UNIVERSITAT POLITÈCNICA DE VALÈNCIA

Contributions to modelling and control for improved hypoglycaemia and variability mitigation by dual-hormone artificial pancreas systems

PhD Dissertation

Author: Vanessa Moscardó Garcia

Supervisors: Dr. Jorge Bondia Company
Dr. Paolo Rossetti

Instituto Universitario de Automática e Informática Industrial
Departamento de Ingeniería de Sistemas y Automática
Universitat Politècnica de València

February 2019

Acknowledgements

Cuando llegas a este punto, en el que has logrado plasmar de la mejor forma posible el trabajo llevado a cabo durante tus últimos años, es inevitable reflexionar y darte cuenta de que todo el trabajo realizado en la presente tesis no hubiese sido posible sin el apoyo, la ayuda y la implicación de ciertas personas. Es por eso que estas personas se merecen ser las protagonistas de siguientes líneas.

En primer lugar, quiero mostrar mi agradecimiento y admiración a mis supervisores, Jorge Bondia y Paolo Rossetti. Gracias por vuestro apoyo y la confianza depositada en mi trabajo; también por vuestro esfuerzo y capacidad para guiarme en el desarrollo de la tesis. Gracias por contribuir en mi crecimiento tanto a nivel profesional como personal. Además de ser excelentes profesionales, sois grandes personas.

Quiero expresar también mi agradecimiento al Centre for Bio-Inspired Technology Imperial College que me permitió realizar con ellos la estancia de investigación. Especialmente a Pantelis Georgiou y Pau Herrero por su amabilidad y por todo el soporte profesional y logístico que tuve para alcanzar los objetivos perseguidos. Muchas gracias por permitirme vivir una experiencia realmente importante en mi formación como investigadora.

En segundo lugar, mencionar todo el apoyo recibido por parte de mi familia. Gracias por darme alas y dejar labrar mi futuro, haciendo posible que ahora esté aquí y así. Chelo, gracias por tu paciencia, preocupación y ánimos. Vicente, gracias por darme ese claro ejemplo de voluntad y constancia que no te cansas cada día de demostrar. ¡Juntos podemos con todo! Ainhoa, tú has vivido de muy cerca

todas las fases por las que he pasado durante el doctorado. En cada una de ellas has estado ahí como hermana, amiga y cómplice. Has tenido paciencia, has sabido cómo animarme, cómo sacarle partido a cada historieta y aventura que hemos vivido; me has ayudado a que todo fuese un poquito más fácil. Entre nosotras la distancia no ha importado y estoy segura que nunca importará, ¡siempre juntas! Y, como siempre te digo: Pilar, eres imprescindible.

Quiero extender mis agradecimientos a los compañeros de la *Sala* y del *Nuevo Lab*. Gracias por vuestro apoyo, interés y buenas palabras siempre que os he ido con alguna historieta de las mías. Me llevo tan buenos momentos: Henry con la prensa corrupta, Ale y Yadira con su especial y encantadora manera de ser, Nóbel con "El juego", Juanfer con su "he perdido" al ver a Nóbel, Clara con su sonrisa y capacidad de relativizar las cosas, Iván con su cabezonería y buen fondo, Frank y Gloria con sus conversaciones y risas durante los mediodías, y Eslam con sus "tienes tres broblemas Vanessa". También, he de agradecer sus consejos y amistad a aquellos que formaron parte de "la antigua Sala", Gilberto, Jopipe, Diego, Gabi, Manuel y Jesús. He de reconocer que os tengo mucho aprecio a todos vosotros y que el "jamón de los viernes" y la costumbre de "las cervecitas de los viernes" me han hecho pasar muy buenos momentos rodeados de gente brillante pero también muy humilde y sensata.

En este punto, no puedo olvidarme de hacerle mención aparte a una persona que, aunque ha sido especial pero sigiloso durante todo el proceso, se ha convertido en uno de los pilares fundamentales en esta fase final y en mi gran compañero de viaje. Gracias Temo por tu paciencia, por tu calma, tu gran ayuda y por creer en mí.

En última estancia, quiero agradecer a mis amigos más cercanos por su cariño, ánimos y comprensión cuando alguna de nuestras citas se ha pospuesto por algún deadline. Mireia, María, Alicia, José, Andrés, Raimon, Gal·la, Laura habéis sido indispensables.

Finalmente, debo agradecer al Ministerio de Educación y Formación Profesional por su financiación con concesión de la beca de Formación del Profesorado Universitario (FPU).

A todos vosotros, gracias por confiar y creer en que algún día estaría escribiendo estas líneas.

Abstract

People with Type 1 Diabetes lack the ability to secrete insulin and therefore need to regulate their blood glucose with exogenous insulin delivery. The Artificial Pancreas is presented as the ideal technological solution to reach the therapeutic goals of normoglycaemia, freeing the patient from the current burden of self-control and management. Nevertheless, the risk of hypoglycaemia and the high glycaemic variability are still a limiting factors in the current control algorithms integrated in the Artificial Pancreas.

The purpose of the present thesis is to delve into knowledge of hypoglycaemia and to advance in the artificial pancreas control algorithms in order to minimise hypoglycaemia incidence and reduce glycaemic variability. After providing an overview of the state of the art in the field of glucose control and artificial pancreas, this thesis addresses issues on modelling and control, with the following contributions:

An extension of the Bergman Minimal model accounting for counterregulatory response to hypoglycaemia is presented. This model explains the relationship between the several physiological changes produced during hypoglycaemia, with adrenaline and free fatty acids as main players. As a result, a better understanding of hypoglycaemia is gained, allowing to explain a paradoxical auto-potentiation of hypoglycaemia as modeled through functional approaches in the widespread used UVA-Padova Type 1 Diabetes simulator, which will be used in this thesis for in silico validation of the developed controllers.

An assessment of glucose variability metrics and control quality indices is carried out. The evaluation of the glycaemic variability on the controllers performance is

necessary; but there is not a gold standard variability metrics yet. Therefore, an analysis of the variability metrics available in literature is conducted in order to define a recommendable set of indicators.

Due to the limitations of single-hormone artificial pancreas systems in mitigating hypoglycaemia in challenging scenarios such as exercise, this thesis focuses on the developement of new dual-hormone control algorithms, with concomitant infusion of insulin and glucagon. *A coordinated dual-hormone controller with parallel control structures is proposed* as a feasible control algorithm for hypoglycaemia mitigation and glycaemic variability reduction, demonstrating superior performance as currently used control structures with independent insulin and glucagon control loops. The controllers are designed and evaluated in-silico under challenging scenarios and their performance are assessed mainly with the set of metrics defined previously as the recommendable ones.

Resumen

Las personas con diabetes tipo 1 carecen de la capacidad de secretar insulina y, por lo tanto, necesitan regular su glucosa en sangre con la administración de insulina exógena. El páncreas artificial se presenta como la solución tecnológica ideal para alcanzar los objetivos terapéuticos de la normoglucemia, liberando al paciente de la carga actual de autocontrol y manejo. Sin embargo, el riesgo de hipoglucemia y la variabilidad glucémica siguen siendo factores limitantes en los algoritmos de control actuales integrados en el páncreas artificial.

El propósito de la presente tesis es profundizar en el conocimiento de la hipoglucemia y avanzar los algoritmos de control del páncreas artificial para minimizar la incidencia de hipoglucemia y reducir la variabilidad glucémica. Después de proporcionar una visión general del estado del arte del control de la glucosa y el páncreas artificial, esta tesis aborda temas relacionados con el modelado y el control, con las siguientes contribuciones:

Se presenta una extensión del modelo de Bergman Minimal que tiene en cuenta la respuesta contrarreguladora a la hipoglucemia. Este modelo explica la relación entre los diversos cambios fisiológicos producidos durante la hipoglucemia, con la adrenalina y los ácidos grasos libres como actores principales. Como resultado, se obtiene una mejor comprensión de la hipoglucemia, lo que permite explicar una auto-potenciación paradójica de la hipoglucemia como se modela a través de enfoques funcionales en el ampliamente utilizado simulador de diabetes tipo 1 UVA-Padova, que se utilizará en esta tesis para la validación in silico de los controladores desarrollados.

Se realiza una evaluación de las métricas de variabilidad de la glucosa y los índices de calidad de control. La evaluación de la variabilidad glucémica en el desempeño de los controladores es necesaria; pero todavía no hay un conjunto de métricas de variabilidad glucémica que sea considerado como el "gold estándar". Por tanto, se lleva a cabo un análisis de las métricas de variabilidad disponibles en la literatura para definir un conjunto de indicadores recomendables.

Debido a las limitaciones de los sistemas de páncreas artificiales unihormonales para mitigar la hipoglucemia en escenarios difíciles como el ejercicio, esta tesis se centra en el desarrollo de nuevos algoritmos de control bihormonales, con infusiín simultanea de insulina y glucagón. *Se propone un controlador coordinado bihormonal con estructuras de control paralelas* como un algoritmo de control factible para la mitigación de la hipoglucemia y la reducción de la variabilidad glucémica, demostrando un rendimiento superior al de las estructuras de control utilizadas actualmente con lazos de control independientes de insulina y glucagón. Los controladores están diseñados y evaluados in silico en escenarios desafiantes y su rendimiento se evalúa principalmente con el conjunto de métricas definidas previamente como las recomendables.

Resum

Les persones amb diabetis tipus 1 no tenen la capacitat de secretar insulina secreta i per tant, necessiten regular la seva glucosa en sang amb l'administració d'insulina exògena. El Pàncrees Artificials es presenta com la solució tecnològica ideal per assolir els objectius terapèutics de la normoglucèmia, alliberant al pacient de la càrrega actual d'autocontrol. No obstant, el risc d'hipoglucèmia i l'alta variabilitat glucèmica continuen sent un factor limitant en els algoritmes de control actuals integrats en el Pàncrees Artificials. El propòsit de la present tesi és aprofundir en el coneixement de la hipoglucèmia i millorar els algoritmes de control per corregir amb antelació la dosi excessiva d'insulina, minimitzant la incidència d'hipoglucèmia i reduint la variabilitat glucèmica.

Després de donar una visió general de l'estat de l'art del control de la glucosa i el pàncrees artificial, aquesta tesi aborda aspectes de modelització i control, amb les següents contribucions:

Es presenta una extensió del model Minimal de Bergman amb la contrarregulació. Aquest model explica la relació entre els diversos canvis fisiològics produïts durant la hipoglucèmia. Així, permet comprendre millor la hipoglucèmia i comparar els resultats amb els proporcionats per l'enfocament funcional del simulador de diabetis tipus 1 més utilitzat a la comunitat científica.

Es realitza una avaluació de les mètriques de variabilitat glucèmica i dels índexs de qualitat de control. Es necessària l'avaluació de la variabilitat glucèmica en el rendiment dels controladors; però encara no hi ha un conjunt de mètriques considerades com les "gold standard". Per tant, es realitza una anàlisi de les mètriques

de variabilitat disponibles a la literatura per definir un conjunt d'indicadors recomanables.

Es proposa un controlador bi-hormonal coordinat amb estructures de control paral·leles com un algoritme de control viable per a la mitigació d'hipoglucèmia i la reducció de la variabilitat glucèmica. Els controladors estan dissenyats i avaluats in-silico en escenaris desafiadors i el seu rendiment es valora principalment amb el conjunt de mètriques definides prèviament com les mètriques recomanables.

Contents

Chapter 1

Introduction

This chapter introduces the main ideas of the thesis, which is concerned with the generalisation of the current state of diabetes and the advances in the Automatic Insulin Delivery Systems, in order to put the reader into context. Besides, the ongoing limitations of the glucose control algorithms are briefly presented since they are the principal motivation of this work. Then, the objectives that have lead the way in the consecution of the present thesis are exposed. The chapter concludes with a brief overview of the contents.

1.1 Motivation and background

Diabetes is a chronic disease with a high individual and social impact, and with an important prevalence. It is estimated that the number of people with diabetes in the world will reach about 10% of the adult world population between 20 and 79 years by 2045 (Shaw et al. 2010). In addition, diabetes is responsible for more than 10% of healthcare spending in most countries of the European Union (Federation of European Nurses in Diabetes 2008).

Type 1 diabetes Mellitus (T1D) affects approximately 10% of diabetic patients and is characterized by self-destruction of beta cells in the pancreas, which are responsible for insulin secretion. This causes a constant state of hyperglycaemia (glucose levels above 180 mg/dL) that can lead to chronic microvascular and macrovascular complications besides of other short term complications. In the 1990s, the DCCT study (Control and Group 1993) showed that an improvement in glycaemic control

reduces the risk of suffering the chronic complications associated with diabetes. Therefore, normoglycaemia (glucose levels between 70 and 180 mg /dL) has been established as a control objective in patients with T1D. Currently, patients follow insulin replacement therapy with multiple daily inyections (MDI, 4 or more per day) or continuous subcutaneous insulin infusion, based on usually intermittent (3-6 per day) self-monitoring of capillary blood glucose. Patients education is a cornerstone of the treatment, as they must learn how to interpret blood glucose profiles and adjust the insulin dose in response to changes in meal intake, physical activity, illness, etc. This represent a considerble burden for both the patients and the health care professionals and, despite considerable efforts and the spreading of continuous glucose monitoring, glycaemic control is still not satisfactory (Kowalski 2009), with huge variations in plasma glucose concentrations. The result is a significant exposure to both hyperglycaemia (an average of 9h/day plasma glucose values above 180 mg/dl) and hypoglycaemia (an average of 1h/day below 70 mg/dl), which poses the patient at risk for acute and chronic complications.

The Artificial Pancreas (AP), or Automatic Insulin Delivery Systems, is a technology that arouses great interest in the scientific community (Gibney 2013) since it represents an important advance in the management of Type 1 Diabetes (T1D). As long as the cure for T1D is not found, the artificial pancreas is presented as the ideal technological solution to reach the therapeutic goals of normoglycaemia, freeing the patient from the current burden of self-control and management. Advances in continuous glucose measurement technology led in 2006 to the creation of an international consortium in artificial pancreas by the Juvenile Diabetes Research Foundation (JDRF) (Jaeb Center for Health Research 2018). In addition, that same year, the Food and Drug Administration (FDA) declared the artificial pancreas a priority in its Critical Path Initiative. Then, the National Institutes of Health (NIH) in the USA and the EU in the seventh framework program was also joined to this commitment. Thus, all of those gave a crucial impulse to the research in the area.

The current effort of the scientific community focuses on providing the system with the necessary efficiency and safety in the daily living conditions of the patient. One of the problems of the ongoing control strategies is the overcorrection of the controller inducing an excess of insulin when it tries to compensate the meal intake, which increases the risk of late postprandial hypoglycaemias. However, reduction of overcorrection is a difficult task because patients with T1D exhibit high glycaemic variability (glucose response is not the same even under theoretically identical conditions, i.e. the same meal and insulin dose). Additionally, controllers must be robust also against the errors in continuous glucose monitoring, which performance has improved during the last years but that is far from being perfect.

High glycaemic variability is associated with a greater risk for hypoglycaemia, so that a good control must also consider the reduction of glucose variability as a control objective.

However, we are not yet able to emulate the insulin secretion of a healthy pancreas. That is, the current insulin replacement in people with diabetes is still a bit far from being perfect. There are several reasons why it is difficult to replace insulin. First, insulin is replaced in the wrong place, i.e. it is delivered in the subcutaneous tissue instead of the intravascular space. This is responsible for slow insulin absorption at meal times with excessive increase in post-prandial blood glucose concentrations (Dimitriadis and J. E. Gerich 1983). Besides, subcutaneous insulin delivery induces systemic hyperinsulinemia (Bolli 1990). Such hyperinsulinemia is itself a risk factor for hypoglycaemia, despite insulin resistance (DeFronzo et al. 1982).

Second, despite the use of insulin formulations with improved action profile and patient empowerment with structured educational programmes, exogenous insulin replacement cannot perfectly match insulin requirements, which vary greatly depending on the physiological changes of insulin sensitivity and meal size and composition (Kelley 2003).

Thereby, the challenges for the development of the AP are multiple: the accuracy of continuous glucose monitors must be even more improved, especially in hypoglycaemia; there are physiological delays due to the infusion of insulin subcutaneously compared to pancreatic secretion; the patient presents high variability; and there are important disturbances such as meal, exercise and stress. Moreover, the problem with the insulin delivery is that the effect of insulin is unidirectional promoting a decrease in plasma glucose concentration. This means that if insulin is delivered in excess, there are serious limitations to compensate for an excessive drop in blood glucose concentration, being necessary rescue carbohydrates intake.

The home use of the artificial pancreas requires safety mechanisms that allow its use without additional risk for the patient besides of an efficient controller that is able to cope with the conditions of daily life. The hypoglycaemia prevention and the efficient control involve providing the system with the ability to react. The strategies based on MPC predict blood glucose in a given prediction horizon by means of the calculation of the insulin infusion that maximizes the performance of the controller (Hovorka et al. 2004). In the PID control schemes, a predicted insulin feedback is added from a pharmacokinetic model (Steil et al. 2011). Additionally, supervisory algorithms for patient safety employ predictions of the risk of hypoglycaemia (Patek et al. 2012). The used modelling techniques range from autoregressive models based on data (Ståhl and Johansson 2009; Finan et al. 2009)

to physiological models, from greater to lesser complexity (Hovorka et al. 2004; Dalla Man et al. 2007b).

The simplest strategy proposed in literature is the hypoglycaemia detection by threshold and defining the hypoglycaemia risk when the glucose concentration is lower than a second risk threshold after a certain time period (Choleau et al. 2002; Children Network (DirecNet) Study Group 2004). Other technique proposed to classify glucose measurements are the stochastic models based on the kernel density model (Signal et al. 2012) and linear statistical predictive models (Cameron et al. 2008). Both techniques manage to be a robust event classifier but do not have an optimal prediction horizon. About simple linear models, Bremer and Gough 1999 showed that predictions could be obtained with a prediction horizon of 10 min if representative data were available. However, the data were not representative since they did not take into account the variability of human factors and the fact that the dynamics of glucose follows a non-linear regime. In order to adjust the system to the glucose variability, Daskalaki et al. 2013 proposed adaptive prediction models (autoregressive model, autoregressive model with correction module and recurrent neural networks); whereas Buckingham et al. 2009 developed a partial-square-regression autoregressive algorithm to model and predict future glucose concentrations and used it in an alarm system of hypoglycaemia. So as to give robustness to the system, other authors (Dassau et al. 2010; Buckingham et al. 2010) developed voting algorithms that operated in parallel to a threshold alarm system consisting of linear prediction algorithms, statistical prediction, Kalman filter, HIIR (hybrid impulse response filter) and another numerical logic algorithm. These systems aimed to offer better prediction than a system formed by a single Kalman filter as Palerm suggested (Palerm and Bequette 2004; Palerm and Bequette 2007; Harvey et al. 2012).

In the proposed algorithms, the prediction depends on the level of glucose, although hypoglycaemic episodes physiologically begin with more hormonal changes. The current models are focused on insulin and glucose. However, insulin is only one part of the glucose regulation especially during hypoglycaemia, where hormones such as adrenaline, cortisol and growth hormone have an active role in T1D patients, as well as the lipid and glucidic metabolism.

Presently, several AP prototypes based on proportional-integral-derivative (PID) algorithms or model-based predictive control (MPC) have been validated clinically in controlled environments and outpatient studies. In the second case, linear approaches have been used, based on autoregressive models (ARX) (Magni et al. 2009) or the physiological models linearization (Magni et al. 2007). Both the PID and the MPC have been shown to be efficient at nocturnal control (Hovorka et al. 2010; Kumareswaran et al. 2011; El-Khatib et al. 2010; Kovatchev et al. 2010).

In addition, other clinical trials have been also performed out to test fuzzy algorithms (Dovc et al. 2017) and a switched Linear Quadratic Gaussian (LQG) controller combined with a Safety Auxiliary Feedback Element (SAFE) algorithm (R. Sánchez-Peña et al. 2017; R. Sánchez-Peña et al. 2018). Nevertheless, postprandial control (compensation of a meal intake) is still an open problem due to the overacting of the controller. This causes an excessive insulin infusion, inducing late hypoglycaemia that can have unwanted consequences for the patient. Other challenge is the control during physical activity since the glycaemic response depends on the characteristics of the exercise (type, intensity, duration) as well as the variability of the patient.

The problem of excessive insulin infusion has been approached from various perspectives: (1) the limitation of insulin infusion and (2) the use of glucagon as a counterregulatory control action. Several prototypes have incorporated insulin on board restrictions (IOB - insulin that is already in the body and has not yet acted-), both by means of ad hoc solutions in PID algorithms (Weinzimer et al. 2008) and integrated in the design of MPC controllers (Ellingsen et al. 2009). However, the results have not been completely satisfactory. In the new prototypes based on MPC, strategies that reduce the aggressiveness of the controller performance have been included. This works as an open loop system with a basal insulin infusion when the patient is in euglycaemia (control-to-range algorithms). It has been demonstrated that these new algorithms improve the glycaemic control compared to the standard therapy with insulin pumps in controlled studies of 22 hours which included meal, nocturnal period and 30minutes of exercise (Breton et al. 2012). The Sliding Mode of Reference Conditioning (SMRC) was applied in (Revert et al. 2013) in order to design an external loop that allow to limit the IOB in a generic controller. Results were satisfactory in a clinical controlled study that included 8 postprandial hours (Rossetti et al. 2017).

Alternatively, dual-hormone systems have been developed in order to complement the action of insulin with a subcutaneous infusion of glucagon, promoting the release of glucose in blood (unidirectional signal in the opposite direction to insulin). The first results were validated in humans with good results in 51-hour trials (Russell et al. 2012). Then, Taleb et al. 2016 showed better results in dual-hormone systems during studies with exercise. Besides, Castle et al. 2018 demonstrated recently that the addition of glucagon delivery to the closed-loop system with automatic exercise detection reduces hypoglycemia after aerobic exercise. So far, the great limitation of these dual-hormone systems was the short stability period of glucagon solutions for continuous pump infusion. However, currently, the new formulation enables a viable use of glucagon in the glucagon pumps. This gives a boost to the dual-hormone configuration of the AP, and makes possible that both

the single-hormone AP and the dual-hormone AP can already play in the same league.

As it can be concluded from the discussion above, there is a worldwide interest in the improvement of the Automatic Insulin Delivery Systems. Recent AP configurations have achieved acceptable nocturnal control performance and a reduction of time in hypoglycaemia in postprandial scenarios if they are compared with the previous AP options. Nevertheless, the problem of hypoglycaemia is still relevant, especially during the postprandial period and physical activity. Hypoglycaemia is intimately related to glycaemic variability (Gimenez et al. 2018), and both are associated with a significant patient burden. Therefore, both issues should be addressed by the new proposals of control algorithms.

This thesis studies the hypoglycaemia from a physiological point and develops a model considering the hormones and mechanisms that are involved in the hypoglycaemia process. This model allows to understand better the glucose behaviour in T1D patients, and it can be used as a reference for the validation tools of the controllers (i.e. the in-silico simulators). In regard to the improvement of control algorithms faced with hypoglycaemia, the development of dual-hormone control algorithms is carried out. Then, the features of the proposed dual-hormone controller are analysed by the times in ranges and the glycaemic variability metrics, which have been also evaluated in the present work.

1.2 Objectives

The main objective of this thesis is the development of more efficient control algorithms mitigating hypoglycaemia and reducing glycaemic variability in the challenging scenarios of patient's daily life. To achieve this, a dual-hormone configuration of the controller is proposed besides of the previous study of a new hypoglycaemia model, which is the main current limitation of the controllers along with the glycaemic variability.

In order to attain its consecution, this general objective is divided into three specific sub-objectives:

1. *Assesment of counterregulatory response modelling under hypoglycaemia for in silico evaluation of controllers.* The first step towards achieving the global objective is to review the existing literature and research concerning the physiological mechanisms hypoglycaemia stimulates and its changes due to T1D. The key concept here is the counterregulatory response, thus, the next step is to analyse the implementation of the counterregulation in the current

available simulators used for in-silico validation. To this end, the functional approach of the model used in the UVA-Padova simulator is evaluated. Then, the physiology of the counterregulation is modelled, and compared with the outcomes from the model used in the UVA-Padova Simulator.

2. *Assessment of glycaemic variability metrics.* Evaluation of the glycaemic variability on the controller performance is necessary; but there is not a gold standard variability metrics yet. Therefore, an analysis of the variability metrics available in literature and, then, the definition of the recommendable indicator is conducted.

3. *Controllers design and evaluation for hypoglycaemia mitigation and glycaemic variability reduction under challenging scenarios.* Due to the limitations of single-hormone systems, especially under exercise, dual-hormones systems will be considered here. The design of the controllers is carried out using a suitable in-silico simulator (taking into account the results from objective 1), and the proposed systems are evaluated considering the recommendable metrics resulting of the objective 2.

Figure 1.1 shows the links between the contributions of the present thesis.

1.3 Structure of the thesis

This thesis is divided into two parts:

- Part I. This part summarises the most relevant concepts and results in literature related to the objectives of this thesis. In Chapter 2, the mechanisms involved in glucose control are introduced. Besides, the main failures in this process that are associated with Type 1 diabetes are presented, focusing on defective counterregulatory response to hypoglycaemia.

  Chapter 3 presents a summary on the Artificial Pancreas research, presenting with deeper detail the strategies that have been taken into account in the development of this thesis. These are the dual-hormone approach and the strategies for the limitation of the insulin on board in order to avoid an insulin overdose. Moreover, the glycaemic variability, which is considered the other target along with hypoglycaemia avoidance, is assessed with the indicators available in literature.

  Finally, Chapter 4 carries out a revision of the mathematical models proposed in literature. The Bergman Minimal Model is explained in more detail since it is of relevance to this thesis, which extends this minimal model with

the mechanisms involved in hypoglycaemia. Besides, the extended version of the original Bergman Model with the Fatty acids are also described because it is partially used in this work.

- Part II. This part contains the contributions of this work. The first contribution is presented in Chapter 5, where the physiological model of glucose autorregulation is presented. It is an extension of the Bergman Minimal Model with the counterregulatory response which is involved in the hypoglycaemic ranges. Previously, a more detailed study of the physiological behaviour related to hypoglycaemia is also realized.

  Chapter 6 deals with the assessment of glucose variability. As said before, glycaemic variability is a control target, but there is not a consensus on the best method to measure it. Several authors have given their proposal, but any analysis about their features have not been done. Therefore, in order to determine the proper metrics to characterise our proposed glucose controller, an analysis of variability metrics is conducted.

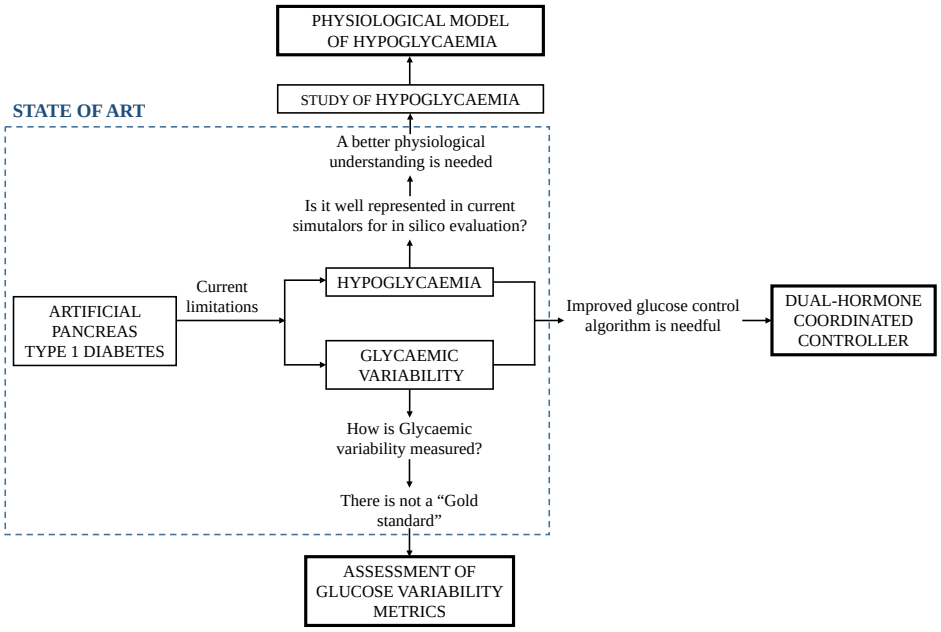

Figure 1.1: Routemap of the present thesis.

Chapter 7 presents the dual-hormone controller proposed to achieve a good glycaemic control. The controller is evaluated in several scenarios with meal, snack and exercise perturbations. In the most challenging scenario (exercise), hypoglycaemia is not completely avoided; thus, a limitation of the insulin on board is included.

- This thesis ends in Chapter 8, drawing some concluding remarks and providing some suggestions for future work.

Note that a full list of publications by the PhD candidate is presented in page 171.

Part I

State of the Art

Chapter 2

Glucose control

This chapter presents an overview on the mechanisms involved in glucose control. Particular failures on this process drive to the onset of Diabetes. Specific interest has the Type 1 Diabetes in this thesis, whose particularities are also explained. Hypoglycaemia is one of the most serious complications in the treatment of this disease, and the current technological solutions are focused on avoiding it. Thus, the first step is to understand well the physiological processes and interactions that participate in it.

2.1 Glucose control

Homeostasis is the process by which the internal environment of the body is maintained stable allowing optimal function and physiological balance. Control of blood glucose is a fundamental part of this process. Plasma glucose concentration in healthy people is subjected to a rigorous control that maintains the glucose concentration in a narrow range ($\sim 70 - 180$ mg/dL) despite wide variability in meal intakes size and composition, and physical activity, among others factors. The upper limit is defended because high glucose concentration (hyperglycaemia) can cause both acute (diabetic ketoacidosis -DKA-, coma, diabetic atherosclerosis) and chronic long-term complications (micro- and macrovascular damage); and the lower limit is guarded in order to avoid glucose values under that threshold (hypoglycaemia) since the brain cannot function properly without an adequate supply of glucose.

Glucose regulation is a complex process which involves many organs. Figure 2.1 shows the major players in the regulation and utilization of plasma glucose, and the role of each one is discussed below.

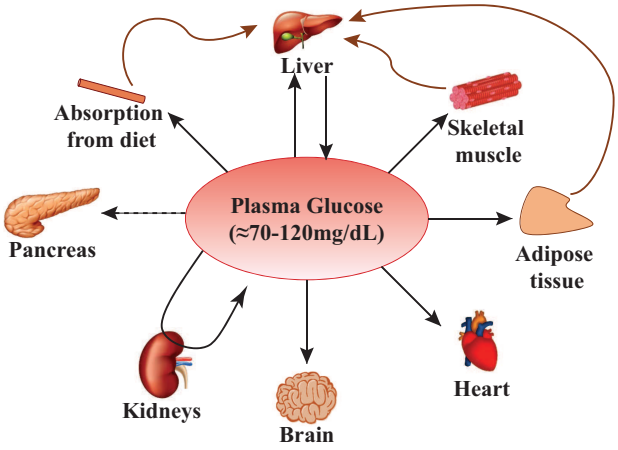

Figure 2.1: Main organs that are involved in the plasma glucose regulation.

The **brain** function depends exclusively on glucose supply from plasma so that it consumes a $\sim 50\%$ of whole body glucose production under resting conditions. Although alternative fuels (ketone and lactate) can be used in extreme conditions (prolonged fasting, starvation), when plasma glucose fall acutely below ~ 50 mg/dL brain disfunction ensues; when glucose levels decrease persistently and consistently below 40 mg/dL, this can lead to permanent damage and/or death.

The **liver** is the major metabolic regulatory organ. In the basal (fasting) state, about 90% of all circulating glucose comes from the liver. The liver contains significant amounts of stored glycogen available for rapid release into circulation (glycogenolysis), and is capable of synthesizing large quantities of glucose from other substrates like lactate and amino acids released by other tissues (gluconeogenesis). During prolonged starvation, the liver is the source of glucose and the ketone bodies demanded by the brain to replace glucose.

The **kidney** has also the ability to release glucose into the blood. Under normal conditions gluconeogenesis (glucose production from precursors like glycerol, lactate, and amino acids) provides only a small contribution to the total circulating

glucose; however, during prolonged starvation and fasting, the kidney contribution may be comparable to that of the liver. Nevertheless, the role of kidney is crucial in the glucose homeostasis because plasma glucose must be reabsorbed when it passes through the kidney to prevent losses.

The **muscle** cannot deliver glucose to the bloodstream; however it is able to increase quickly its glucose uptake for dealing with sudden increases in plasma glucose. In addition, the skeletal muscle has also a role in maintaining plasma glucose levels since it can realise free amino acids into circulation to be used as substrates for the liver gluconeogenesis. The muscle can use glucose, FFA, and ketone bodies for energy whereas it usually maintains significant amounts of stored glycogen, small amounts of FFA and large reserve of proteins that can be broken down in critical situations.

The **adipose tissue** is the main triglyceride (glycerol and three FFAs) storage. In conditions when liver gluconeogenesis is necessary, the adipose tissue supplies FFA as an alternative fuel to glucose, and glycerol as a substrate for hepatic. gluconeogenesis.

Finally, the **pancreas** is the source of insulin and glucagon, two of the most important regulatory hormones. Besides, the **Hypothalamic-pituitary-adrenal axis** (HPA) has also an important role with the catecholamines adrenaline and noradrenaline, cortisol and Grown Hormone secretion during hypoglycaemic situations.

Fasting and fed state are two physiological conditions that require to be distinguished in the glucose regulation process due to differences in their physiological response. During **fasting**, insulin concentrations are reduced and glucagon increased, which maintains blood glucose concentrations within the normoglycaemic limits. The net effect is to reduce peripheral glucose utilization, to increase hepatic glucose production and to provide non-glucose fuels for tissues not entirely dependent on glucose. In addition, plasma free fatty acids and ketone body concentrations also increase. These changes are mainly due to the decrease in plasma insulin concentration which permits accelerated lipolysis with increased FFA release and ketone body formation. As fasting prolongs, muscle and other tissues use FFA and ketone bodies more efficiently.

Muscle and other tissues become progressively more dependent on free fatty acids and ketone bodies. When plasma glucose tend to decrease, ketone bodies can be used as an alternative fuel by the neural tissues, thus reducing - but not eliminating - the need for glucose. After a short fast (e.g. overnight), glucose production needs to be 5-6g/h to maintain blood glucose concentration. The required glucose

comes from glycogenolysis (60-80%) and gluconeogenesis (20-40%). Otherwise, in prolonged fasting, glycogen becomes depleted and glucose production is primarily from gluconeogenesis, with an increasing proportion from the kidney compared to the liver. In extreme situations renal gluconeogenesis can contribute as much as 45% of glucose production. Thus glycogen is the short term or "emergency" fuel source.

After meal (**fed state**), the rise in glucose concentrations results in an increase in insulin and reduction in glucagon secretion. This balance favours glucose utilization and reduction of glucose production, and increases glycogen, triglyceride and protein formation. At the same time, the fatty acids are taken up into the adipose tissue and re-esterified to triglyceride (using glycerol derived from glucose) before being stored. In addition, glucose uptake is increased (in proportion to plasma glucose) in the liver. Lastly, hepatic glycogenolysis is suppressed and glycogen deposition stimulated due to insulin concentration increase.

Figure 2.2 represents the profiles of glucose and insulin concentrations throughout 24 h in non-diabetic subjects. As it can be observed, plasma glucose is maintained below 100 mg/dL (5.56 mmol/L) during fasting and below $\sim$ 135 mg/dL (7.5 mmol/L) in the post-prandial period, even after a carbohydrate-rich meal. In the

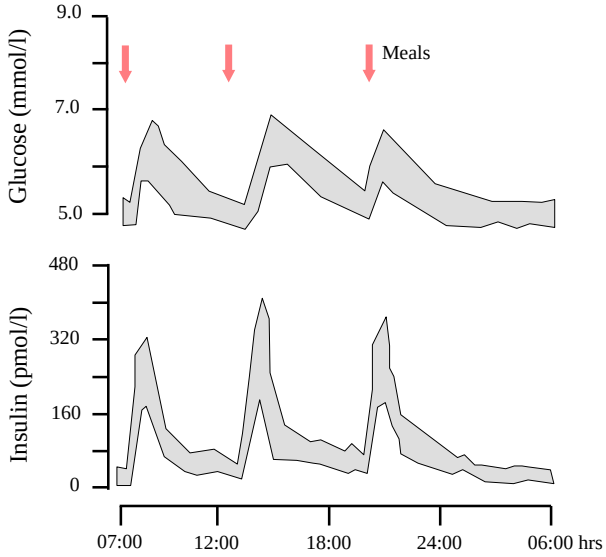

Figure 2.2: Physiology of glucose homeostasis in non-diabetic subjects (adapted from Rossetti et al. 2008).

fasting state, maintenance of normoglycaemia is possible because of the continuous release of insulin from the pancreas which restrains hepatic glucose production (2-3 mg/kg/min) as to match peripheral glucose uptake (50% the brain, 50% the rest of the tissues). In the fed state, pancreas releases insulin very rapidely in response to meal ingestion promoting the disposal of ingested glucose and controlling in this way postprandial glucose excursions. However, of similarly importance is prompt decrease of plasma insulin 60-90 minutes after meal ingestion, which prevents hypoglycaemia in the post-prandial state. Finally, the fact that between-meal plasma insulin is flat and peakless is the key factor in preventing interprandial and fasting hypoglycaemia, especially during the nocturnal fasting hours.

2.1.1 Pancreas and neuroendocrine responses

The pancreas has two major functions: (1) synthesis and release of digestive enzymes, and (2) production and delivery of the two major hormones responsible for the endocrine glucose metabolism control (insulin and glucagon).

The endocrine pancreas is composed of small groups of cells distributed throughout the organ, the Islets of Langerhans. These groups are four and each one secretes one major hormone: apha-cells are the insulin producing cells; beta-cells produce glucagon; gamma-cells secrete somatostatin; and, PP-cells deliveries Pancreatic polypeptide (I. A. Macdonald and King 2007).

The most relevant hormones involved in the glycaemia regulation are the following five ones: insulin, glucagon, adrenaline, cortisol, and growth hormone. They are described in detail because it is important to know the mechanisms of which each one is responsible and the relationship between them in order to be able to reproduce it mathematically.

- **Insulin** is a peptide hormone. It is secreted in response to elevated plasma glucose, mannose, and some amino acids. On the other hand, insulin release is inhibited by somatostatin, by cortisol, and by catecholamines. Insulin effects on glucose metabolism are the stimulation of lipid synthesis and liberation in the liver and protein synthesis. In addition, insulin stimulates glucose uptake into adipose tissue and in muscle.
- **Glucagon** release is activated by low plasma glucose and by catecholamines and glucocorticoids whereas it is inhibited by insulin and somatostatin. Glucagon delivery is also inhibited by glucose but it is unknown if it is due to a direct effect of glucose on alpha-cells or it is an indirect consequence of elevated insulin levels. This hormone has an antagonistic actions

of insulin. However, glucagon action is probably limited to the liver, with limited effects in other tissues. Glucagon stimulates liver amino acid uptakes, gluconeogenesis, and glucose release, and inhibits glycolysis and FFA synthesis.

- The **catecholamines** adrenaline and noradrenaline, cortisol, and growth hormone all acts to raise plasma glucose levels. Their behaviours are against those of insulin, and they with glucagon are called **counterregulatory hormones**. Due to the dependence of the brain on plasma glucose for energy, hypoglycaemia can quickly end up in unconsciousness, brain damage, and death. Thus, the counterregulatory hormones act to prevent hypoglycaemia and avoid severe consequences.

  Adrenaline is released by the adrenal medulla in response to hypoglycaemia, and as part of the preparation for exercise. On the other hand, **noradrenaline** is released from sympathetic neurons. Both catecholamines have significant roles in maintaining glucose levels in exercise; nevertheless, adrenaline secretion has a more important contribution in terms of hypoglycaemia prevention. Catecholamines stimulate glucagon secretion and inhibit insulin delivery causing a decrease in the insulin-glucagon rate and having indirect effects on liver glucose metabolism. Adrenaline also stimulates liver gluconeogenesis, muscle glycolysis, and glycogen breakdown in liver and muscle.

  Cortisol is released from the adrenal cortex in response to stress of falling plasma glucose levels. It stimulates gluconeogenesis and glycogen synthesis in the liver, and reduce muscle and adipose tissue glucose uptake. It also acutely inhibits insulin release and insulin action. **Growth hormone** is secreted in response to dropping down glucose levels, and its counterregulatory action is the stimulation of lipolysis and an inhibition of insulin action.

2.2 Diabetes

Diabetes Mellitus is a condition characterized by chronic hyperglycaemia due to absolute or relative insulin deficiency (the pancreas cannot produce any or enough insulin to match tissue requirements). Hyperglycaemia, if left unchecked over the long term, can cause damage to various body organs, leading to the development of disabling and life-threatening health complications such as cardiovascular diseases, neuropathy, nephropathy, and eye disease (retinopathy leading to blindness). However, if appropriate management of diabetes is achieved, these serious complications can be delayed or prevented (Heinemann 2017).

The classification is complex. However, $\sim 90\%$ of patients have Type 1 Diabetes (T1D) (10%) and Type 2 Diabetes (T2D) (80%). Less common types of diabetes include the gestational diabetes (GDM), the monogenic diabetes and secondary diabetes. Monogenic diabetes is the result of a genetic mutation; secondary diabetes arises as a complication of other diseases such as hormone disturbances. The present thesis addresses problems related to T1D. Therefore, T1D is the only one explained below in more detail.

Diabetes complications can be divided into acute and chronic complications (Melmed et al. 2016, Chapter 33). Acute complications include diabetic ketoacidosis (DKA), hyperglycaemic hyperosmolar state (HHS), hyperglycaemic diabetic coma, seizures or loss of consciousness and infections. Chronic microvascular complications are nephropathy, neuropathy and retinopathy, whereas chronic macrovascular complications are coronary artery disease (CAD) leading to angina or myocardial infarction, peripheral artery disease (PAD) contributing to stroke, diabetic encephalopathy and diabetic foot. In addition, diabetes has also been associated with increased rates of cancer, physical and cognitive disability, tuberculosis, and depression.

2.3 Type 1 diabetes

Type 1 Diabetes is an autoimmune disease that causes the destruction of the beta cells of the pancreas. This destruction produces the lack of endogenous insulin secretion that leads to hyperglycaemia; then, endogenous insulin delivery has to be provided. Figure 2.3 illustrates the difference between glucose regulation in T1D subjects compared with the healthy ones.

Non-diabetic subjects maintain plasma glucose concentrations below 100mg/dL during fasting state, and below 140mg/dL in the postprandial period. During fasting, maintenance of normoglycaemia is possible due to the continuous secretion of insulin from pancreas, which restrains hepatic glucose production and prevents hyperglycaemia. At meal times, the pancreas releases insulin in response to meal ingestion and drives the glucose levels to the basal concentrations. 60-90 minutes after meal ingestion, the basal glucose concentration is achieved and the insulin secretion is reduced to the basal levels to regulate hepatic glucose production to maintain euglycaemia. This flatted insulin secretion is also crucial to prevent the interprandial and fasting hypoglycaemias.

In contrast, the T1D patient has to replace this endogenous insulin production (that is null) by an exogenous insulin delivery to avoid acute and chronic complications. The insulin delivery should imitate the model of insulin dynamics of

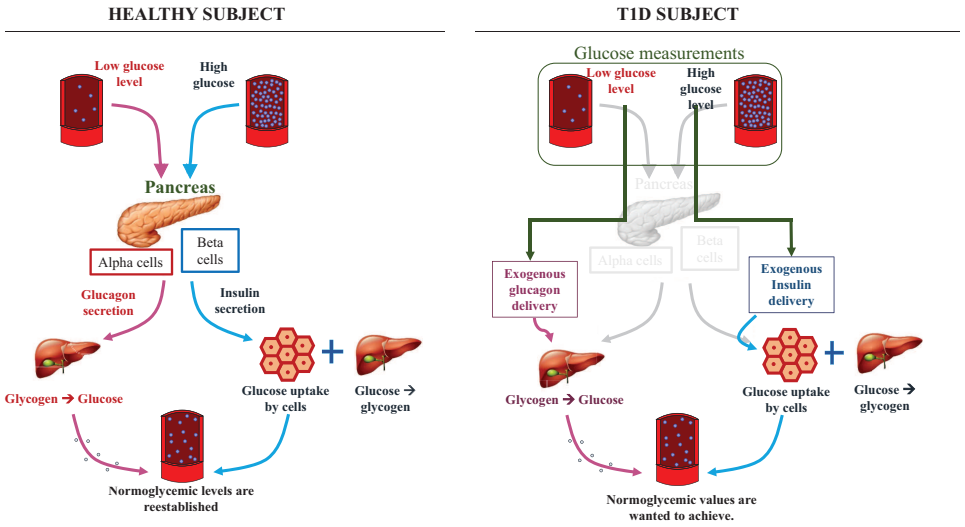

Figure 2.3: Glucose regulation in T1D people compared with healthy people.

non-diabetic subjects (Melmed et al. 2016, Chapter 32) (see Figure 2.2). That is, in fasting state, insulin should be replaced using a preparation of "basal" insulin ideally reproducing a flat and peakless concentration for all day long; at meal times, a bolus injection of a rapid-acting insulin is needed in order to reproduce the early and elevated peak plasma insulin in coincidence with carbohydrate ingestion. The delay associated to the abosrption from the subcutaneous tissue to plasma retards insulin action until after starting carbohydrates absorption. This fact increases the risk of post-prandial hyperglycaemia combined possibly with the problem of late post-prandial hypoglycaemia due to continuing absorption of insulin beyond the meal absorption. Hence, the insulin preparation (analogues) and the insulin delivery must mimic the healthy human physiology (the pharmacokinetics and pharmacodynamics characteristics must be close to the ideal human insulin). However, physiological insulin replacement is a hard task, resulting into a mismatch between insulin needs and supply. This causes hyper- and hypoinsulinemia, generating hypo- and hyperglycaemic peaks, respectively. Figures 2.4 shows the differences between healthy and T1D patients in terms of plasma insulin concentration (secreted endogenously in Healthy people; delivered exogenously in T1D patients), and glucose concentration. Here, it also can be observed the different performance of the regular and rapid-acting insulin analogues.

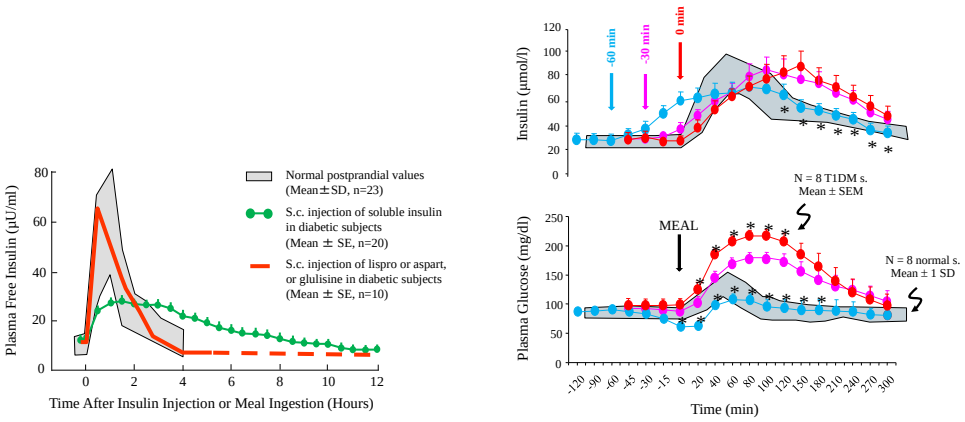

(a) **(b)**

Figure 2.4: (a) Pharmacokinetics following subcutaneous injection of regular human insulin, and rapid-acting insulin analogues. (b) Post-prandial insulin and glucose profiles in T1D patients vs healthy subjects. Both adapted from (Rossetti et al. 2008)

The treatment of T1D lie generally in an intensive therapy consisted of insulin administration by an external pump or by three or more daily insulin injection (Melmed et al. 2016, Chapter 32). The first one involves administering a rapid-acting insulin preparation by CSII (continuous subcutaneous insulin infusion) through a catheter that is usually inserted into the subcutaneous tissues of the anterior abdominal wall. The pump delivers insulin as a preprogramed basal infusion in addition to patient-directed boluses given before meals or snacks or in response to elevations in the blood concentrations outside the desired range. This leads to greater flexibility for the patients compared by the multiple insulin injections. The sensor-augmented-pump (SAP) therapy is also other alternative that add a continuous glucose monitor to the CSII which enables to transmit glucose values to the pump allowing patients and clinicians to monitor treatment. The newest SAP includes the availability of low-glucose suspend features that suspend insulin delivery when glucose levels reach a programmed lower limit or when hypoglycaemia is predicted (Heinemann 2017).

The most serious complication of intensive regimens of insulin replacement is hypoglycaemia, and this is usually the factor that limits patients ability to achieve tight glucose control. This is because patients with T1D have serious defects in mechanism responsible for glucose counterregulation and this is the major underlying reason for the predisposition.

The severity of hypoglycaemia increases with lower glucose concentrations. Nonsevere hypoglycaemia may lead to anxiety, nausea, confusion, blurred vision, and difficulty in speaking; while severe hypoglycaemia is defined as the one that necessitates third party assistance, and if it is not solved, it leads to coma or seizure. Hypoglycaemia is currently a factor of life for patients with type 1 diabetes with an incidence rate of around 2.7 episodes of nonsevere hypoglycaemia per patient per week (Leese et al. 2003). The incidence of severe hypoglycaemia is around 1.3 episodes per patient per year (Omar et al. 2018). The aim of novel therapeutic options is to increase the time spent in normoglycaemia without increasing the risk of hypoglycaemia.

2.3.1 Hypoglycaemia in type 1 diabetes

As said before, hypoglycaemia is the consequence of the mismatch between insulin requirements and exogenous insulin infusion resulting in insulin excess. During hypoglycaemia, while the glucose concentration is decreasing, central and peripheral glucose sensors activate mechanisms to evoke the corresponding neuroendocrine, autonomic and behavioural response (the so-called **counterregulatory response**) (P. E. Cryer 2001). Thus, the hormones involved, which oppose the action of insulin with its own mechanisms, are the counterregulatory hormones. Many hormones are released when blood glucose is lowered, but glucagon, the catecholamines -adrenaline and noradrenaline-, growth hormone, and cortisol are the most important.

In healthy humans, the initial response to prevent a decline in blood glucose concentration is a reduction in insulin secretion which begins while plasma glucose concentration is still in the physiologic range, at approximately 80mg/dL (C. Fanelli et al. 1994). Glucagon and adrenaline are secreted as glucose levels fall slightly below the physiologic range, at approximately 68mg/dL (C. Fanelli et al. 1994; Mitrakou et al. 1991; Schwartz et al. 1987). Besides, there is an activation of the autonomic nervous system which increases the amounts of noradrenaline and adrenaline in the circulation. Beyond the suppression of insulin secretion, glucagon plays the primary role in the hypoglycaemia correction whereas adrenaline has a secondary role (J. Gerich et al. 1979; Rizza et al. 1979). If glucose continues falling down, others counterregulatory factors are also activated: secretion of growth hormone occurs at a plasma glucose threshold of approximately 66mg/dL, and secretion of cortisol at approximately 58mg/dL.

The well-orchested counterregulatory response is managed by the following effects on the glucose metabolism: The decrease in insulin secretion favours the increment of hepatic and renal glucose production besides of the decrease of glucose

utilization by insulin-sensitive tissues (e.g. skeletal muscle). Glucagon acutely raises plasma glucose concentration by stimulating hepatic glucose production via glycogenolysis and gluconeogenesis. Adrenaline increases glycogenolysis and gluconeogenesis at the liver; reduces insulin secretion while increasing glucagon release from the pancreatic islets; reduces glucose uptake and utilization and increases glycolysis by muscle; and increases lypolysis in adipose tissue providing alternative fuel (FFA) and substrate for gluconeogenesis (P. E. Cryer 1994). Cortisol and Growth hormone increase the gluconeogenesis (glucose production from precursors like glycerol, lactate, and amino acids mostly in the liver, although it can occur in the kidneys too) and reduce glucose utilization. Note that glucagon and adrenaline act within minutes to raise plasma glucose concentrations whereas the actions of growth hormone and cortisol to support glucose production and limit glucose utilization are delayed.

Although the primary role of the counterregulatory hormones is on glucose metabolism, any effects on fatty acid (FFA) utilization has an indirect effect on blood glucose. Thus, the increase in plasma adrenaline stimulates lipolysis in adipose tissue and muscle and release FFA which are used as an alternative fuel to glucose, making more glucose available for the central nervous system (brain) which is always glucose dependent.

On the other side, the counterregulatory response to hypoglycaemia is altered in T1D patients (Beall et al. 2012). Firstly, due to exogenous insulin therapy, patients with T1D cannot imitate physiology and reduce systemic insulin levels when blood glucose concentrations begin to decline, unless an artificial pancreas or sensor-augmented pump is used (with the inherent limitations of subcutaneous insulin delivery). Thus, subjects with T1D lack the first line of defence against hypoglycaemia. Secondly, glucagon secretion in response to hypoglycaemia is lost soon after the onset of the disease. And thirdly, the response of adrenaline to a given level of hypoglycaemia is blunted and the glycaemic threshold for its secretion is shifted to lower plasma glucose concentration (about 46mg/dL) (P. E. Cryer 1994), together with reduced autonomic symptoms. The same decrease happens to the glucose activation threshold of Growth hormone and Cortisol. However, these two hormones do not have an immediate role in the recovery from hypoglycaemia. Due to the loss of glucagon secretion and despite blunted response, adrenaline becomes the main actor of the counterregulation

Comparison between the chain of counterregulatory physiological actions in T1D patients and healthy humans are shown in Figure 2.5. It is important to remark that the magnitude of the hormonal response also depends on the exposure to hypoglycaemic episode (Mitrakou et al. 1991). In contrast, this response is attenuated as a result of a previous episode of hypoglycaemia (Heller and I. Macdonald

1996) and even by prolonged exercise the day before hypoglycaemia is produced. Recurrent hypoglycaemias can produce that glycaemia for initiation counterregulatory responses shift to lower plasma glucose concentrations each hypoglycaemic event, and can lead to hypoglycaemia unawareness. This phenomenon is known as hypoglycemia-associated autonomic failure (HAAF) in type 1 diabetes. It was defined by P. E. Cryer 2001 as "recent antecedent iatrogenic hypoglycemia causes both defective glucose counterregulation and hypoglycaemia unawareness, and thus a vicious cycle of recurrent hypoglycaemia". This concept is summarized in Figure 2.6.

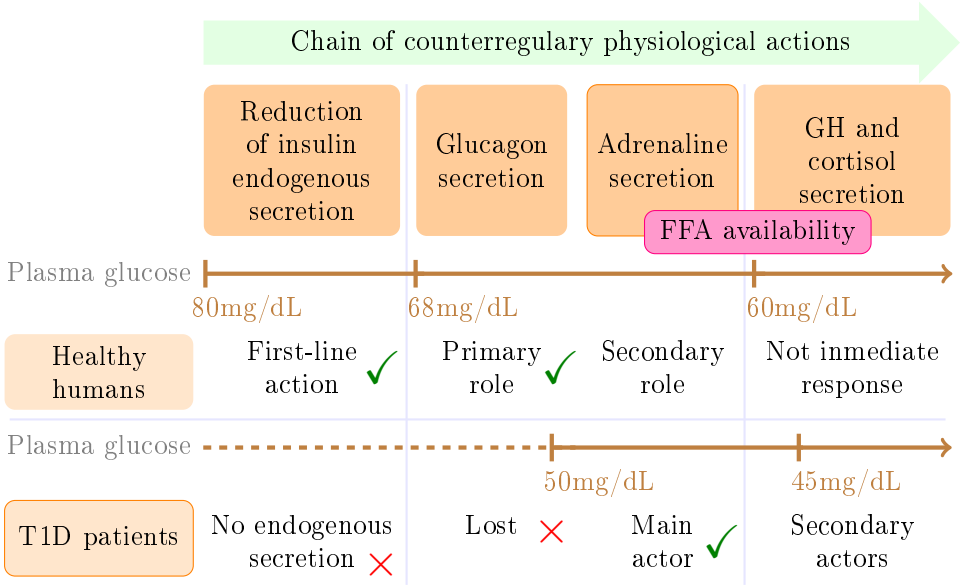

Figure 2.5: Chain of counterregulatory physiological actions.

Despite the relevant contribution of the counterregulatory response to hypoglycaemia to glucose control in T1D, it is often neglected in simulation studies for control strategies design or predictive algorithms for hypoglycaemia prevention.

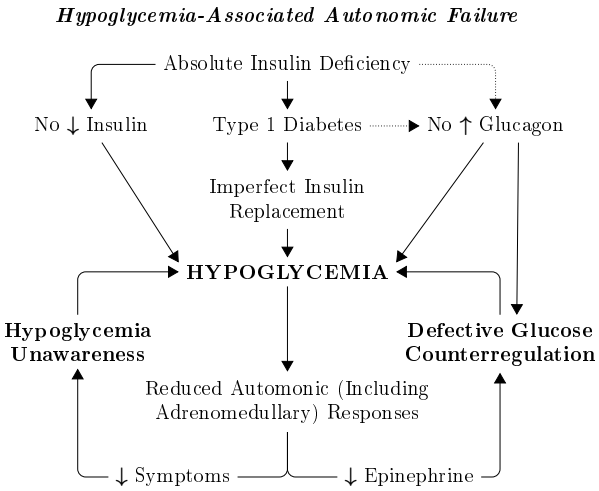

Figure 2.6: Schematic representation of the concept of hypoglycemia-associated autonomic failure in diabetes. Adapted from (P. E. Cryer 2001).

Chapter 3

Artificial Pancreas

This chapter gives a summary on the Artificial Pancreas (AP) research. This introduces the type of control strategies that have been proposed recently in order to face with the challenge of glycaemic control. Likewise, one section is dedicated to go into detail with the control objectives considered in the configuration of the AP proposed. In addition, variability metrics to assess the performance of the control algorithms are presented. Finally, the strategies that have been used in the development of this thesis are more detailed.

3.1 Artificial Pancreas

The AP, or also so-called Automatic Insulin Delivery, is a closed-loop control system that delivers insulin to the patient, who is considered the plant or process of the system. It is composed of three components: (1) a continuous glucose monitoring system (CGM), (2) an infusion pump as the actuator of the system, and (3) a controller that regulates glucose concentrations through automatic adjustments of hormonal delivery based on glucose measurements. The generic control scheme of AP is depicted in Figure 3.1.

CGM is the **glucose sensor** that computes plasma glucose values from a catalytic reaction based on the enzyme glucose oxidase immobilized into a polymeric membrane covering an electrode sensing element. The glucose sensor is inserted through the skin and placed at a depth of 8-12mm in the subcutaneous tissue. It means that the sensor measures glucose in the interstitial fluid rather than

the blood. Therefore, dynamics of glucose transport between plasma and the interstitial fluid introduce a measurement lag about 10 min (Hovorka 2006). This physiological lag time is a factor to consider.

The infusion pump consists of a refillable insulin cartridge, a pump mechanism, and a programmable user interface, which can be used by the patient to establish a basal infusion rate or give a discrete bolus in order to make up for a meal or correct the hyperglycaemia. Since insulin is infused until its peak effect, approximately 80 minutes pass (Hovorka 2006). Therefore, this lag due to the insulin absorption (from the sc tissue into plasma) besides the glucose sensor lag must be taken into account by the controller.

Note that Implantable insulin pumps that infuse insulin into the peritoneum were also proposed by Renard et al. 2010 in an attempt to closely emulate the pancreas. Nevertheless, they were not considered feasible for a commercial AP since they were invasive.

The **controller** is based on a control algorithm that suggests a certain insulin infusion depending on the values provided by the glucose sensors. Particularly, this is the component that has the most interest in this thesis.

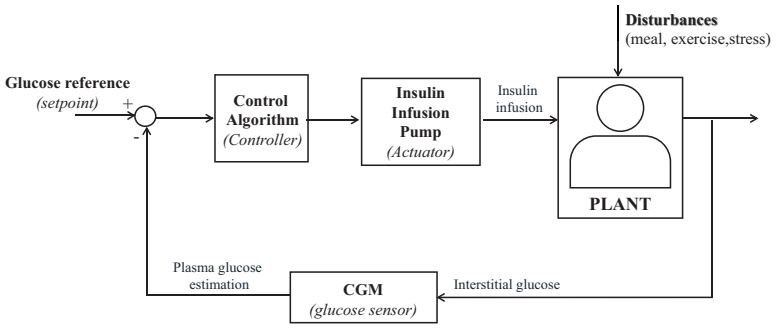

Figure 3.1: Generic control scheme of AP.

Two configurations of the artificial pancreas have been proposed: a single-hormone AP (delivers insulin alone) and a dual-hormone AP (delivers both insulin and glucagon). Figure 3.2 illustrates the control scheme of a generic dual-hormone AP.

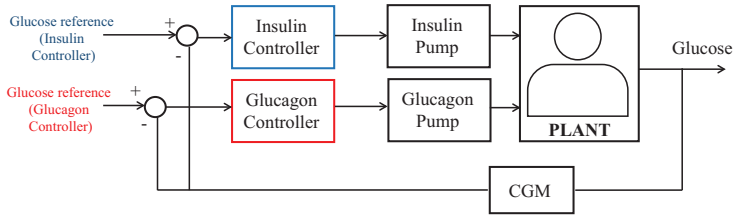

Figure 3.2: Generic control scheme of dual-hormone controller.

3.2 Control algorithms

The ideal closed-loop system would control blood glucose (BG) levels within a target range, preventing postprandial and exercise-induced hypoglycaemia besides of reducing glycaemic variability. Nevertheless, current AP systems still suffer from hypoglycaemia, especially in the late post-prandial state.

A wide range of control algorithms have been proposed for the artificial pancreas, but only a few have been tested experimentally. The algorithms that have been extensively tested fall under three classes of controllers: (1) Proportional-integral-derivative (PID) (Weinzimer et al. 2008; El Youssef et al. 2011), (2) model predictive control (MPC) (El-Khatib et al. 2010; Gondhalekar et al. 2015a) and, (3) fuzzy logic Control (FL) (Atlas et al. 2010; Mauseth et al. 2013; Capel et al. 2014; Dovc et al. 2017).

Besides, controllers with pilot studies or tested only in simulations are H_∞ controllers (P. Colmegna et al. 2014), sliding-mode controllers (Abu-Rmileh et al. 2010), neural-network controllers (Trajanoski and Wach 1998),linear parameter-varying controllers (Sánchez Peña and Ghersin 2010; P.H. Colmegna and R.S. Sánchez-Peña 2014), switched LPV controllers (P.H. Colmegna et al. 2016b; P.H. Colmegna et al. 2016a), adaptative controllers (see Cinar and Turksoy 2018, and robust controllers (Kovács et al. 2008).

PID controllers have been linked to the dynamics of beta cells insulin secretion in response to varying glucose levels in healthy individuals. They tried to adapt to the changes in insulin sensitivity or rates of endogenous appearance without steady-state errors in fasting glucose. Steil et al. 2003 presented an algorithm to insulin

delivery predicted by a PID controller. From this configuration, the next proposal was the PID with a modification to include the feedback of a model-predicted insulin profile (Steil et al. 2006). This Insulin feedback (IFB) tried to reproduce better the functioning beta cell, which reduces insulin secretion as plasma insulin levels increase. The effect of insulin feedback on closed loop was assessed in (Steil et al. 2011) particularly in the break fast-meal profile, after the good overnight performance of PID controller was demonstrated in (Steil et al. 2006). Nevertheless, the occurrence of hypoglycaemia 2-3 hours post meals required rescue glucose administration. In order to reduce the frequency of postprandial hypoglycaemia associated with PID algorithms, a hybrid system in which basal insulin is raised prior to the beginning of an intake to prevent or reduce the aggressive increase in insulin delivery due to the fast rise of BG after meal was developed (Weinzimer et al. 2008). (Ruiz et al. 2012) reported that PID + IFB markedly reduced the occurrence of hypoglycaemia without increasing meal-related glucose excursions. (percentage in hypoglycaemia of 9% vs 2% during 24h studies without exercise, PID and PID+IFB respectively). Therefore, an important underlying problem of the PID strategy is the difficulty in hypoglycaemia prevention associated with an inaccurate or overestimated insulin dose. In that context, a predictive hypoglycaemia alarm by means of hypoglycaemia models incorporation is advantageous since the alarm suspends the insulin delivery and can markedly reduce the occurrence of moderate hypoglycaemia as (Buckingham et al. 2009) showed. Following the same purpose, (Revert et al. 2013) developed a safety algorithm for glucose control based on the PID controller with the addition of a IOB restriction by means of sliding mode reference conditioning (SMRC) method and the IOB estimation. The results in simulation showed a significant reduction of time in hypoglycaemia (7% vs 15.75%, in scenarios of 16hours with three meals). This controller was tested in a clinical trial and resulted consistent in the postprandial control without an increase of the time in hypoglycaemia (Rossetti et al. 2017).

On the other hand, MPC is based on prediction of glucose dynamics using a model of the patient metabolic system; besides, it is able to predict the effects of meals and can introduce constraints on insulin delivery rate and glucose values. Specifically, it solves a finite-horizon optimization problem every 5-15 min to obtain an optimal insulin delivery profile that minimizes an objective function. The objective function consist of 1) term that penalizes the mismatch between future model-predicted glucose concentration and the target glucose level, 2) a term that penalizes the control signal, and 3) a term that penalized the mismatch between the model-predicted glucose concentration and the target glucose level. The controller can handle meals and meal-time insulin boluses in a straightforward manner. If the patients have a meal or deliver an insulin bolus, the algorithm will be updated before the next cycle. The meal and the bolus will then change the

predicted future glucose levels and affect the optimal insulin profile (Cobelli et al. 2009).

Several configuration of MPC controllers are found in literature: among others, Patek et al. 2007 propose a linear MPC where a linear quadratic Gaussian based-feedback control algorithm was implemented, with the incorporation of a Kalman filter used to estimate different metabolic states of the patient based on subject-specific parameters. Results in-sillico were good (0.8% of time in hypoglycaemia), but the duration of the simulation was one-day simulation, and exercise and inter-day variability were not considered. Later, a non-linear state feedback MPC scheme was proposed by Magni et al. 2008 and compared to open loop performance in overnight and post-prandial studies. The improvement in hypoglycaemia events with the MPC was during the night (1.63 vs 0.13 events), but there was not any difference during the postprandial period (Clarke et al. 2009). In order to deal with the insulin overdose, Ellingsen et al. 2009 suggested an insulin on board (IOB)-MPC, which uses the IOB as a safety constraint based on IOB estimations; the IOB-MPC showed relatively robust results in silico. Percentage of hypoglycaemia was 0.75% and 18.6%, MPC with and without IOB constraint respectively, in a 24 hours study with three meals.

Grosman et al. 2010 presented a control algorithm based on zone-MPC that uses mapped-input data, it is adjusted automatically by linear difference personalized models, and the control variable objective is expressed as zone. Results showed a reduction of glycaemic variability. Gondhalekar et al. 2013 proposed the "periodic zone model predictive control" (PZMPC) strategy that employs periodically time-dependent blood glucose output target zones and enforces periodically time-dependent insulin input constraints in order to modulate its behaviour based on the time of the day. Results showed improvements in nocturnal hypoglycaemia.

Gondhalekar et al. 2015b included a velocity weighting mechanism in the MPC cost function, such that a predicted zone excursion is penalized taking into account both its value and also the rate of change of the blood glucose trajectory. (Lee et al. 2016) used and exponential-quadratic shaping for the cost function utilized within an MPC block. It showed improved performance compared to previous controllers that were validated in clinical settings. In (El Hachimi et al. 2017), a MPC configuration was proposed with a new formulation of the cost function which includes an exponential asymmetric weighting of the glucose excursions in order to accelerate the speed of control of AP and tackle the nonlinearity of the control problem. In addition, other recent proposal for the MPC has been to model the unavoidable uncertainty in probabilistic terms by means of Bayesian network (Lackinger et al. 2017). Recently, the proposal of Renard et al. 2016 showed percentage of time in hypoglycaemia of 2.1% and 3.2%, AP vs SAP.

In contrast, FL allows the development of a fuzzy controller without any patient model by means of fuzzy rules inclusion. In this way, the controller rules are provided by "experts" with knowledge of the system at hand and by medical expertise (L. Wang 1997). In addition, multiple inputs and multiple outputs can be included in a natural way. Different groups have proposed an AP based on fuzzy-controllers (Nimri et al. 2012; Mauseth et al. 2013; Mauseth et al. 2015) and insulin limitation based on predictions of IOB are also applied in FL systems in order to avoid insulin overdose (Kircher et al. 2015).

As seen above, there is a significant number of approaches suggested with relevant results. Nevertheless the hypoglycaemia due to challenging situations, such as postprandial period or exercise, continues being the most important limitation of all of them.

3.3 Challenges of Artificial Pancreas controllers

The daily use of the AP gives ambitious challenges to the controller performance. These challenges are summarized in Figure 3.3. The most important challenges for the closed loop are those that are inherent to human physiology: the hypoglycaemia avoidance and the robustness against glycaemic variability. The insulin delivered by the pump cannot be removed from the body once it is there; thus, the controller should not be aggressive in excess. Additionally, insulin sensitivity varies (Scheiner and Boyer 2005) due to factors such as time of day, stress, and exercise; glycaemia is also affected differently depending on the meal composition; and, temperature along with other factors have also effect on the glycaemia variation. Thus, controllers must be sufficiently robust to these variations. Furthermore, the significant dynamic lag due to the insulin subcutaneous route poses other challenge to glucose control since the insulin effect cannot be easily counteracted by the controller once insulin is infused.

For these reasons, it should take into account the insulin on board or follow other control strategies in order to prevent the glucose descent towards hypoglycaemic levels. Hypoglycaemia models that allow the prediction of hypoglycaemic events and a dual-hormone control approach which push the glucose concentration up in critical situations could be the keys in the optimal glucose control in T1D patients.

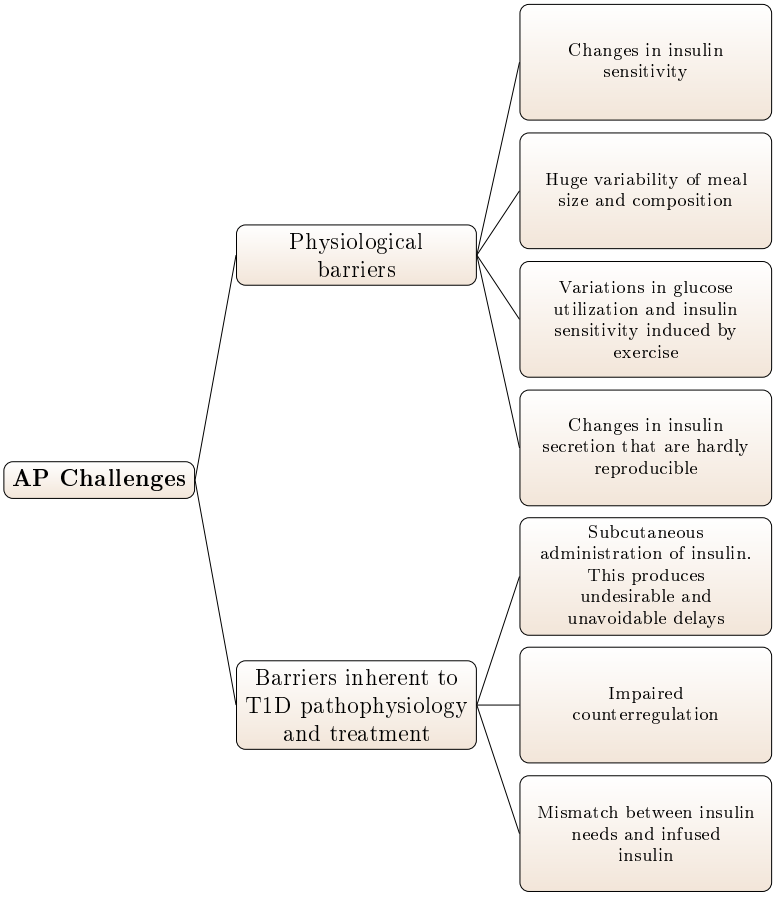

Figure 3.3: Challenges of Artificial Pancreas controllers

3.3.1 Control strategies

In order to face with the above explained problems, two different perspectives have been addressed, not mutually-exclusive: (1) The incorporation of mechanisms for insulin on board (IOB) limitation (Ellingsen et al. 2009; Revert et al. 2013; R. Sánchez-Peña et al. 2017; R. Sánchez-Peña et al. 2018; P. Colmegna et al. 2018a); and (2) the introduction of dual-hormone artificial pancreas systems which infuse glucagon as counterregulatory action to increase plasma glucose (El-Khatib et al. 2010; Castle et al. 2010; Haidar et al. 2013; Herrero et al. 2012).

Furthermore, it is worth noting that several groups have also proposed configurations which include the insulin estimation in order to avoid the controller over-actuation because of slow insulin absorption (even rapid-acting insulin analogues are slower in comparison with physiological prandial insulin secretion) also increase the risk of insulin stacking, particularly in the early post-meal periods. This is so-called insulin feedback configuration, which was originally proposed by (Steil et al. 2011), and it has been incorporated to some control schemes based on PID (Revert et al. 2013), MPC (Ellingsen et al. 2009), and FL (Kircher et al. 2015) to improve the controller performance.

The IFB algorithm emulates the physiological reduction of insulin production with falling glucose levels. This is achieved through inhibition of insulin infusion as plasma insulin levels are estimated to increase. The prediction of plasma insulin is fed on the forward delivery of insulin of the control algorithms. The action suggested by the controller is limited by an action proportional to the increment of predicted plasma insulin concentration from the basal insulin concentration. Thus, the IFB do not have effect on the total insulin action during basal (stationary) conditions.

In order to avoid the over-insulination by means of IOB estimation, other strategy is proposed in literature. This consists in the inclusion of a safety auxiliary feedback element based on SMRC technique (Revert et al. 2013). The formulation related to this technique is detailed due to its relevance in the development of this thesis.

SMRC uses the modulation of glucose targets as a new degree of freedom for glucose regulation. A prediction of IOB, $IOB(t)$, drives a switching function $\sigma_{sm}(t)$, triggering a discontinuous signal $\omega(t)$ that, after a filtering step, sums to the standard glucose target/reference. Upper and lower limits for IOB can be defined if desired. The upper limit of IOB definition promote an increase in the glucose target value resulting in a decrease in the insulin delivery. Although the controller response is in favour of insulin delivery reduction, the opposite effect could be when a lower limit of IOB is defined. SMRC originates from concepts of invariance control and sliding regimes as a transitional mode of operation. In contrast to the conventional sliding mode control, the aim here is not evolving toward the equilibrium point. Only when the system reaches a given sliding surface separating the space into feasible and unfeasible regions (characterized by the constraint on the IOB) is the sliding regime stabilized by conditioning the reference until the system returns to the feasible region.

Then, given an upper limit on IOB (or time varying $\overline{IOB}(t)$) and the system state $x(t)$, the set

$$\Sigma = \left\{ x(t) | IOB(t) \leq \overline{IOB}(t) \right\} \tag{3.1}$$

is invariant for a discontinuing signal $\omega(t)$ of the form

$$\omega(t) = \begin{cases} \omega^{+} & if\ \sigma_{SM}(t) > 0 \\ 0 & otherwise \end{cases} \tag{3.2}$$

with $\omega^{+} > 0$ large enough and

$$\sigma_{SM}(t) = IOB(t) - \overline{IOB}(t) + \sum_{i=1}^{l-1} \tau_i \left(IOB(t)^i - \overline{IOB}(t)^i \right) \tag{3.3}$$

where l is the relative degree between the output $IOB(t)$ and the input $\omega(t)$, superscript i denotes i-th derivative, and τ_i are constant gains.

The first order filter

$$\frac{dG_{RF}}{dt} = -\alpha G_{RF}(t) + \alpha \left(G_R(t) + \omega(t) \right) \tag{3.4}$$

keeps all signals in the control loop smooth, where $G_{RF}(t)$ is the modulated glucose target fed to the controller, $G_R(t)$ is the standard glucose target, and α defines the filter cut-off frequency. Stability of the system is guaranteed, since SMRC loop acts only on the setpoint, which is always bounded.

Relative degree l is determined by the relative degree of the filter (Dalla Man et al. 2014) and the relative degree of the IOB predictor. The IOB estimation was obtained from the Hovorka subcutaneous insulin pharmacokinetic model (Hovorka et al. 2004):

$$\frac{dS_1(t)}{dt} = I(t) - \frac{1}{t_{maxI}} S_1(t) \tag{3.5}$$

$$\frac{dS_2(t)}{dt} = \frac{1}{t_{maxI}} (S_1(t) - S_2(t)). \tag{3.6}$$

Then, the $IOB(t)$ was defined by:

$$IOB(t) = S_1(t) + S_2(t). \tag{3.7}$$

The equations for the IOB estimation (3.5), (3.6), and (3.7) have a relative degree of one, giving rise to a total relative degree of $l = 2$. According to the interest

of limiting the Insulin delivery, $\overline{IOB}(t)$ must be considered and the switching function (3.3) is

$$\sigma_{SM}(t) = IOB(t) - \overline{IOB}(t) + \tau \left(\frac{dIOB(t)}{dt} - \frac{d\overline{IOB}(t)}{dt} \right). \tag{3.8}$$

The switching function $\sigma_{SM}(t)$ will be positive when $IOB(t) + \tau\,(dIOB(t)/dt)$ is higher than the $\overline{IOB}(t)$. How close IOB is allowed to approach its limit will depend on the IOB tend, weighted by the parameter τ. This defines a threshold on IOB, which corresponds to $\overline{IOB} - \tau\,(dIOB(t)/dt)$. A rapidly changing IOB will lower this threshold, compared to an IOB slowly approaching the limit. When IOB goes beyond this threshold, an increment on the glucose setpoint is triggered, resulted by the discontinuous signal $\omega(t)$ and amounting ω^{+}, after a transient state given by the filter. As a reaction to the new glucose reference, the controller will reduce the insulin delivery, impeding violation of the IOB limit. The glucose reference will return to its original value after the transient state imposed by the filter, when IOB returns below the threshold, in which case $\omega(t) = 0$.

The IOB limitation with SMRC was evaluated in a clinical study (Rossetti et al. 2017), where it showed an improvement of postprandial control with a significant decrement of postprandial peak and increment of the time in range; nevertheless, hypoglycaemia continued being the main weakness.

Dual-hormone approach

Current dual-hormone systems are based on two control loops with an insulin controller and a glucagon controller. The latter is activated in certain circumstances with the goal of triggering a counterregulatory control action to mitigate hypoglycaemia. It has been commonly thought that dual-hormone systems may allow being more aggressive with the insulin infusion compared to a single hormone system since it is possible to modulate the excessive insulin action with the glucagon infusion. However, recent studies demonstrate that the excess of insulinemia reduces the glucagon effectiveness and have negative effect on hypoglycaemia incidence (El Youssef et al. 2014).

The viability of a dual-hormone system in humans was demonstrated in (El-Khatib et al. 2010). The system was based on an MPC controller for insulin infusion and a PD controller for the glucagon infusion which was only activated when glycaemia was lower than a given target threshold or close to this threshold with a fast falling down. Similar structure has been used in other groups for glucagon and insulin infusion. As an example, a Fading Memory Proportional Derivative

(FMPD) algorithm for the insulin and glucagon action with different parameters and target glucose in each hormone was presented in (Ward et al. 2008). However, in (Haidar et al. 2013), an MPC controller was used for the insulin delivery that takes into account the glucagon on board, whereas glucagon is delivered following heuristic rules. Other approach available in literature is the use of a bio-inspired controller for the insulin and a PD controller for the glucagon (Herrero et al. 2012).

Current clinical trials have not demonstrated a clear superiority of the dual-hormone systems compared to single-hormone ones since the hypoglycaemia incidence is similar in both. Nevertheless, single and dual- hormone systems are clearly better than the conventional therapy (P. A. Bakhtiani et al. 2013; Weisman et al. 2017). Comparisons between the single- and dual-hormone approach have been carried out by several authors. During nocturnal control, the single-hormone systems is able to perform an efficient control (Haidar et al. 2015). However, the dual-hormone system showed superior results during studies with exercise (Taleb et al. 2016), the percentage time in hypoglycaemia ($<$72mg/dL) was 0% vs. 11%, and the percentage of time in range (72-180 mg/dL) was 100% vs 71.4%. Nevertheless, this good point has not been proved in outpatient studies (Haidar et al. 2017) since there were not significant differences between the hypoglycaemia events (6 events in dual-hormone configuration vs. 14 events in single-hormone system), but authors proposed larger studies to assess properly the differences due to the complexity of dual-hormone systems. Recently, (Castle et al. 2018) have demonstrated that the incorporation of glucagon delivery to the closed-loop system with automatic exercise detection reduces hypoglycemia after exercise.

Physiologically, in pancreatic islets (contains a network of cells responsible for different hormonal secretion), there is communication between the beta and alpha cells, responsible for the insulin and glucagon secretion, respectively (Jain and Lammert 2009). In (B. A. Cooperberg and P. E. Cryer 2009) it is demonstrated that an increment in plasma and intra-islets insulin levels produces a suppression in glucagon secretion, and a decrement in insulin levels with low plasma glucose concentrations stimulate glucagon secretion. Furthermore, authors in (Rodriguez-Diaz et al. 2011a) showed that the alpha cell anticipates the possible hyperglycaemic rebounds due to the glucagon secretion by means of beta cell stimulation, confirming the tight paracrine communication in both directions. Thus, coordination between the secretion of both hormones is a relevant factor to take into account in the glycaemic control. In a recent work, a coordinated biologically inspired glucose control strategy was presented (Herrero et al. 2017), achieving in silico a reduction of hyperglycaemia without increasing hypoglycaemia when compared to its non-coordinated configuration (1.79% of time below 70mg/dL).

However efficient hypoglycaemia mitigation in dual-hormone systems is still an open issue.

Of note one of barriers to implementation of the dual-hormone controllers was the unavailability of stable glucagon formulations (the available subcutaneous glucagon formulation was only stable for 24 hours). Fortunately, a novel stable peptide analogue of human glucagon has been recently developed (Dasiglucagon is the proposed international non-proprietary name) (Hövelmann et al. 2018), allowing its use in pump delivery devices in the clinical outpatient setting.

In order to improve AP performance, Chapter 7 shows the dual-hormone control algorithm we have developed in this thesis. The controller is based on a collaborative parallel control formulation for multiple-input single output processes.

3.4 Control targets

3.4.1 Hypoglycaemia avoidance

Hypoglycaemia prevention remains one area that can still be improved since a majority of studies reported at least one episode during the closed-loop evaluation. Moreover single and dual hormone AP have shown reduction in time spent in hypoglycaemia compared with the conventional treatment (SAP, multiple insulin injections), but have not yet been able to eradicate it completely. Therefore, a study of the causes that promote hypoglycaemia and its effects, besides of a better understanding of the factors that determine hepatic glucagon sensitivity in T1D and the mechanisms involved in hypoglycaemia are needed. There are many factors related to the Hypoglycaemia events and, thus, they must be considered in order to face with this problem.

During exercise, especially aerobic exercise, blood glucose concentrations often fall rapidly, increasing the risk of hypoglycaemia (Children Network (DirecNet) Study Group 2006). Many factors affect the variations in glucose concentrations during exercise: type, intensity, and duration of exercise are prominent factors; but starting glucose level, time since last insulin bolus, and insulin injection site are important factors too (Riddell et al. 2015). The risk of hypoglycaemia increases during exercise due to the rapid utilization of glucose by muscle and the short-term improvement in the insulin sensitivity. Additionally, the latter prolongs also several hours after exercise increasing the risk for late evening and nocturnal hypoglycaemia (Maran et al. 2010; Iscoe and Riddell 2011). Different types of exercise (resistance vs. aerobic) can have contrasting effects on the duration

and severity of exercise-induced hypoglycaemia and post-exercise hypoglycaemia (Yardley et al. 2012).

Nowadays, patients use several strategies in order to prevent exercise-induced hypoglycaemia as suppression of basal insulin (Diabetes Research in Children Network (DirecNet) Study Group et al. 2006), ingestion of carbohydrates (Riddell et al. 1999), or, reduction of pre-meal insulin dose (Rabasa-Lhoret et al. 2001); nevertheless, the hypoglycaemia problem is not yet solved, and it continues to be common during exercise. Other factor to consider is the mental stress and sickness affect glucose control through peripheral and hepatic insulin resistance leading to hypoglycaemia.

Finally, it is also to highlight that the hypoglycaemia affect the relationship between interstitial glucose and plasma glucose concentrations (Moscardo et al. 2018). Since sensors measure glucose concentration in the interstitial fluid, control action calculations might be affected.

3.4.2 Glycaemic variability reduction

Glucose variability describes within-day and between-day fluctuations in glucose concentration and is elevated in people with type 1 compared with people with healthy glucose tolerance.

Clinical observations in T1D suggested that glucose profiles can greatly differ even among people with glycated hemoglobin (HbA1c) values approaching target, defining that glucose variability is an important component of dysglycaemia (C. Wang et al. 2012). Indeed, increased glycaemic variability is also associated with a higher incidence of severe hypoglycaemia in patients with T1D (Kovatchev and Cobelli 2016). Reduction of glucose variability to address the risk of hypo- and hyperglycaemia is a target in diabetes treatment; besides, variability has been also associated with macro- and microvascular complications (Quagliaro et al. 2005; Schiekofer et al. 2003; Monnier et al. 2006; Ali et al. 2008), neuropathy (Krinsley 2008), retinopathy (Kilpatrick et al. 2007), atherosclerosis (Rodbard 2009a), kidney disease (Hill et al. 2011), cardiovascular disease (Health Research (JCHR) 2018), and impairment of cognitive function (Whitelaw et al. 2011).

- Variability within the same patient (Intrapatient variability).

Insulin sensitivity within the same patient may exhibit random day-to-day variations ($\pm 30\%$) depending on the stress level, exercise level, and food intake (El Youssef et al. 2011; Taplin et al. 2010; Pańkowska et al. 2012; Swan et al. 2009; Cavallo et al. 2001; Burstein et al. 1985). For example, the lower insulin sensitivity

after exercise event (Taplin et al. 2010), and the insulin sensitivity changes due to the sickness/stress (El Youssef et al. 2011) or menstrual cycles (Trout et al. 2007).

Other source of variability is the meal absorption since meals with identical carbohydrates content but different fat and protein contents show different absorption profiles (Elleri et al. 2013). It means that the calculated bolus taking into account the amount of carbohydrates could not have the same effect on the glucose levels in different meals with same carbohydrates amount.

In addition, variability of the pharmacokinetics of insulin formulations after its injection in the subcutaneous tissue can contribute to inter day variability of plasma insulin and therefore glucose levels.

- Variability between patients.

Insulin sensitivity vary significantly between patients. Basal insulin needs can be as low as 0.2U/hours in young children and as high as 2.0U/hour in obese adults. Similarly, total daily insulin needs can vary between 0.3U/kg in insulin-sensitive patients to 1.3U/Kg in insulin resistant patients (Haidar 2016). Most controllers are thus designed so that their gain is individualized using clinical variables such as total daily insulin as a surrogate of insulin sensitivity (El Youssef et al. 2011). For instance, PID are individualized by their coefficients (Steil et al. 2011; El Youssef et al. 2011) and model predictive controllers are individualized through either the weighting parameters of the objective function or the models used for predictions (El-Khatib et al. 2010; Toffanin et al. 2013; Harvey et al. 2014; Haidar 2012). Adaptive algorithms adjust and individualize the controllers gain in real time.

As commented before, for intrapatient variability, pharmacokinetics of insulin formulation affects also the variability between patients. For instance, time-to-peak of insulin absorption varies between individuals by as much as fivefold and can be anywhere between 30 and 150 min. Absorption time cannot be predicted reliably from clinical variables but may be estimated in real time by means of the insulin-glucose data relationship (Haidar 2012; Hovorka et al. 2010; Mazor et al. 1998).

Other factors obviously related to the variability are, among others, physical activity (varying types and intensities), meals (varying sizes and composition), health status, and biological factors (puberty, menstrual cycles, pregnancy, and menopause).

Alternative classification of glycaemic variability factors is shown in (Kudva et al. 2014), where the physiologic factors that could affect the glycaemic variability are grouped by time scale considerations. This classification is shown below.

- Time scale of minutes to hours: mixed-meals with different macronutrient composition; gastrointestinal dysmotility, type of physical activity, alcohol ingestion, medication effects.
- Time scale of days: menstruation, workdays vs nonwork days, working day vs nonwork days, shift workers.
- Time scale of months: weight gain or loss, physical training program, closed-loop use, kidney function changes.
- Life cycle-related issues: puberty, menstruation, pregnancy, trimester of pregnancy, menopause, postmenopausal.

It is clear that a good glycaemic control in the context of the AP can be achieved only if the control action is robust enough to compensate for intra- and between patients variability.

Glycaemic variability metrics

Currently available continuous glucose monitoring (CGM) devices provide glucose data every 5 minutes and from these data, multiple indices or glycaemic variability metrics can be calculated. In order to quantify glucose variability, several authors have defined indicators. Nevertheless, there is not a clear consensus on the gold-standard method to measure glucose variability in clinical practice and research. The easiest way to get an impression of the glucose variability in an individual patient is to calculate the SD of glucose measurements and/or the coefficient of variation. However, in this way, a lot of useful information about glycaemic performance can be lost.

The indicators that can be founded in literature are listed below and their mathematical formulations are available in appendix A. Introducing them is essential to carry out the first objective of this thesis.

- *Standard deviation (SD), mean glucose and coefficient of variation (CV).* SD is an index of dispersion of data around mean blood glucose. It was the simplest approach for the evaluation of glucose variability, beyond the simple determination of mean blood glucose (Whitelaw et al. 2011).

- *Mean Amplitude of Glucose Excursion (MAGE).* MAGE is the mean of the daily glucose excursions that exceed the SD measured over the 24h period (Hill et al. 2007).
- *Continuous overlapping net glycaemic action over n-hour period (CONGAn).* This is an indicatior of within-day glucose variability. It calculates the difference between current observation and observation in the previous n hours. The higher CONGA value, the greater the glycaemic excursion (McDonnell et al. 2005).
- *Mean of Daily Differences (MODD).* MODD quantifies the phenomenon of between-day variability from CGM readings. It is the mean of the absolute difference between glucose values taken on two consecutive days at the same time (Molnar et al. 1972).
- *M-value of Schlichtkrull (M-VALUE).* This metrics measures the stability of glucose excursions in comparison with an ideal glucose value (Service 2013).
- *J-INDEX.* The J-INDEX is an indicator that correct the SD for mean blood glucose (Service 2013).
- *Mean Absolute Glucose (MAG).* MAG assesses short-term within-day temporal variability (Service 2013).
- *Absolute Average rate of change (AARC)* (Whitelaw et al. 2011).
- *Lability Index (LI).* It is also known as Hypo Index. It assesses glycaemic lability (Ryan et al. 2004).
- *Glycaemic Risk Assessment Diabetes Equation (GRADE).* It is the mean approximation of the results from a function relating risk to glycaemia (Hill et al. 2007). The GRADE formula generated by this process allowed the assessment of each discrete point in a glycaemic profile. The contribution of hypoglycaemia, euglycaemia and hyperglycaemia to the GRADE score is expressed as percentages: %GRADE-hypo, %GRADE-eu, %GRADE-hyper.
- *Risk index (RI), Low blood glucose index (LBGI), and High blood glucose index (HBGI).* These parameters were developed by Kovatchev et al. 2006. They are a logarithmic transformation of the blood glucose data. LBGI and HBGI represent the frequency and extent of low and high blood glucose measurements, respectively. Higher LBGI and HBGI values indicate more frequent or more extreme hypo- and hyperglycaemia, respectively.

- *Average Daily Risk Range (ADRR).* It is the average sum of the HBGI for maximum glucose plus the LBGI for minimum glucose for each day. It is equally sensitive to hypoglycaemic and hyperglycaemic blood glucose (Kovatchev et al. 2006).

Newer metrics for the assessment of glycaemic control based on CGM data have been defined for use in clinical practice and in the research setting. They are:

- *Index of Glycaemic Control (IGC).* This metrics combines the results from a Hyperglycaemia Index and a Hypoglycaemia Index (Rodbard 2009a; Rodbard 2009b).
- *Personal Glycaemic State (PGS).* It evaluates four dimensions of glycaemic control: mean glucose, glycaemic variability, percent time in range and frequency and severity of hypoglycaemia (Hirsch et al. 2017).
- *Glycaemic Variability Percentage (GVP).* It is based on the length of the continuous glucose monitoring temporal trace normalized to the duration under evaluation (Hirsch et al. 2017).

The availability of an excessive number of variability indices leads to an increase of the existing confusion surrounding this important issue. Interrelationship between them must be assessed. Likewise, the vulnerability faced with inter-, intra- variability must be studied in order to find the best and rigourous indicator. Finally, a differentiation between glucose variability metrics and quality control indices will be also useful in the analysis of controllers performance.

Chapter 4

Models of glucose regulation in type 1 diabetes

One of the main problems for glucose control is the insufficient accuracy of existing mathematical models for describing the physiology of the glucoregulatory system. In this chapter the modelling and simulation context for the artificial pancreas will be reviewed, and the state of the art of mathematical models in literature will be described. The models described in detail are the ones which are considered in this thesis.

4.1 Mathematical representation of glucoregulation

Models that describe dynamics of glucose regulation are crucial in the context of the AP. These are generally used for three main purposes: (1) to support physiology studies, (2) to perform simulations, and (3) as part of the closed-loop controllers.

1. Models to support physiology studies.

These models are usually **minimal models**. It means that the models are parsimonious descriptions of the key components of the system functionality and are able to measure crucial processes of glucose metabolism, thus also improving our understanding of the system. Bergman et al. 1981 introduced the minimal model method to describe an IVGTT (intravenous glucose tolerance test) in order to

analyse the glucose metabolism by means of insulin and glucose measurements. From these measurements and with that Minimal Model, an index of insulin action, called insulin sensitivity, was obtained.

The features of the minimal models are (Cobelli et al. 2009): 1) physiology based; 2) parameters estimated with reasonable precision; 3) parameter values within physiologically plausible ranges; and, 4) system dynamics described with the smallest number of identifiable parameters. Moreover, a good minimal model is a small-scale one because it is not necessary that every known substrate or hormone was included in the model because the macro-level response of the system would be relatively insensitive to many micro-level relationships.

The most popular model is Bergman's minimal model, which is widely used to estimate insulin sensitivity (Bergman et al. 1979). Nevertheless, other models have been developed to assess the beta-cell responsiveness (Hovorka et al. 1998) and glucose effectiveness (Vicini et al. 1997) and, to estimate the time-varying metabolic functions such as endogenous glucose production and rate of glucose consumption (Steele et al. 1968; Radziuk et al. 1978; Mari 1992), among others.

2. Models for simulation.

Models used for simulations are often complex, physiologically inspired, nonlinear, high order; these adopt the compartmental approach, and are built from smaller submodels such as glucose-kinetics, insulin-action, insulin-absorption, and meal-absorption submodels. Those are **maximal models**. They are comprehensive descriptions that attempt to implement fully the body of knowledge about the system. This class of models cannot be identified easily, generally.

It is important to note that the large-scale models are very useful as a research tool. The Dalla Man model (Dalla Man et al. 2007b) is one of the most widely used maximal model in the AP community. Indeed, it is the kernel of the UVA-Padova T1D Simulator (Dalla Man et al. 2014), a simulation tool for the evaluation of glucose controllers accepted by the FDA as a substitute for animals trials. Hovorka Model (Hovorka et al. 2004), (Wilinska et al. 2010) is the other one popular maximal model, which considers the meal component and includes carbohydrate digestion and absorption. The Identifiable Virtual Patient Model (S. S. Kanderian et al. 2012) is other example.

3. Models for control systems.

Glucose models have also constituted an integral part of the closed-loop predictive glucose controllers. Control-oriented models are generally simplifications of

simulation models and are considered at the controller design phase since most of the well-established theory of control law design accommodates only simpler models. That is, although control-oriented models have to represent the underlying dynamics to some degree, they are mainly obtained for synthesis purposes and have a much simpler mathematical formulation (P. Colmegna et al. 2018b). These models can be characterized as being parametric low-order models such as those used in physiology studies (Parker and Doyle III 2001) or proposed in (van Heusden et al. 2012; P. Colmegna et al. 2018b), parametric high-order models but with a low number of free parameters to allow real-time estimation, and non-parametric models, such ARMAX models and impulse response models. Most of these models were derived from existing ones that were originally developed for simulations (Sorensen 1985) or physiological studies (Parker and Doyle III 2001) but some models were derived specifically to be used in closed-loop controllers (Fabietti et al. 2006).

Regardless of the different purpose of the model, modelling of the glucose regulation for any subcutaneous insulin therapy (Single-hormone AP) must involve the following three subprocess or components:

- A subcutaneous insulin pharmacokinetic model describing how insulin appears in blood after subcutaneous infusion.
- An insulin action model describing how plasma insulin concentration exerts its effect on glucose metabolism.
- A glucose metabolism model describing the comprehensive effect of insulin on plasma glucose concentration.

In the case of dual-hormone therapy, the following four additional subprocesses must be also considered:

- A subcutaneous glucagon pharmacokinetic model describing how glucagon appears in blood after subcutaneous infusion.
- A glucagon action model describing how plasma glucagon concentration exerts its effect on glucose metabolism.
- A glucose metabolism model describing the comprehensive effect of glucagon on plasma glucose concentration.
- Model of the interaction between insulin and glucagon.

4.2 Simulation models for in silico testing of control algorithms in T1D

The main uses of maximal models and simulation in AP are: (1) to develop and test theories about insulin signalling (e.g. Sedaghat et al. 2002) and secretion (e.g. Grodsky 1972 and Cerasi et al. 1974); (2) with educational purpose, interacting with the models, clinicians and patients gain understanding of glucose regulation (e.g. AIDA educational package (Lehmann et al. 1993), KADIS system (Rutscher et al. 1994), and DIAS (Andreassen et al. 1994)); (3) to use as a test beds for examining the empirical validity of models intended for clinical applications, i.e. the substitution of animal trial with in silico experiments in T1D (Cobelli et al. 2014). Of special interest in the context of this thesis is the simulator used as a validation tool for assessing the control algorithms, especially the representation of hypoglycaemia, whose mitigation is the main target of the to-be-developed controllers.

In metabolism and diabetes, there are situations where in silico experiments with complex models could be of enormous value. In fact, it is often not possible, appropriate, convenient, or desirable to perform an experiment on the glucose system, because it cannot be done at all, or it is too difficult, too dangerous, or unethical. In such cases, simulation offers an alternative way of in silico experimenting on the systems. Indeed, simulation models have been published and already used to examine various aspects of diabetes control (for assessing different control algorithms and different insulin infusion routes). Nevertheless, it is important to mention that good in silico performance of a control algorithm does not guarantee in vivo performance.

Algorithms for closed-loop insulin delivery in subjects with type 1 diabetes can be designed and tuned empirically, and evaluated during clinical testing. However, a validated simulation model of glucose regulation in type 1 diabetes accelerates the design and the evaluation process. The recent simulators are built from smaller already existing submodels that represent the glucose regulation. Hence, the simulators core often include a submodel of the glucose kinetics and insulin action. Notice that if the simulation model is to be used for testing the artificial pancreas that drives a subcutaneous insulin infusion pump based on subcutaneous glucose measurements, it is also necessary to consider submodels that represent both the subcutaneous insulin kinetics and the interstitial glucose kinetics. The principal simulation environments and their related models available in literature are presented below.

- Sorensen model (Sorensen 1985).

Sorensen model belongs to the class of complex physiological based on compartmental models. The model was based on earlier work (Guyton et al. 1978). It divides the body into six physiologic compartments: the brain, the heart, the periphery (includes skeletal muscle and adipose tissue), the gut, the liver, and the kidneys. Glucose and insulin subsystems are considered separately, with coupling through metabolic effects.

The parameters values were derived from the literature and hence could only represent a nominal "average" virtual subject with type 1 diabetes. Therefore the model fails to represent the within subject variability. Sorensen model was further developed (Parker et al. 1999; Parker et al. 2000) to test glucose controllers.

– Fabietti model (Fabietti et al. 2006).

The model is based on a modified Bergman Minimal model. External inputs of the model such as meals and intravenous glucose boluses were added together with the submodel of the glucose absorption from the gastrointestinal tract. The circadian variability of insulin sensitivity was represented by a sinusoidal signal. In addition, most of the parameters were obtained from the literature or by fitting published data. Thus, this is the most important limitation.

– Hovorka model (Hovorka et al. 2004).

This simulation model is based on the compartment model of glucose kinetics and insulin action described by Hovorka et al. 2002. From this, two-compartment models of the subcutaneous insulin and subcutaneous glucose kinetics are included as well as two compartment model of the glucose absorption from the gastrointestinal tract.

An important property of this simulation environment is its ability to represent between and within subject variability. The between subject variability is represented by a population of 18 virtual subjects with T1D. The model parameters were obtained either from clinical studies in subjects with type 1 diabetes or from informed probability distributions. The within subject variability of the glucoregulatory system was implemented by superimposing sinusoidal oscillations on a subset of model parameters.

The main weakness of the Hovorka virtual patient model is that the representation of glucose absorption from the gut is simple and it may need to be refined. Moreover, the within subject variability may also require refinement (Wilinska and Hovorka 2008).

– Medtronic virtual patient (S. Kanderian et al. 2006).

The simulation model used Bergman minimal model at its core interacting with two-compartment models of the subcutaneous insulin kinetics and the meal absorption. Nevertheless, diurnal variations of minimal model parameters such as insulin sensitivity and glucose effectiveness at zero insulin concentration, and the endogenous glucose production were introduced.

The principal limitation is the simplistic representation of the glucose kinetics by Bergman minimal model which includes a short duration of insulin action and overestimation of glucose effectiveness (Wilinska and Hovorka 2008).

– Dalla Man model (Dalla Man et al. 2007a; Dalla Man et al. 2014; Visentin et al. 2018).

The Padova University team, led by Prof. Claudio Cobelli, developed a meal-simulation model of glucose-insulin system utilising data collected in 204 healthy subjects. The simulation model is made up of several parsimonious submodels describing the various unit processes (liver, gastrointestinal tract, muscle and adipose tissue, and beta cell process) (Dalla Man et al. 2007b). There are two main systems in the model (glucose and insulin subsystems); both are described by two compartment models.

The simulation model was employed to simulate a typical day of a non-diabetic subject with three meals. To account for diurnal variations in insulin sensitivity and beta-cell responsiveness, it was assumed that insulin sensitivity is fast and the lunch and beta-cell responsiveness is 25% lower during the lunch and the evening meal compared to the breakfast. As the simulator model was obtained in healthy subjects, for T1D simulations, authors substituted the insulin secretion model with the model of subcutaneous insulin kinetics. To account for the higher basal glucose in T1D, the endogenous glucose production was also increased.

The weakness of this proposal was the fact that the diurnal variations of certain model parameters were not been modelled. Besides, the hypoglycaemia implications and counterregulation were not included in the first version (UVA-Padova Type 1 Diabetes Simulator, S2008).

Later versions, the UVA-Padova Type 1 Diabetes Simulator, S2013 (Dalla Man et al. 2014), incorporated a nonlinear glucose response to hypoglycaemia and a model of counterregulation. Besides, it was also included a population of 300 in-silico subjects (100 adults, 100 adolescents, and 100 children), as in its first version. The limitations of this version was the "single-meal" domain of validity.

The latest version, the UVA-Padova Type 1 Diabetes Simulator, S2017 (Visentin et al. 2018), includes the model of intraday insulin sensitivity variability (the

circadian variability of insulin sensitivity demonstrated by Hinshaw et al. 2013). In addition, its domain of validity was extended from “single-meal” to “single-day”. Finally, S2017 incorporates new models implementing the current performance of insulin delivery and glucose sensing. It is worth remarking, that despite the label "single-meal" or "single-day" considered in FDA documentation, the simulator has been extensively used in the artificial pancreas community to simulate long complex scenarios for controllers testing prior to clinical studies.

Notice that the above-mentioned simulation environments does not consider the particularities of hypoglycaemia nor counterregulation effect, excepting the UVA-Padova Type 1 Diabetes Simulator, S2013 and S2017. Recently, the simulator whose use is more spread in the scientific community is the UVA-Padova Type 1 Diabetes Simulator, S2013

4.3 Models considered

Many models are found in literature to describe the relationship between insulin, glucose and other possible factors that each model also may include. For the sake of brevity, only the models which are relevant in the context of this thesis are explained in detail below.

4.3.1 Bergman minimal model and extensions

Bergman et al. 1979 quantified the pancreatic responsiveness and insulin sensitivity of a diabetic patient using a three-compartment model, namely, I, X and G which represent plasma insulin ($\mu U/mL$), insulin action from a remote compartment (min^{-1}) and plasma glucose (mg/dL) concentrations respectively. The model compartmental representation can be observed in Figure 4.1. The equations (4.1), (4.2), and (4.3) defined the Bergman Minimal model. It is a second-order, nonlinear model relating plasma insulin concentrations (input) and plasma glucose concentration (output). Plasma insulin, $I(t)$, enters from the circulatory system into the remote compartment, $X(t)$, which is modelled with a first-order system representing a lagged action of insulin. This promotes the uptake of plasma glucose ($G(t)$) by the hepatic and extrahepatic tissues. The plasma glucose concentration $G(t)$ is inhibited by the glucose itself and insulin effect. A constant hepatic glucose production $p_1 \cdot G_b$ is considered that drives the system to equilibrium for a basal insulin concentration I_b. p_1, p_2, and p_3 are kinetic parameters. p_1 is the kinetic parameter that governs the rate at which glucose is removed from the plasma space independently of the insulin influence (the so-called glucose effectiveness);

lastly, Insulin Sensitivity is defined by p_3/p_2.

$$\dot{I}(t) = -nI(t) + \frac{u_1(t)}{Vol_I} \tag{4.1}$$

$$\dot{X}(t) = -p_2X(t) + p_3\left(I(t) - I_b\right) \tag{4.2}$$

$$\dot{G}(t) = -p_1G(t) - X(t)G(t) + p_4 + \frac{u_2(t)}{Vol_G} \tag{4.3}$$

$$x(0) = 0, \quad G(0) = G_b, \quad I(0) = I_b.$$

Glucose and insulin distribution volumes are indicated by Vol_G and Vol_I, respectively.

Roy and Parker 2006b proposed an extension of the Minimal Model with the intention of developing a model of T1D patient that fully characterizes endogenous energy production. That was the addition of the FFA dynamics and its interactions with glucose and insulin dynamics. In Figure 4.2, the compartmental representation of this extension is depicted in order to identify visually the relationship between the compartments.

The equations representing plasma insulin and remote insulin remain the original ones (4.1). The plasma glucose dynamics was modified as follows:

$$\dot{G}(t) = -p_1G(t) - p_4X(t)G(t) + p_6G(t)Z(t) + p_1G_b - p_6G_bZ_b + \frac{u_2(t)}{Vol_G} \tag{4.4}$$

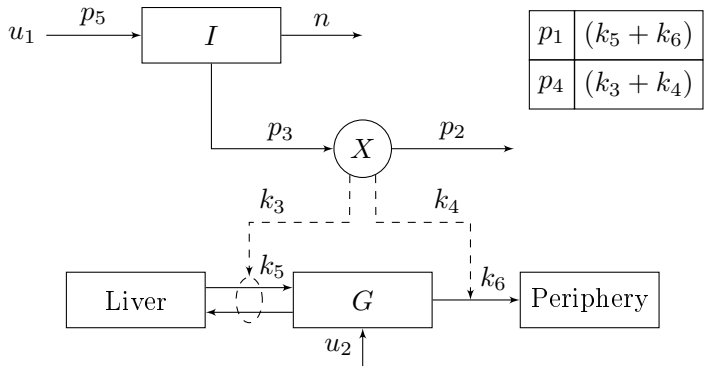

Figure 4.1: Compartmental representation of Bergman Minimal Model. Adapted from (Roy and Parker 2006b).

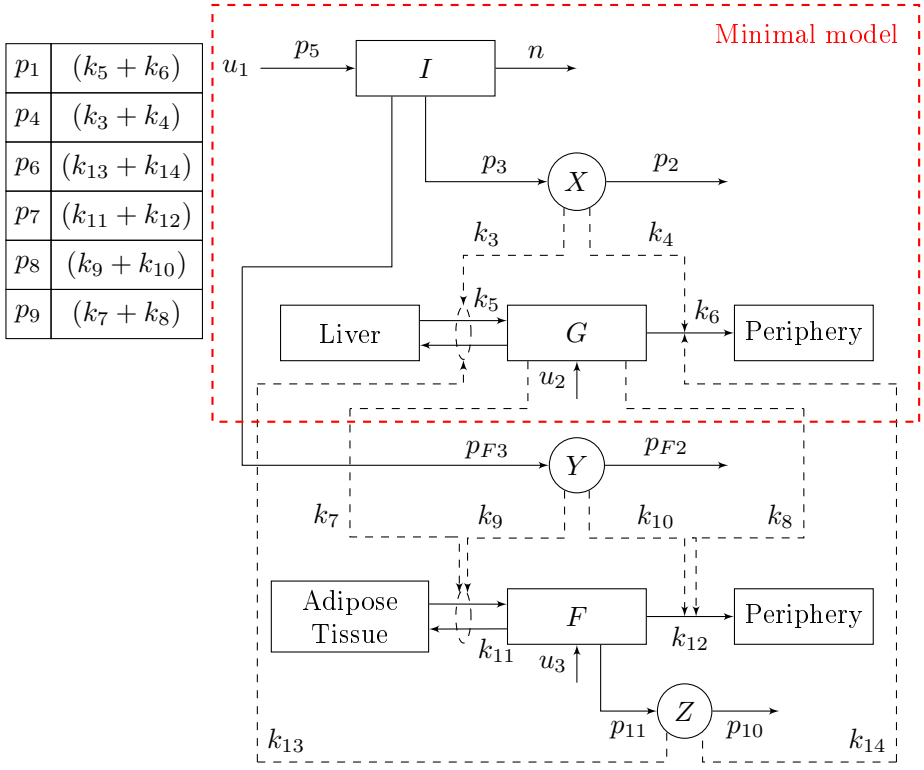

Figure 4.2: Compartmental representation of FFA extension of Bergman Minimal Model. Adapted from (Roy and Parker 2006b).

Parameters p_1, p_4, G_b, Vol_G, and $u_2(t)$ are the same as in equation (4.3). The imparing action of plasma FFA on glucose uptake is represented by the parameter p_6.

Insulin from the circulatory system enters the compartment Y(t), with dynamics:

$$\dot{Y}(t) = -p_{F2}Y(t) + p_{F3}I(t). \tag{4.5}$$

This promotes uptake of plasma FFA into the adipose tissue for storage, which is known as lipogenesis The rate of disappearance of insulin from this remote insulin compartment is managed by the parameter p_{F2}, and the rate at which plasma insulin enters into this remote insulin compartment is governed by the parameter p_{F3}.

Plasma FFA is taken up by the periphery (including the adipose tissue). High glucose levels, representative of low insulin levels, are associated with lipolysis,i.e. the release of FFA is promoted from the adipose tissue into the circulatory system. That is,

$$\dot{F}(t) = -p_7 F(t) - p_8 Y(t) F(t) + p_9(G) F(t) G(t) + p_7 F_b - p_9(G) F_b G_b + \frac{u_3(t)}{Vol_F} \quad (4.6)$$

F_b is the basal FFA concentration, Vol_F is the FFA distribution volume. $u_3(t)$ is the exogenous contribution of FFA. The insulin independent dynamics of FFA is governed by p_7. p_8 represents the rate of disappearance of plasma FFA under the influence of insulin (the antilipolytic effect of insulin). The lipolytic effect associated with plasma glucose concentration level is indicated by the parameter $p_9(G)$, where

$$p_9(G) = 0.00021 e^{-0.00556}.$$

The remote FFA dynamics are represented by the compartment Z, which affects glucose uptake in the hepatic and peripheral tissues:

$$\dot{Z}(t) = -k_2 Z(t) + k_1 F(t) + k_2 Z_b - k_1 F_b. \quad (4.7)$$

Z_b represents the basal remote FFA concentration. The rate of disappearance and appearance of FFA from the remote FFA compartment are driven by the parameters k_2 and k_1, respectively.

Simulations with this model demonstrated a successful performance, achieving a good representation of the physiological interaction between plasma insulin, glucose and FFA concentrations.

Other extensions

Notice that Cobelli et al. 1986 and Cobelli et al. 1999 developed a revised minimal model in order to separate the effects of glucose production from utilization. (Hovorka et al. 2002) extended the original minimal model even further by adding three glucose and insulin subcompartments in order to capture the observed absorption, distribution, and disposal dynamics, respectively. In addition, Roy and Parker 2006a also extended the Bergman Minimal Model to include the major effects of exercise on plasma glucose and insulin levels. Differential equations were developed to capture the exercise-induced dynamics of plasma insulin clearance and the elevation of glucose uptake and hepatic glucose production rates. The changing liver glucose output resulting from prolonged exercise was modelled using an equation depending on exercise intensity and duration.

4.3.2 Hypoglycaemia models

As seen in Chapter 2, counterregulation is a relevant factor when hypoglycaemia occurs. However, counterregulation is often neglected in simulation studies for control strategies design and is not considered in the models that are part of the hypoglycaemia prediction algorithms.

To date, few works have partially included counterregulatory response in predictive or simulation models for a more accurate description of hypoglycaemia episodes and time-course recovery from them. A main difficulty is the quantification of counterregulatory plasma hormonal concentrations. Kovatchev in (Kovatchev et al. 1998) presented a mathematical model of insulin-glucose dynamics that includes estimations for the onset and rate of counterregulatory responses. In that work, a dynamical network model of insulin, glucose, physical activity, and counterregulation interactions was presented. The system was defined in terms of five dependent state variables: plasma glucose levels, insulin, food intake, physical activity, and liver stores. The counterregulatory process was represented by the loop between liver stores and plasma glucose concentration. Then, this process was modelled as a release of glucose from a multicompartmental storage pool. It was assumed that during euglycaemia no counterregulatory response occurred, whereas the model expected onset of counterregulation during descent into hypoglycaemia. Moreover, the counterregulation term was defined as a uni- or bi-modal function depending of the subject data. Finally, they used plasma adrenaline concentrations only to validate models results, showing a high correlation with counterregulation rates. This contribution demonstrated that counterregulation is a process that is directly involved in glucose metabolism, specifically during hypoglycaemia, and its relevance as a part of the glucose dynamics mathematical models. Besides, it promoted the idea that a deeper study of this was needed.

More recently, Dalla Man (Dalla Man et al. 2014) have included in the UVA-Padova T1D Simulator an improved description of glucose kinetics during hypoglycaemia by means of a functional approach. They have incorporated glucagon secretion and action, as well as a paradoxical increment of glucose utilization during hypoglycaemia. This paradoxical increase of glucose comsumption when plasma glucose decreases under a given threshold was obtained from data of hyperinsulinemic clamps in T1D (Bergman et al. 1981; Schwartz et al. 1987), and it was represented by a nonlinear increase of insulin-dependent glucose utilization. However, during hypoglycaemia counterregulation response actually achieves a reduction (not an increase) or peripheral glucose uptake, promoving the use of alternative fuels (FFA) in order to maintain glucose supply to the brain.

The formulation of the insulin-dependent glucose utilization, and the risk function included by the authors are described in the following equation:

$$U_{id}(t) = \frac{[V_{m0} + V_{mx} \cdot X(t) \cdot (1 + r_1 \cdot risk)] \cdot G_t(t)}{K_{m0} + G_t(t)} \tag{4.8}$$

$$risk = \begin{cases} 0 & \text{if } G \geq G_b \\ 10 \cdot [f(G)]^2 & \text{if } G_{th} \leq G \leq G_b \\ 10 \cdot [f(G_{th})]^2 & \text{if } G \leq G_{th} \end{cases} \tag{4.9}$$

$$f(G) = \log\left(\frac{G}{G_b}\right)^{r_2} \tag{4.10}$$

where $U_{id}(t)$ is the insulin-dependent utilization, $X(t)$ the insulin effect, G_t is the plasma glucose concentration, G_b the basal glucose concentration, G_{th} the hypoglycaemic threshold, which is modified by the risk function when glucose is below basal, and V_{m0}, V_{bmx}, K_{m0}, r_1, r_2 are model parameters.

This functional approach achieves good performance, as shown in Chapter 5. Nevertheless, the physiological mechanisms involved in hypoglycaemia are not taken into account and have no mathematical representation. The paradoxical behaviour needs to be clearly understood in order to be confident with the mathematical approximation done. Therefore, a faithful representation of counterregulation during hypoglycaemia could be complementary or improve these findings.

Part II

Contributions

Chapter 5

Physiological modelling of hypoglycaemia

Hypoglycaemia is one of the most important limitations in type 1 diabetes management. However, counterregulatory response to hypoglycemia is often neglected in current simulators, or modelled through functional approaches with no clear physiological explanation. The first step towards achieving the complete understanding of the hypoglycaemic response morphology is to review the existing literature concerning the physiological mechanisms hypoglycaemia stimulates and changes due to T1D. Hence, firstly, in this chapter, a deeper explanation of the counterregulatory mechanisms is provided. From the physiological knowledge, a physiological model of counterregulatory response to hypoglycaemia is built, and the current functional approach in the FDA-accepted UVA-Padova simulator for in silico evaluation of controllers for the artificial pancreas is assessed.

5.1 Preliminaries

Hypoglycaemia is one of the greatest limitations of the glycaemic control in T1D patients, as seen in Chapter 3. Hence, it is important to understand the mechanisms involved in hypoglycaemia, besides of its representability by means models. It will help to evaluate the simulator that we will use for the in silico validation of our controllers.

Several glucose dynamics models have been proposed and proven to be useful in tacking various aspects and several physiological responses in T1D patients. However, the hypoglycaemia continues being their weak spot.

Most of the models assume the same dynamics across the different glycaemic ranges (i.e. euglycaemia, hyperglycaemia and hypoglycaemia) although it is known that there are additional mechanisms that act defending the organisms against low (and dangerous) glucose concentrations during hypoglycaemia.

Therefore, the good understanding of the hypoglycaemia and the mechanisms that it involves is necessary to current models limitations. During hypoglycaemia, while the glucose concentration is decreasing, central and peripheral glucose sensors activate mechanisms to elicit the neuroendocrine, autonomic and behavioural response (the so-called counterregulatory response) (P. E. Cryer 2001).

To date, few works have partially included counterregulatory response in prediction or simulation models for a more accurate description of hypoglycaemia episodes and time-course recovery from them. A main difficulty is the quantification of counterregularoty plasma hormonal concentrations. In (Kovatchev et al. 1998) a mathematical model of insulin-glucose dynamics that include estimates for the onset and rate of counterregulatory responses is presented. This approach considered an additional counterregulation term to be a uni- or bimodal function, corresponding to a one- or two-compartment model. This term could have one, two or more additive components depending on the subject data. In (Thomaseth et al. 2014), the role of the counterregulatory response in healthy humans was assessed modelling the glucose and the free fatty acid (FFA) kinetics during insulin-modified intravenous glucose tolerance test. They worked in a modification to the glucose minimal model using the glucose concentration below a threshold as a signal for the counterregulation and model predictions improved for both glucose and FFA concentrations. More recently, the UVA-Padova T1D Simulator (Dalla Man et al. 2014) has included an improved description of glucose kinetics during hypoglycaemia by means of a functional approach (risk function based on the high blood glucose index (HBGI), the low blood glucose index (LBGI) and a glucose transformation (Kovatchev et al. 2006)). They have incorporated glucagon secretion and action, as well as a paradoxical increment of glucose utilization during hypoglycaemia.

Being the UVA-PADOVA simulator the main tool used for in silico validation of controllers for the artificial pancreas, it is necessary a better understanting and assessment of response to hypoglycaemia, especially in the context of the design of controllers aiming at a better hypoglycaemia mitigation.

Thus,the work presented in this chapter is focused on a deeper study and physiological modelling of hypoglycaemia, particularly in the counterregulatory response, for which the counterregulatory hormones are responsible.

Adrenaline becomes the main actor of counterregulatory response to hypoglycaemia in T1D. Subjects with T1D lack the first line of defence against hypoglycaemia since they cannot reduce systemic insulin levels as blood glucose concentrations begin to decline, unless an artificial pancreas or sensor-augmented pump is used (with the inherent limitations of subcutaneous insulin delivery). Secondary, glucagon secretion in response to hypoglycaemia is lost soon after the onset of the disease. Additionally, the response of adrenaline to a given level of hypoglycaemia is blunted; but the glycaemic threshold for its secretion is shifted to lower plasma glucose concentration (around 60mg/dL) if it is compared with the response of healthy subjects (Schwartz et al. 1987; Tesfaye and Seaquist 2010). It means that due to the absence of endogenous insulin and glucagon response, adrenaline, although blunted, is the most important hormone in the recovery from hypoglycaemia. For this reason, the model of the counterregulatory response proposed in this chapter is based on adrenaline secretion and action. Besides, the FFA dynamics is also added since it improves the representability of the model giving a physiological explanation to certain interactions within it. Of note, a high insulin level leading to hypoglycaemia results in an inhibition of lypolysis, which reduces substrates for glucose production by the liver.

This chapter is organized as follows: a physiological description of the counterregulation and the hypoglycaemia problem is presented in Section 5.2; in Section 5.3, the description of the methodology followed throughout this chapter is addressed. In Section 5.4, the adrenaline secretion model is proposed; the adrenaline action model is presented in Section 5.5; finally, the integration of the two previous models, as well as the incorporation of the FFA dynamics, leading to a complete extension of the Bergman minimal model with counterregulatory response is carried out in Section 5.6; besides of the comparison between the physiological model obtained and the functional approaches used in the UVA-Padova simulator. Conclusions are shown in Section 5.7.

5.2 Counterregulation

Plasma glucose concentration remains normally within a narrow safe physiological range by means of a combination of neural, hormonal, and cellular factors. Then, hypoglycaemia occurs when plasma glucose drops below this normal physiological range. The American Diabetes Association defined in 2004 the hypoglycaemic threshold as 70mg/dL. Nevertheless, there is a recent proposal to set also 54mg/dL as a glycaemic threshold to consider (Amiel et al. 2017). The variable activation of a single counterregulation in an individual makes difficult the definition of a single glucose threshold for a biochemical definition of hypoglycemia. Thus, three levels of hypoglycemia need to be considered: Level 1: glucose alert value is 70 mg/dL; Level 2: glucose alert value is 54 mg/dL; and Level 3: severe hypoglycemia, denoting severe cognitive impairment and need of external help.

Once hypoglycaemia starts, the counterregulatory response is also activated. The counterregulatory response to hyapoglycaemia is defined in (Tesfaye and Seaquist 2010) as: "The counterregulatory response to hypoglycaemia is a complex and well-coordinated process. As blood glucose concentration declines, peripheral and central glucose sensors relay this information to central integrative centers to coordinate neuroendocrine, autonomic, and behavioural responses and avert the progression of hypoglycaemia". That is, the counterregulatory response is a defense mechanisms against low glucose concentrations and its consequences.

The first response to prevent the drop in glucose concentration is the reduction in insulin secretion. However, T1D patients cannot reduce systemic insulin levels when blood glucose concentrations begin to decline. Secondary, the expected increment in glucagon secretion in response to hypoglycaemia is also compromised because the glucagon delivery is mostly suppressed in T1D. The next actor in the action line is the adrenaline secretion, which increases glycogenolysis and glucogenesis at the liver, reduces insulin secretion while increasing glucagon released from the pancreatic islets (in healthy subjects), reduces glucose uptake and utilization, increases glycolysis by muscle, and increases lipolysis in adipose tissue. Nevertheless, the threshold that activates the adrenaline action is lower in T1D than healthy subjects. That is, in healthy subjects, glucagon plays the primary role in the correction of hypoglycaemia while adrenaline has a secondary role. By contrast, adrenaline has the primary role in T1D patients although its activation threshold is lower than in healthy subjects ($\approx$ 50 mg/dL vs 69 mg/dL).

As glucose levels fall further, other counterregulatory factors are activated: secretion of growth hormone and cortisol. Both induce changes in metabolic processes over longer periods of time (hours) by stimulating lipolysis in adipose tissue, ketogenesis and gluconeogenesis in the liver. Moreover, they do not have an immediate

role in the recovery from hypoglycaemia, but they have more prominent roles in the setting of prolonged hypoglycaemia. As it was the case with adrenaline, the activation threshold of these hormones is lower in T1D patients. Thus, there is a delay in the onset of secretion for both hormones with respect to healthy patterns. Cortisol and growth hormone responses start two hours after hypoglycaemia (Amiel et al. 1988). Remark that, preceding hypoglycaemia, severe or recurrent hypoglycaemias shift glycaemic thresholds for initiation of counterregulatory hormones response (Galassetti et al. 2006).

Considering the works reported in (P. E. Cryer 2001; Tesfaye and Seaquist 2010; Watts and Donovan 2010; Marty et al. 2007), Figures 5.1 and 5.2 were built in order to give a general idea about the different interactions and mechanisms that are involved in the glucoregulation when glucose concentrations starts to decrease from 70mg/dL. The physiological terms that are named in the diagram are introduced in Chapter 2.

Figures 5.1 and 5.2 are simplified and customized for T1D patients in Figure 5.3. Figure 5.3 will be useful to obtain a counterregulation model. In addition, Figure 5.4 shows the typical performance of the four counterregulatory hormones (glucagon, adrenaline, cortisol, and growth hormone) that are responsible for pushing glucose concentration up when hypoglycaemia occurs. Data is from the eu-hypoglycaemic clamp carried out with T1D patients in the Clinic University Hospital of Valencia, Spain, whose results were published in (Moscardo et al. 2018).

As it can be observed, glucagon secretion is not activated when hypoglycaemia starts, and the concentration remains practically constant throughout the clamp. By contrast, adrenaline secretion starts as soon as glucose concentration is lower than a given threshold. Cortisol and GH are also incremented during hypoglycaemia, but such increase is lower than the adrenaline. Finally, FFA secretion shows also an increment in hypoglycaemia with respect to euglycaemic phase.

According to the above-described, the adrenaline plays the role of counterregulation conductor in T1D. Cortisol and growth hormone reinforce the effect of adrenaline on glucose concentration but in case of prolonged hypoglycaemias. Therefore, the development of a model that includes the counterregulatory response must be based mainly on adrenaline. That is, this consideration was carried out in order to reduction of the complexity and because the most immediate effect in glucose concentration during hypoglycaemia is provided by adrenaline. Cortisol and Growth hormone are neglected due to their weak and delayed response faced with the onset of the hypoglycaemia event.

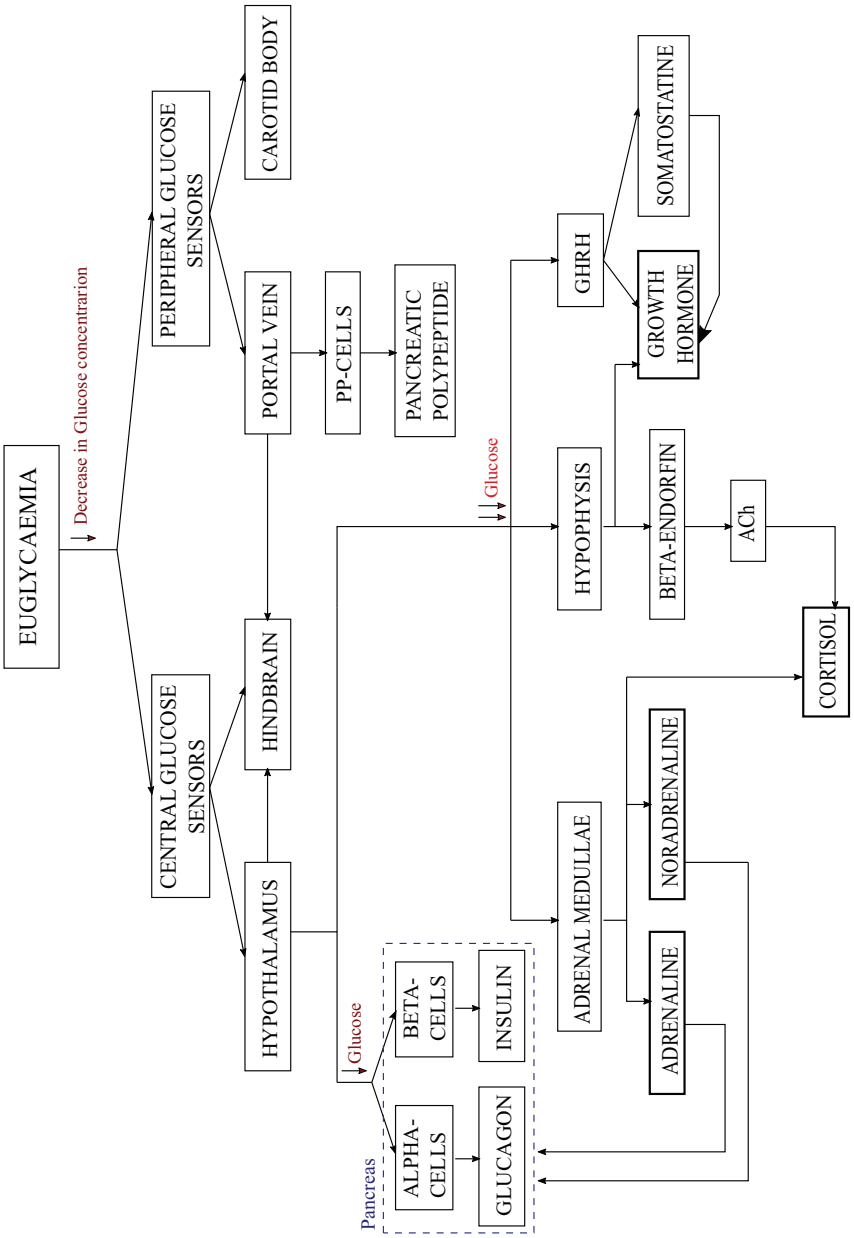

Figure 5.1: Relation between the hormones and mechanisms involved in counterregulation: Part 1.

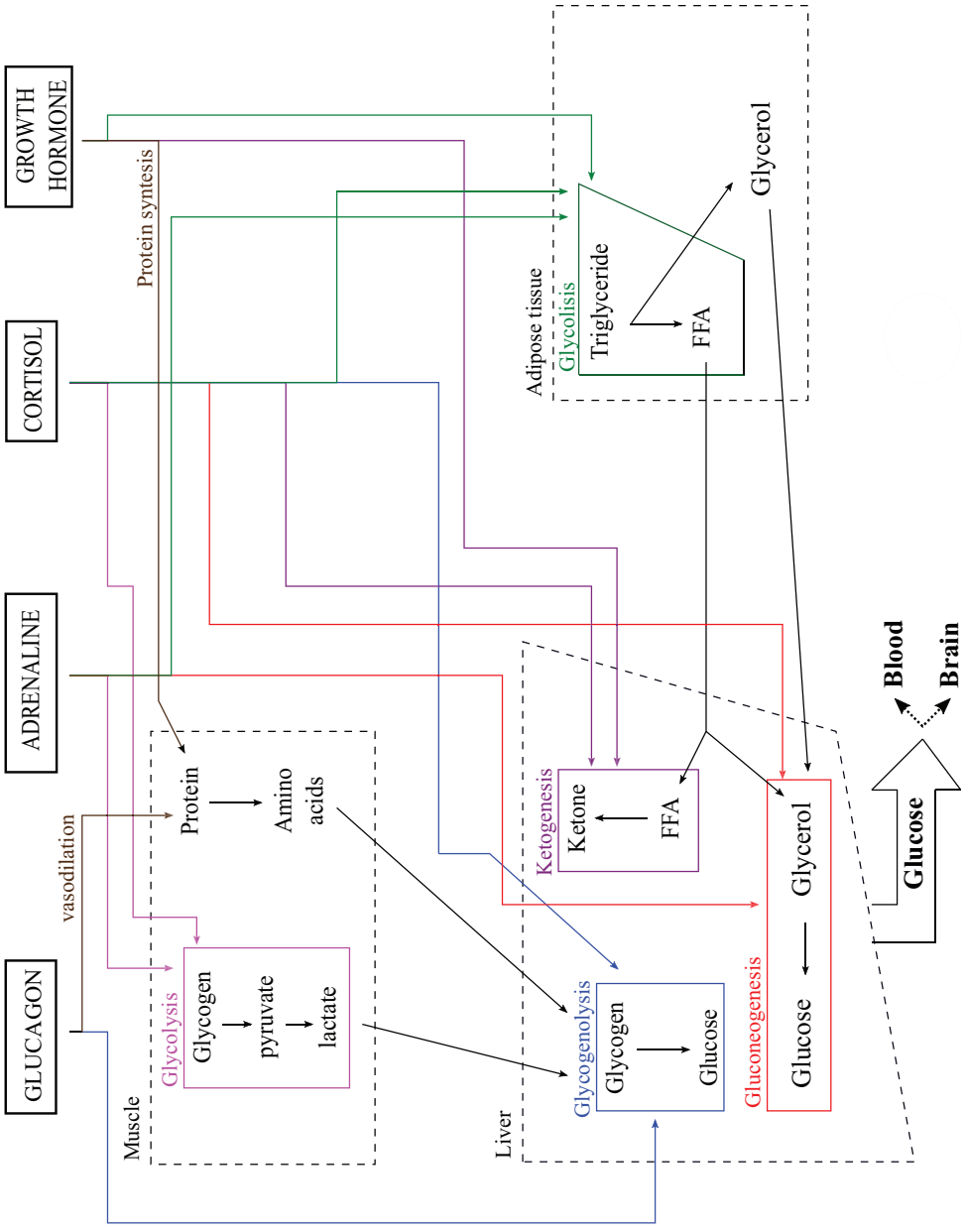

Figure 5.2: Relation between the hormones and mechanisms involved in counterregulation: Part 2.

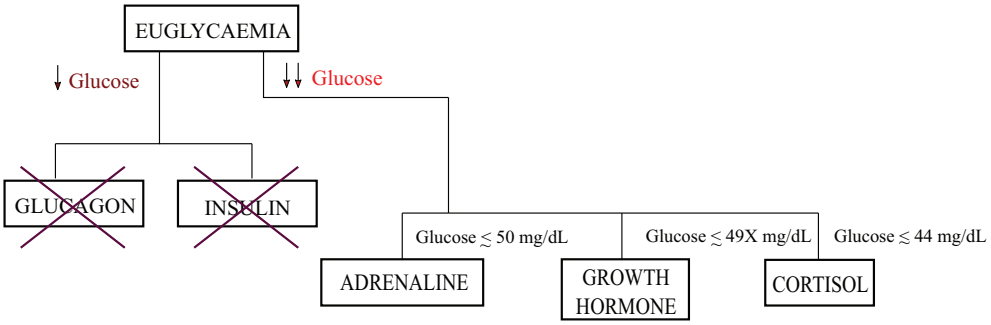

Figure 5.3: Response of counterregulatory hormones in T1D patients.

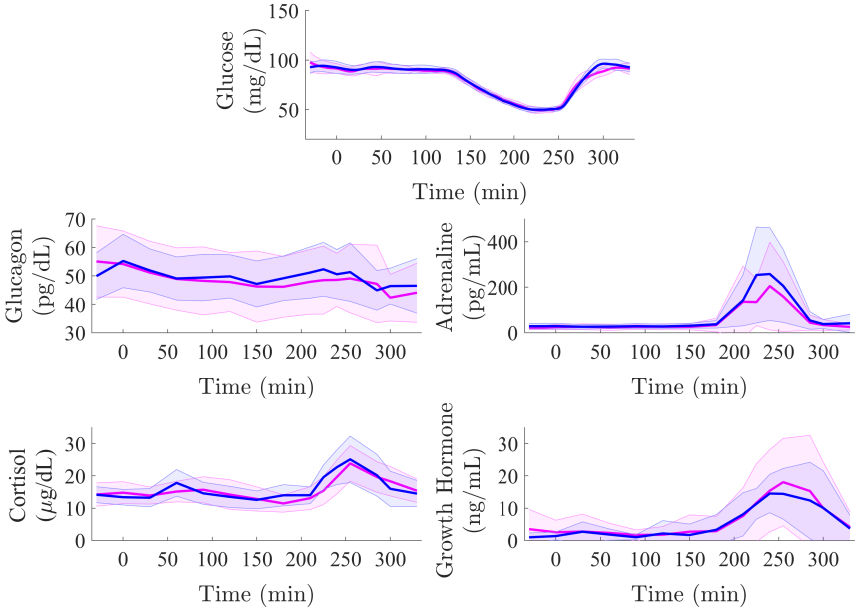

Figure 5.4: Representation of counterregulatory hormones faced with glucose concentration daring a eu-hypoglycaemic clamp (glucose, adrenaline, FFA, cortisol, and glucagon).

5.3 Methods

The modelling process starts with the assessment of the available experimental data in order to determine if they are sufficiently (or not) rich to enable estimations to be made of all the known parameters. After that, the structure of the model and its corresponding parameters need to be defined in order to get the system's model. Once data are properly processed and model structure and parameters are established, the value of unknown parameters are obtained by means of parameter identification techniques. This process continues with the model validation, that is, examining whether the model performance is good enough in relation to its intended purpose. In order to quantify the goodness of fit of the model, several statistical metrics must be defined. Finally, the simulation of the formulated model is carried out in order to reproduce the system dynamics and assess its output behaviour. Figure 5.5 summarizes all the above-described process, particularizing in the methodology followed in this chapter.

5.3.1 Experimental data

Data from an eu-hypoglycaemic clamp study was used in the identification of the models proposed in this chapter. Fourteen subjects with T1D (age 36.5 ± 9.1 years, 9 female, BMI 25.3 ± 3.0 kg/m^2, diabetes duration 15.2 ± 9.8 years, HbA1c $7.9 \pm 0.4\%$ or 62.8 ± 2.02 mmol/mol; all data mean$\pm$SD) were enrolled in the study performed at the Clinic University Hospital of Valencia, Spain. The study protocol was approved by the Ethical Committee of the Clinic University Hospital of Valencia and patients were informed of the objective, methodology, benefits and risks of the study before they signed their informed consent.

Each individual participated in two eu-hypoglycaemic clamp studies with different levels of insulinemia (0.3 mU/Kg/min -Low Insulin- vs 1 mU/Kg/min -High Insulin-). In addition, two patients dropped out the study. That is, a total of 24 clamps were performed. In an initial phase glucose was normalized to 90 mg/dL by using a variable intravenous (i.v.) insulin infusion. Then a hypoglycaemic plateau at 50 mg/dL was induced for 45 minutes with previous and subsequent phases of euglycaemia. The total duration of the study was 8.5 hours. Figure 5.6 illustrates the phases of the studies.

Plasma glucose was measured every five minutes (YSI 2300, YSI Incorporated Life Sciences, Yellow Springs, Ohio, USA). Plasma adrenaline concentration was measured by HPLC (Waters Corporation) every 30 minutes due to blood sampling limitations. Plasma insulin was measured with the same frequency by chemiluminescence immunoessays (Abbot Architect).

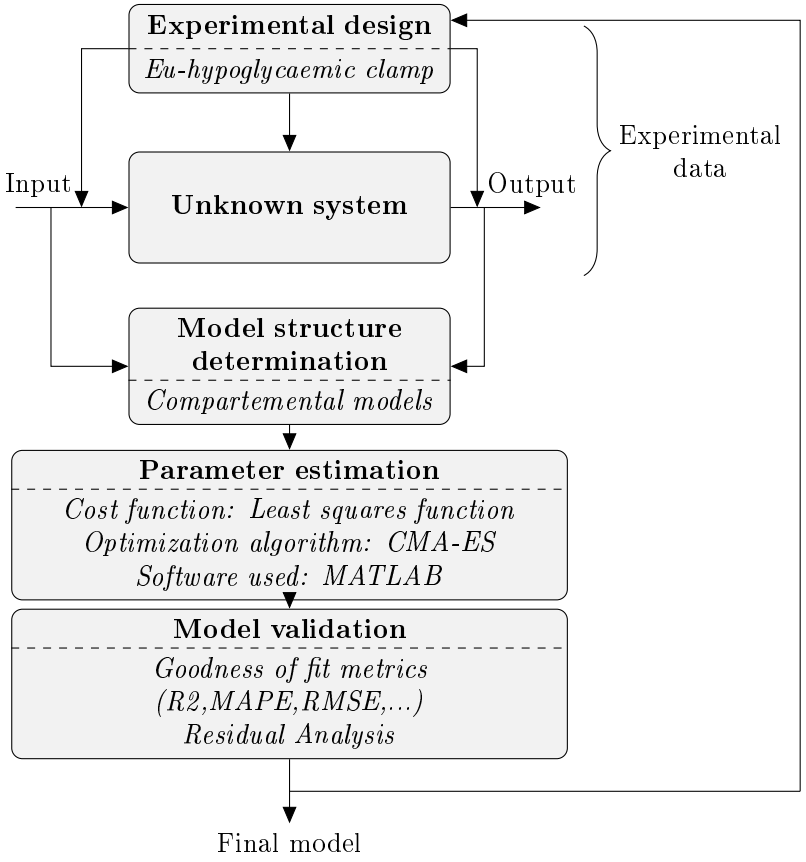

Figure 5.5: Overview of the methodology followed in this chapter for the models identification

Glucose, insulin and adrenaline measurements were available from 24 clamp studies. Before starting with identification, data from three clamp studies were excluded because of inaccurate adrenaline measurements (noise greater than response to hypoglycaemia). Data from another one was not included neither, due to the lack of counterregulatory response (adrenaline behavior was oscillatory around its basal values until the end of study). It means, the number of experiments considered in the models identification was 21 (N=21).

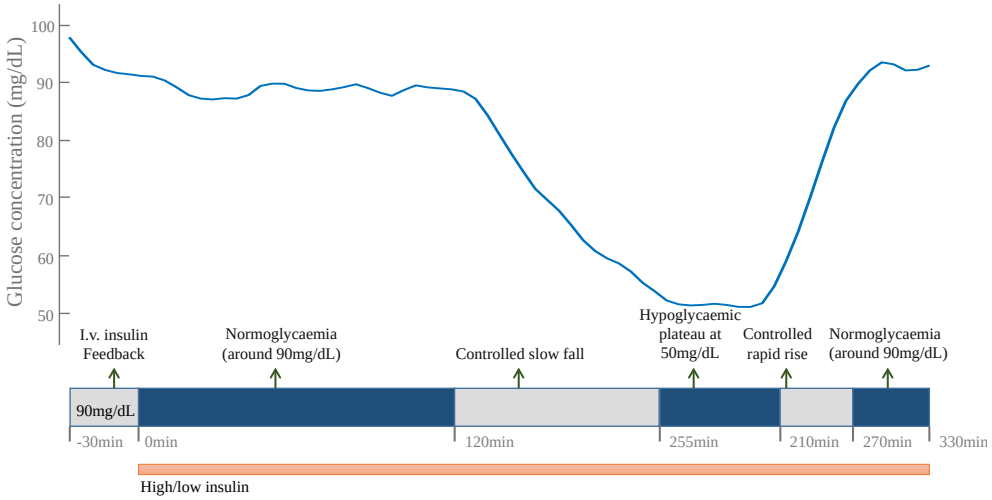

Figure 5.6: Experimental design of the eu-hypoglycaemic clamp.

5.3.2 Identifiability of the model

The identifiability analysis studies if the unknown parameters of the proposed model can be estimated in a unique way, assuming ideal observation conditions and independence between particular values of the parameters and the experimental conditions.

The identifiability analysis provides the knowledge of which combination of parameters are identifiable. In case that the number of identifiable parameters is lower than the number of model parameters, a reduction of the number of parameters to estimate or a modification of the model structure is required.

For linear systems, a common method is the analysis of the number of solutions of the following equation:

$$y_m(s, \hat{p}) - y_m(s, p) = 0, \quad \forall s, u(s) \tag{5.1}$$

where y_m is the system output Laplace transform, p the unknown actual values of the model parameters; $\hat{p}$ the fictitious model parameter values leading to the same output; and $u(s)$ the system input.

In order to analyse the identifiability of the systems presented in this chapter when it is needed and the systems are linear, the equation (5.1) is solved by means of the transfer function method (Walter and Pronzato 1997; Bellman and Aström 1970).

Given the state-space structure described by:

$$\frac{dx(t)}{dt} = A(p)\,x(t) + B(p)\,u(t); x(0) = 0 \tag{5.2}$$

$$y_m(t) = C(p)\,x(t,p) + D(p)\,u(t), \tag{5.3}$$

where A is the state matrix; B is the input matrix; C is the output matrix; D is the feedforward matrix; and p is the p-dimension vector containing the A, B, C, D parameters belonging to the space P (a subspace of the real space $\mathbb{R}$).

The system output expressed in the Laplace domain is:

$$y_m(s,p) = H_1(s,p)\,u(s) + H_2(s,p)\,x_0(p), \tag{5.4}$$

where

$$H_1(s,p) = C(p)\left(sI - A(p)\right)^{-1} B(p) + D(p), \tag{5.5}$$

$$H_2(s,p) = C(p)\left(sI - A(p)\right)^{-1}. \tag{5.6}$$

Then, the equation (5.1) is solved by comparison of transfer functions coefficients leading to a set of algebraic equations whose solutions determine the identifiability of the system according to: the single parameter p_i is a priori globally identifiable if, and only if, for almost any $\hat{p} \in P$, the system of equations has the one and only solution; p_i is locally identifiable if, and only if, for almost any $\hat{p} \in P$, the system of equations has for p_i more than one, but finite number of solutions; p_i is non-identifiable if, and only if, for almost any $\hat{p} \in P$, the system of equations has for p_i an infinite number of solutions.

On the other hand, when the system is nonlinear, the identifiability analysis needs to be studied by other available methods (Carson and Cobelli 2014). In this thesis, the differential algebra algorithm proposed in (Saccomani et al. 1997) is used. Given the model:

$$\frac{dx(t)}{dt} = f(x(t), p, u(t)), \tag{5.7}$$

$$y(t) = f(x(t), p, u(t)), \tag{5.8}$$

where $x(t)$ is the states variable vector, p is the parameters vector, $u(t)$ is the inputs vector, and $y(t)$ is the output vector.

The goal is to calculate the characteristic set of the model, which is the minimal set of differential polynomials that, when set to zero, has the same solutions as the original model. To accomplish this, the Ritt's algorithm is used (Audoly et al. 2001).

This algorithm requires the introduction of a ranking among the variables; in particular, the higher ranked variables are eliminated first. The unknown state variables and their derivatives are ranked highest so they are preferentially eliminated. Then the polynomials defining the system (equations 5.7-5.8) are reduced using Ritt's pseudo-division algorithm. Once the system can no longer be reduced, the characteristic set has been obtained. Then, the corresponding system of differential polynomial equations results in:

$$f_i\left(p\right)\left(y_1, \dot{y_1}, \ddot{y_1}, \ldots, y_r, \dot{y_r}, \ddot{y_r}, \ldots, u_1, \dot{u_1}, \ddot{u_1}, \ldots, u_m, \dot{u_m}, \ddot{u_m}, \ldots\right) = 0, i = 1, \ldots r \tag{5.9}$$

where r is the number of system outputs, and m the number of inputs.

Therefore, equation 5.9 is a function of only the model inputs, outputs, and their derivatives, which are all theoretically known variables. Hence its coefficients in the parameter vector, p, are known. In order to uniquely fix the coefficients, these are extracted to form the exhaustive summary of the model. The Buchberger algorithm is applied to solve it, and the Gröbner basis provides the number of solutions for each unknown parameter (Forsman and Glad 1990).

If all the parameters have only one solution, then the model is a priori globally identifiable. If there are a finite number of possible parameter sets then the model is locally identifiable, and if there are an infinite number of parameter sets the model is non-identifiable. The reader is referred to Section 5.5.2 for an application of this method.

5.3.3 Parameter estimation

The identification procedure is established as an optimization problem based on the minimization of the weighed distance between the experimental values (y) and the predicted values ($\hat{y}$). The cost function used in all identifications carried out in this chapter is the least square function, which is defined as:

$$J\left(p\right) = \sum_{i=1}^{n} w_i \left(\hat{y}_i - y_i\left(p\right)\right)^2, \tag{5.10}$$

where w_i is the weigh coefficient for the instant i-th. The weight coefficients are positive or zero, and they are set a priori (their value can be chosen empirically). The greater the w_i, the more it costs the model to deviate from the experimental data y_i. The value of w_i represents, then, the relative confidence in both the experimental data and the importance of each component of y and its value in the model performance.

Therefore, the optimization problem results in finding the value of the parameter p that minimizes the function $J(p)$. That is,

$$\hat{p} = \arg\min_{p} J(p). \tag{5.11}$$

Since the introduced optimization problem cannot be solved analytically, an iterative optimization procedure is proposed for the problem resolution. Firstly, the structure of the model, experimental data, and the parameters to estimate are defined. Starting from initial values for the parameters (p_0), the optimization routine is based on calculating the value of the objective function and generating new values for the parameters in such a way that they decrease the value of the defined objective function. This process is repeated iteratively until reaching a solution within the previous specified tolerance.

These routines can be solved using local methods since they are efficient and converge in a proper solution (global solution) if initial values are good quality (inside of the area of attraction of the global solution) or if the problem is convex. However, optimization problems are often multimodal (they present local optimal solutions), so these methods will converge on local solutions. Thus, in order to avoid this limitation, global optimization algorithms are used in this work.

The global optimization algorithm CMA-ES (which stands for Covariance Matrix Adaptation - Evolution Strategy) (Auger and Hansen 2005; Hansen et al. 2003; Hansen 2006; Hansen 2016) was used for the estimation of the parameter vectors in our models identifications. CMA-ES is a stochastic, derivative-free method for numerical optimization of non-linear or non-convex continuous optimization problems. This algorithm considers a black box search scenario where parameters vector is considered as the input and the cost function to be minimized is the output. The aim is to find candidate values of evaluated parameters with an objective function value as small as possible.

5.3.4 Goodness of fit assessment

The accuracy of the data fit is tested by the coefficient of determination (R2), usually interpreted as the percentage of the total variation of the dependent variable around its mean that is explained by the fitted model, and by the normalized root mean square error (NRMSE) where lower values indicate less residual variance of the model adjustment. In addition, the mean absolute percentage error (MAPE) is calculated as a measure of model prediction accuracy. Therefore, the goodness of fit of the model is evaluated by the closeness of its coefficient of determination to 100% and its NRMSE to 0. Besides, the smaller the MAPE, the smaller the

estimation error. The coefficient of variation of the RMSE, CV(RMSE), is also considered to observe its variability. These metrics are calculated as:

$$R2 = 1 - \frac{VAR_{res}}{VAR_{tot}}; \tag{5.12}$$

$$MAPE = \frac{\sum_{i=1}^{n} \frac{|y_i - \hat{y}_i|}{y_i}}{N}; \tag{5.13}$$

$$RMSE = \sqrt{\frac{\sum_{i=1}^{n} (\hat{y}_i - y_i)^2}{N}}; \tag{5.14}$$

$$NRMSE = \frac{RMSE}{y_{\max} - y_{\min}}; \tag{5.15}$$

$$CV(RMSE) = \frac{RMSE}{\bar{y}}; \tag{5.16}$$

where VAR_{res} and VAR_{tot} are the variance of the model residual and the observations respectively; $\hat{y}_i$ is predicted value at instant i-th; y_i is measured value at instant i-th; $y_{\max}$ and $y_{\min}$ are the maximum and minimum value of y_i; $\bar{y}$ is the mean value of y_i; and n is the number of predictions.

The proper and valid results of the parameters from an identification process are the ones in which the residual error is random, not autocorrelated, and, then, unpredictable. Hence, the residual error evaluation is required.

Therefore, the assessment of the model residuals is carried out with the study of residuals autocorrelation by means of the Ljung-Box Q-test for residual autocorrelation. In the Ljung-Bos Q-test, the number of lags used was $min(20, T-1)$ as Box et al. 2015 suggested. In addition, the residual independence is also tested with the Wald-Wolfowitz Runs tests (Box et al. 2015).

5.4 Model of adrenaline secretion

As said before, the counterregulatory hormones play an important role in recovery from hypoglycaemia. Particularly, in T1D patients, adrenaline is the first line of counterregulatory hormone response to hypoglycaemia. For this reason, this section is focused on analysing and modelling the effect of glucose concentration on adrenaline secretion. That is, the model considers the glucose concentration as the input of the model, and adrenaline concentration as the output. This general idea is represented in Figure 5.7.

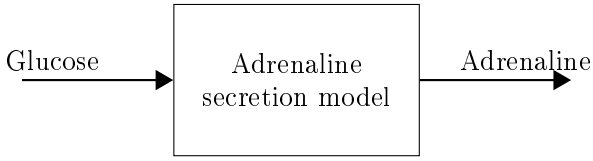

Figure 5.7: General representation of the adrenaline secretion model. Glucose is considered as the input and adrenaline as the output.

5.4.1 Physiological description of the system and the signals to model

Figure 5.8 represents a typical response for adrenaline in our dataset after data interpolation. Adrenaline secretion presents a biphasic nature: the first phase is a quick response against hypoglycaemia that starts when glycaemia is lower than a given threshold; the late phase is associated to the recovery presenting different dynamics. Adrenaline concentration remains constant at basal values until counterregulatory response begins.

The glucose threshold that activates the adrenaline secretion will be subject-dependent. Remark that this does not refer to the hypoglycaemia level of 70 mg/dL. It is known that this threshold can be affected by the number of severe hypoglycaemias, the incidence of unawareness hypoglycaemia or the occurrence of recurrent hypoglycaemias (Beall et al. 2012; de Galan et al. 2003). Likewise, the amplitude of adrenaline signal is also subjected to the physiological condition of the individual.

5.4.2 Model proposal

According to the characteristics that the adrenaline temporal signal presents, a four-compartmental model is proposed. The structure of the model is defined by two chains. One chain is formed by two compartments which represent the slow phase of the adrenaline behaviour; the other one is composed by one compartment representing the fast phase. The last compartment, Q_3 is the measuring compartment of adrenaline concentration. Figure 5.9 depicts the scheme of the model.

The parallel-input compartmental model represented in Figure 5.9 is described by the following equations:

$$\dot{Q}_1(t) = -k_{a1}Q_1(t) + \beta_1 u_a(t) \tag{5.17}$$

$$\dot{Q}_2(t) = k_{a1}\left(Q_1(t) - Q_2(t)\right) \tag{5.18}$$

$$\dot{Q}_3(t) = k_{a1}Q_2(t) - k_eQ_3(t) + k_{a2}Q_4(t) \tag{5.19}$$

$$\dot{Q}_4(t) = -k_{a2}Q_4(t) + \beta_2 u_a(t) \tag{5.20}$$

$$u_a(t) = \begin{cases} 0 & G(t) \geq G_{th} \\ G_{th} - G(t) & G(t) < G_{th} \end{cases} \tag{5.21}$$

$$A(t) = \frac{Q_3(t)}{Vol_A} + A_{basal}$$

$$Q_1(0) = Q_2(0) = Q_3(0) = Q_4(0) = 0;$$

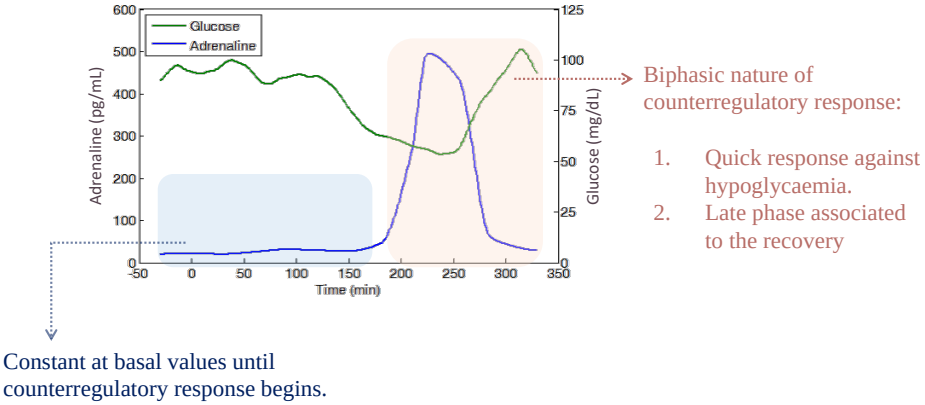

Figure 5.8: Example of adrenaline response to hypoglycaemia.

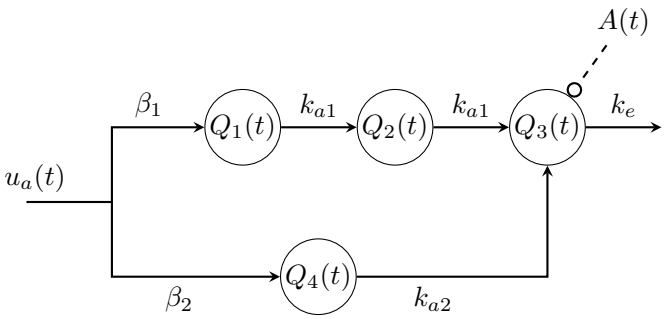

Figure 5.9: Compartmental model of adrenaline secretion.

where $A(t)$ is plasma adrenaline concentration (pg/mL); A_{basal} is basal adrenaline concentration (pg/mL); Vol_A is the distribution volume of adrenaline (dL); $G(t)$ is plasma glucose concentration (mg/dL); G_{th} is the glucose concentration value that activates the counterregulatory response of adrenaline (mg/dL); $u_a(t)$ is the model input corresponding to glucose deviation from the activation threshold G_{th} (glucose does not affect adrenaline secretion unless it goes below this threshold); $Q_3(t)$ (pg) is the measurement compartment of adrenaline mass; the rest of compartments, $Q_1(t)$ (pg), $Q_2(t)$ (pg) and $Q_4(t)$ (pg), define the dynamics of each secretion phase (second and first order, respectively); β_1 (dL$\cdot$min^{-1}) and β_2 (dL$\cdot$min^{-1}) represent the gain of physiological response; k_{a1} (min^{-1}) and k_{a2} (min^{-1}) are transfer rate constants between compartments; and k_e (min^{-1}) is adrenaline rate of disappearance.

Notice that $u_a(t)$ is preceded by a minus sign $(-)$. It is because the influence of glucose concentration on adrenaline secretion is in the opposite direction. That is, the more negative the value of $u_a(t)$, the greater the adrenaline secretion should be since the glycaemic values are closer to severe hypoglycaemia.

Looking at the equations (5.17)-(5.21), β_1, β_2, k_{a1}, k_{a2}, k_e are unknown parameters which must be estimated. Then, the parameter vector is defined as $p = [\beta_1, \beta_2, k_{a1}, k_{a2}, k_e, G_{th}]^T$. In contrast, Vol_A can be considered known, with a population value (Dejgaard et al. 1989). Therefore, from (5.17)-(5.21), the adrenaline concentration at time t_i, $A(t_i)$ is predicted by a function of the unknown parameter vector p and the unknown constant threshold G_{th}, and t_i, i.e., $A(t_i) = h(t_i, p, G_{th})$.

5.4.3 Identification and validation

A priori (structural) identifiability deals with the uniqueness of the solution with respect to model parameters p in the whole complex space under the ideal conditions of error-free model structure and noise-free data. There are many methods for testing identifiability of the models. As mentioned previously, the transfer function method is the one used in this work. Thus, equation (5.1) is particularized for the adrenaline secretion system: y_m corresponds to the system output Laplace transform, i.e. the plasma adrenaline concentrations A; and $u(s)$ corresponds to the system input $u_a(s)$.

In order to apply the transform function method, the output of the system needs to be expressed in the Laplace domain.

Considering the state-space of the model defined by equations (5.17)-(5.21):

$$A = \begin{bmatrix} -k_{a1} & 0 & 0 & 0 \\ k_{a1} & -k_{a1} & 0 & 0 \\ 0 & k_{a1} & -k_e & k_{a2} \\ 0 & 0 & 0 & -k_{a2} \end{bmatrix}, \quad B = \begin{bmatrix} -\beta_1 \\ 0 \\ -\beta_2 \\ 0 \end{bmatrix}, \tag{5.22}$$

$$C = \begin{bmatrix} 0 & 0 & \dfrac{1}{Vol_A} & 0 \end{bmatrix}, \quad D = 0. \tag{5.23}$$

Laplace Transform of the output is:

$$y(s,p) = H_1(s,p)u_a(s) + H_2(s,p)x_0(p), \tag{5.24}$$

$$H_1(s,p) = C(p)\left[sI - A(p)\right]^{-1} B(p) + D(p), \tag{5.25}$$

$$H_2(s,p) = C(p)\left[sI - A(p)\right]^{-1}; \, x_0(p) = 0 \tag{5.26}$$

$$y(s,p) = -\left(\frac{\beta_2 k_{a2}}{Vol_A\,(k_{a2}+s)\,(k_e+s)} + \frac{\beta_1 k_{a1}^2}{Vol_A\,(k_{a1}+s)^2\,(k_e+s)} \right) u_a(s). \tag{5.27}$$

Remark that the $H_2(s,p)$ is not used since the initial conditions are in the equilibrium, i.e. $x_0(p) = 0$.

Evaluating the equality (5.1), there is only one set of parameters p that can lead to a given output. This is,

$$\beta_1 = \hat{\beta}_1;\ \beta_2 = \hat{\beta}_2;\ k_{a1} = \hat{k}_{a1};\ k_{a2} = \hat{k}_{a2};\ k_e = \hat{k}_e. \tag{5.28}$$

Thus, the model is structurally identifiable.

In order to reduce the number of dimensions in the global optimisation problem, prior to the identification of the model parameters vector p, an identification of the glucose threshold (G_{th}) was carried out for each clamp study by detecting a significant change in the slope of the adrenaline temporal signal. To this end, the rate of change of adrenaline concentration was assessed as Figure 5.10 shows. The results across all clamp studies indicated that basal oscillations were always lower than 1 pg·mL^{-1}·min^{-1}. Hence, the G_{th} was obtained as the value of glucose concentration from which the adrenaline slope is greater than 1 pg·mL^{-1}·min^{-1} and glucose concentration is lower than 70 mg/dL. That is,

$$\text{If } \frac{\Delta A_y(t)}{\Delta A_x(t)} > 1 \text{ pg·mL}^{-1}\text{·min}^{-1} \text{ and } G(t) < 70 \text{ mg/dL}. \tag{5.29}$$

The values estimated for each clamp study are summarized in Table 5.1. The average value was approximately 60 mg/dL (60.58 ± 6.57 mg/dL), consistent with

the findings of other studies (Schwartz et al. 1987; Tesfaye and Seaquist 2010). Variability of this value could be caused by extra-patient variability (for example variability from noise in the data), by physiological inter-individual variability or likely by previous episodes of hypoglycaemia affecting both the degree and the threshold of the adrenergic response to hypoglycaemia (Beall et al. 2012; de Galan et al. 2003). The identified values were consistent as demonstrated by a successful posterior identification of the model parameters p.

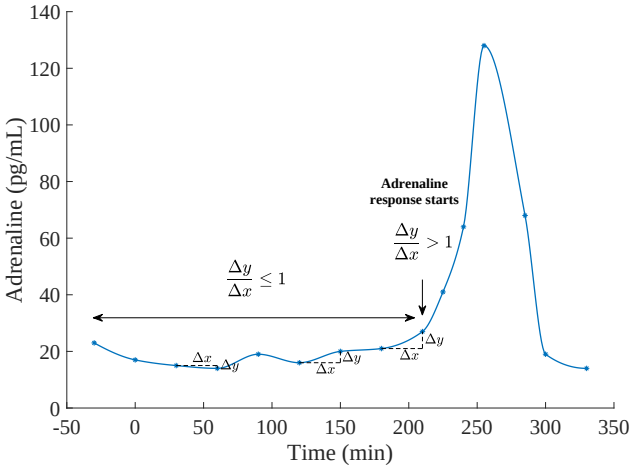

Figure 5.10: Assessment of adrenaline concentration rate of change

In addition, the distribution volume of adrenaline, Vol_A, was set to 200 dL, taking as a reference studies in the scientific literature (Dejgaard et al. 1989) for an average patient.

Once G_{th} was set for each clamp study, parameter vector $p = [\beta_1, \beta_2, k_{a1}, k_{a2}, k_e]^T$ was estimated for each clamp study using the global optimization algorithm CMA-ES. A least squares error function was considered as the cost function to be minimized:

$$\hat{p} = \arg\min_{p} \sum_{i=1}^{N} \left(\hat{A}_i(p,t) - A_i(t) \right)^2 \tag{5.30}$$

where $\hat{A}_i(p,t)$ is the predicted adrenaline value at instant t, $A_i(t)$ is the measured value and N is the number of data points. $\hat{p}$ and p are the estimated parameters vector and the parameter vector respectively. During the optimization process, a

#	$\mathbf{G_{th}}$ $(\mathbf{mg \cdot dL^{-1}})$	#	$\mathbf{G_{th}}$ $(\mathbf{mg \cdot dL^{-1}})$	#	$\mathbf{G_{th}}$ $(\mathbf{mg \cdot dL^{-1}})$
1	52.61	**8**	61.95	**15**	58.86
2	58.65	**9**	71.27	**16**	60.49
3	52.46	**10**	65.53	**17**	63.74
4	50.78	**11**	63.39	**18**	63.55
5	74.53	**12**	60.15	**19**	49.19
6	65.28	**13**	52.87	**20**	62.29
7	67.31	**14**	59.28	**21**	57.95

Table 5.1: Individual estimation of G_{th}.

#	$\boldsymbol{\beta_1}$	$\boldsymbol{\beta_2}$	$\boldsymbol{k_{a1}}$	$\boldsymbol{k_{a2}}$	$\boldsymbol{k_e}$
	$(10^{-7}\mathrm{dL}\cdot\mathrm{min}^{-1})$	$(10^{-7}\mathrm{dL}\cdot\mathrm{min}^{-1})$	(min^{-1})	$(10^{-2}\,\mathrm{min}^{-1})$	(min^{-1})
Mean (SD)	209.52(115.32)	1.36(1.09)	3.87(2.63)	6.94(4.83)	0.96(1.78)
Median [IQR]	177.1[139.45; 294.68]	0.21[0.14; 1.24]	1.1[0.22; 4.66]	6.45[2.68; 9.03]	0.49[0.18; 0.81]

Table 5.2: Values of the estimated parameters of the adrenaline secretion model.

fourth-order Runge-Kutta method (ode45 in Matlab) was used for model simulation.

The estimated values for the model parameters, considering the corresponding glucose threshold G_{th} are shown in Table 5.2. Individual values for each clamp study are shown in Appendix B.1. Variability of parameters β_1 and β_2 between subjects is due to a significant difference in peak values of adrenaline in each subject, although the adrenaline dynamics remains the same among subjects. It thus reflects a change in the system gain. Parameters k_{a1} and k_{a2} have lower order of magnitude. Inter-patient variability was also lower reflecting more uniform dynamics among patients.

The fact that the second chain has lower gains and that dynamics is slower than the first chain demonstrated that the first chain manages the quick secretion of adrenaline to correct the hypoglycaemic state since it is an emergency situation. However, this emergency is not latent when glycaemia starts to going up. Therefore, from this moment, the adrenaline concentration is going to come back its basal values by means of a more relaxed response.

The accuracy of model fitting was tested by the coefficient of determination (R2) and NMRSE. The median coefficient of determination across clamp studies was 95.45% with a maximum of 99.67% and a minimum 76.22%. The most unfavourable case corresponded to an "outlier" behaviour with a fast increase of glucose level and slow stop of adrenaline secretion which requires further investigation. Nevertheless, Figure 5.12 shows a general acceptable estimation across the studies since the mean of estimated and measured adrenaline concentration are quasi-concordant.

The values of the model accuracy are shown in Table 5.3. Nine clamp studies had R2 above 98%, while only three clamp studies had coefficients of determination below 90%. The median NRMSE of the model fits was 0.1166 ± 0.067 with a range from 0.045 to 0.284. This indicates a good model fit for all studies because lower values of it indicate less residual variance.

Moreover, the residual analysis showed that the residual error from the estimation was random and unpredictable. The analysis of residual correlation with Ljung-Box Q-test run proved that they were not autocorrelated ($p > 0.05$ for all studies parameter estimations). Besides, the Wald-Wolfowitz run tests also proved the residual independence across all individual estimations ($p > 0.05$ for all studies). Overall, it means that the estimated values of the model parameters are not likely to be biased. Individual p-values of each test are shown in Appendix B.2 along with the individual parameters value for each clamp study.

Remark that the different levels of insulinemia (low and high insulin) affected slightly the amplitude values of adrenaline secretion (see Figure 5.4). However, it was not relevant to include an insulin-dependent factor in the model because insulin effect was comparable to the other variability sources that were not included. Some variability sources might be recurrent hypoglycaemias (Moheet et al. 2014), previous adrenaline response or antecedent increase in plasma cortisol (de Galan et al. 2003), differences in the treatment and the goodness of the glycaemic control (Amiel et al. 1988), and moderate physical activity during the day previous to the study (Galassetti et al. 2006) among others.

#	**R2 (%)**	**MAPE (%)**	**NRMSE**	**CUV (NRMSE)**
Mean (SD)	93.19 (6.00)	17.89 (6.30)	0.12 (0.06)	0.24 (0.20)
Median [IQR]	95.45 [89.64;95.93]	17.10 [13.92;21.03]	0.07[0.05;0.21]	0.12[0.08;0.25]

Table 5.3: Statistical metrics of adrenaline secretion model fitting (goodness-of-fit).

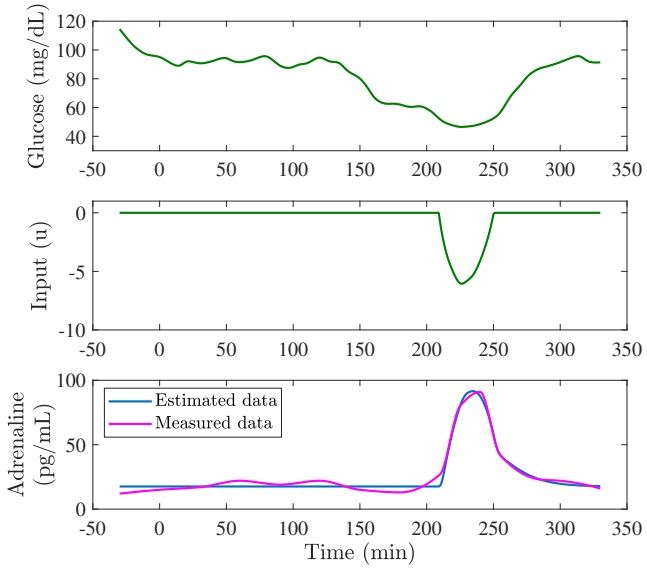

Figure 5.11: Model fit in study #9. (Top) glucose measurements, (middle) input considered in our model, (bottom): adrenaline concentration estimated compared with adrenaline measurements.

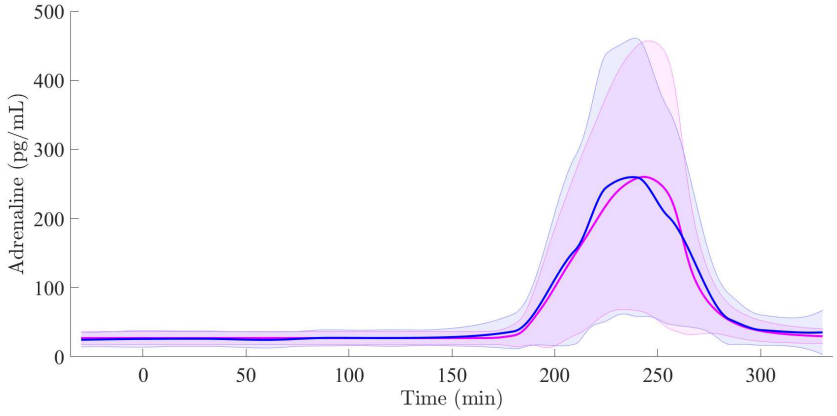

Figure 5.12: Mean temporal signal of the adrenaline experimental data (blue) versus the adrenaline secretion model output (magenta), considering the 21 studied subjects.

As an example, Figure 5.11 presents the data fit for study #9 (it is not the best case, but the average one) whose R2 was 97.78% and NRMSE was 0.1127. It is

worth remarking that in this example, data showed an increment of adrenaline sooner than the model fit, which may indicate an overestimation of the glucose threshold. This may have been caused by the oscillatory behaviour of basal secretion, which was neglected. According to the results, the model proposed can reproduce the adrenaline behaviour in spite of several disturbance sources (sensor noise, measurements error, among others).

The main limitation found has been the variability in adrenaline response (perceptible in Figure 5.4, even in the same subject, which may be due to the occurrence of previous hypoglycaemic episodes affecting counterregulatory response. Then, results could be improved by repeating the analysis on different datasets and increasing the number of studied subjects. Nevertheless, the features of the model are acceptable to take it into account and integrate it in the subsequent extension of the Minimal model as a part of the counterregulatory response.

5.5 Model of adrenaline action

Adrenaline acts as a brake to hypoglycaemia. Hence, a model that includes the adrenaline counterregulatory action ensures a more complete physiological description of plasma glucose regulation. It will provide a better description of hypoglycaemia severity and its recovery phase besides of an improvement in the overall performance of the glucoregulatory model. To this end, an extension of the Bergman Minimal Model of insulin-glucose dynamics (Bergman et al. 1981) is considered, including the counterregulation as a new term within the model. For the sake of reduced complexity, the counterregulation in the model proposed in this section is led by the adrenaline concentration as the first line of action in type 1 diabetes. The general idea is represented in Figure 5.13.

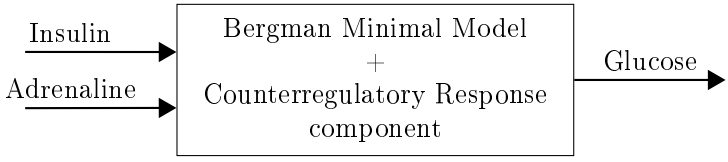

Figure 5.13: General representation of the glucoregulatory model that is addressed to better explain hypoglycaemic profiles. Glucose is considered as the output, and Adrenaline and insulin as the input. The mathematical relationship between them is represented by the box.

5.5.1 Model proposal

Bergman Minimal model (Bergman et al. 1981) quantifies the pancreatic responsiveness and insulin sensitivity of a diabetic patient using a three-compartment model, $I(t)$, $X(t)$, and $G(t)$ which represent plasma insulin, insulin action from a remote compartment and plasma glucose concentrations respectively, as showed in Chapter 4. Adrenaline has no effect on insulin secretion, thus, the modification is carried out on glucose compartment. The extension of the Minimal Model considering adrenaline response is based on a modification in the glucose dynamics (equations (4.1)-(4.3) in Chapter 4) by the addition of two terms, as follows,

$$\dot{I}(t) = -nI(t) + \frac{u_1(t)}{Vol_1} \tag{5.31}$$

$$\dot{X}(t) = -p_2X(t) + p_3I(t) \tag{5.32}$$

$$\dot{G}(t) = -p_1G(t) - X(t)G(t) + p_4 + \frac{u_2(t)}{Vol_G} + p_aA_d(t) - p_h \max\left(G_{b2} - G(t), 0\right) \tag{5.33}$$

$$A_d(t) = \begin{cases} 0 & G(t) > G_{th} \\ A(t) - A_{basal} & G(t) \leq G_{th} \end{cases} \tag{5.34}$$

where lack of endogenous insulin secretion is considered thereby modelling the insulin-dependent diabetic patient. All the necessary insulin must then be infused exogenously. Insulin secretion is thus substituted by i.v. insulin infusion, u_1 (μU/min), and i.v. glucose infusion, u_2 (mg/min), is also added in order to represent the clamp experimental conditions used for model fitting. p_3 (min^{-1}) represents the kinetic parameter that governs the rate of appearance of insulin in the compartment $X(t)$ ($\mu\text{U}\cdot\ \text{mL}^{-1}$). n (min^{-1}) is the rate of disappearance, and p_2 (min^{-1}) is the kinetic parameter that governs the rate of disappearance from $X(t)$. p_1 (min^{-1}) is the kinetic parameter that governs the rate at which glucose is removed from the plasma space independently of the insulin influence. $X(t)G(t)$ represents glucose uptake under the influence of insulin. p_4 ($\text{mg}\cdot\ \text{dL}^{-1}\cdot\text{min}^{-1}$) represents hepatic glucose production rate (given by the original Bergman model as G_bp_1, where G_b is the glucose basal value yielding a given steady state). Glucose and insulin distribution volumes are indicated by Vol_G (dL) and Vol_I (mL), respectively. In addition, $A(t)$ is the plasma adrenaline concentration (pg/mL); A_{basal} is basal adrenaline concentration; G_{th} (mg/dL) is the glucose threshold that activates adrenaline response; and $A_d(t)$ is the adrenaline "effect" activated below the glucose threshold G_{th}, expressed as the increment of adrenaline concentration from its basal value. This increment is associated with the counterregulatory response of this hormone during a hypoglycaemic event, which is modulated by the parameter p_a (min^{-1}). It is considered that adrenaline effect is immediate,

representing a very fast counterregulatory action in face of hypoglycemia. G_{th} values are coincident with the glucose threshold used in the adrenaline secretion model (Section 5.4). It is the glucose value that activates the adrenaline counterregulatory response. Parameter G_{b2} is other glucose threshold that triggers a paradoxical glucose use modulate by parameter p_h (min^{-1}). The above model considers that plasma insulin, I, enters from the circulatory system into the remote compartment, X, which is proportional to remote insulin denoting its action in promoting the uptake of plasma glucose (G) by the hepatic and extrahepatic tissues.

Adrenaline acts estimulating hepatic and renal glucose production, inhibiting glucose peripheral uptake, and estimulating lipolysis (which is an indirect route to estimulate gluconeogenesis in the liver) (Bolli and C.G. Fanelli 1999). However, for the sake of model identifiability, a lumped effect is considered here as expressed by the first new term, $p_a A_d(t)$. This term depends on the deviation of plasma adrenaline concentration from its basal value and it is null until counterregulatory response of adrenaline begins (i.e., when $G(t) \leq G_{th}$). The second term considered, $p_h \cdot \max(G_{b2} - G(t), 0)$, represents an increase in glucose use when glucose is below a given threshold G_{b2} (always inside of hypoglycaemic range and greater than G_{th}). The physiological explanation of this term is controversial. However, data indicated that such effect should be included in order to get a good model fit. Figure 5.14 depicts such need showing the hypoglycaemia overestimation of the model if the second term is not added. This is in line with the approach of (Dalla Man et al. 2014), where a "paradoxical" increment of glucose utilization during hypoglycaemia is considered. However, this contrasts with the inhibition of glucose uptake and insulin resistance induced by the stimulation of free fatty acids due to the adrenaline effect. As a possible hypothesis, a stimulatory effect on blood flow by insulin was reported (Enoksson et al. 2003) which might be relevant during hypoglycaemia. This will be subject of further investigation in Section 5.6.

The model equilibrium point, for a given basal plasma insulin concentration I^* is given by:

$$G^* = \frac{p_4}{p_1 + \frac{p_3}{p_2} I^*}. \tag{5.35}$$

As $G^* > G_{b2}$ and $G^* > G_{th}$ in equilibrium initial condition, the equilibrium initial conditions correspond to:

$$X(0) = \frac{p_3}{p_2} I^*; \quad G(0) = G^*; A(0) = A_{basal}. \tag{5.36}$$

Remark that since plasma insulin measurements are available, equation (5.31) is not relevant in the identification process. Instead the measurement of plasma

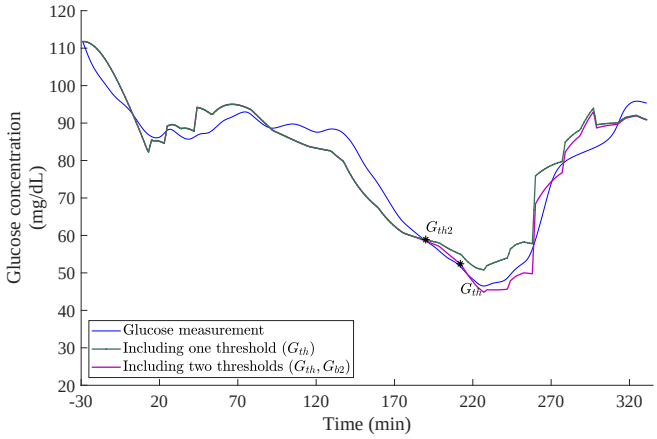

Figure 5.14: Representation of glucose measurements and the estimations of the model including one term or two terms.

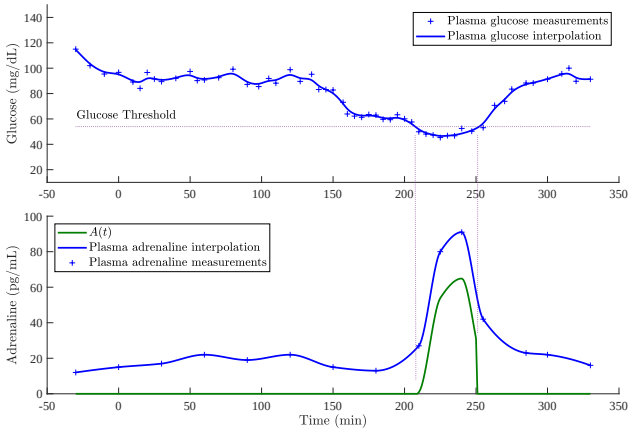

Figure 5.15: Individual profile of plasma glucose and adrenaline concentration during the eu-hypoglycaemic clamp. $A(t)$ is the temporal signal used as input in the model; it represents the increase of plasma adrenaline concentration from basal value.

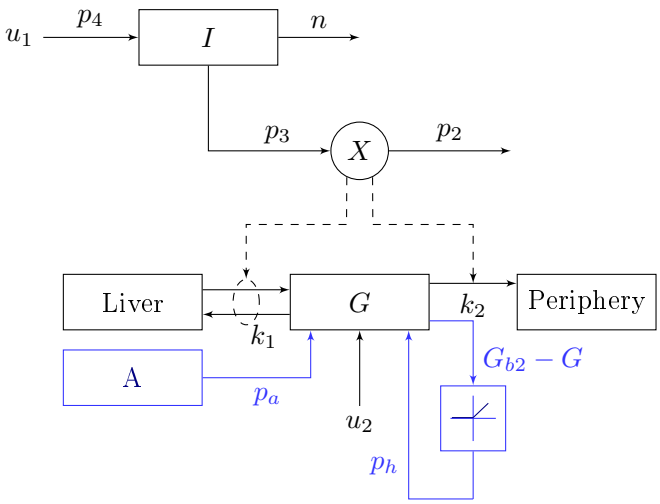

Figure 5.16: Bergman Minimal Model diagram of insulin and glucose dynamics with the modification to account counterregulatory effect.

insulin concentration ($I(t)$) is considered as an input of the model in equation (5.32). Similarly, $A(t)$ is also considered as an input since its measurements are available. Nevertheless, they could be also an estimated measurement using the adrenaline secretion model (obtained in previous section), but it was preferable not to add complexity (more equations) to the system identification at this stage in order to validate the proposed model structure.

As an illustration, Figure 5.15 shows the temporal evolution of plasma adrenaline and plasma glucose concentrations for subject #3 during the High Insulin study. Adrenaline remains in its basal value (around 20 pg/mL for this patient) while plasma glucose concentration keeps in the normoglycaemic range. When glucose concentration begins to decline below the activation threshold of adrenaline, adrenaline counterregulatory response starts in order to prevent plasma glucose to continue falling, reaching peak adrenaline concentration at the hypoglycaemic plateau. By contrast, adrenaline secretion rapidly decreases when hypoglycaemia recovery begins, returning to its basal value.

Likewise, the diagram of the proposed model is shown in Figure 5.16. As mentioned before, the concentration of compartment I is known since insulin concentration was measured. For this reason, the insulin flow coming from the insulin system, u_1, and parameter n, rate of disappearance from I, is not part of the equations used in the extension of the model that has been proposed.

5.5.2 Identification and validation

Equation (5.31)-(5.36) were used in the model parameters identification. According to the identification procedure, parameters that determine the output of our model are: p_1, p_2, p_3, p_4, Vol_G, p_a, p_h, G_{b2}, G_{th}. Values for parameter G_{th} were taken from the previous work (Section 5.4); and, the distribution volume of glucose, Vol_G, was fixed to 117dL, taking as a reference studies in the scientific literature (Roy and Parker 2006b) for an average patient. The rest of parameters, $p = [p_1, p_2, p_3, p_4, p_a, p_h, G_{b2}]^T$, were estimated for each study.

The estimation process was carried out in two stages: (1) Estimation of the characteristic parameters of the Bergman Minimal model during euglycaemic phase, i.e. $p_{MM} = [p_1, p_2, p_3, p_4]^T$; (2) Estimation of the parameters that define the glucose dynamics due to the counterregulation, i.e. $p_{CR} = [p_a, p_h, G_{b2}]^T$.

The a priory identifiability of the system considered at each stage of the identification procedure was analysed by means of the differential algebra algorithm proposed by Saccomani et al. 1997 as exposed below.

The polynomials obtained from the model defined by equations (5.31), (5.32), and (5.33) are:

$$-p_2X + p_3I - \dot{X}, \tag{5.37}$$

$$-p_1G - XG + p_4 + \frac{u_2}{Vol_G} + p_aA_d - p_h(G_b2 - G) - \dot{G}, \tag{5.38}$$

$$y - G, \tag{5.39}$$

At the first stage (1), the parameters vector to identify was p_{MM}, parameter p_a and p_h were considered zero, and $G_{b2} \leq G(t)$. Thus, the two terms p_aA_d and $p_h(G_b2 - G)$ of the polynomial 5.38 were null. Besides, I(t) was considered an available measurement. The polynomials were ordered and reduced according the rank: $u_2 < I < A_d < y < \dot{y} < \ddot{y} < X < G < X < G$. Hence, the differential polynomial that contains the information on the model identifiability (i.e. the polynomial that does not contain the state variables (X, G) or its derivatives as variable) was:

$$y^{-1}\left(-p_2p_4 - p_2\frac{u_2}{Vol_G} + p_2\dot{y} + \ddot{y}\right) + p_2p_1 + p_3I + y^{-2}\left(p_4 + \frac{u_2}{Vol_G} - \ddot{y}\right) \tag{5.40}$$

The coefficients were extracted to form the exhaustive summary, the Buchberger algorithm was applied, and the Gröbner basis was:

$$-p_2p_4, p_2, p_3, p_4, p_2p_1 \tag{5.41}$$

By equating the polynomials (5.41) to known symbolic values α, β, γ, δ, and ϵ, it was determined if the parameters can be uniquely identifiable. That is,

$$-p_2p_4 = \alpha, p_2 = \beta, p_3 = \gamma, p_4 = \delta, p_2p_1 = \epsilon, \tag{5.42}$$

This systems could be solved for $p_1 = \beta/\epsilon$, $p_2 = \beta$, $p_3 = \gamma$, and $p_4 = \delta$. Therefore, the model is globally identifiable.

Likewise, an analogous analysis was carried out at the second stage of the identification procedure. In that case, the parameters vector to estimate was p_{CR}, and p_{MM} was considered known. Hence, the differential polynomial that contains the information on the model identifiability was:

$$y^{-1}\left(-p_2p_4 - p_2\frac{u_2}{Vol_G} + p_2\dot{y} + p_2p_hG_{b2} + p_2p_aA_d + \ddot{y}\right) + p_2p_1 + p_2p_h + p_3I + y^{-2}\left(p_4 + \frac{u_2}{Vol_G} - p_hG_{b2} - p_aA_d - \ddot{y}\right), \tag{5.43}$$

and the extracted coefficients were:

$$-p_h, p_hG_{b2}, p_a, \tag{5.44}$$

By equating the polynomials (5.44) to known symbolic values α, β, and γ, the system could be solved for $p_h = \alpha$, $G_{b2} = \beta/\alpha$, and $p_a = \gamma$. Thus, the model is globally identifiable when parameters estimation is carried by the two stages above described.

The least-square-error function was considered as the cost functions to be minimized:

$$\hat{p}_{MM} = \arg\min_{p_{MM}} \sum_{i=1}^{n} \omega_i \left(\hat{G}_i(p_{MM}, t) - G_i(t)\right)^2 \tag{5.45}$$

where

$$\omega_i = \begin{cases} 0 & \text{if } G_i < 70\text{mg/dL} \\ 1 & \text{otherwise} \end{cases} \tag{5.46}$$

$$\hat{p}_{CR} = \arg\min_{p_{CR}} \sum_{i=1}^{n} \left(\hat{G}_i(p_{CR}, t) - G_i(t)\right)^2 \tag{5.47}$$

where $\hat{G}_i$ is the predicted plasma glucose value at instant i, G_i is the measured value and n is the number of data points. $\hat{p}_{MM}$ and $\hat{p}_{CR}$ are the estimated parameters vectors; and, p_{MM} and p_{CR} are the parameters vector. ω_i is the weight of the i-th residual in order to exclude data affected a priori by counterregulation (hypoglycaemic range).

The parameters vector $\hat{p}_{MM}$ was estimated considering equations (5.32)-(5.36) and forcing $p_h = 0$ and $p_a = 0$. After that, parameter vector $\hat{p}_{CR}$ was obtained taking into account the equations (5.32)-(5.36) and the values of $\hat{p}_{MM}$ as known parameters, i.e., the values identified previously. These results are shown in Table 5.4. Parameter p_a presents significant variability (CV=0.88). It is due to the variability of the maximum value of adrenaline secretion across the subjects during hypoglycaemia. This is demonstrated with the strong correlation that exists between p_a and the peak value of adrenaline concentration (correlation coefficient=0.67). This parameter is responsible for modulating the counterregulation which is represented in our model by the adrenaline signal.

By contrast, the parameter G_{b2} shows lower variability (CV=0.21). This parameter is related to the not fully explained effect of hypoglycaemia on plasma glucose concentration by increasing glucose uptake. The influence of hypoglycaemia "per se" is done uniformly across the patients when a strong hypoglycaemic tendency occurs. The glycaemic profile of the studied subjects is almost the same due to data coming from a clamp. For this reason, the variability of parameter G_{b2} could be due to the hypoglycaemia sensibility of each patient and the history of severe hypoglycaemic events.

#	p_1	p_2	p_3	p_4	p_a	p_h	G_{b2}
	(min^{-1})	(min^{-1})	$10^{-5}min^{-1}$	$mg \cdot dL^{-1} \cdot min^{-1}$	($10^{7}min^{-1}$)	(min^{-1})	(mg/dL)
Mean (SD)	0.010(0.008)	0.046(0.082)	6.180(4.230)	0.821(0.445)	0.192(0.106)	0.036(0.021)	63.940(9.500)
Median [IQR]	0.008 [0.004;0.017]	0.027 [0.014;0.033]	3.390 [2.390;7.010]	0.730 [0.309;1.234]	0.156 [0.054;0.312]	0.021 [0.014;0.043]	63.049 [57.294;70.952]

Table 5.4: Value of estimated parameters.

Figure 5.18 represents the scatter matrix of the parameters. It demonstrates that there is no dependence between the parameters identified and thus the soundness of the new model presented is proved. Parameters draw a lognormal distribution; this can be also observed in the figure.

The accuracy of data was tested by the coefficient of determination (R2) and NMRSE. The median coefficient of determination across clamp studies was 91.22% with a maximum of 96%. The most unfavorable case corresponded to a study with a poorer adjustment in euglycaemia phase, while showing a good fit in the hypoglycaemic phase (R2=85%). As our modification of the Minimal Model aims at improving the adjustment during hypoglycaemia, it has been also calculated the value of goodness of fit indicators considering only the hypoglycaemic phase. All values are shown in Table 5.5.

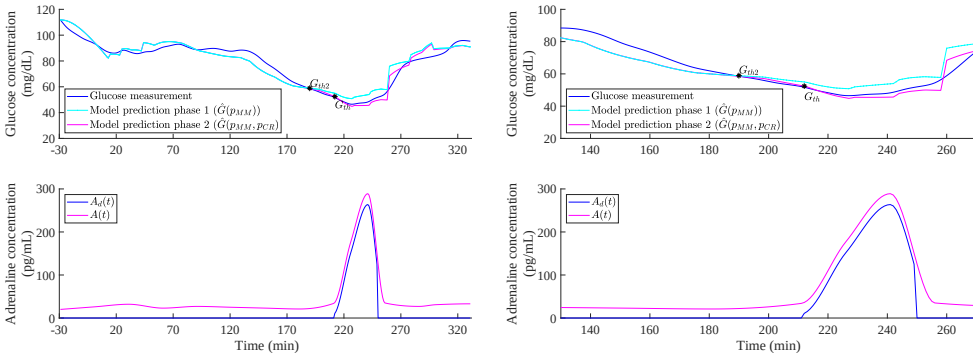

Figure 5.17: Comparison of the model output considering and non-considering counterregulation extension. (a) All phases of the study (feedback, normoglycaemia, controlled slow fall, hypoglycaemic plateau, controlled rapid rise, and normoglycaemia); (b) Considering two phases: controlled slow fall and hypoglycaemic plateau.

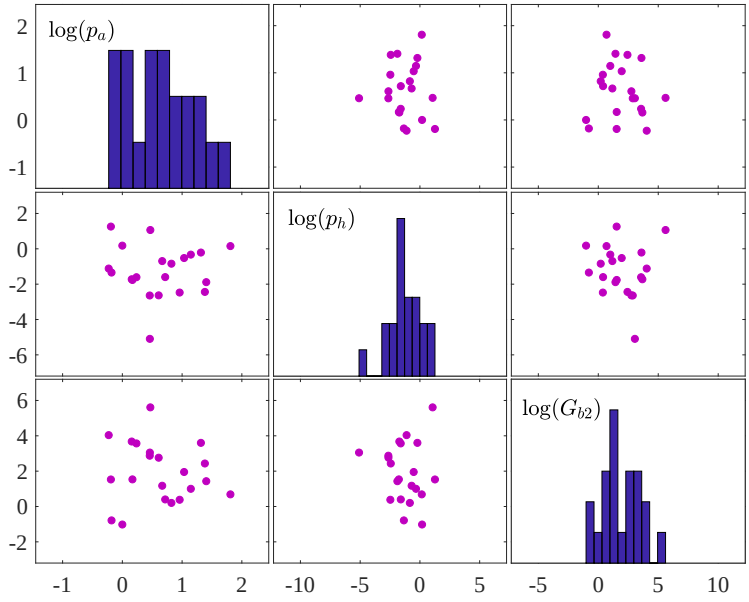

Figure 5.18: Scatterplots and histograms of the individual parameter values, as obtain after model parameters estimation.

Phase	Statistical indicators		
	R2(%)	**NRMSE**	**CV(RMSE)**
Euglycaemia and Hypoglycaemia	91.22 (13.94) 90.94[86.94;94.04]	0.089 (0.034) 0.084[0.065;0.109]	0.060(0.020) 0.048[0.035; 0.076]
Hypoglycaemia	84.39 (11.93) 84.62[79.31; 91.32]	0.094 (0.103) 0.103 [0.065; 0.174]	0.028 (0.017) 0.033 [0.019;0.042]

Table 5.5: Statistical metrics of the model fit.

Figure 5.19 presents a data fit for study #1 whose R2 is 86.6% and NRMSE is 0.08. As it can be observed, the hypoglycaemia phase is well characterized by this model. This case is not the best, but it is an average one. Across the clamp studies, the NRMSE average of the model fits was 0.094 ± 0.034. This indicates a good model fit for all studies because lower values indicate less residual variance. Likewise, the low coefficient of variation of RMSE (0.06 ± 0.02) points out a good adjustment across clamp studies. Figure 5.17a manifests the improvement that counterregulation consideration in the model achieves during hypoglycaemic range. This is not the best case, but it demonstrated that the model works.

Moreover, the residual analysis showed that the residual error from the estimation was random and unpredictable. The analysis of residual correlation with Ljung-Box Q-test run proved that they were not autocorrelated ($p > 0.05$ for all clamp studies parameter estimations). Besides, the Wald-Wolfowitz run tests also proved the residual independence across all individual estimations ($p > 0.05$ for all studies). Overall, it means that the estimated values of the model parameters are not likely to be biased. Individual p-values of each test are shown in Appendix B.2 along with the individual parameters value for each clamp study.

To sum up, the extension of Bergman Minimal Model with the adrenaline dynamics can reproduce the physiological behaviour during hypoglycaemia. These modifications mean that the inclusion of two terms which represent the counterregulatory response and the "influence of hypoglycaemia per se" on glucose homeostasis.

However, this latter term still remains paradoxical, as it was the case with the functional model in UVA-Padova simulator motivating this work, and requires further analysis for a physiological explanation. This will be carried out in next Section with the study of the role of free fatty acids in counterregulation. In addition, the integration of the adrenaline secretion model will lead to the final complete model of counterregulation proposed in this work.

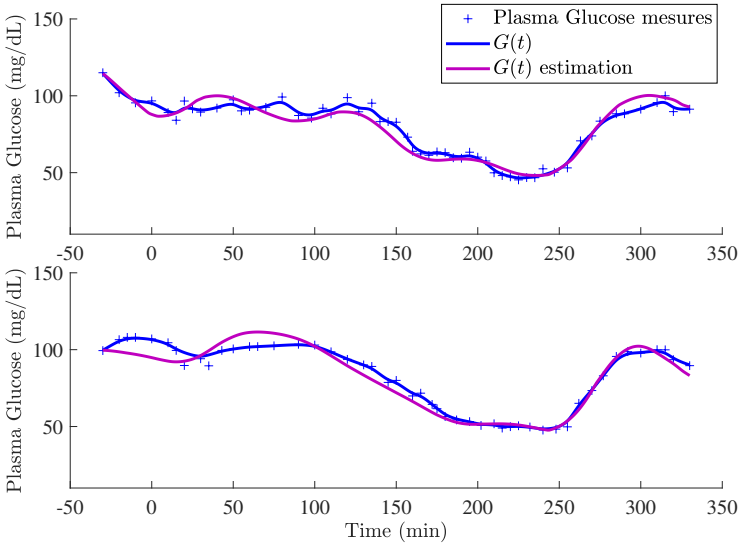

Figure 5.19: Model fit in subject #1 during the High insulin study (top) and during the Low insulin study (bottom).

5.6 Role of free fatty acids in counterregulation: a comprehensive physiological model of hypoglycaemia

The behaviour of Bergman Minimal model improves when a counterregulation dynamics is included, as demonstrated in the previous section. Thus far, the counterregulatory factor has been defined only as a function of adrenaline response since it is the main actor of such mechanism in T1D subjects. However, its mathematical formulation still shows a paradoxical increment of glucose utilization during hypoglycaemia that needs to be physiologically explained.

As studies demonstrated in (DeFronzo et al. 1980; Clutter et al. 1980), adrenergic mechanisms do play a role in the prevention of severe hypoglycaemia at a very early as well as late phase of hypoglycaemia with its contribution in the increase in hepatic glucose production and with the activation of lipolysis as the other powerful counterregulatory mechanism. Besides, there is a substrate competition between FFA and glucose in the oxidation and in the utilization processes of peripheral tissues during hypoglycaemic conditions. For this reason, FFA dynamics during counterregulation deserves a much deeper attention.

Figure 5.20 shows the profiles of adrenaline and FFA considering different ranges of plasma glucose concentrations (euglycaemic and hypoglycaemic ranges). Pro-

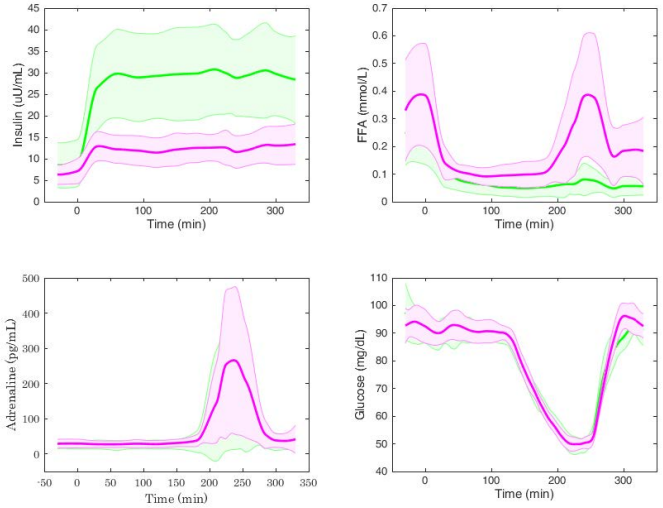

Figure 5.20: Database (average of 12 T1D patients, shading area represents mean±SD). Insulin plasma concentrations (top panel, left), FFA (top panel, right), Adrenaline (bottom panel, left) and Glucose (bottom panel, right). Each one is plotted during Low insulin studies (magenta) and High insulin studies (green).

files are grouped by insulin levels, high (green line) and low (magenta line) levels, to provide a better physiological understanding. As it can be observed, when the hypoglycaemic event occurs during both high and low insulin studies, the counterregulatory response of adrenaline is clear. Adrenaline remains in basal values while plasma glucose concentration is within the normoglycaemic range. When glycaemia begins to decline below the activation threshold, around 60 mg/dL (Schwartz et al. 1987; Tesfaye and Seaquist 2010), counterregulation response of adrenaline starts in order to prevent plasma glucose continues falling. This adrenaline secretion decreases when hypoglycaemia recovery begins. On the other hand, the FFA response is mostly modulated by insulin plasma levels. When insulin levels are high, FFA secretion is practically suppressed although adrenaline concentrations tend to stimulate some FFA secretion (much lower than basal secretion). On the contrary, when insulin concentration is low, FFA is suppressed but less, and insulin does not get to inhibit the FFA estimulation by adrenaline; besides, this secretion is strengthened by the adrenaline response (DeFronzo et al. 1980).

To incorporate FFA dynamcs into counterregulation, the model proposed by A. Roy (Roy and Parker 2006b), which extends Bergman minimal model with FFA,

was considered. Roy's model was then extended with adrenaline secretion and action and the relationship between FFA and adrenaline. Hence, the model was modified as the subsequent equations show. The reader is referred to Section 4.3 for the presentation of the Roy model on which this work is based on.

The equations of insulin (4.1) and remote insulin (4.2) compartments remain unmodified from the Bergman Minimal model as follows:

$$\dot{I}(t) = -nI(t) + \frac{u_1(t)}{Vol_1} \tag{5.48}$$

$$\dot{X}(t) = -p_2 X(t) + p_3 I(t) \tag{5.49}$$

where u_1 (μU/min) is the i.v. insulin infusion, n the rate of disappearance from I (μU/mL); p_3 represents the kinetic parameter that governs the rate of appearance of insulin in the compartment X (μU/mL), and p_2 (min^{-1}) is the kinetic parameter that governs the rate of disappearance from X.

About the FFA dynamics, the remote insulin concentration promoting FFA storage and utilization (Y), and the remote FFA concentration which affects glucose uptake (Z) are taken from the Roy A. model (Roy and Parker 2006b) without any modifications:

$$\dot{Y}(t) = -p_{F2} Y(t) + p_{F3} I(t) \tag{5.50}$$

$$\dot{Z}(t) = k_2 \left(Z_b - Z(t)\right) + k_1 \left(F(t) - F_b\right) \tag{5.51}$$

where k_1 (min^{-1}) and k_2 (min^{-1}) modulate the remote FFA concentration effect; p_{F2} (min^{-1}) and p_{F3} (min^{-1}) are the rate constants representing plasma FFA concentration with insulin influence; and F_b (μmol/L) and Z_b (μmol/L) are the basal values concentration of the F (μmol/L) and Z (μmol/L) compartments respectively.

The incorporation of adrenaline response and FFA dynamics into the model was based on: 1) a modification of glucose dynamics by the addition of the direct effect of the adrenaline deviation from its basal value, i.e. $p_a \cdot A_d(t)$ (as done in Section 5.5); and, 2) a modification of FFA dynamics adding the adrenaline contribution to its secretion mechanisms (as a substitute of the paradoxical term in Section 5.5). The second part was carried out by means of the incorporation of two terms which depend on the deviation of adrenaline concentrations from the basal adrenaline value when glucose is below the given threshold G_{th2} (always within hypoglycaemic range and greater than G_{th}), i.e. $k_{1w} \cdot A(t) \cdot \max(G_{th2} - G(t), 0)$; and, the adrenaline rate of change, $k_{2w} \cdot F(t) \cdot dA(t)/dt$. k_{1w} (μL·pg^{-1}·min^{-1}) is the kinetic parameter of the adrenaline effect on the FFA secretion (lipolysis), and

k_{2w} (mL/pg) is defined as the parameter which controls the effect of the adrenaline rate of change in FFA dynamics. This term incorporates the effect of the rate of change of the plasma adrenaline on FFA secretion so that lypolysis increase and, then, the increase of substrates for gluconeogenesis is promoted in the onset of the counterregulatory response due to an emergency situation (DeFronzo et al. 1980). These considerations modified the original formulations as follows:

$$\dot{F}(t) = -p_7F(t) - p_8Y(t)F(t) + p_9(G)F(t)G(t) + p_7F_b - p_9(G)F_bG_b + \frac{u_3(t)}{Vol_F} + k_{w1}A(t)\max\left(G_{th2} - G(t), 0\right) + k_{w2}F(t)\frac{dA(t)}{dt} \tag{5.52}$$

$$\dot{G}(t) = -p_1G(t) - X(t)G(t) + p_6Z(t)G(t) + X_bG_b + \frac{u_2(t)}{Vol_G} + p_aA_d(t) \tag{5.53}$$

where p_1 (min^{-1}) is the rate at which glucose is removed from the plasma space independently of the insulin influence; $u_2(t)$ is the external glucose infusion rate ($\text{mg}\cdot\text{dL}^{-1}\cdot\text{min}^{-1}$); Vol_G (dL) is the glucose distribution space; p_6 ($\text{min}^{-1}\cdot\mu\text{mol}^{-1}$) is the constant rate that represents the effect of plasma FFA on glucose uptake, X_b is the basal insulin of the insulin remote compartment; p_7 (min^{-1}) the constant rate representing plasma FFA concentration without insulin influence (taken from adipose tissue and periphery); $X(t)G(t)$ represents glucose uptake under the influence of insulin; $Z(t)G(t)$ represents glucose production under the influence of FFA; G_b is the basal glucose concentrations; $A(t)$ is the adrenaline concentration (pg/mL); $A_d(t)$ is the deviation of adrenaline concentration from its basal value A_{basal} (pg/mL); and p_9 (G) is the lipolytic effect of glucose obtained by:

$$p_9(G) = 0.00021e^{-(0.0055\cdot G)}. \tag{5.54}$$

Lastly, the adrenaline secretion model developed in Section 5.4, was included as well. The corresponding equations of the model are the following ones:

$$\dot{Q}_1(t) = -k_{a1}Q_1(t) + \beta_1u_a(t) \tag{5.55}$$

$$\dot{Q}_2(t) = -k_{a1}\left(Q_1(t) - Q_2(t)\right) \tag{5.56}$$

$$\dot{Q}_3(t) = -k_{a1}Q_2(t) - k_eQ_3(t) + k_{a2}Q_4(t) \tag{5.57}$$

$$\dot{Q}_4(t) = -k_{a2}Q_4(t) + \beta_2u_a(t) \tag{5.58}$$

$$u_a(t) = \begin{cases} 0 & G(t) > G_{th} \\ G_{th} - G(t) & G(t) \leq G_{th} \end{cases} \tag{5.59}$$

$$A_d(t) = \begin{cases} 0 & G(t) > G_{th} \\ \dfrac{Q_3(t)}{Vol_A} & G(t) \leq G_{th} \end{cases} \tag{5.60}$$

$$A(t) = \begin{cases} A_{basal} & G_(t) > G_{th} \\ A_d(t) + A_{basal} & G(t) \leq G_{th} \end{cases} \tag{5.61}$$

where Vol_A is the distribution volume of adrenaline (L); G_{th} the glucose concentration value that activates the counterregulatory response of adrenaline; $u_a(t)$ the glucose deviation from the activation threshold G_{th} (glucose does not affect adrenaline secretion when above this threshold); $Q_3(t)$ is the measurement compartment of adrenaline mass; rest of compartments, $Q_1(t)$, $Q_2(t)$, and $Q_4(t)$, define the dynamics of each secretion phase; β_1 and β_2 represent the gain of physiological response; k_{a1} and k_{a2} are transfer rate constants between compartments; and k_e is adrenaline rate of disappearance. Finally, it worth to note that X_b is considered as a equilibrium value of the insulin remote compartment defined by $p_3/p_2 \cdot I_b$. Likewise, Z_b was taken as $(k_1 F_b)/k_2$.

5.6.1 Model identification

A scheme of the system which relates each compartment of the complete model proposed is shown in Figure 5.21. Given the complexity of the model, identifiability and computational issues arise when model inputs and plasma measurements of glucose, FFA, adrenaline and insulin are considered. For this reason, the model is divided into three unit-processes of Adrenaline, FFA and Glucose (Figure 5.22). Thus, the parameters that are responsible of the dynamics of each unit were identified from individual data with a forcing function strategy (Cobelli and Carson 2008). It means that some variables were considered as the input of the unit process (although these are not the inputs of the model) and were assumed to be known without error.

Unit 1. FFA subsystem

FFA submodel is composed of two compartments (Y and F) and the corresponding equations are (5.50) and (5.52). In order to estimate the parameters, measurements of plasma insulin ($I(t)$), plasma glucose ($G(t)$) and plasma adrenaline concentration ($A(t)$) are considered as the model inputs. Then, the equilibrium point, for a given basal plasma insulin concentration (I^*), basal adrenaline concentration (A^*), and glucose concentration (G^*), is given by:

$$Y(0) = I^* \frac{p_{F3}}{p_{F2}}; \quad F(0) = \frac{F_b \left(p_7 - p_9(G^*)\right) G_b}{p_7 + I^* \dfrac{p_{F3}}{p_{F2}} - p_9(G^*)}. \tag{5.62}$$

Initially, an adrenaline remote compartment was considered, but the quick influence of this hormone in the FFA dynamics forced to remove it. By contrast, this intermediate compartment (Y) does exist in the insulin-FFA relationship.

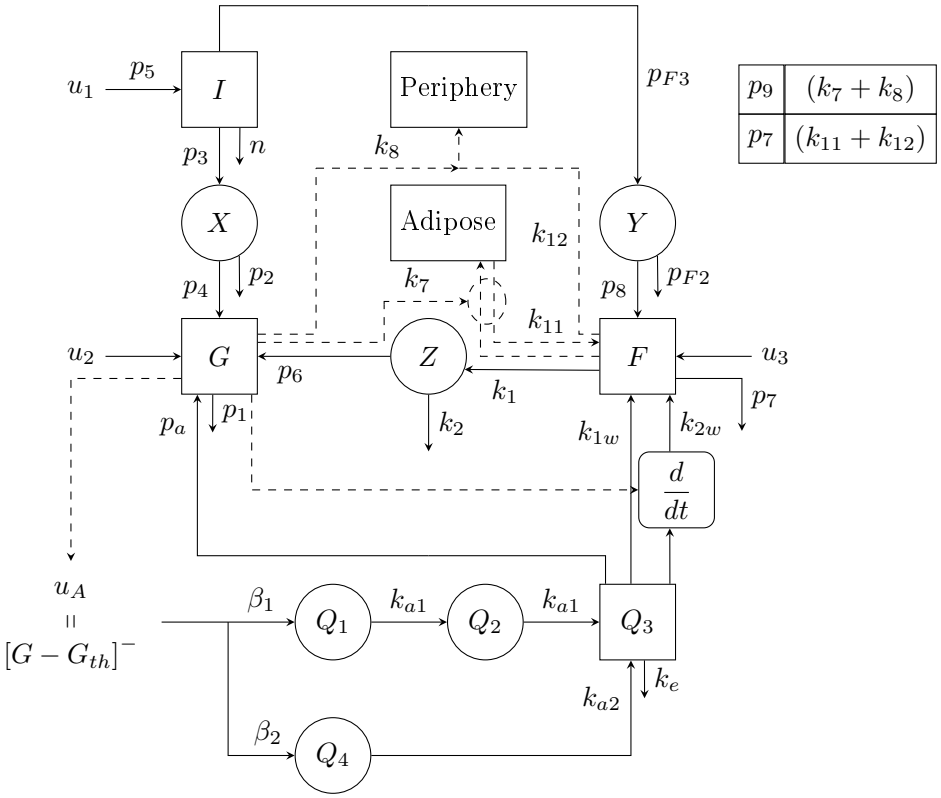

Figure 5.21: Modification of Model diagram based on Bergman Minimal Model, FFA dynamics and adrenaline counterregulatory behaviour.

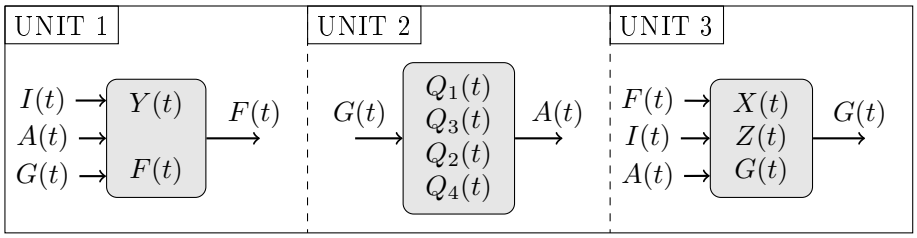

Figure 5.22: Unit processes division. Unit 1: FFA subsystem; Unit 2: Adrenaline subsystem; and, Unit 3: Glucose subsystem.

To reduce identification issues, the parameters estimation process was divided into two phases. The first one took into account the isolated influence of plasma insulin; this implied considering only the euglycaemic glucose profiles since the counterregulatory response has not yet started in this phase. It means that, according to the protocol, the considered data was the data between time -30 and time 120min; and between time 270 and time 330; and the equation corresponding to the output F, in this phase was considered as:

$$\begin{aligned}\dot{F}_{phase1}(t) = &- p_7 F_{phase1}(t) - Y(t)F_{phase1}(t) + p_9(G)F_{phase1}(t)G(t) + p_7 F_b \\ &- p_9(G)F_b G_b + \frac{u_3(t)}{Vol_F}.\end{aligned} \tag{5.63}$$

Therefore, the equations included in the identification process were (5.50) and (5.63), and the estimated parameters vector in this phase, $p_{U1_{phase1}}$ resulted in:

$$p_{U1_{phase1}} = [p_7, p_{F2}, p_{F3}, F_b]\,. \tag{5.64}$$

Regarding the second phase, complete profiles of glucose concentrations were considered, i.e. from time -30 to time 330 min in order to estimate the parameters related to FFA and adrenaline interaction. To this end, equations (5.50) and (5.52) were used, i.e.,

$$\begin{aligned}\dot{F}_{phase2}(t) = &- p_7 F_{phase2}(t) - Y(t)F_{phase2}(t) + p_9(G)F_{phase2}(t)G(t) + p_7 F_b \\ &- p_9(G)F_b G_b + \frac{u_3(t)}{Vol_F} + k_{w1}A(t)\max\left(G_{th2} - G(t), 0\right) \\ &+ k_{w2}F_{phase2}(t)\frac{A(t)}{dt}.\end{aligned} \tag{5.65}$$

Adrenaline concentration was considered as a measurement; and the value of parameters that were estimated in the previous phase were included as known parameters. Thus, the estimated parameters vector in this phase, $p_{U1_{phase2}}$ was:

$$p_{U1_{phase2}} = [k_{1w}, k_{2w}, G_{th2}]\,. \tag{5.66}$$

Remark that there was not exogenous infusion of FFA in the data used. Thus, $u_3(t)$ was null during the whole study for all subjects and Vol_F was not estimated.

The identification process was carried out with the global optimization algorithm CMA-ES. Besides, the estimation was individual for each clamp study considered. The parameter estimator in each phase was:

$$\hat{p}_{U1_{phase1}} = \underset{p_{U1_{phase1}}}{\arg\min} \sum_{i=1}^{n} \omega_i \left(\hat{F}_{phase1_i}\left(p_{U1_{phase1}}, t\right) - F_{phase1_i}(t)\right)^2, \tag{5.67}$$

Params.	Mean (SD)	Meadian [IQR]	Unit
p_7	0.058 (0.010)	0.055 [0.0505; 0.065]	min^{-1}
p_{F2}	1.330 (0.569)	1.381 [0.0.750; 1.781]	min^{-1}
p_{F3}	5.006 (2.256)	4.943 [2.971; 7.320]	10^{-4}min^{-1}
F_b	239.327 (110.645)	230.972 [170.144; 289.681]	μmol/L
G_b	83.649 (17.313)	87.145 [78.268; 94.050]	mg/dL
k_{1w}	0.079 (0.050)	0.073 [0.039; 0.110]	$(\mu\text{L}\cdot\text{pg}^{-1}\text{min}^{-1})$
k_{2w}	2.397 (0.694)	1.923 [1.132; 2.389]	mL/pg
G_{th2}	64.6876 (12.3778)	58.0549 [59.9370; 76.49148]	mg/dL

Table 5.6: Parameter estimation of unit 1.

#	R2 (%)	NRMSE	MAPE (%)
Mean (SD)	86.13 (6.23)	0.081 (0.031)	24.12(6.69)
Median [IQR	84.67 [84.15;91.59]	0.0758[0.066;0.0984]	25.32[18.94;28.35]

Table 5.7: Statistical metrics of unit 1 (goodness-of-fit)

where

$$\omega_i = \begin{cases} 1 & \text{if } t_i \leq 120 \\ 0 & 120 < t < 270 \\ 1 & \text{otherwise} \end{cases} \tag{5.68}$$

$$\hat{p}_{U1_{phase2}} = \underset{p_{U1_{phase2}}}{\arg\min} \sum_{i=1}^{n} \left(\hat{F}_{phase2_i} \left(p_{U1_{phase2}}, t \right) - F_{phase2_i}(t) \right)^2, \tag{5.69}$$

where $\hat{F}_{phase1_i}$ is the predicted plasma FFA value at instant i, F_{phase1_i} is the measured value and n is the number of data points. $\hat{p}_{U1_{phase1}}$ and $\hat{p}_{U1_{phase2}}$ are the estimated parameters vectors; and, $p_{U1_{phase1}}$ and $p_{U1_{phase2}}$ are the parameters vector. ω_i is the i-th element of the weight vector.

The results of the identification routine for the parameters of the model are shown in Table 5.6. Furthermore, the statistical characteristics of the goodness of fit of the model adjustment are presented in Table 5.7. Notice that the similar values of G_{th2} to the values of parameter G_{b2} from the model presented in previous section ($p = 0.978$) demonstrates that the effect observed previously can be explained with the adrenaline indirect effect through the FFA.

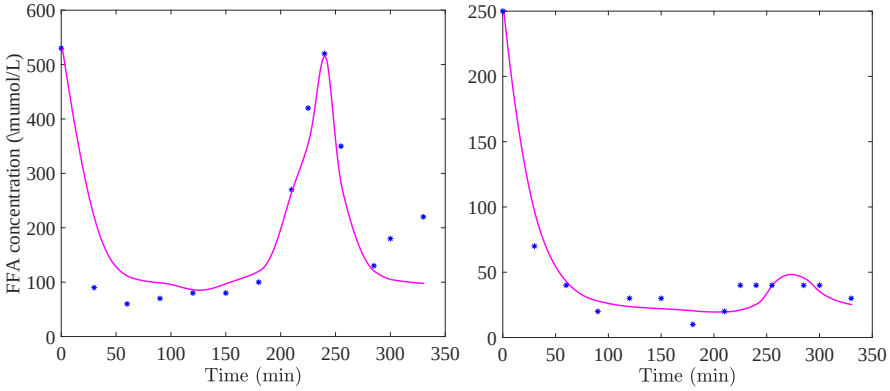

Figure 5.23: Unit 1 estimation outcomes. Measured (blue) vs estimated FFA concentration (magenta) during Low (left) and High (right) insulin clamp.

Quantitatively, model predictions were consistently within on standard deviation of the mean of experimental data. The model was able to reproduce the two phases of the FFA behaviour. The basal state is managed by the insulin concentration which remains constant during the clamp whereas the FFA secretion due to the lower glucose concentrations were successfully fitted with the contribution of adrenaline effect. In Figure 5.23, the good fitting of the Unit 1 can be observed; however, it is important to note that in the last part of the clamp, the submodel was less accurate in the latest new basal concentrations of FFA. It could be explained by the lack of FFA plasma-interstitium equilibrium.

The unit 1 or FFA subsystem includes the effect of the adrenaline counterregulatory response on FFA secretion. Thus, this implies an indirect effect on glucose concentration through FFA.

During the identification process, the need for including another term in addition to the insulin impact on FFA secretion, which was reported and demonstrated previously (Roy and Parker 2006b), was proved with the improvement achieved in the glucose concentration fitting due to adrenaline effect addition. Periwal et al. 2008 suggested that the physiology of glucose and FFA regulation may have unknown mechanisms. This hypothesis could be supported by the above results where the unknown mechanism could be identified as the counterregulatory response or the interaction between Glucose-Adrenaline-FFA.

The relationship between insulin and FFA is known (Li et al. 2016), insulin reduces the blood glucose levels with the promotion of glucose uptake, decreases FFA secretion in the liver, and increases glucose utilization. During hypoglycaemia, as

FFA secretion occurs in an emergency situation, the systemic increase of glucose is not manifested since the glucose utilization increase in order to achieve "emergency fuel" to face with the hypoglycaemic conditions and maintain the central nervous system with enough substrate. Then, this paradoxical effect appears.In addition, counterregulatory response is also risen. It means that the secretion mechanism of FFA is not just dependent or modulated by insulin; but counterregulatory response (adrenaline) also has an important role, specifically during the hypoglycemic range.

FFA concentrations are managed by insulin until hypoglycaemia occurs and also by adrenaline concentration when glucose concentration is below a threshold (G_{b2}). From this glucose value, adrenaline promotes the FFA secretion which is also enhanced by the rate of change of adrenaline concentration (because of quick response requirement).

Unit 2. Adrenaline subsystem

The adrenaline block is explained by four compartments which are well defined by the adrenaline secretion model presented and successfully identified in Section 5.4. Table B.1 summarizes the value of the parameters of this unit.

The adrenaline subsystem results in a compartmental model which was able to reproduce the biphasic dynamic of adrenaline secretion. As observed in the equations of the model, the adrenaline concentration depends on glucose concentrations, being this the only input of the submodel.

Unit 3. Glucose subsystem

The three compartmental submodel of unit 3 was also identified on individual plasma glucose with the forcing function strategy: plasma insulin, plasma FFA and plasma adrenaline concentration are the inputs of the system and plasma glucose concentration is the output. These variables were assumed to be known without error. To avoid identification problems, as occurred in unit 1, the parameters of the system were estimated gradually in different phases. Considering the system inputs and their expected effect in plasma glucose concentration, three steps were carried out.

The first evaluated group of parameters was the parameters of the model without the proposed extensions. It was addressed during the euglycaemic period of the clamp in order to exclude the effect of the counterregulatory mechanisms (adrenaline and FFA effects) on glycaemic dynamics. That is, the considered data

was, according to the protocol, the data between time -30 and time 120 min; and between time 270 and time 330; and the equation corresponding to the output G, in this phase (phase$_1$)was considered as:

$$\dot{G}_{phase1}(t) = -p_1 G_{phase1}(t) - X(t)G_{phase1}(t) + p_1 G_b + \frac{u_2(t)}{Vol_G}. \tag{5.70}$$

Therefore, the equations included in the identification process were (5.49), (5.51), and (5.53), and the equilibrium conditions for a given basal insulin (I^*), basal FFA concentration (F^*), and basal adrenaline (A^*), were:

$$Z(0) = \frac{k_1 F^*}{k_2}; \quad X(0) = \frac{p_3}{p_2} I^*; \quad G(0) = \frac{G_b}{p_1 - p_6 \dfrac{k_1}{k_2} F^*}. \tag{5.71}$$

The estimated parameters vector in this phase, $p_{U3_{phase1}}$ resulted in:

$$p_{U3_{phase1}} = [p_1, p_2, p_3, G_b, Vol_G]\,. \tag{5.72}$$

However, the parameter G_b was estimated in the subprocess unit 1. Hence, G_b is considered as known parameter, and then the definitive estimated parameters vector is:

$$p_{U3_{phase1}} = [p_1, p_2, p_3, Vol_G]\,. \tag{5.73}$$

The second step was the evaluation of the influence of the FFA into glucose dynamics during hypoglycaemia (phase 2). As shown before, it was based on the addition of several terms and compartments to the Bergman minimal model equations. In that case, measurements from all study (euglycaemia, hypoglycaemia and recovery) were used and the value of the parameters estimated in the previous step ($p_{U3_{phase1}}$) were considered known parameters. As only the FFA contribution was taken into account in this phase, the corresponding equation to the output G was:

$$\dot{G}_{phase2}(t) = -p_1 G_{phase2}(t) - X(t)G_{phase2}(t) + p_6 Z(t) G_{phase2}(t) + X_b G_b + \frac{u_2(t)}{Vol_G}. \tag{5.74}$$

Thus, the equations included in the identification process were (5.49), (5.51), (5.53), and (5.71). The estimated parameters vector in this phase, $p_{U3_{phase2}}$ resulted in:

$$p_{U3_{phase2}} = [p_6, k_1, k_2, F_b]\,. \tag{5.75}$$

Nevertheless, parameter F_b was already estimated in the unit 1. Then, the definitive estimated parameters vector was:

$$p_{U3_{phase2}} = [p_6, k_1, k_2]\,. \tag{5.76}$$

Notice that the indirect effect of the adrenaline was also considered by means the promotion of FFA secretion.

Finally, the third stage (phase 3) addressed the complete extended model through the addition of the direct adrenaline effect on glucose dynamics to the previous phase. Therefore, the corresponding equation to the output $G(t)$ was the complete equation (5.53), i.e. $G_{phase3}(t) = G(t)$, then,

$$\begin{aligned}\dot{G}_{phase3}(t) = &- p_1 G_{phase3}(t) - X(t)G_{phase3}(t) + p_6 Z(t) G_{phase3}(t) + X_b G_b \\ &+ \frac{u_2(t)}{Vol_G} + p_a A_d(t);\end{aligned} \tag{5.77}$$

and the parameter in this phase, $p_{U3_{phase3}}$ was:

$$p_{U3_{phase3}} = p_a. \tag{5.78}$$

The identification process was carried out with the global optimization algorithm CMA-ES. Besides, the estimation was individual for each clamp study considered. The parameter estimator in each phase was:

$$\hat{p}_{U3_{phase1}} = \underset{p_{U3_{phase1}}}{\arg\min} \sum_{i=1}^{n} \omega_i \left(\hat{G}_{phase1_i} \left(p_{U3_{phase1}}, t \right) - G_{phase1_i}(t) \right)^2, \tag{5.79}$$

where

$$\omega_i = \begin{cases} 1 & \text{if } t \leq 120 \\ 0 & 120 < t < 270 \\ 0 & \text{otherwise} \end{cases}. \tag{5.80}$$

$$\hat{p}_{U3_{phase2}} = \underset{p_{U3_{phase2}}}{\arg\min} \sum_{i=1}^{n} \left(\hat{G}_{phase2_i} \left(p_{U3_{phase2}}, t \right) - G_{phase2_i}(t) \right)^2, \tag{5.81}$$

$$\hat{p}_{U3_{phase3}} = \underset{p_{U3_{phase3}}}{\arg\min} \sum_{i=1}^{n} \left(\hat{G}_{phase3_i} \left(p_{U3_{phase3}}, t \right) - G_{phase3_i}(t) \right)^2, \tag{5.82}$$

where $\hat{G}_{phase1_i}$ is the predicted plasma glucose value at instant t, G_{phase1_i} is the measured value and n is the number of data points. $\hat{p}_{U3_{phase1}}$, $\hat{p}_{U3_{phase2}}$, and $\hat{p}_{U3_{phase2}}$ are the estimated parameters vectors; and, $p_{U3_{phase1}}$, $p_{U3_{phase2}}$, and $p_{U3_{phase3}}$ are the parameters vector. ω_i is the i-th element of the weight vector.

The values of the identified parameters of the glucose subsystem, unit 3, are provided by Table 5.8. Moreover, the goodness of fit of the model adjustments is shown in Table 5.9.

Params.	Mean (SD)	Meadian [IQR]	Unit
$p1$	0.064(0.114)	0.014 [0.009; 0.034]	min^{-1}
p_2	0.040(0.032)	0.026 [0.014; 0.034]	min^{-1}
p_3	5.452(5.790)	3.332 [2.080; 6.67]	$10^{-5}\,\text{min}^{-1}$
p_6	6.0996(4.0837)	3.4600 [2.4643; 7.7558]	$10^{-5}(\text{min}\cdot\mu\text{mol})^{-1}$
Vol_G	122.845(25.526)	119.729 [105.916; 140.229]	dL
p_a	0.064(0.231)	0.043 [0.011; 0.023]	$10^{7}\,\text{min}^{-1}$

Table 5.8: Parameter estimation of unit 3.

#	R2 (%)	NRMSE	MAPE (%)
Mean (SD)	88.29(8.29)	0.094 (0.034)	5.46 (2.91))
Median [IQR]	90.03 [83.26;94.68]	0.089 [0.065;0.109]	5.14 [4.02;5.70]

Table 5.9: Statistical metrics of unit 3 (goodness-of-fit).

In addition, Figure 5.24 exposes an example of the fitting model with the glucose experimental data at the different phases of the identification process: (1) considering only the FFA contribution, and (2) adding both FFA and adrenaline contribution.

As expected in the unit 3 evaluation, adrenaline response plays an essential role in the glucose kinetics during hypoglycaemia. Without considering the counterregulatory mechanisms (phase 1), the predicted glucose completely failed to match experimental data during hypoglycaemia period since glucose concentration was overestimated. When FFA secretion was considered, the fitting improved; nevertheless, some compensatory additional factor was needed as it can be observed in Figure 5.24. For this reason, the addition of the direct effect of adrenaline secretion to the model improved the model performance during hypoglycaemia, and the glucose behaviour was also better explained. Besides, the goodness of fit of glycaemic profile was greater during the whole clamp (R2=$88.30 \pm 8.20\%$, MAPE $= 5.65 \pm 1.83$).

In addition, the residual analysis showed that the residual error from the estimation was random and unpredictable. The analysis of residual correlation with Ljung-Box Q-test run proved that they were not autocorrelated ($p > 0.05$ for all studies parameter estimations). Besides, the Wald-Wolfowitz run tests also proved the residual independence across all individual estimations ($p > 0.05$ for

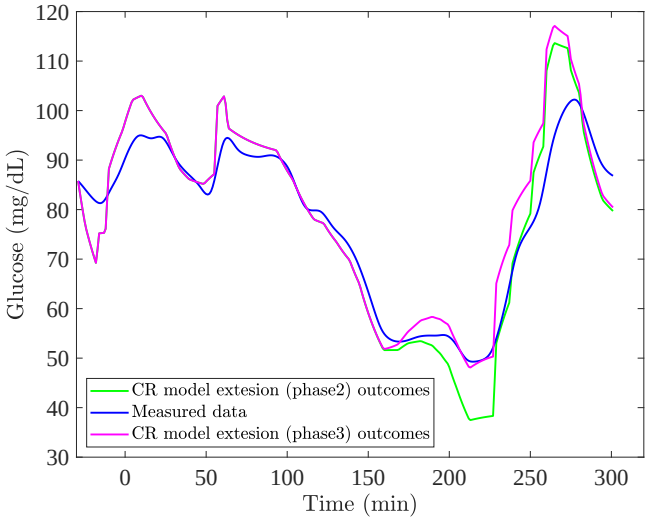

Figure 5.24: Unit 3 fit in clamp study #13 resulting in the phase 2 of the identification process (green line) and in phase 3 (magenta line).

all studies). Overall, it means that the estimated values of the model parameters are not likely to be biased. Individual p-values of each test are shown in Appendix B.2 along with the individual parameters value for each clamp study.

The novel terms of the model represent the straight counterregulatory response along with the increase in glucose clearance promoted by hypoglycaemia (Clutter et al. 1980), which is activated when glucose level is below a given threshold G_{th2} (this value is always inside of hypoglycaemic range and greater than G_{th}). The increase in glucose clearance leads to an increment of the glucose utilization besides of a simultaneous promotion of the FFA secretion in order to compensate the rising in glucose uptake while glucose continues decreasing.

These findings are supported by the physiological behaviour since the effect of adrenaline in glucose concentration is demonstrated by several studies (C.G. Fanelli et al. 1992) and the impact of this hormone in the FFA secretion, especially during hypoglycaemia.

5.6.2 Model comparison with other model approaches

The physiological model approach presented in this chapter was compared to both the Bergman Minimal Model (Bergman et al. 1981) and the Minimal Model extended with the functional approach suggested by Dalla Man et al. 2014, which were introduced in Chapter 4, and used in the UVA-Padova simulator. The core of both approaches is the Bergman Minimal model; besides an important goal of this work is explaining the functional approach of Dalla Man by means of the modelling of physiological interactions. For this reason, the following comparisons will show the improvements achieved with both extensions, and the performance of the functional approach.

Simulations were carried out for each model using the experimental data from the clamp. Outcomes from each model were evaluated by several metrics: apart from the metrics computed to assess the goodness of fit of the model (R2, NRSME, and MAPE), outcome metrics such percentage of values in hypoglycaemia and area under the curve (AUC) for hypoglycaemic values were calculated in both the measured data and each model predicted data. Then, the difference between AUCs of each model predicted and measured glucose concentration was calculated (dAUC), i.e., $dAUC = AUC_{measurement} - AUC_{estimation}$, where $AUC_{measurement}$ is the area under the curve of the experimental data and $AUC_{estimation}$ is the one calculated with the estimated data. Finally, a Kruskal-Wallis test was used to assess the statistical differences between the several approaches and a subsequent post-hoc analysis showed where the differences were. The significance level set at p-value=0.05.

Table 5.10 summarizes the statistical indicators calculated for each model in order to compare them during hypoglycaemia period. Additionally, Figure 5.25 shows a graphical comparison between the estimated glucose concentration for each model. Here, the glucose profile estimation is represented for two random clamp studies.

From metrics showed in Table 5.10, it is important to note that the 18.19% of hypoglycaemic values were unnoticed by the Minimal Model compared to the 6.93% and 7.58% of the Dalla Man and our approach respectively. Moreover, the average of dAUC with negative value demonstrated a glucose overestimation during hypoglycaemia.

Statistical analysis of the considered metrics shown that there are significant differences between approaches ($p = 0.005$, $p = 0.006$ and $p = 0.001$, $p = 0.006$ for MAPE, R2, dAUC, and unnoticed hypoglycaemia respectively). Post hoc analysis proved that Bergman minimal model is different from the other approaches ($p < 0.05$ in all comparisons). Nevertheless, there were not statistical differ-

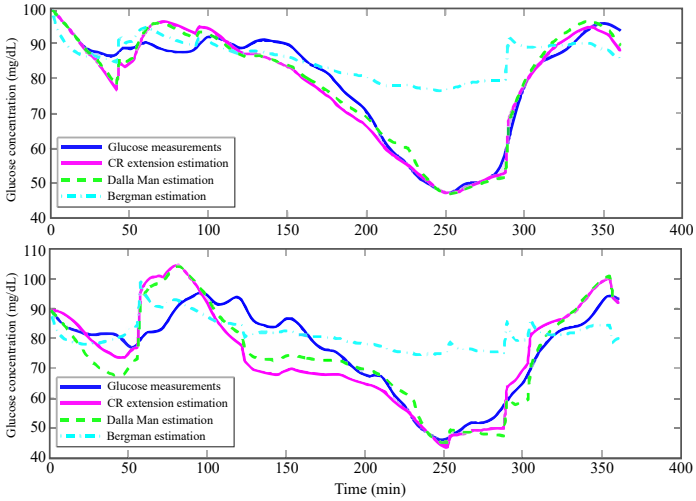

Figure 5.25: Comparison between the physiological and functional approaches (Bergman Minimal Model, Dalla Man approach, physiological model with counterregulatory response extension).

ences between the Dalla Man functional approach and our physiological approach ($p = 0.452$, $p = 0.091$, $p = 0.058$, and $p = 0.784$; MAPE, R2, dAUC, and unnoticed hypoglycaemia respectively).

Looking at comparisons, the functional approach and our physiological approach work in a similar way (both behaviours are not statistically different). It means

Metrics (hypoglycaemic phase)	**Approach**		
	Bergman et al. 1981	**Dalla Man et al. 2014**	**Our approach**
MAPE (%)	25.99(37.63)†	5.20 (2.08)*	5.37 (2.08)*
R2(%)	54.33(34.12)†	79.56 (20.85)*	77.88 (15.41)*
dAUC (mg/dL)	−362.76(462.78)†	-8.68 (290.61)*	8.38 (271.24) *
Unnoticed hypoglycaemic values (%)	18.19(26.33)†	6.93 (12.10)*	7.58 (13.32)*

(*) Significantly different from Bergman Minimal Model.
(†) Significantly different from Dalla Man Model.

Table 5.10: Model approaches comparison.

that both perspectives could be equivalent in terms of outcomes since both were capable of reproducing the hypoglycaemic periods. Thus, our proposal is able to link the mathematical terms with physiological relationships and behaviours. Indeed, our model allows to provide a physiological explanation to the functional approach, in principle paradoxical, used in the UVA-Padova simulator, which will be used in clinical validations in Chapter 7.

5.7 Conclusions

In this chapter, an exhaustive study of physiology was carried out and the better understanding of counterregulatory mechanisms were achieved. From this study, adrenaline was found as the main counterregulatory hormone during hypoglycaemia events since glucagon delivery is practically suppressed in T1D patients. The assessment of the adrenaline secretion and action were also conducted in order to extend the Bergman Minimal Model.

From the adrenaline action model, a paradoxical increment of glucose utilization during hypoglycaemia was observed. This led to find some physiological explanation to the phenomenon. Finally, the consideration of FFA mechanisms, which are involved also in the hypoglycaemia avoidance, provided a suitable model approach.

Therefore, an extension of Bergman Minimal Model was proposed based on adrenaline response as the main counterregulation line. The effect of adrenaline was included as a direct effect on glucose concentration and indirectly through the influence on FFA secretion. In addition, the adrenaline secretion model was also incorporated to the model extension presented.

The goodness of fit of the model showed an acceptable performance and an improvement in hypoglycaemia reproduction compared to the Minimal Model. Moreover, the features of the physiological approach proposed in this work were compared with the functional approach in UVA-Padova simulator (i.e. a risk function explanation of hypoglycaemic glucose levels) and both worked similarly. It means that our proposal is able to associate the mathematical terms with physiological mechanisms and hormones and metabolites interactions.

The main limitation is the variability of the adrenaline response, even in the same subject, which may be due to occurrence of previous hypoglycaemic episodes affecting counterregulatory response. The differences between the amplitude of the adrenaline responses could also be due to the large adrenaline sampling period (30min) since this fact could cause that the real adrenaline peak was not exactly registered. Nevertheless, increasing the sampling frequency was not possible since

patient safe blood extraction volume have to be guaranteed. However, this limitation affects mainly to the gain of the system since the morphology (i.e. the structure of the system) is not affected by such variability. However, it is considered that this has no major impact according to the model objectives, which were to derive a physiological explanation of hypoglycaemia, and above all, the paradoxe introduced by the functional modelling carried out in the UVa-Padova simulator which will be used for in silico evaluation of controllers derived in Chapter 7.

Other limitation could be the reduced number of subjects and the duration of the clamp. For this reason, a future work could be a validation with experimental data from clinical studies with longer duration and greater number of participants. It would provide subjects with a broader range of adrenaline response variation and a better representation of T1D population. Nevertheless, results obtained with the Minimal Model extended with counterregulatory response are successful and relevant.

Chapter 6

Glucose Variability Assessment

Reduction of glucose variability, along with the avoidance of hypoglycaemia events, is a control target which must be considered during the controller design in order to improve the Artificial Pancreas performance. In literature, there are multiple indicators that are used to quantify such glucose variability. Nevertheless, these could be intrinsically affected by the intra- and inter-subject variability besides that there is not a consensus about which metrics are the most rigorous ones. In this chapter, the assessment of the performance of multiple glucose variability metrics is carried out to determine their ability to discriminate between different subjects (inter-subject variability) and attenuate the effect of within-subject variability. To this end, the discriminant ratio (DR) is used to compare them, and the relevant information from the correlation analysis is also included.

6.1 Preliminaries

Glucose variability describes within-day and between-day fluctuations in glucose concentration (intra-patient variability), and it is elevated in people with type 1 diabetes. Moreover, the glucose profiles can also greatly differ even among people with HbA1C[1] values approaching target (inter-patient variability). The

[1] The term HbA1c refers to glycated haemoglobin. By measuring glycated haemoglobin, clinicians are able to get an overall picture of what average blood sugar levels have been over a period of weeks/months. For people with diabetes this is important as the higher the HbA1c, the poorer control of blood glucose levels.

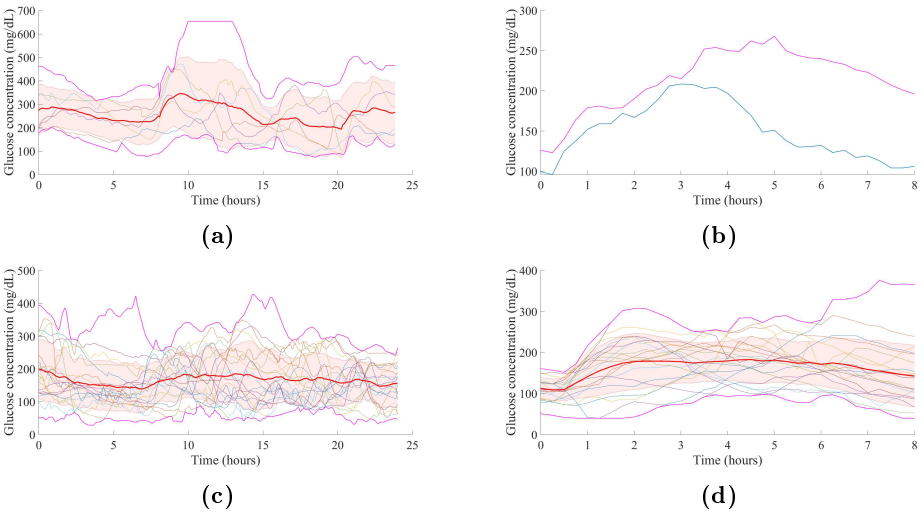

Figure 6.1: Glucose variability. (a) Daily glucose profile of one patient in 7 consecutive days; (b) Glucose profile of one patient during 8 hours in clinical trial; (c) Glucose profile of 20 patients during one day; (d) Glucose profile of 20 patients during 8 hours in clinical trial.

relevance of Glucose variability comes from the association of this factor with a higher incidence of severe hypoglycaemia in patients with type 1 diabetes (T1D) (Kilpatrick et al. 2007), besides the suggestion that glucose variability is an important component of dysglycaemia, i.e. abnormalities in blood sugar stability such as hypoglycaemia and hyperglycaemia (Monnier et al. 2008). In (Gimenez et al. 2018), the association between higher HbA1C values and increased glucose variability is demonstrated.

In order to illustrate this concept, Figure 6.1, shows the several definitions of variability mentioned above. Figure 6.1a represents the daily profile of one patient in seven consecutive days. Days have been superposed to represent more clearly the between-day fluctuations.

As observed, changes within subjects are considerable, that is, even being from the same person, glycaemia is not easily predictable. Profiles of the same patient from two different days but identical study conditions are represented in Figure 6.1b. This controlled environment, which reduces the effect of the underlying external variability factors, proves the intra-patient variability.

Figure 6.1c represents the glycaemia of 20 patients during one day. The pattern of each line is different for each other. Inter-patient variability is shown here. Nevertheless, part of this variability may be due to the differences in the meal time, the amount of carbohydrates, and physical activity or lifestyle. In order to exclude these factors, Figure 6.1d represent the profile of 20 patients during eight hours of study in the same conditions (same meal, same time, same physical activity). The differences in the glucose excursions in this Figure confirms that there are other factors that have an effect on glucose variability across the subjects since even in the same conditions, glycaemia discerns significantly. Profiles of figures 6.1b and 6.1d are taken from the study carried out by (Rossetti et al. 2017). Likewise, data of the figures 6.1a and 6.1c are taken from a Juvenile Diabetes Research Foundation (JDRF) database which is widely used in the present contribution. More details about it are given in Subsection 6.3.1.

Currently available continuous glucose monitoring (CGM) devices provide immediate feedback on the glucose concentration, and the magnitude, direction and rate of change (Kohnert et al. 2015). These measurements enable direct assessment of the dynamics of glycaemic fluctuatios and calculation of variability metrics. There are a large number of measures of glycaemic variability, including standard deviation (SD), percentage coefficient of variation (%CV), mean amplitude of glucose excursion (MAGE), mean absolute Glucose(MAG), mean of daily differences (MODD), and continuous overlapping net glycaemic action over an n-hour period (CONGAn).

Similarly, there are numerous measures of quality of glycaemic control like the Glycaemic Risk Assessment Diabetes Equation (GRADE), the Index of Glycaemic Control (IGC), the High Blood Glucose Index (HBGI), the Low Blood Glucose Index (LBGI), the Average Daily Risk Range (ADRR), Personal Glycaemic State (PGC) and percentage of time under, within and above specified glucose ranges. All of these metrics are described in Section 3.4. As an illustration, they have been calculated for the JDRF database patient #4 depicted in Figure 6.1a and shown in Table 6.1 in order to understand how each indicator gives information related to the glycaemic profile.

GLUCOSE MEAN	SD	CV	MAG	GVP (%)	LI	M-VALUE	J-INDEX	$CONGA_1$	MAGE
259.31	117.60	0.45	3.14	52.46	12.35	58.20	142.06	4.25	202.75

ADDR	RI	LGBI	HBGI	GRADE	%GRADE HYPO	IGC	PGS	PTIR	PT HYPO	PT HYPER
62.16	26.64	0.13	26.52	19.76	0.00	7.01	21.50	29.60	0.00	70.40

Table 6.1: Metrics for subject #4 of Figure 6.1a.

According to the values of the calculated metrics, all of them suggest that the subject has a poor glycaemic control and a moderate-high variability. This affirmation is based on: ADDR $>$ 40 (ADDR $<$ 30 is Low risk; 20 $\leq$ ADDR $\leq$ 40 is moderate risk; ADDR $>$ 40 is high risk (Hill et al. 2007)); M-VALUE $\geq$32 ($0 \leq M \leq 18$ is good control, $19 \leq M \leq 31$ is fair control, and $32 \leq M$ is poor control (Service 2013)); J-INDEX $>$ 40 ($10 \leq J \leq 20$ is ideal control, $20 < J \leq 30$ is good control, $30 < J \leq 40$ is poor control, and J $>$ 40 is lack of control (Service 2013)); GRADE $>$ 5 (GRADE $\leq$ 5 is good control, besides 50 is the maximum value for GRADE representing this value a bad control). Looking at the time in hyperglycaemia, the reason of this bad control is that the glycaemia is above the target control. About variability, GVP are around the 50% which is a significant value of variability. Besides, MAG is not around zero which confirms the presence of glucose variability.

As seen, the assessment of glucose variability is a specific area where several methods are at hand to the researcher. The advantages, limitations, and interrelationships among the available mentioned methods have been described previously (Rodbard 2009a). However, a gold standard measurement has not been identified, limiting efforts to demonstrate a relationship between variability and clinically relevant micro- and macrovascular diabetes complications, and making heterogeneous the analysis of the glycaemic control outcomes.

In artificial pancreas context, these metrics are used as indices that describe the controller's performance in T1D patients, specifically the glucose variability improvements. Nevertheless, a consensus on which is the recommendable indicator is necessary since the comparison between controllers would be easier and the definition of a good controller more robust.

A set of basic outcome measures was identified in (Maahs et al. 2016), but it was focused mostly on the glycaemic range control that includes time spent in desired ranges (70-140 mg and 70-180 mg(dL) as well as time in hypo- (defining three different thresholds: 50, 60, and 70 mg/dL) and hyperglycaemia (defining also three different thresholds: 180, 250, and 300mg/dL), mean glucose, standard deviation, coefficient of variation, severe hypoglycaemic events, total daily dose of insulin and total daily dose of glucagon or other hormones. However, as said before, this is not enough and a consensus remains challenging; a concise definition of desired range is recommendable besides that the definition of consistent indicators to measure the glucose variability must also be considered.

Discriminant ratios suggest which test is better able to distinguish individual variation within a population and have been used previously to compare insulin sensitivity measures by calculating the ratio of the underlying between-subject stan-

dard deviation to the within-subject standard deviation (Hermans et al. 1999; Verkest et al. 2010). Hence, in the work here presented, we have applied discriminant ratios to commonly used measures of glucose variability and quality of glycaemic control in order to demonstrate which metric is the most effective at distinguishing between-subject glucose variability differences in a large population with type 1 diabetes using CGM data.

This work is organized as follows: the discriminant Ratio is introduced in Section6.2; in Section6.3, the metrics comparison is shown and the main results about it are presented; the interrelationship between metrics by means of correlation analysis is carried out in Section 6.4. Conclusions in Section 6.5 gather some final remarks.

6.2 Discriminant ratio

The Discriminant Ratio (DR) methodology compares different tests or indicators measuring the same underlying physiological variable by determining the ability of a test to discriminate between different subjects, and the comparison of discrimination between different tests (Hermans et al. 2011; Levy et al. 1999; Hermans et al. 1999). In our case, the variable under study is the glucose variability, and the different tests are the several metrics available in literature to measure it.

DR is defined as the ratio of the unbiased between-subject standard deviation (SD_u) and within-subject standard deviation (SD_w) (Hermans et al. 1999). That is,

$$DR = \frac{SD_u}{SD_w}, \tag{6.1}$$

$$SD_u = \sqrt{SD_B^2 - \frac{SD_w^2}{k}}, \tag{6.2}$$

where SD_B is the between-subject standard deviation of the metrics values, and k is the number of replicate measurements performed in each subject, i.e., the number of temporal windows considered in each subject.

The between-subject standard deviation (SD_B) is obtained as the SD of the subjects mean values calculated from the k replicates that are performed in each subject. This overestimates the underlying SD_u due to the presence of within-subject variation. Thus, it is important to adjust it using a standard formula (6.2) to yield an unbiased estimate, the SD_u.

The within-subject standard deviation (SD_w) is the variation underlying each subject which is obtained for each subject from its recordings.

Glucose temporal signal is divided into k windows or replicas in each subject; and the variability metrics are calculated for each window in each patient. Then, the following matrices are defined for each metrics:

$$X = \begin{bmatrix} x_{11} & x_{12} & \cdots & x_{1k} \\ x_{21} & x_{22} & \cdots & x_{2k} \\ \vdots & \vdots & \ddots & \vdots \\ x_{n1} & x_{n2} & \cdots & x_{nk} \end{bmatrix} \tag{6.3}$$

$$X_{mean} = \begin{bmatrix} \sum_{j=1}^{k} \frac{x_{1j}}{k} & \sum_{j=1}^{k} \frac{x_{2j}}{k} & \cdots & \sum_{j=1}^{k} \frac{x_{nj}}{k} \end{bmatrix}^T \tag{6.4}$$

where $X \in \mathbb{R}^{n \times k}$, being i-th row the i-th subject, and j-th column the j-th window. X is the metrics considered and X_{mean} is the mean of the metric obtained for each subject considering all windows.

Particularly, from matrices above, the SD_w for the i-th subject (denoted as SD_{wi}) and SD_B are calculated for each metrics as follows:

$$SD_{w_i} = \sqrt{\sum_{j=1}^{k} \frac{(x_{ij} - x_{meani})^2}{k}} \tag{6.5}$$

$$SD_B = \sqrt{\sum_{i=1}^{n} \frac{\left(\overline{X_{mean}} - x_{mean_i}\right)^2}{n}} \tag{6.6}$$

where $\overline{X_{mean}}$ is the mean of X_{mean}. Therefore, (6.1) and (6.2) are rewritten as follows:

$$DR_i = \frac{SD_{u_i}}{SD_{w_i}} \tag{6.7}$$

$$SD_{u_i} = \sqrt{SD_B^2 - \frac{SD_{w_i}^2}{k}} \tag{6.8}$$

The absolute value of DR is the mean or median (depending on the distributions) of DRs across the subjects.

Notice that the DR is calculated using the same glucose recordings in all metrics. This fact enables the proper comparison between tests (metrics) since the absolute DR values are not comparable between outcomes from different populations.

6.3 Metrics comparison

6.3.1 Data description

Data from the Juvenile Diabetes Research Foundation (JDRF) CGM study were used. The JDRF dataset is freely accessible and was obtained from the Jaeb Center for Health Research (Health Research (JCHR) 2018). The study was a 26-week randomised, parallel group, study that evaluated the impact of continuous glucose monitoring on glucose control in children and adults with T1D.

The rules to standardize the data in our work were:

- 24 weeks of complete CGM data were used for each participant although incomplete day recordings due to sensor changes were allowed.
- Data were processed each five minutes and the lack of data in a period larger than two hours was considered as a gap. Missing data were interpolated by linear method interpolation.

As a result of data normalization, 179 patients were included in the analysis (55.3% males; ages= 24.12 ± 14.60 years; HbA1c=7.44 ± 0.88%; T1D duration=14.07 ± 12.39 years).

Data from each patient were divided into windows in order to obtain the values of the different assessed metrics per window. The length of the temporal window was set at 12 days since this value was previously defined by (Neylon et al. 2014) as the minimum duration of sensor data from which glycaemic variability can be consistently evaluated.

6.3.2 Metrics assessement with DR

The glycaemic variability measures that were evaluated are: AARC; CONGA1; CV; GVP; J-INDEX; LI; MAG; MAGE; MODD; and, M-VALUE. Likewise, the quality of glycaemic control indices assessed were: ADRR; GRADE; %GRADE-Hypo; HBGI; LBGI; PGS; RI; IGC; the percentage of time between several ranges (pTIR50-140, pTIR70-180); the percentage of time below 54mg/dL (pT$<$54) and

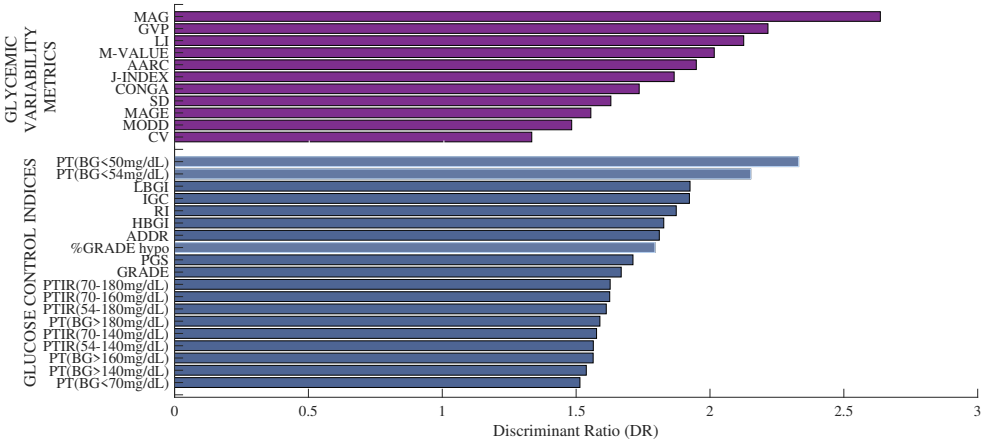

Figure 6.2: Median of DR corresponding to the evaluated Glycaemic Variability metrics and Glucose Control indices.

70mg/dL (pT<70); and, the percentage of time above 140mg/dL (pT>140) and 180mg/dL (pT>180). Previous to the analysis, the implementation of these indicators was carried out in MATLAB 2017 according to their original formulation (see appendix A). It is important to note that the M-VALUE, PGS, and IGC were calculated using the default values of their parameters, i.e. M-VALUE$_{100}$, IGC$_1$.

Each metrics was calculated in each window of each patient across the 24 weeks of data. Then, matrices (6.3) and (6.4) were defined for each metrics and (6.7) and (6.8) were computed. For example, the matrix (6.3) is defined for MAGE calculations as (6.9) where $k = 14$ and $n = 179$. This matrix for the other metrics are defined by the same token.

$$MAGE = \begin{bmatrix} MAGE_{11} & MAGE_{12} & \cdots & MAGE_{1k} \\ MAGE_{21} & MAGE_{22} & \cdots & MAGE_{2k} \\ \vdots & \vdots & \ddots & \vdots \\ MAGE_{n1} & MAGE_{n2} & \cdots & MAGE_{nk} \end{bmatrix} \tag{6.9}$$

Due to the non-normality of the data, DRs were expressed as the median [IQR]. The values obtained are shown in Table 6.2, and Figure 6.2 is added to make easier the comparison between metrics.

In addition, in order to assess the effect of k value consideration, statistical comparison was carried out between the results obtained with a different number of

windows (i.e. different lengths of the recordings consideration, $k \in \{3, 4, 5, \cdots, 14\}$ where $k = 14$ is equivalent to 24 weeks of recordings). Then, DR was considered constant from the k value whose results were statistically different from the immediately lower k results and not significantly different from the results of the subsequent higher k values.

For sake of clarity, it is worth to mention that the evaluation of the parameter k is independent of the glucose variability analysis. That is, the analysis of the parameter k evaluates the metrics DR metrics instead of the glucose variability directly. In each window $(1, 2, \ldots, k)$, glucose variability needs to be properly assessed; thus, the number of days included in each windows must be 12 days. As commented before, 12 days are defined as the minimum duration of sensor data from which glycaemic variability can be consistently evaluated (Neylon et al. 2014).

For the evaluated glycaemic variability metrics, the MAG has the highest DR value and is statistically significantly greater than the other metrics ($p < 0.001$) except for the GVP ($p = 0.430$), indicating that both metrics may be the most unbiased and most effective at distinguishing between variability differences across individuals. However, the LI, M-Value and J-index also showed no significant differences from GVP ($p = 0.989$; $p = 0.977$; $p = 1.00$; respectively).

In Figure 6.3, the mean of DRs versus weeks considered are represented in order to determine the effect of the parameter k and the vulnerability of the metrics. The study of this parameter implies the analysis of the effect of the inter-day variability in the assessment of glycaemic variability by means of the available metrics. MAG converges faster to a stable value at $k = 8$ compared with the slightly slower convergence of GVP at $k = 9$ ($p < 0.001$) and M-Value and J-Index at $k = 13$ ($p = 0.012$ and $p = 0.019$, respectively). That means that MAG and GVP indicators are less vulnerable to the effect of inter-day variability and, then, a better discriminators.

By looking at data, percentage of time below 50mg/dL and 54mg/dL showed the highest DR values. However, these values are biased due to both metrics are concentrated around similar values describing a left skewed distribution (the number of severe hypoglycaemia are low). They are therefore relatively less affected by variability and cannot be properly evaluated as a good discriminators in relation to intra and inter-patient variability.

For Glucose Control Indices, LBGI presents the most favourable value for DR. However, it is not significantly different from the HBGI, RI and IGC ($p = 0.976$; $p = 0.998$; and, $p = 1.000$ respectively). Considering the k screening, the ro-

GLYCAEMIC VARIABILITY METRICS	
Metrics	**Median [IQR]**
MAG	2.98 [1.64; 3.67]
GVP	2.20 [1.39; 3.01]
LI	2.11 [1.20; 3.10]
$M-VALUE$	2.00 [1.30; 2.94]
$AARC$	1.95 [1.41; 2.64]
$J-INDEX$	1.85 [1.34; 2.59]
$CONGA_1$	1.73 [1.37; 2.18]
SD	1.62 [1.21; 1.99]
$MAGE$	1.56 [1.22; 1.93]
$MODD$	1.47 [1.11; 1.98]
CV	1.33 [1.08; 1.63]

GLUCOSE CONTROL QUALITY INDICES	
Metrics	**Median [IQR]**
$LBGI$	1.93 [1.15; 3.44]
IGC	1.92 [1.27; 2.93]
RI	1.87 [1.32; 2.72]
$HBGI$	1.83 [1.34; 2.72]
$ADDR$	1.81 [1.40; 2.28]
$\%GRADE\ hypo$	1.79 [1.04; 4.46]
PGS	1.71 [1.44; 2.02]
$GRADE$	1.67 [1.30; 2.27]

GLUCOSE CONTROL QUALITY INDICES (Time in ranges)	
Metrics	**Median [IQR]**
$PT\ (BG < 50mg/dL)$	2.33 [1.06; 6.35]
$PT\ (BG < 54mg/dL)$	2.15 [1.08; 5.28]
$PTIR\ (70-180mg/dL)$	1.74 [1.31; 2.02]
$PTIR\ (70-160mg/dL)$	1.63 [1.29; 2.01]
$PTIR\ (54-180mg/dL)$	1.61 [1.32; 2.09]
$PT\ (BG > 180mg/dL)$	1.59 [1.27; 2.09]
$PTIR\ (70-140mg/dL)$	1.58 [1.36; 1.85]
$PTIR\ (54-140mg/dL)$	1.56 [1.31; 2.09]
$PT\ (BG > 160mg/dL)$	1.56 [1.32; 1.97]
$PT\ (BG > 140mg/dL)$	1.54 [1.29; 1.85]
$PT\ (BG < 70mg/dL)$	1.51 [1.07; 2.77]

Table 6.2: DR values for the evaluated glycaemic metrics expressed as median [IQR].

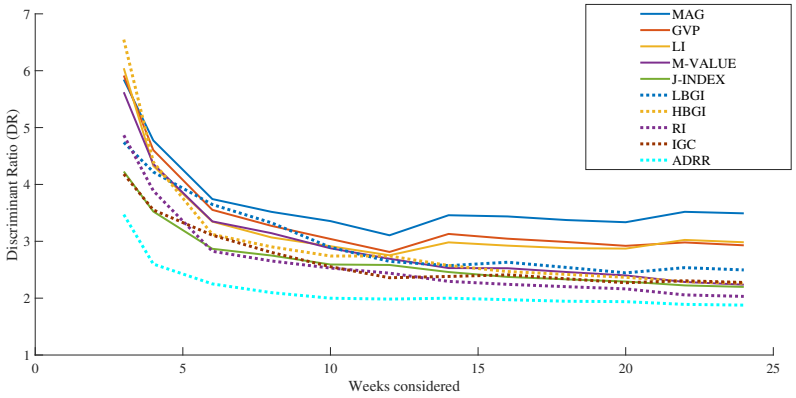

Figure 6.3: Discriminant Ratio versus temporal length consideration (number of weeks) used to obtain the calculations. Only the metrics which have the highest DR are represented.

bustness of the LBGI and IGC is demonstrated (they were constant from $k = 9$ and $k = 8$ respectively) while HBGI stabilized at $k = 13$ and RI is not stable at $k = 13$). Therefore, IGC may be preferable to LBGI as the inter-day variability has less effect on its calculation.

In addition, several time in range indices were evaluated separately. Based on these results, the optimal ones are the commonly used percentage of time between 70mg/dL and 180mg/dL followed by the range defined by 70mg/dL and 160mg/dL without a statistically significant difference between both ranges ($p = 0.197$).

6.4 Interrelationship between metrics

Apart from the robustness of the metrics faced with glucose variability, interrelation between them is also important in order to identify redundancies in the information that all of them provide. In order to assess this behaviour, the correlation between metrics was calculated since the correlation represents the degree to which the tests are assessing the same physiological trait. From this analysis, it is possible to define a small number of recommendable metrics to evaluate the efficacy and safety of therapies, devices, and algorithms. That means identifying which metrics could be taken as the reference, and which others could be in the background. In order to assess the correlation between metrics, Spearman's correlation coefficient (r_s) was used due to the Non-normality of the data (Mukaka 2012). Table 6.3 summarizes the interrelationships between the metrics that were strongly correlated with PTIR, PT(BG<th), and PT(BG>th), for the different

	PTIR			
	[54-140]	[54-180]	[70-140]	[70-180]
M-VALUE	-0.63	-0.83	-0.70	-0.88
J-INDEX	-0.85	-0.92	-0.84	-0.87
HBGI	-0.87	-0.95	-0.86	-0.90
RI	-0.77	-0.93	-0.82	-0.95
GRADE	-0.93	-0.95	-0.93	-0.91
IGC	-0.47	-0.68	-0.59	-0.79
PGS	-0.72	-0.87	-0.80	-0.92
	PT (BG $<$ th)			
th	*50*	*54*	*70*	
LGBI	0.77	0.82	0.96	
GRADE-hypo	0.73	0.76	0.74	
	PT (BG $>$ th)			
th	*140*	*160*	*180*	
J-INDEX	0.84	0.90	0.94	
HBGI	0.87	0.93	0.97	
RI	0.70	0.80	0.86	
GRADE	0.89	0.93	0.93	
PGS	0.64	0.74	0.79	
GRADE-hyper	0.59	0.61	0.60	

Table 6.3: Spearman's correlation coefficient for the metrics correlated with the times in ranges (PTIR), percentage of times in hypoglycaemia PT (BG $<$ th), and percentage of times in hyperglycaemia PT (BG $>$ th).

evaluated thresholds (th). In addition, Table 6.4 abridges the correlation between the metrics more correlated with the time in ranges considered. The purpose of differentiation by range is to identify which metrics are more associated with the characterization of the hypo-, eu- and hyperglycaemic range.

Results showed a high correlation between the percentages of times in ranges and M-Value, J-Index, RI, GRADE, PGS and IGC. The IGC, PGS include two components corresponding to hypo- and hyperglycaemia limits besides penalty scores. That is, the metrics are customizable to weight hypoglycaemia and hyperglycaemia. The default values, which are used in the present analysis, usually assign the same weight to both glycaemic zones. For this reason, the high correlation showed with the euglycaemic range. Nevertheless, the relationship with IGS is weaker with a narrower range since it is strongly dependent of the upper and lower range threshold definition. The same phenomenon occurred with PGS, but

less markedly since this metrics also depends on other parameters. Therefore, the customisation of range in both IGC and PGS (penalty scores) is the determinant that defines the relative influence of hypo-and hyperglycaemia in the outcomes.

On the other hand, RI and GRADE are a functional approximation which are based on fixed parameters. Nevertheless, the correlation remains high across the several considerate ranges, but with two particularities: (1) values of RI correlation lessen when the hyperglycaemic threshold is reduce; (2) the r_s coefficients of GRADE practically do not change with the different thresholds. It demonstrates that in case that the control target range change, GRADE is even able to provide proper results according to the target. Likewise, if the upper threshold change, a reformulation of RI could be required.

About the correlation between these *glycaemic control range* metrics (Table 6.4), they are greatly correlated between them ($r_s > 0.75$ in all cases). This fact proves that all of them are describing the same physiological trait.

Percentages of time in hypoglycaemia are highly correlated with LBGI and GRADE%hypo. However, LBGI shows better r_s for the threshold equal to 54 and 70mg/dL. The weaker correlations with the threshold equal to 50 mg/dL might be due to the small number of glucose values under this threshold. Correlation between LGBI and GRADE%hypo are marginally high, but the discrepancies could be due to the different functional approaches of each index.

Regarding the percentages of times in hypergycaemia, J-INDEX, HBGI, RI and GRADE are highest correlated. The performance of GRADE and RI that has been commented previously in the time in ranges is also observed in this case. The r_s of RI is higher with the hyperglycaemia threshold definition as 180mg/dL; instead, the differences in the coefficient across the several thresholds is not observed in the GRADE. However, HBGI is more correlated with time in hyperglycaemia than GRADE%hyper, although HBGI shows the same effect of the threshold definition on r_s values than RI. PGS shows lower correlation with the threshold equal to 140 mg/dL due to the customization of the hypo- and hyperglycaemia were the default ones (70 mg/dL and 180 mg/dL respectively). Nevertheless, as said before, this metrics is customizable depending the glycaemic zone that is considerate as the critical one. It means that this lower correlation coefficient value could be improve if the hyperglycaemia is higher weighted.

To summarise, although percentage of time in ranges has the theoretical limitation that it assigns the same penalty score to all glucose values; calculations suggested that simple indices such as PTIR, PT(BG<th), PT(BG>th) may be as informative as the "risk index" criteria, as proposed previously (Rodbard 2018). IGS and

PGS are able to accomplish the same function with parameter tunings. Besides, this possibility of customization allows to configure the metrics to study the overall glycaemic control, hypoglycaemic or hyperglycaemic range. By contrast, the times in ranges showed higher vulnerability to intra- and interpatient variability than the risk indices with lower values of DR.

	M-VALUE	J-INDEX	LGBI	HBGI	RI	IGC	PGS	GRADE	GRADE-LOW	GRADE-HIGH	GRADE-EU
M-VALUE	1.00										
J-INDEX	0.81	1.00									
LGBI	0.11	-0.33	1.00								
HBGI	0.81	0.99	-0.36	1.00							
RI	0.97	0.90	-0.06	0.91	1.00						
IGC	0.93	0.61	0.36	0.61	0.86	1.00					
PGS	0.90	0.80	0.05	0.81	0.92	0.86	1.00				
GRADE	0.78	0.89	-0.34	0.93	0.89	0.63	0.82	1.00			
GRADE-LOW	0.24	-0.07	0.71	-0.10	0.13	0.45	0.26	-0.04	1.00		
GRADE-HIGH	0.28	0.54	-0.60	0.59	0.40	0.04	0.28	0.50	-0.65	1.00	
GRADE-EU	-0.73	-0.63	0.00	-0.67	-0.75	-0.65	-0.70	-0.67	-0.05	-0.58	1.00

Table 6.4: Spearman's correlation coefficient between glycaemic control quality indices.

With regard to variability metrics, MAG is correlated with LI ($r_s = 0.87$); CONGA with LI ($r_s = 0.89$); and GPV with AARC ($r_s = 0.9$). This correlation is explained by the fact that they are sensible to the time parameter and this parameter is the same although they compute different glucose functions. In the case of GVP and AARC, the great interrelationship is due to both represent the rate of change but with different formulation. Lastly, MAGE, MODD, and ADDR are correlated with no times in ranges, suggesting that they are able to describe glucose variability independently of the glucose zone.

In summary, considering these results along with the results from the previous analysis with the DR, the ICG is suggested as the recommendable control quality index since is a good discriminator, besides that it is able to carry out the same function that the percentage of times in ranges giving an overall glycaemic control view. Moreover, MAG is proved as the crucial glucose variability outcome for

people with type 1 diabetes since it is the most effective one at distinguishing between and within subject variability differences using CGM data.

6.5 Conclusions

Increasing adoption of continuous glucose monitoring (CGM) technologies to support self-management of type 1 diabetes is creating a large volume of data for people with diabetes, their careers, and healthcare professionals to reflect on. Conventional glucose metrics such as mean glucose, HbA1c, and time in range are accessible and easily understood but may not be sensitive to variability in glucose and there is potential benefit from standardising measurement to assess variability and to measure the impact of an intervention, especially in clinical research. Several measures of glycaemic variability have been described. These can be broadly subdivided into measures to evaluate glycaemic variability (e.g. SD, CV, MAGE, CONGA, MODD, LI, J-Index, M-Value, and MAG), and measures to evaluate glucose control quality that are also sensitive to glycaemic variability (e.g. GRADE, pTIR, ADRR, IGC, PGS, RI, LBGI, and HBGI). The interrelationship analysis between them suggests that simple metrics such as times in ranges are correlated and could be as informative and useful as the risk indices are, provided that they are good discriminators of glucose variability.

The results reported in this chapter are obtained from the largest freely-available CGM dataset and describe the ability of different glycaemic variability metrics and glucose control quality indices to discriminate between individuals. Mean Absolute Glucose (MAG), a glycaemic variability metric that is the measure of glucose rate of change over time, has the highest discriminant ratio while LBGI and IGC have the higher DR values for measures of glucose control quality. These LBGI outcomes are supported by an analysis of glucose variability metrics in children using principal components analysis (PCA) (Guilmin-Crépon et al. 2018).

For times in ranges, time between 70 and 180 mg/dL is most effective at discriminating between individuals. To specifically assess time in hypoglycaemia the International Hypoglycaemia Study Group defined threshold of 54 mg/dL appears to discriminate effectively when time below threshold is assessed. The limitations of this work include the exclusion of glycaemic profiles which include episodes of severe hypoglycaemia. This may result in a bias in the analysis of the percentage of time below 50 and 54 mg/dL due to relatively fewer samples in these ranges. An analysis with data from studies that includes people with higher risk of hypoglycaemia could reinforce the results of these both metrics.

In summary, the data presented do not define an absolute gold standard for glycaemic variability measurement but strongly support the use of MAG as an important glucose variability outcome for people with type 1 diabetes that may be used, alongside HbA1c and a measure of hypoglycaemia, to assess glucose and the impact of interventions in a meaningful way. The most robust time in range is 70 to 180 mg/dL and we advocate standardization of this as the primary time in range metric whereas LBGI and IGC should be considered the optimal glucose quality metrics. LBGI is recommended particularly in performances where the hypoglycaemia assessment is one of the object of study.

Chapter 7

Dual-hormone coordinated control

The main goal of control algorithms for the Artificial Pancreas is to maximize the percentage of time in target and to avoid hypoglycaemia events. Besides, a reduction in glycaemic variability is also pursued. Due to the limitations of single-hormone artificial pancreas systems in mitigating hypoglycaemia in challenging scenarios such as exercise, this thesis focuses on the developement of new dual-hormone control algorithms, with concomitant infusion of insulin and glucagon. In this chapter, a dual-hormone artificial pancreas system is presented. This is designed according to coordinated insulin and glucagon delivery strategies, which may play a key role in glucoregulation since a bi-directional communication among beta and alpha cells in the pancreas exists. Then an insulin on board limitation is incorporated to the initial coordinated scheme. The performance of the controllers is assessed in order to test if the proposed controller achieves low time in hypoglycaemia and a reduction in the glycaemic variability.

7.1 Preliminaries

A crucial aspect in the design of control algorithms in the Artificial Pancreas area is the unidirectional effect of insulin, which promotes the reduction of blood glucose concentration. In case of an excessive insulin delivery, there are some restrictions to compensate for the substantial drop in plasma glucose concentration, inducing then hypoglycaemias or severe hypoglycaemias. This problem has been addressed from two main perspectives as reviewed in Section 3.2: (1) the inclusion of mechanisms that restrict the insulin on board (IOB) in the single-hormone systems (Ellingsen et al. 2009; Revert et al. 2013); and, (2) the use of dual-hormone systems, which define the glucagon as the contrarregulatory action since it has an opposed effect to insulin on glucose concentration (El-Khatib et al. 2010; Haidar et al. 2013; Herrero et al. 2012; Ward et al. 2008).

The lack of a significant reduction in hypoglycaemia has been associated with excessive circulating insulin. Moreover, high levels of plasma insulin concentration may limit the effects of glucagon (El Youssef et al. 2014). It was also demonstrated that high insulin on board increases significantly the risk of glucagon failure in preventing hypoglycaemia (P. Bakhtiani et al. 2015). On the other hand, the antagonistic effect of insulin and glucagon along with the structure of the current systems based on independent control loops, might cause unwanted oscillations between hypoglycaemia and hyperglycaemia (El Youssef et al. 2014).

A better understanding of physiology can help the development of new bio-inspired strategies. The drop in glucose concentration during hypoglycaemia triggers the counterregulatory response. In healthy people, the first counterregulatory response is the reduction of endogenous insulin secretion, which occurs when blood glucose levels fall below 81 mg/dL, still within the normal glycaemic range. When blood glucose falls outside this range, below 65-70 mg/dL, the secretion of glucagon and adrenaline begins, among other neuroendocrine responses, (see Chapter 5 to more detail).

Thus, glucagon secretion is always preceded in healthy subjects by a reduction in the plasma insulin level, which prevent high insulin concentrations accompanying the glucagon secretion. This means that glucagon should be used as a rescue from hypoglycaemia along with stopping the insulin infusion. The success will depend on the current insulin on-board due to the subcutaneous infusion. Besides, glucagon can help to mitigate the excessive aggressiveness of the insulin infusion to achieve better postprandial control and lower blood glucose average. Hence, a recommendable artificial pancreas approach will be one that uses glucagon as a modulator to prevent hypoglycaemia.

In addition, according to physiology, there is paracrine communication between alpha and beta cells, glucagon and insulin secretors respectively (Jain and Lammert 2009). Beta cells inhibit the effect of alpha cells. In patients with T1D, it was demonstrated that the increase in insulin levels produces a suppression of glucagon secretion, and that the decrease of insulin levels combined with low glucose values stimulates glucagon secretion (B. Cooperberg and P. Cryer 2010). However, this stimulation did not exist during normoglycaemia. It means that insulin is a paracrine glucagon inhibitor whereas the secretion of glucagon as a counterregulatory response is signalled by the decrease in insulin concentrations. On the other hand, alpha cells sensitize the beta cells by means of glucagon secretion and acetylcholine in order to respond optimally to the subsequent glucose increase (Rodriguez-Diaz et al. 2011b). Thus, alpha cells anticipate possible hyperglycaemic rebounds by means of the beta-alpha cells communication. Therefore, paracrine communication is observed in both directions. This fact reveals that the coordination between the secretion of both hormones is a relevant factor in the glycaemic control.

The work presented in this chapter is focused on the development of new control algorithms based on a dual-hormone configuration which incorporate the coordination above described between insulin and glucagon infusion. They are able to improve the features of the artificial pancreas. From the coordinated dual-hormone proposal, an insulin on board limitation is also included in such configuration in order to manage the excessive amount of circulating insulin, which could interfere in the glucagon effect on glucose concentration and in the rate of glucose decrease. Therefore, this chapter is organized as follows: Section 7.2 introduces briefly the current dual-hormone systems; Section 7.3 presents a description of the glucose-insulin-glucagon model that is used in this work; then, the control strategy followed here in order to define our controller proposal is described in Section 7.4. Section 7.5 describes the coordinated controller proposal and shows the results from the comparison between coordinated and non-coordinated configurations; Section 7.6 exposes the new controller configuration with the addition of the insulin on board limitation; here, a comparison between the previous coordinated controller and the new proposal of coordinated dual-hormone controller with insulin on board limitation is also carried out. Finally, Section 7.7 shows the conclusion of this work.

7.2 Current dual-hormone systems structure

The current dual hormone control systems are founded on the control structure of Figure 7.1. All of them are based on an insulin controller, to which a new glucagon control loop is added. The glucagon controller is activated under certain circumstances with the aim of triggering a counterregulatory action that prevents or minimizes the hypoglycaemia generated by the insulin controller.

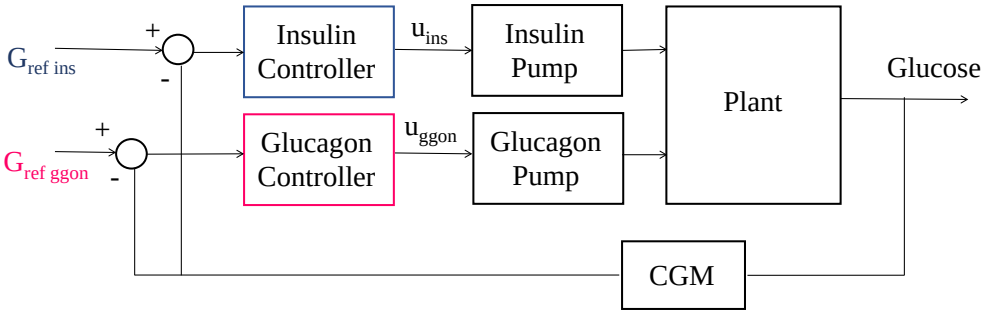

Figure 7.1: Dual-hormone control system based on independent loops for the insulin and glucagon controllers.

The ongoing implementation of dual hormone systems include ad-hoc solutions with heuristic components such as controller activation rules, action saturation, rules to compensate for unwanted interactions between controllers and different considerations of glucose reference for insulin and glucagon controllers. Considering two different references implies an additional degree of freedom for tuning, although the goal of each controller from the physiological point of view is common (normoglycaemia).

In addition, the dual hormone system allows more aggressive insulin infusion, compared to a single hormone system, since the dual configuration uses the glucagon infusion as a modulator to avoid hypoglycaemia. However, as discussed in the previous section, excess of insulin may reduce the effectiveness of glucagon resulting in hypoglycaemia incidence despite glucagon counterregulatory action. Besides, insulin and glucagon secretion are intimately coordinated through paracrine communication between the alpha and beta cells of the pancreas. These aspects justify the interest in new control structures that permit a more systematic design, as well as the coordination of the delivery of both hormones.

7.3 Models of the glucose-insulin-glucagon system

The development of new dual hormone control algorithms requires models that describe the action of insulin and glucagon in glucose regulation, as well as the respective pharmacokinetics of subcutaneous infusion.

As exposed in Chapter 4, there are three models that are widely used: Bergman minimal model (Bergman et al. 1981), the Hovorka model (Hovorka et al. 2004), and the Dalla Man model (Dalla Man et al. 2007b). This last model is integrated in the UVA/Padova simulator which is used in the present chapter to carry out the simulations and validations.

The Bergman minimal model is a non-linear second order model that relates plasma insulin concentration and plasma glucose concentration. This model was obtained in order to measure the insulin sensitivity from plasma glucose and plasma insulin data. Thus, the model did not include neither the pharmacokinetics of insulin nor the model of carbohydrates absorption. The Hovorka model is a non-linear seventh order model that relates the intake and subcutaneous insulin infusion with the plasma glucose concentration. The pharmacokinetics of insulin is represented by a linear, third order system.

The Bergman minimal model has been widely used in combination with models of subcutaneous insulin pharmacokinetic and carbohydrates absorption from the intake since it is simple and identifiable. The Identifiable Virtual Patient (IVP) model (S. S. Kanderian et al. 2012) is one example that join the Bergman model with the carbohydrates absorption model from Hovorka model and a reduction of the pharmacokinetics model of insulin considering only one compartment.

The incorporation of the effect of glucagon on the models was carried out in analogous procedure. The Bergman minimal model was extended by (Herrero et al. 2013) in order to incorporate the pharmacokinetics and pharmacodynamics of exogenous glucagon infusion. This model is relevant in our work since its equations will reveal some characteristics of our coordinated control scheme. Such model is described by the following equations:

$$\dot{F}(t) = \frac{1}{t_{maxG}} \left(-F(t) + A_G D_G\right) \tag{7.1}$$

$$\dot{R}_a(t) = \frac{1}{t_{maxG}} \left(-R_a(t) + F(t)\right) \tag{7.2}$$

$$\dot{S}_1(t) = u(t) - \frac{S_1(t)}{t_{maxI}} \tag{7.3}$$

$$\dot{S}_2(t) = \frac{S_1(t) - S_2(t)}{t_{maxI}} \tag{7.4}$$

$$\dot{I}(t) = -k_e I(t) + \frac{S_2(t)}{V_I t_{maxI}} \tag{7.5}$$

$$\dot{X}(t) = -p_2 X(t) + p_2 S_I \left(I(t) - I_b\right) \tag{7.6}$$

$$\dot{Z}_1(t) = w(t) - \frac{Z_1(t)}{t_{maxN}} \tag{7.7}$$

$$\dot{Z}_2(t) = \frac{Z_1(t) - Z_2(t)}{t_{maxN}} \tag{7.8}$$

$$\dot{N}(t) = -k_N N(t) + \frac{Z_2(t)}{V_N t_{maxN}} \tag{7.9}$$

$$\dot{Y}(t) = -p_3 Y(t) + p_3 S_N \left(N(t) - N_b\right) \tag{7.10}$$

$$\dot{G}(t) = -\left(S_G + X(t) - Y(t)\right) G(t) + S_G G_b + \frac{R_a(t)}{V_G} \tag{7.11}$$

Equations (7.1)-(7.2) are related to the intake, as well as equations (7.3)-(7.6) are associated with to pharmacokinetics and effect of insulin effect. Likewise, (7.7)-(7.10) corresponds to the pharmacokinetics and effect of glucagon. Lastly, the glucose metabolism is described by equation (7.11).

The terms about the intake and the model of the insulin pharmacokinetics are corresponded with the Hovorka model. In the meal absorption model, R_a (mg/min^{-1}kg^{-1}) is the plasma glucose rate of appearance, F is the glucose appearance in the first compartment. A_G is the carbohydrate bioavailability, and D_G (mg) is the amount of carbohydratres ingested, and lastly, $t_{\max G}$ is the time-to-maximum of carbohydrate absorption.

In the pharmacokinetic and absorption insulin model, I (μU/ml) is the plasma insulin concentration, k_e (min) is the first-order decay rate for insulin in plasma, u (μU/kg) is the subcutaneous insulin infusion rate, V_I (ml/kg) is the distribution volume of plasma insulin, $t_{\max I}$ (min) is the time-to-maximum insulin absorption, and S_1 and S_2 are a two-compartment chain representing absorption of subcutaneously administered insulin.

The pharmacokinetics and the effect of glucagon are incorporated and modelled by the same model structure as the one defined for the insulin where N (pg/ml) is the plasma glucagon concentration, k_N (min^{-1}) is the first-order decay rate for glucagon in plasma, Z_1 and Z_2 are the two-compartment chain that represents the absorption of the glucagon administered subcutaneously. $w(t)$ (ng/kg) is the subcutaneous glucagon infusion rate, V_N (mL/kg) is the distribution volume of

plasma glucagon, and t_{maxN} (min) is the time-to-maximum glucagon absorption. The effect of glucagon on glucose is also modelled following a similar approach to the one used in the Bergman Minimal model, $y(t)$ is glucagon action on glucose production, N_b is the glucagon basal value, S_N (min^{-1} per pg/mL) is glucagon sensibility, and p_3 (min^{-1}) is the constant rate that describes the dynamics of glucagon action. Lastly, the effect of glucagon on glucose concentration is incorporated in (7.11) with opposite sign to insulin. This effect is modulated by the glucose concentration, $Y(t) \cdot G(t)$.The hepatic production is modulated by the glucagon sensitivity.

In a control context, the analysis of the insulin and glucagon dynamics is a point of interest. In the system defined by equations (7.1)-(7.11), the parameters that are responsible of the mentioned dynamics are t_{maxI}, k_e and p_2 for the insulin whereas t_{maxN}, k_N and p_3 for the glucagon. The value of these parameters in the patients identified in (Herrero et al. 2013) demonstrated that the glucagon dynamics is faster that the insulin one, i.e. $t_{maxN} > t_{maxI}$, $k_N > k_e$ and $p_3 > p_2$. Therefore, this feature about the differences between dynamics must be considered in the configuration of our control system.

7.4 Control of Multiple Input-Single Output systems

The control problem of the dual-hormone AP can be casted as the design of a controller for a MISO plant, where insulin and glucagon infusion are the plant inputs and glucose the output. The system to be controlled in this chapter is described by the model (7.1)-(7.11). According to them, the system can be expressed as:

$$\dot{x}(t) = f(x(t), u(t), w(t), d(t)), \tag{7.12}$$

$$G(t) = h(x(t)), \tag{7.13}$$

where $x \in \mathbb{R}^n$ is the system state, $u \in \mathbb{R}$ is the subcutaneous insulin infusion, $W \in \mathbb{R}$ is the subcutaneous glucagon infusion, and $d \in \mathbb{R}$ is a perturbation that contains the glucose flux due to the ingestion. Therefore, the exposed system is a non-linear MISO system that has two inputs (insulin and glucagon delivery) and one output (glucose concentration).

MISO systems are common in the industrial processes. Within these MISO systems, the control strategies can be divided into non collaborative and collaborative ones (Rico-Azagra et al. 2014). Non collaborative control selects a plant inside a battery of them, which covers a wide range of operating points for the output. The selection criterion is based on the stationary capacity of each plant. Thus, the control law is designed for an equivalent SISO system. A selector splits online

the control action to the plant or plants with capacity to regulate the output in the actual operating point.The split-range method is the most representative of this class of controllers where design reduces to a pure SISO system, which closes a single feedback loop around a plant. That is, only one control input is acting to one plant at any given time. The inputs to the other plants could be manipulated manually or are left constant. On the other hand, collaborative strategies benefit from dynamic strengths of each plant to improve the performance of the controlled output considering the restrictions of the manipulated variables and individual outputs (Rico-Azagra et al. 2014). In the literature, the concept of collaborative MISO has been developed under several nomenclatures, such as VPC (Valve Position Control) (Shinskey 1978; Yu and Luyben 1986), habituating control (Henson et al. 1995; McLain et al. 1996), main-vernier control (Lurie and Enright 2011), PQ design method (Schroeck et al. 2001), or Midranging control (Allison and Isaksson 1998).

The coordinated control strategies are of special interest in this work. The concept of *habituating control strategy* was introduced by (Henson et al. 1995); it is used to coordinate the available manipulated inputs so that the outputs are maintained at their references whereas the overall cost of control actions is minimized. Most control systems employ only slow and "cheap" variables as the manipulated inputs, although additional fast, but "expensive" inputs are available. In habituating control systems, the fast (secondary) inputs can be used to track reference changes and reject disturbances rapidly. As the slower (primary) inputs begin to affect the outputs, the fast inputs can be habituated by slowly returning to their desired values. Improved performance can be obtained with little additional cost because the expensive secondary inputs are not used at steady state.

A cardiovascular system that employs a habituating control strategy for regulating arterial blood pressure was inspired by (Henson et al. 1995). The arterial pressure is determined basically by two physiological variables: 1) the sympathetic system, which acts slower on the peripheral resistance, and 2) the parasympathetic system that acts faster on the cardiac output. A continuous action on cardiac output is costly. For this reason, the brain coordinates both physiological variables in order to achieve the best features at expenses of the minimum possible cost. That is, as long as the sympathetic response on the peripheral resistance is being greater, the parasympathetic system is "being habituated" in order to provide an equilibrium value for the cardiac output. This system has similarities with the dual-hormone problem since two control actions are also considered, glucagon and insulin infusion; besides that glucagon can be categorized as the "fast and expensive" control action whereas insulin can be defined as "slow and cheap" action. Glucagon can be identified as the secondary action due to the amount of glucagon delivered must be

as low as possible (side effects could be manifested if the glucagon administration was higher that a daily limit around 1mg). Hence, glucagon provides a quick and optimal response to avoid the hypoglycaemia while a decrease in insulin delivery has a later effect.

In that cardiovascular system, the steps proposed to design the controllers are: 1) definition of the desired transfer function between the output and its reference; 2) definition of the desired transfer function between the secondary action and its reference; 3) decoupling of the response between the reference of the secondary action and the output; 4) achievement of asymptotic tracking of both references; 5) Ensuring nominal closed-loop stability. However, in our dual-hormone problem, a reference for the glucagon infusion different from zero has no sense since the glucagon infusion is only in case of hypoglycaemia emergency. From the good results obtained with this methodology, the habituating control methodology was extended to the case of non-linear processes in (McLain et al. 1996). Then, the application of the methodology to the voltage control problems in quasi-resonant converters was proposed by (Cevantes and Alvarez-Ramirez 2004). The control strategy was tested in a reactor control problem in (Monroy-Loperena et al. 2004).

Other interesting approach is the *cooperative-feedback control*, which considers the use of additional actuators in order to avoid the saturation of the main actuator. To this end, a parallel structure with a switch function is able to define the contribution of each control action in the output response. A design of cooperative controllers based on the plant factorization was suggested by (Alvarez-Ramirez et al. 2004). It consists in two steps: 1) design the controller for one of the factors; 2) design of a divisor in order to split the total "control effort" into the two available control actions so that the closed-loop performance is preserved. The effectiveness of this approach was tested in (Velasco-Perez et al. 2009) and (Velasco-Pérez et al. 2011). In the glucose control context, a glucose control system was proposed in (Sun et al. 2012) using the MPC control from (Henson et al. 1995) with intravenous insulin and glucose infusion as control variables. This control configuration could be interpolate to our problem, but as mentioned above, the reference of glucagon action cannot be different from zero unlike the case of glucose as the secondary control action.

The parallel control structures are the most suitable approach to assess the dual-hormone problem. This kind of structures arise for instance in the plant factorization presented in (Alvarez-Ramirez et al. 2004) , which will set the foundations of the design strategy of the controller proposed in the present chapter. Thus, it is explained in more detail below.

Consider the plant:

$$y(s) = H_1(s)u_1(s) + H_2(s)u_2(s) \tag{7.14}$$

where

$$H_1(s) = \frac{N_1(s)}{D_1(s)}e^{-d_1 s},\ H_2(s) = \frac{N_2(s)}{D_2(s)}e^{-d_2 s},\ d_1 \geq d_2. \tag{7.15}$$

Then, (7.14) can be expressed as:

$$y(s) = \frac{N_1^+(s)N_2^+(s)}{Q(s)}e^{-d_1 s}\left(\frac{N_1^-(s)Q(s)}{N_2^+(s)D_1(s)}u_1(s) + \frac{N_2^-(s)Q(s)}{N_1^+(s)D_2(s)}e^{(d_1-d_2)s}u_2(s)\right) \tag{7.16}$$

$$y(s) = H'(s)e^{-d_1 s}\left(F_1(s)u_1(s) + F_2(s)e^{(d_1-d_2)s}u_2(s)\right) \tag{7.17}$$

where

$$H'(s) := \frac{N_1^+(s)N_2^+(s)}{Q(s)},\ F_1(s) := \frac{N_1^-(s)Q(s)}{N_2^+(s)D_1(s)},\ F_2(s) := \frac{N_2^-(s)Q(s)}{N_1^+(s)D_2(s)} \tag{7.18}$$

where $N_i^+(s)$ is the factor that contains all the right-hand side zeros (including those in the imaginary axis) of the transfer function $H_i(s)$, $i = 1, 2$ with $N_i^+(0) = 1$ and $Q(s)$ is a stable polynomial satisfying $Q(0) = 1$ such that $H'(s)$ is a proper transfer function and $F_1(s)$ and $F_2(s)$ are non-strictly proper transfer function. To guarantee these characteristics, the following condition must be met:

$$\deg(Q(s)) \geq \max\left\{\deg(N_1^+(s)N_2^+(s)), \deg\left(\frac{N_1^-(s)}{N_2^+(s)D_1(s)}\right), \deg\left(\frac{N_2^-(s)}{N_1^+(s)D_2(s)}\right)\right\} \tag{7.19}$$

Notice that "deg" denotes degree of polynomial.

As a consequence:

- H' is stable and non-invertible where $H'(0) = 1$ and

$$\deg(Q(s)) \geq \deg\left(N_1^+(s)N_2^+(s)\right).$$

- F_1 and F_2 are invertible, and $F_1(s)^{-1}$ and $F_2(s)^{-1}$ are proper; where $F_i(0) = H_i(0)$, and $r\deg(F_i(s)) \leq 0, i = 1, 2$. Notice that "$r$ deg" denotes relative degree.

From (7.17), the virtual action is defined as:

$$\mu(s) := F_1(s)u_1(s) + F_2(s)e^{(d_1-d_2)s}u_2(s). \tag{7.20}$$

Considering that $v_2(s)$ represents the secondary action which presents the faster dynamics faced with the primary action, $v_1(s)$ and $v_2(s)$ are defined as:

$$v_1(s) := F_1(s)u_1(s), \tag{7.21}$$

$$v_2(s) := F_2(s)e^{(d_1-d_2)s}u_2(s). \tag{7.22}$$

Thus,

$$\mu(s) = v_1(s) + v_2(s). \tag{7.23}$$

Therefore the SISO plant of the system is summarized in:

$$y(s) = H'(s)\mu(s) \tag{7.24}$$

This is an equivalent representation of plant (7.14) with control input $\mu(s)$ and control output $y(s)$. After plant factorization, the controller design is carried out following the subsequent steps:

1. The design of the master controller $C(s)$ according to the plant.

   $$\mu(s) = C(s)e(s), \text{ where } e(s) \text{ is the error, i.e., } e(s) = y_{ref}(s) - y(s). \tag{7.25}$$

2. The design of the divisor, which is responsible to distribute the virtual action $\mu(s)$ to the primary and secondary control actions ($v_1(s)$ and $v_2(s)$). To this end, as described by (Alvarez-Ramirez et al. 2004), the following optimization problem is posed:

   $$\min_{(v_1,v_2)} \frac{1}{2}\left(\alpha v_1(s)^2 + (1-\alpha)\, v_2(s)^2\right) \tag{7.26}$$

   with the restriction

   $$\mu(s) = v_1(s) + v_2(s). \tag{7.27}$$

   where $\alpha \in [0, 1]$ is a customizable parameter that weights each control action.

   The optimization problem solution is:

   $$v_1(s) = (1-\alpha)\,\mu(s),\ v_2(s) = \alpha\mu(s). \tag{7.28}$$

3. Definition of the real control actions u_1 and u_2 considering v_1 and v_2. That is,

   $$u_1(s) = F_1^{-1}v_1(s); \quad u_2(s) = F_2(s)^{-1}e^{(d_1-d_2)s}v_2(s). \tag{7.29}$$

Then, the stability and features of the MISO system are determined by the stability and features of the SISO system whose closed loop transfer function is defined by

$$H_{cl}(s) = \frac{C(s)H'(s)}{1 + C(s)H'(s)} \tag{7.30}$$

The resultant control structure described above is shown in Figure 7.2.

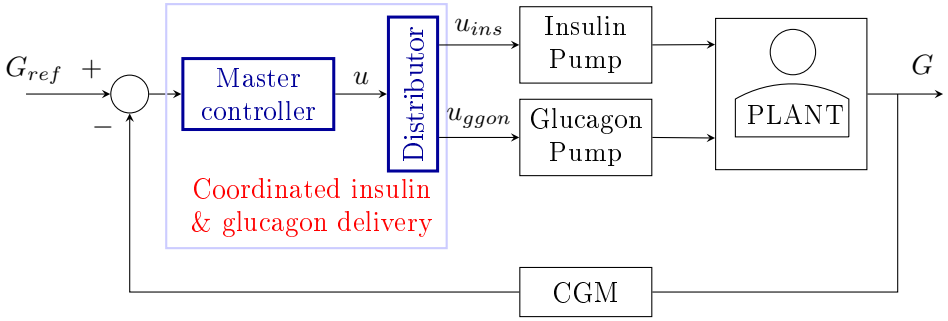

Figure 7.2: General block diagram of the parallel control structure applied to the dual-hormone artificial pancreas system.

7.5 Coordinated controller proposal

In a dual-hormone artificial pancreas systems, an analogy of the "fast and cheap" is established with glucagon action due to a faster subcutaneous pharmacokinetics and pharmacodynamics, although its delivery must be constrained to 1 mg/day due to the possible side effects; then, the "slow and cheap" action is identified with the insulin action. Glucagon can respond quickly when hypoglycaemia occurs while insulin decreases to produce a latest effect on plasma glucose concentrations. Besides, glucagon may ultimately act as a secondary control action when either insulin is saturated (insulin infusion cannot have negative values) or insulin delivery is below a given threshold for hypoglycaemia mitigation.

Overall, the control effort provided by the combined action of insulin and glucagon must be the one needed to maintain the glucose control targets. To this end, the general parallel control structure in Figure 7.2 is proposed in this work, as opposed to independent control loops for insulin and glucagon used in the most current systems (see Figure 7.1). A master controller computes a virtual control action representing a control effort, which is then distributed among insulin and glucagon according to given logics leading to a coordinated hormones delivery.

The design of the control system in Figure 7.2 is adapted from (Alvarez-Ramirez et al. 2004) according to the theory exposed in previous section, leading to the controller depicted in Figure 7.3. It is expected that the relation between insulin, glucagon and glucose presents nonlinear and even time-varying dynamics. However, for simplicity, a system linearized at its basal values is considered in this thesis for the controller design. Hence, the design steps, which will be illustrated considering the glucose-insulin-glucagon model in Section 7.3, are defined as follows:

1. Linearization and factorization of the system.

Considering the equations (7.1)-(7.11) that describe the system to be controlled, the system is linearized as follow:

$$\Delta G(s) = H_1(s)\Delta u(s) + H_2(s)\Delta\omega(s) + H_3(s)\Delta R_a(s), \tag{7.31}$$

where

$$H_1(s) = \frac{G^* S_I p_2}{V_I t_{maxI}^2} \frac{1}{\left(s + \frac{1}{t_{maxI}}\right)^2 (s + k_e)(s + p_2)(s + S_G)} \tag{7.32}$$

$$H_2(s) = \frac{G^* S_N p_3}{V_N t_{maxN}^2} \frac{1}{\left(s + \frac{1}{t_{maxN}}\right)^2 (s + k_N)(s + p_3)(s + S_G)} \tag{7.33}$$

$$H_3(s) = \frac{1}{V_g} \frac{1}{(s + S_G)} \tag{7.34}$$

$\Delta G(s)$ is the deviation of plasma glucose concentration from the equilibrium value G^*, ($\Delta G(t) := G(t) - G^*$); $\Delta u(s)$ is the deviation of insulin infusion from the equilibrium value u^*, ($\Delta u(t) := u(t) - u^*$); $\Delta\omega(s)$ is the deviation of glucagon infusion from the equilibrium value ω^*, which is null ($\Delta\omega(t) := \omega(t)$); and, $\Delta Ra(s)$ is the disturbance due to the meal intake ($\Delta Ra(t) := Ra(t)$). Transfer functions $H_1(s)$, $H_2(s)$, and $H_3(s)$ are the linearized plants representing the glycaemic effect of insulin, glucagon and meal intake respectively, with $H_1(0) = 1$, and $H_2(0) = 1$. Thus, gains α and β correspond to the insulin and glucagon sensitivities, respectively. Remark that, due to subcutaneous pharmacokinetics and pharmacodynamics of insulin and glucagon, $H_1(s)$ will have a slower dynamics than $H_2(s)$ (see Section 7.3).

In the absence of disturbance, the plant with faster dynamics (i.e., $H_2(s)$) can be factorized as follows:

$$\Delta G(s) = H_2(s)\left(\frac{H_1(s)}{H_2(s)}\Delta u(s) + \Delta\omega(s)\right) \tag{7.35}$$

where

$$\frac{H_1(s)}{H_2(s)} = -\frac{S_I}{S_N}\frac{p_2}{p_3}\frac{V_N}{V_I}\left(\frac{t_{maxN}}{t_{maxI}}\right)^2 \frac{\left(s+\dfrac{1}{t_{maxN}}\right)^2 (s+k_N)(s+p_3)}{\left(s+\dfrac{1}{t_{maxI}}\right)^2 (s+k_e)(s+p_2)} \tag{7.36}$$

with static gain equal to:

$$\frac{H_1(0)}{H_2(0)} = -\frac{S_I}{S_N}\frac{k_N}{k_I}\frac{V_N}{V_I} = -\frac{S_I}{S_N}\frac{Cl_N}{Cl_I}, \tag{7.37}$$

where $Cl_N = k_N V_N$ and $Cl_I = k_I V_I$ are the "clearance" of glucagon and insulin. This concept corresponds to the plasma volume of each hormone per time unit that is cleared.

Altenatively to equation (7.31), model linearisation can be expressed as

$$\Delta G(s) = \alpha H_1(s)\Delta u(s) + \beta H_2(s)\Delta\omega(s) + H_3(s)\Delta R_a(s), \tag{7.38}$$

where $\alpha = -S_I/Cl_I$ and $\beta = S_N/Cl_N$ so that $H_1(0)/H_2(0) = 1$. This will be the representation considered henceforth, for an explicit representation of gain α and β, that will need individualization.

Defining now

$$\Delta\mu(s) := \Delta v_1(s) + \Delta v_2(s), \tag{7.39}$$

$$\Delta v_1(s) := \alpha\frac{H_1(s)}{H_2(s)}\Delta u(s), \tag{7.40}$$

$$\Delta v_2(s) := \beta\Delta w(s). \tag{7.41}$$

Equation (7.35) can be expressed as a SISO system in terms of a new virtual control action as follows:

$$\Delta G(s) = H_2(s)\cdot\Delta\mu(s) \tag{7.42}$$

where $\Delta\mu(s)$ represents the "control effort" without saturation constraints, unlike insulin, $\Delta u(s)$, and glucagon, $\Delta w(s)$, infusion that must be non-negative.

2. Design of master controller $C(s)$ for the equivalent SISO plant.

A controller design can thus be carried out for the SISO system (7.42), with closed-loop dynamics given by

$$H_{cl}(s) = \frac{C(s)H_2(s)}{1 + C(s)H_2(s)} \tag{7.43}$$

yielding the master controller $C(s)$ in Figure 7.5.2. In this work, a PD controller is considered:

$$C(s) = \frac{\Delta\mu(s)}{G_{ref}(s) - G(s)} = kp(1 + T_d s) \tag{7.44}$$

$$\Delta\mu(s) = kp(1 + T_d s)\left(G_{ref}(s) - G(s)\right) \tag{7.45}$$

where k_p is the proportional gain, T_d is the derivative time, and G_{ref} is the value of the glucose reference.

3. Divisor design to distribute the total virtual control action $\Delta\mu(s)$ in both primary $\Delta v_1(s)$ and secondary $\Delta v_2(s)$ actions.

The control action computed in (7.45) can be distributed in terms of $\Delta v_1(s)$ and $\Delta v_2(s)$ with consideration of the constraint imposed by (7.39), i.e., both actions must add up the total control effort needed. Then, by inverting (7.40) and (7.41), the final insulin and glucagon infusions can be obtained as:

$$\Delta u(s) = \frac{1}{\alpha}\left(\frac{H_1(s)}{H_2(s)}\right)^{-1}\Delta v_1(s), \tag{7.46}$$

$$\Delta w(s) = \frac{1}{\beta}\Delta v_2(s), \tag{7.47}$$

$$u(t) = \Delta u(t) + u^*, \tag{7.48}$$

$$w(t) = \Delta w(t). \tag{7.49}$$

For the design of the divisor that distributes the virtual control action $\Delta\mu(s)$, an optimization problem with restrictions was considered, equivalently to (Alvarez-Ramirez et al. 2004). The restriction is expressed by the equation (7.39) and the function to minimize is:

$$\arg\max_{\Delta v_1, \Delta v_2} \frac{1}{2}\left(\gamma\Delta v_1(s)^2 + (1-\gamma)\Delta v_2(s)^2\right) \tag{7.50}$$

where $\gamma \in [0, 1]$ is a design parameter to fix the relative weight of each control action $(\Delta v_1, \Delta v_2)$ determining the degree of collaboration between them. The solution of the optimization problem is

$$\Delta v_1(s) = (1-\gamma)\Delta\mu(s), \tag{7.51}$$

$$\Delta v_2(s) = \gamma\Delta\mu(s). \tag{7.52}$$

Intuitively, insulin delivery should be prioritized with respect to glucagon. The latter should be delivered only when insulin infusion is below a given threshold,

u_{th}. Thus, the following divisor is defined

$$\gamma = \begin{cases} 0 & \tilde{u}(t) > u_{th} \\ 1 & \tilde{u}(t) \leq u_{th} \end{cases} \tag{7.53}$$

where $\tilde{u}(t)$ is the would-be insulin infusion if directing the control effort through the insulin input channel. In the extreme case where $u_{th} = 0$, glucagon would act when the insulin pump is shut off in response to impending hypoglycaemia. However, delays due to glucagon subcutaneous absorption may be a limitation to successfully avoid hypoglycaemia. For this reason, $u_{th} \geq 0$ will be considered here. Remark that for $\gamma = 1$ (activation of glucagon delivery), the insulin infusion will correspond to the free response of the system (7.46), since $\Delta v_1(s) = 0$.

The switching due to (7.53) does not affect the closed-loop transfer function. When $\gamma = 0$, the closed-loop transfer function is

$$H_{cl}^0(s) := \frac{C(s)\frac{1}{\alpha}\left(\frac{H_1(s)}{H_2(s)}\right)^{-1}\alpha H_1(s)}{1 + C(s)\frac{1}{\alpha}\left(\frac{H_1(s)}{H_2(s)}\right)^{-1}\alpha H_1(s)} = \frac{C(s)H_2(s)}{1 + C(s)H_2(s)} \tag{7.54}$$

and, when $\gamma = 1$:

$$H_{cl}^1(s) := \frac{C(s)\frac{1}{\beta}\beta H_2(s)}{1 + C(s)\frac{1}{\beta}\beta H_2(s)} = \frac{C(s)H_2(s)}{1 + C(s)H_2(s)}. \tag{7.55}$$

Therefore, the closed-loop transfer function remains unaltered and it will be stable by the design conditions on $C(s)$.

7.5.1 Tuning of the coordinated controller (CC) proposed.

- Master controller, $C(s)$.

The master controller is defined by equation (7.44), and the parameters that determine its dynamics are K_p, T_d, and G_{ref}. K_p and T_d were manually tuned to achieve the best possible glycaemic outcomes in the average patient, i.e. percentage time in target range [70, 80] mg/dL and percentage time below target. Figure 7.4 shows a representation of the parameter values screening. G_{ref} was fixed to 100 mg/dL because it is the desirable value for an optimal glycaemia. One day scenario with three meals (7am (50g), 1pm (80g), 8pm (60g)) was used for the

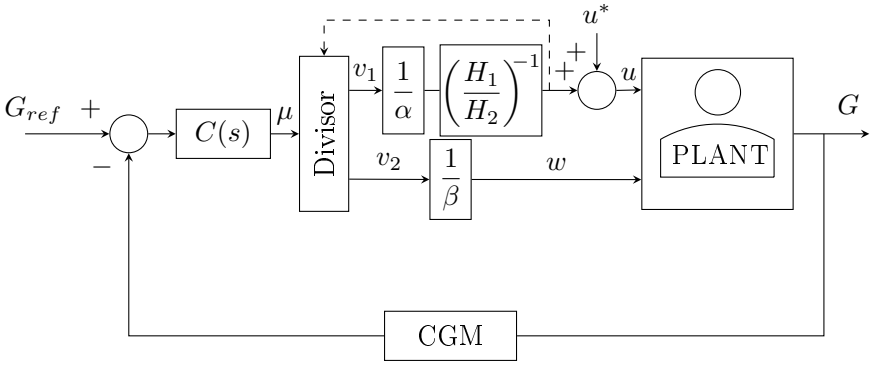

Figure 7.3: Block diagram of the closed-loop system for glucose coordinated control based on the proposed parallel control structure.

parameters tuning. Intrasubjects variability was also included. For all the evaluated subjects, these parameters were fixed to the same value: $k_p = 3.1350 \times 10^4$, $T_d = 90\,\text{min}$ and, $G_{ref} = 100\text{mg/dL}$, considering them as population parameters since they were evaluated in the average patient.

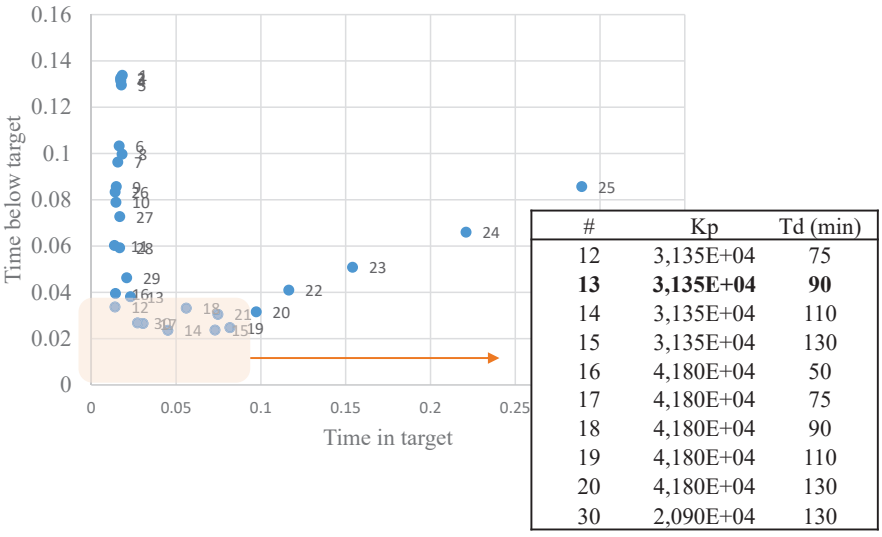

#	Kp	Td (min)
12	3,135E+04	75
13	**3,135E+04**	**90**
14	3,135E+04	110
15	3,135E+04	130
16	4,180E+04	50
17	4,180E+04	75
18	4,180E+04	90
19	4,180E+04	110
20	4,180E+04	130
30	2,090E+04	130

Figure 7.4: Graphical representation of the results from parameters screening.

- Filter

After the identification process, the filter resulted in:

$$\left(\frac{H_1(s)}{H_2(s)}\right)^{-1} = \frac{s^2 + 0.01074s + 4.395 \times 10^{-5}}{0.3522s^2 + 0.008251s + 4.395 \times 10^{-5}} \tag{7.56}$$

with unitary static gain:

$$\left(\frac{H_1(0)}{H_2(0)}\right)^{-1} = 1. \tag{7.57}$$

An identification procedure was conducted using the average patient in the distribution version of the UVA-Padova simulator, resulting in second order systems relating the dynamics of both hormones, which is considered constant in all patients. However, the filter is multiplied by an individualized gain, $1/\alpha$, which depends on the insulin sensitivity.

The parameter α was individualized for each patient following an identification procedure based on the impulse response for a set of bolus doses. As an example, Figure 7.5 shows the identification process output of patient #10. The individualization was carried out to reduce the outcomes variability and reduce the error between a population insulin sensitivity and the real one for each patient. Besides, an interesting point of this parameter is that it could be determined clinically in T1D patients. The value of α identified for each patient is show in Table 7.1. Likewise, β was obtained for each patient analogously to the parameter α. This parameter is related to the glucagon sensitivity. Table 7.1 summarizes the identified values of α and β for each patient.

#	1	2	3	4	5	6	7	8	9	10	11
α	0.0179	0.0147	0.0126	0.0164	0.0135	0.0072	0.0311	0.0119	0.0173	0.0097	0.0124
β	633.20	1214.00	5378.00	459.60	844.60	253.40	103.00	350.80	1285.00	807.20	807.10

Table 7.1: α and β values identified for each patient.

- Divisor

The divisor requires special attention since it determines the performance of the controller in terms of switching between glucagon and insulin. The switch condition is defined in equation (7.53), thus, depending on the value of u_{th}, the delivery of the hormones is simultaneous or non-simultaneous. It means that the configuration of this component allows to define how the delivery of both hormones is

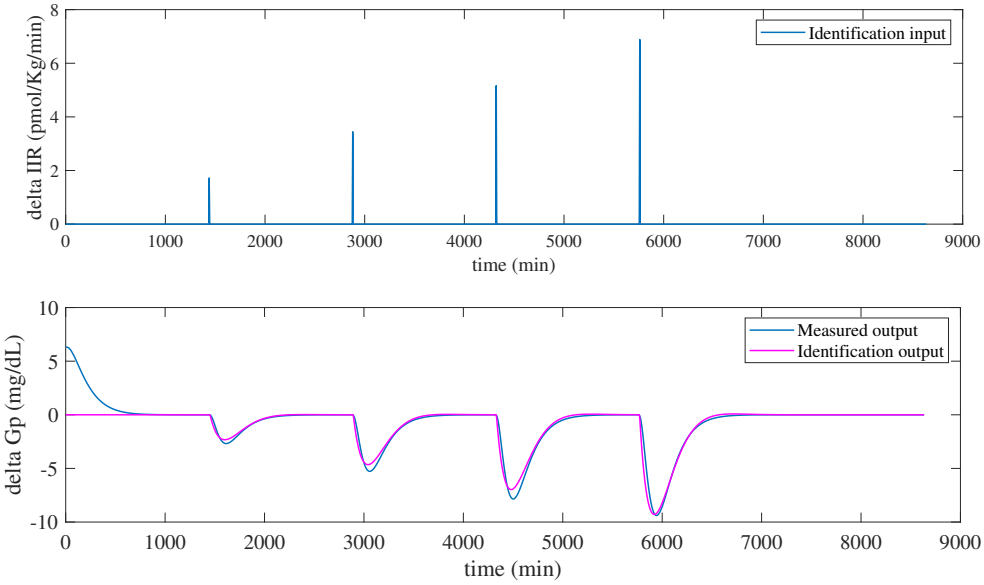

Figure 7.5: Outcomes from insulin sensitivity identification process for patient #10.

distributed. This fact is relevant and can modify significantly the performance of the variable to control because of the differences in the pharmacodynamics and interactions.

Therefore, the effect of the parameter u_{th} on the controller performance was evaluated in order to determine the optimal switch condition for the CC. The following thresholds were considered: $u_{th} \in \{0,\ \ 0.25u^*,\ 0.5u^*,\ 0.75u^*\}$. Each one of them was evaluated in the three different scenarios, which were used in the subsequent in-silico evaluation of the controllers, in order to define the value of u_th with better performance. Results of these simulations (glucose mean, percentage of several times in ranges, and the total amount of insulin and glucagon delivered) are shown in Appendix C. Figure 7.6 summarizes the results of interest to set the optimal value of u_{th} in the CC configuration.

The higher the value of u_{th}, the lower the time in hypoglycaemia, without compromising the time in range. In the case $u_{th} = 0$, the values of hypoglycaemia are significantly high during the scenario with exercise disturbance. This value for the switch condition means that the glucagon delivery only occurs when the insulin delivery suggested by the controller is zero. Therefore, results show that the anticipated glucagon delivery during physical activity is relevant to face with the faster drop in glucose concentrations. $u_{th} = 0.5u^*$ improves the hypoglycaemic

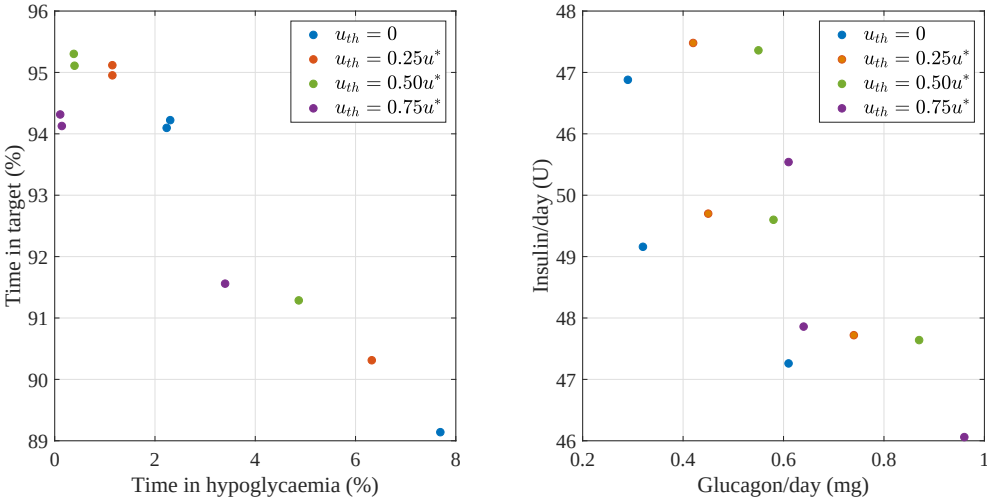

Figure 7.6: Illustration the time in range vs time in hypoglycaemia, and the insulin delivery vs the glucagon delivery for each threshold considered. Data from the three different scenarios are included.

percentages although the insulin delivery is even superior to the case $u_{th} = 0.75u^*$. The total glucagon daily delivered is higher in $u_{th} = 0.75u^*$, but it is within the healthy limits (1mg/day). Definitely, looking at the results, the best controller performance is found with $u_{th} = 0.75u^*$. Therefore, the parameter u_{th} of the CC configuration is set to $0.75u^*$.

7.5.2 Comparison between non-coordinated and coordinated control strategies.

In this section, the contribution of coordination is evaluated, by comparing with a standard independent insulin and glucagon loops structure. The non-coordinated structure (NCC) considered for the comparison is shown in Figure 7.7. In order to be consistent with the structure evaluation, the design and tuning of the insulin loop is the same as the one used in the coordinated controller (CC). It means that the insulin infusion is equivalent to setting $\gamma = 0$ in equations (7.51)-(7.52). Insulin infusion is saturated to be non-negative. The design of the glucagon loop is based on the proportional-derivative controller (PD) proposed in (Herrero et al. 2012), in which the proportional term only acts when glucose is below the glucose reference for the glucagon loop, $G_{ref_{ggon}}$:

$$PD_{ggon}(s) = \kappa + Kp_{ggon}Td_{ggon}s \tag{7.58}$$

$$\kappa = \begin{cases} Kp_{ggon} & \text{if } G_{ref_{ggon}} - G(t) > 0 \\ 0 & \text{otherwise} \end{cases} \tag{7.59}$$

$$w(s) = PD_{ggon}(s)\left(G_{ref_{ggon}}(s) - G(s)\right) \tag{7.60}$$

where PD_{ggon} is the controller transfer function, Kp_{ggon} is the proportional gain and Td_{ggon} is the time derivative.

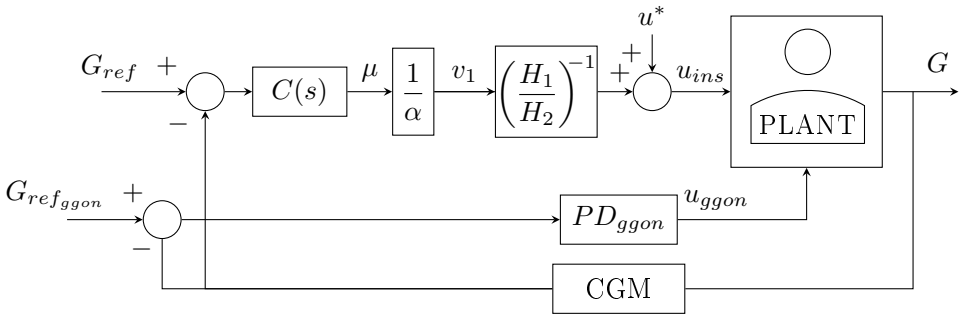

Figure 7.7: Block diagram of the closed-loop system for glucose non-coordinated control (NCC).

In current dual-hormone systems based on insulin and glucagon independent loops structure, an activation condition for the glucagon loop is defined. To evaluate the isolated effect of the coordination on the dual-hormone controller performance, the glucagon loop is activated equivalently to the switching condition (7.53). Thus, the glucagon action is defined as:

$$u_{ggon}(t) = \begin{cases} 0 & u_{ins}(t) > u_{th} \\ w(t) & u_{ins}(t) \leq u_{th} \end{cases} \tag{7.61}$$

Regarding to the tuning of the NCC controller, the values of the parameters that are part of the insulin loop (k_p, T_d, G_{ref}, β, and α) were the same as the values identified in the CC controller. On the other hand, the parameters of the independent glucagon loop ($T_{d_{ggon}}$ and $G_{ref_{ggon}}$) were manually tuned to achieve the best possible glycaemic outcomes in the average patient, i.e., percentage time in target range [70, 80] mg/dL and percentage time below target; instead, $k_{p_{ggon}}$ was expressed as a function of glucagon sensitivity β.

In order to make a rigorous comparison and analyse the effect of the coordination, the value of u_{th} was set to the same value that it was set in the previous case of CC. That is $u_{th} = 0.75u^*$, giving rise to the configuration referenced as NCC-A. This means that glucagon activation will happen at the same time, changing the way it is subsequently delivered.

	CC	NCC-A	NCC-B
$\mathbf{K_p}$	3.1350×10^{-4}	3.1350×10^{-4}	3.1350×10^{-4}
$\mathbf{T_d(min)}$	90	90	90
$\mathbf{G_{ref}mg/dL}$	100	100	100
α	$(*)$	$(*)$	$(*)$
β	$(*)$	$(*)$	$(*)$
$\mathbf{K_{p_{ggon}}}$	-	$0.3228/\beta$	$0.3228/\beta$
$\mathbf{T_{d_{ggon}}(min)}$	-	10	10
$\mathbf{G_{ref_{ggon}}mg/dL}$	-	90	90
$\mathbf{u_{th}}$	$0.75u^*$	$0.75u^*$	0

Table 7.2: Value of the parameters for CC, NCC-A, and NCC-B.

On the other hand, the optimal u_{th} value for the NCC configuration was also identified following a similar procedure to the CC case (more details about this analysis in Appendix C). The analysis proved that the optimal threshold for the non-coordinated configurations was $u_{th} = 0$ (referenced as NCC-B). It means that the glucagon pump is only activated when theoretical insulin delivery has negative values (insulin saturation in zero). Therefore, the anticipation of glucagon delivery is not suitable in this configuration. Table 7.2 summarizes the value of the parameters in the three configurations considered during the controllers assessment.

7.5.3 In silico evaluations

Simulation scenarios description

The simulator UVA-Padova Simulator (Dalla Man et al. 2014) with the addition of the exercise model (Schiavon et al. 2013) and intra-day and intra- subject variability was used to assess the proposed coordinated control structures. Notice that the addition of variability sources provides more realistic scenarios besides of making possible the robustness evaluation of the controller against common uncertainty sources.

Intra-day variability was introduced to the simulator by modifying some of the parameters: meal variability was emulated by introducing meal-size variability ($CV = 10\%$), meal-time variability ($SD = 20$) and uncertainty in the carbohydrate estimation (uniform distribution between -30% and $+40\%$). Variability of meal absorption rate (k_{abs}) and carbohydrate bioavailability (f) were considered

to be ±30% and ±10% respectively. For intra-day meal variability, the 11 meals corresponding to each cohort were randomly assigned at each meal intake.

To emulate intra-subject variability, insulin absorption model parameters (k_d, k_{a1}, k_{a2}) were varied ±30%. Insulin sensitivity parameters (V_{mx}, K_{p3}) were assumed to change along the day following the sinusoidal pattern

$$p(t) = p_0 + 0.3 \cdot p_0 \sin\left(\frac{2\pi}{24 \cdot 60}\right)t + 2\pi \cdot RND, \tag{7.62}$$

where $p(t)$ is the corresponding time-varying parameter (i.e. V_{mx} or k_{p3}); p_0 is the default parameter value in the simulator; and RND is a randomly uniformly generated number between 0 and 1.

Finally, variability into exercise was added modifying the starting time ($STD = 20\,\text{min}$), the exercise intensity ($CV = 10\%$), and the duration ($CV = 10\%$).

Three scenarios were considered, all of them with meal announcement:

- Scenario A. The daily patterns of carbohydrate doses in this scenario are the following : 7am (50g), 1pm (80g), 8pm (60g).
- Scenario B. The daily patterns of carbohydrate doses in this scenario are the same than scenario A with the addition of a daily snack (30g) at 5pm.
- Scenario C. The daily patterns of carbohydrate doses in this scenario are the same than scenario A. The peculiarity lies in the incorporation of an exercise event at 3pm with a duration of 60min and an intensity ($VO_{2max}\%$) of 50%.

The duration of the simulations was two weeks and, the cohort analysed was 100 adults based on the 10 adults that are available in the educational version of the UVA/Padova simulator, with 10 repetitions each getting different instances of variability. The chosen basal insulin infusion rates (u^*) were the ones provided by the simulator for each subject.

Outcomes from simulations

The performance of each configuration (CC, NCC-A, and NCC-B) was assessed in order to compare the features of each one. To quantify the goodness of the glycaemic control, the following internationally accepted metrics (Maahs et al. 2016) were calculated: mean blood glucose (BG); percentage time in target range [70,180] mg/dl (TIR); percentage time below target (< 70 mg/dL); percentage

time below 54mg/dL (< 54 mg/dL); percentage time above target (> 180 mg/dL); standard deviation (STD); daily average of insulin delivered in units of insulin (INS); and daily average of glucagon delivered in mg (GGON). Additionally, MAG, LBGI and IGC were also obtained since it was demonstrated in Chapter 6 that they are the most appropriate metrics to assess glycaemic variability. Then, the differences between the three configurations were evaluated non-parametrically in each scenario, using the Kruskal Wallis test with Fisher's LSD post-hoc analysis.

Table 7.3 shows the results for scenario A. Across the patient cohorts, when there was only meal perturbation, the time in hypoglycaemia was the same in CC and its equivalent non-coordinated configuration, NCC-A, ($p = 0.232$ for percentage of time under 70 mg/dL, and $p = 0.924$ for time under 54mg/dL) although with greater glucagon infusion in the latter ($p < 0.001$). Nevertheless, the mean glucose and the time above range were greater in the non-coordinated configuration ($p < 0.01$) despite higher insulin delivery in NCC-B. These results reflect that, when the glucagon delivery is triggered at the same time, the NCC-A is prone to glucagon and insulin over-delivery resulting in increased hyperglycaemias, compared to CC.

On the other side, comparisons between the CC and the best configuration for NCC, NCC-B, showed the same performance in time in range ($p = 0.652$), and time above 180 mg/dL ($p = 0.233$); but time below 70 mg/dL and 54 mg/dL were lower in CC ($p < 0.01$ in both cases). The hormone delivery was the same for insulin ($p = 0.328$), but it was greater for glucagon in NCC-B ($p < 0.01$). It means that the different way to distribute the glucagon delivery of CC resulted in a reduced time in hypoglycaemia.

The results from scenario B are shown in Table 7.4. The addition of snack perturbation implied an increase on the number of hypoglycaemic events relative to scenario A for NCC-B; this difference was statistically significant ($p < 0.001$) with respect to CC controller, which showed to be most favourable. Glucagon and insulin delivery was the same in both ($p = 0.346$ for insulin delivery, and $p = 0.734$ for the glucagon delivery), although the performance was sub-optimal in NCC-B configuration. However, the percentage of time in hypoglycaemia was statistically similar in CC and NCC-A, although it was at the expense of a higher time in hyperglycaemia in NCC-A ($p < 0.01$), a higher glucose mean and variability ($p < 0.01$ in both), and a higher hormones delivery ($p < 0.01$ in glucagon and insulin delivery). Therefore, the CC configuration showed improved performance.

Lastly, when exercise perturbation was added (scenario C), CC and NNC-A configurations performed similarly as in scenario A although the number of hypoglycaemic events increased. Nevertheless, the amount of glucagon was significantly higher in NCC-A ($p < 0.001$) and the percentile 75 is further of the physiologi-

	CC	NNC-A	NNC-B	CC vs NCC-A	CC vs NCC-B
MG (mg/dL)	129.04(5.55) 129[126.19; 131.63]	141.47(17.58) 137.32[134.72;139.59]	121.60(5.52) 120.71[117.33;124.59]	P-value <0.01	P-value <0.01
TIR(%)	94.13(3.27) 94.49[92.11;96.78]	88.18(15.84) 92.83[89.96;96.22]	94.58(3.62) 95.57[92.37;97.61]	P-value <0.01	P-value= 0.652
>180(%)	5.73(3.35) 5.43[2.90;7.89]	11.81(15.84) 7.17[3.78;9.98]	4.53(3.53) 3.47[1.56;6.78]	P-value <0.01	P-value= 0.233
<70(%)	0.14(0.30) 0.00[0.00;0.00]	0.01(0.04) 0.00[0.00;0.00]	0.89(0.95) 0.57[0.25;1.26]	P-value= 0.232	P-value <0.01
<54(%)	0.00(0.02) 0.00[0.00;0.00]	0.00(0.00) 0.00[0.00;0.00]	0.06(0.13) 0.00[0.00;0.05]	P-value= 0.924	P-value <0.01
INS (U/day)	47.43(11.52) 44.41[40.23;53.25]	52.49(12.50) 51.17[44.38;58.14]	49.10(12.12) 45.80[41.50;55.00]	P-value <0.01	P-value= 0.328
GGON (mg/day)	0.64(0.54) 0.44[0.25;0.92]	2.08(2.48) 1.21[0.65; 2.16]	0.72(0.75) 0.31[0.18;1.11]	P-value <0.01	P-value <0.01
MAG (mg/dL)	1.20(0.21) 1.19[1.01;1.39]	1.28(0.35) 1.23[1.02;1.38]	1.23(0.22) 1.18[1.05;1.43]	<0.01	<0.01
GVP (%)	12.84(3.62) 11.78[9.73;19.96]	13.49(5.42) 12.02[9.44;16.02]	13.19(3.84) 11.75[9.99;16.81]	0.078	<0.01
LBGI	0.13(0.11) 0.09(0.05;0.16)	0.05(0.05) 0.03[0.02;0.05]	0.46(0.25) 0.39[0.28;0.63]	<0.01	<0.01
IGC	0.32(0.12) 0.31[0.23;0.39]	0.63(0.72) 0.42[0.30;0.53]	0.37(0.19) 0.32[0.23;0.46]	<0.01	0.069

Table 7.3: Statistical analysis for comparison CC vs NCC, Scenario A.

cal acceptable limit (1mg/day). If the best configuration for NCC is considered for the comparison, the glucagon delivery was improved but it was even greater ($p < 0.01$) compared with CC configuration whereas the insulin delivery was statistically similar ($p = 0.346$). Looking at Table 7.5, results were acceptable for CC configuration, but hypoglycaemia events were not completely avoided, remaining an average of $3.40 \pm 2.92\%$ of time in hypoglycaemia.

In addition, these comparisons are also shown in Figure 7.8. Median and interquartile range for each scenario and controller configuration are represented for the studied cohort. Two days has been represented instead of all fourteen days of the simulation in order to observe better the behaviour described by the two configurations proposed.

About glucose variability analysis in each controller, a reduction of glucose variability is observed in CC configuration ($p < 0.05$ in all MAG and LBGI compar-

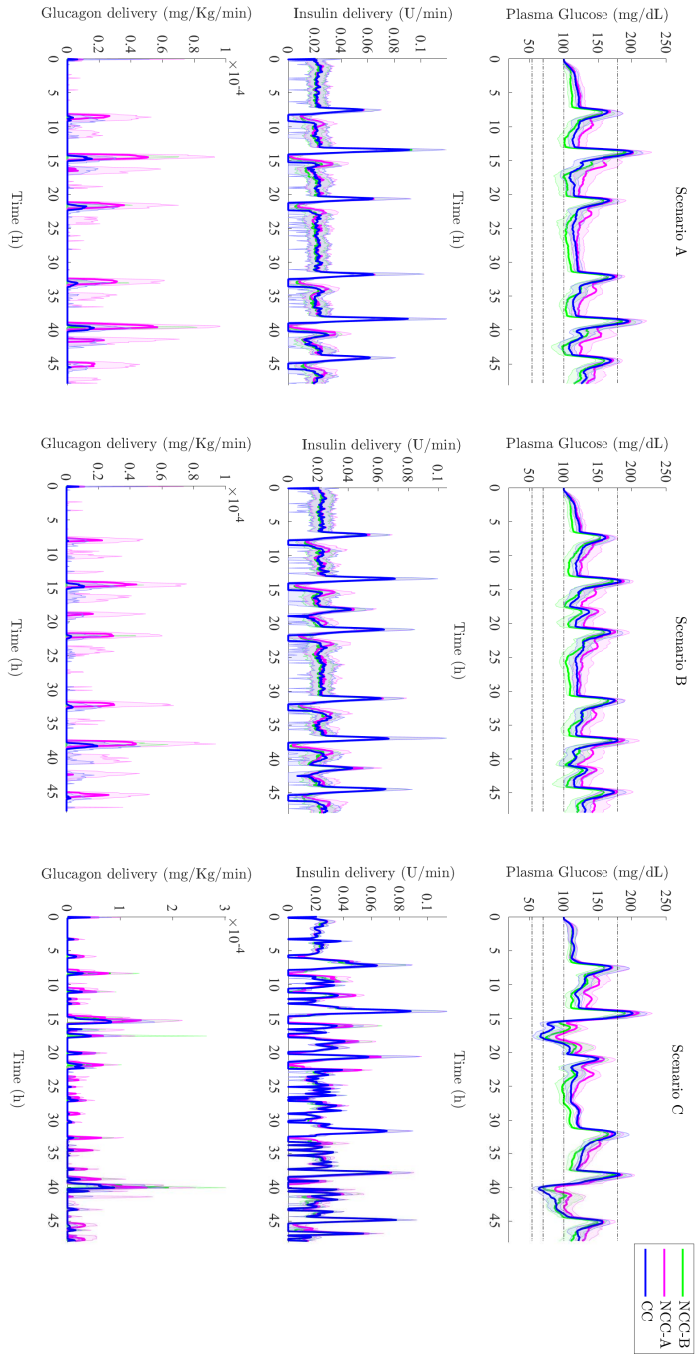

Figure 7.8: Evaluated controllers (CC, NCC-A, and NCC-B) performance during scenario A, B, and C. Median and percentile 25 and 75 are represented for two simulated days.

	CC	NNC-A	NNC-B	CC vs NCC-A	CC vs NCC-B
MG (mg/dL)	130.53(5.53) 130.41[128.03;132.95]	142.52(16.32) 137.99[136.03;141.60]	122.60(5.44) 121.42[118.27;126.81]	P-value <0.01	P-value <0.01
TIR(%)	94.32(3.12) 94.92[92.97;96.49]	88.26(14.66) 92.77[89.93;95.45]	94.54(3.67) 95.54[92.61;97.32]	P-value <0.01	P-value= 0.814
>180(%)	5.57(3.13) 5.02[3.39;7.03]	11.73(14.67) 7.23[4.55;10.07]	4.40(3.32) 3.44[1.96;5.84]	P-value <0.01	P-value= 0.210
<70(%)	0.11(0.27) 0.00[0.00;0.11]	0.02(0.06) 0.00[0.00;0.00]	1.06(1.32) 0.60[0.15;1.38]	P-value= 0.518	P-value <0.01
<54(%)	0.00(0.01) 0.00[0.00;0.00]	0.00(0.00) 0.00[0.00;0.00]	0.21(0.43) 0.00[0.00;0.24]	P-value= 0.968	P-value <0.01
INS (U/day)	48.77(11.87) 45.31[41.98;54.94]	53.85(12.81) 51.96[46.07;59.76]	50.42(12.47) 46.67[43.13;56.68]	P-value <0.01	P-value= 0.346
GGON (mg/day)	0.61(0.51) 0.47[0.23;0.94]	2.01(2.35) 1.20[0.67;2.18]	0.66(0.67) 0.30[0.17;1.12]	P-value <0.01	P-value= 0.734
MAG (mg/dL)	1.21(0.20) 1.21[1.02;1.38]	1.29(0.32) 1.26[1.04;1.42]	1.24(0.21) 1.20[1.04;1.40]	<0.01	<0.01
GVP (%)	12.54(3.44) 11.84[9.56;16.00]	13.17(4.96) 11.90[9.38;15.80]	12.84(3.63) 11.65[9.67;15.74]	0.527	0.001
LBGI	0.11(0.11) 0.08[0.04;0.14]	0.05(0.06) 0.02[0.01;0.05]	0.48(0.29) 0.40[0.25;0.57]	<0.01	<0.01
IGC	0.33(0.14) 0.31[0.24;0.38]	0.64(0.67) 0.45[0.33;0.55]	0.42(0.28) 0.33[0.22;0.61]	<0.01	0.018

Table 7.4: Statistical analysis for comparison CC vs NCC, Scenario B.

isons). The mean absolute glucose (MAG) is lower in CC configuration, which implies a reduction in the within-day variability, the percentage of glucose variability (GVP) is also lower in CC, but it is not statistically different from NCC-A in scenario A ($p = 0.078$) and B ($p = 0.527$). The LBGI is lower in the NCC-A but it is due to the higher glucose mean ($p < 0.001$). In addition, the control quality index (IGC) is more favourable in CC and NCC-B. Nevertheless, the scenario C shows a higher glucose variability metrics and LBGI and IGC indices. This is coincident with the results obtained with the percentage of times in ranges and the approximately 0% of time in hypoglycaemia of NCC-A. However, the CC presents better features related to the NCC configurations.

These behaviours confirmed the positive benefit of the intrinsic coordination in hormones delivery of the CC configuration; it was able to deal with the overlapping between glucagon and carbs and with the severe hypoglycaemia. Nevertheless,

	CC	NNC-A	NNC-B	CC vs NCC-A	CC vs NCC-B
MG (mg/dL)	123.26(5.72) 121.93[119.27;126.80]	136.75(18.28) 132.06[129.88;133.96]	120.04(6.84) 119.39[115.62;120.30]	P-value <0.01	P-value <0.01
TIR(%)	91.56(3.42) 91.53[89.19;94.10]	89.26(15.21) 94.12[92.08;96.01]	93.15(4.32) 94.42[90.61;96.34]	P-value <0.01	P-value= 0.126
>180(%)	5.04(3.11) 4.24[2.47;6.88]	10.32(15.36) 5.43[3.15;7.56]	4.54(4.44) 2.91[1.65;5.28]	P-value <0.01	P-value= 0.623
<70(%)	3.40(2.92) 2.89[0.95;4.84]	0.42(0.65) 0.15[0.00;0.42]	2.31(1.65) 2.12[0.84;3.52]	P-value <0.01	P-value <0.01
<54(%)	0.73(1.29) 0.15[0.00;0.72]	0.02(0.07) 0.00[0.00;0.00]	0.36(1.43) 0.24[0.00;0.58]	P-value <0.01	P-value= 0.603
INS (U/day)	46.53(11.22) 44.02[39.26;52.23]	51.48(12.13) 50.61[43.44;56.77]	48.67(11.70) 46.38[41.27;54.15]	P-value <0.01	P-value= 0.194
GGON (mg/day)	0.96(0.79) 0.69[0.36;1.71]	2.64(3.11) 1.47[0.78;3.52]	1.38(1.39) 0.83[0.43;2.37]	P-value <0.01	P-value <0.01
MAG (mg/dL)	1.35(0.21) 1.35[1.17;1.46]	1.47(0.39) 1.39[1.25;1.51]	1.44(0.25) 1.41[1.28;1.55]	<0.01	<0.01
GVP (%)	15.64(3.74) 14.75[12.59;17.74]	17(6.69) 14.91[13.29;17.95]	17.00(4.67) 15.88[13.66;18.65]	0.005	<0.01
LBGI	0.84(0.57) 0.73[0.43;1.04]	0.20(0.16) 0.19[0.08;0.25]	0.75(0.33) 0.75[0.53;0.93]	<0.01	0.186
IGC	0.82(0.62) 0.62[0.42;0.94]	0.60(0.71) 0.37[0.30;0.50]	0.59(0.30) 0.55[0.33;0.80]	<0.01	0.001

Table 7.5: Statistical analysis for comparison CC vs NCC, Scenario C.

the time in hypoglycaemia during physical activity could be further improved. The hypoglycaemia should not be solved with an over-delivery of glucagon since it could provoke side effects, like nausea, to the patient besides, a higher risk of hyperglycaemic rebounds. For this reason, glucagon must be delivered in an optimal amount and the avoidance of hypoglycaemia during exercise must be addressed with the addition of an insulin limitation block to the coordinated control structure. This proposal is discussed in the subsequent section.

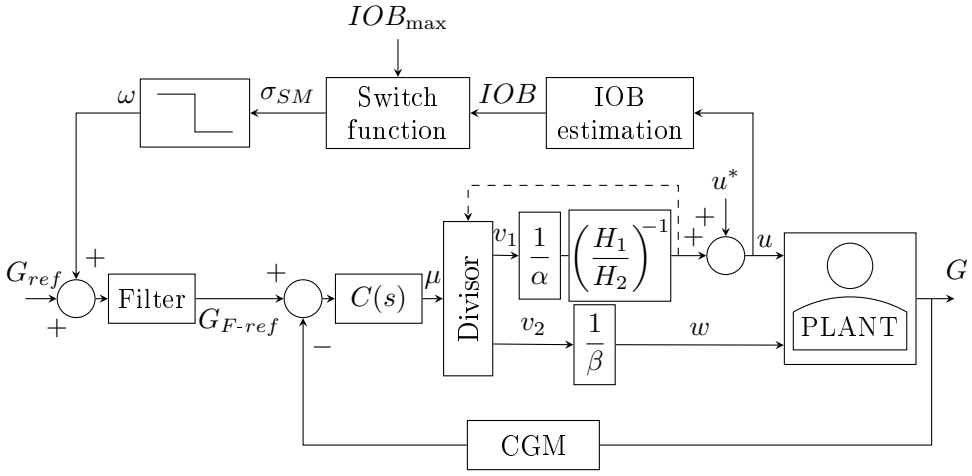

Figure 7.9: Block diagram of the closed-loop system for glucose coordinated control based on Habituating Control strategy with glucagon factorization and SMRC block (CC-SMRC).

7.6 Limitation of insulin on board

The novel dual hormone closed-loop system based on a parallel control structure with intrinsic coordination among insulin and glucagon delivery (CC) presented in previous section demonstrated acceptable values of time in ranges besides a reduction in glycaemic variability. Nevertheless, the hypoglycaemia during exercise can be even more improved.

For this reason, the above coordinated controller (CC) was extended with insulin on board (IOB) limitation through Sliding Mode Reference Conditioning (CC-SMRC), successfully tested in the context of single-hormone systems previously (Revert et al. 2013; Rossetti et al. 2017). The purpose of the incorporation of mechanisms to restrict the IOB is to minimize the insulin to deliver in order to reduce the impact of hypoglycaemia, especially in exercise scenarios where it has been demonstrated that some additional measure is required. The implementation of the Sliding Mode Reference Conditioning (SMRC) is proposed for dual-hormone systems according to the scheme shown in Figure 7.9.

The SMRC block acts on the glucose reference but it does not modify the stability of the closed loop system. It implies the addition of an external loop that imposes limits on the IOB, which is represented by two subcutaneous compartments, $S_1(t)$ and $S_2(t)$. The IOB definition is taken from the pharmacokinetics insulin model

suggested in (Hovorka et al. 2004). That is,

$$\dot{S}_1(t) = u_{SC}(t) - \frac{S_1(t)}{t_{\max I}} \tag{7.63}$$

$$\dot{S}_2(t) = \frac{S_1(t)}{t_{\max I}} - \frac{S_2(t)}{t_{\max I}} \tag{7.64}$$

$$IOB(t) = S_1(t) + S_2(t). \tag{7.65}$$

where $t_{\max I}$ is the time constant that determines the insulin transport, and u_{SC} ($\mathrm{mU{\cdot}kg^{-1}\cdot min^{-1}}$) is the subcutaneous insulin infusion.

Given an upper limit of IOB, $IOB_{\max}(t)$, and the system state denoted by $x(t)$, the set $\sigma := \{x(t)|IOB(t) \leq IOB_{\max}(t)\}$ is invariant for the discontinuous signal ω:

$$\omega(t) = \begin{cases} \omega^+ & \text{if } \sigma_{SM} > 0 \\ 0 & \text{otherwise} \end{cases} \tag{7.66}$$

$$\sigma_{SM}(t) := IOB(t) - IOB_{\max}(t) + \sum_{i=1}^{l-1} \tau_i \left(IOB^{(i)}(t) - IOB^{(i)}_{\max}(t) \right), \tag{7.67}$$

where $\omega^+ > 0$ and l is the relative degree between the output $IOB(t)$ and the input $\omega(t)$, (i) is the i-th derivative, and τ_i are gains to tune.

The first order filter defined by:

$$\frac{dG_{F-ref}(t)}{dt} = \lambda G_{F-ref}(t) + \lambda \left(G_{ref}(t) + \omega(t) \right), \tag{7.68}$$

allows to smooth the signal. $G_{ref}(t)$ is the original glucose reference (mainly constant), $G_{F\text{-}ref}$ is the conditionned reference, and λ defines the cut-off frequency of the filter. Based on the relative degree $l = 2$, determinated by the relative degree of the filter (7.68) and the relative degree of the IOB predictor (7.65), the switch function is defined as follows:

$$\sigma_{SM}(t) := IOB(t) - IOB_{\max}(t) + \tau \left(\frac{dIOB(t)}{dt} - \frac{dIOB_{\max}(t)}{dt} \right). \tag{7.69}$$

After the incorporation of the insulin-on-board limitation block to the control loop, equations (7.44)-(7.45) are modified as follow:

$$C(s) = \frac{\mu(s)}{G_{F\text{-}ref}(s) - G(s)} = kp\left(1 + T_d s\right), \tag{7.70}$$

$$\mu(s) = kp\left(1 + T_d s\right)\left(G_{F\text{-}ref}(s) - G(s)\right). \tag{7.71}$$

7.6.1 Tuning of the coordinated controller with IOB limitation (CC-SMRC) proposed.

The starting point for tuning the controller was the previous adjustments of the CC controller. That is, both structures (CC and CC-SMRC) share the tuning of the master controller parameters, thus, the parameters K_p, T_d, G_{ref}, α, and u_{th} had the same values as in CC.

About the parameters strictly related to the added SMRC block, for all evaluated subjects, parameters were fixed to the same value except the parameter $IOB_{\max}$. $IOB_{\max}$ was time invariant and defined as a constant multiplied by the basal IOB value (IOB_{basal}) of the corresponding patient. ω, λ, and τ were manually tuned to achieve the best possible glycaemic outcomes (i.e. percentage of time in range [70, 180]mg/dL and percentage below target). Table 7.6 summarizes the parameters value of the CC-SMRC controller.

$\mathbf{K_p}$	$\mathbf{T_d}$ (min)	$\mathbf{G_{ref}}$ (mg/dL)	α	$\mathbf{u_{th}}$	τ (min)	ω (min)	$\mathbf{IOB_{min}}$ (U)	$\mathbf{IOB_{max}}$ (U)
3.1350×10^{-4}	90	100	(*)	$0.75 \cdot u^*$ (*)	10	200	0	$1.3 \cdot IOB_{basal}$ (*)

Table 7.6: Values of the parameters for CC-SMRC.

7.6.2 In silico evaluation

The CC configuration was compared to CC-SMRC proposal in order to assess the benefit of the incorporation of the IOB limitation. The scenarios assessed were the same that were used previously with the CC comparison with the NCC configuration: scenario A (meal disturbance), B (meal and snack disturbances), and C (meal and exercise disturbance). Both CC and CC-SMRC performances are illustrated in Figure 7.10, and the quantitative results are presented in Table 7.7.

As determined before, the CC proposal was sufficient to prevent the hypoglycaemia (0.14% considering glucose $<$70 mg/dL, 0.00% considering glucose $<$54 mg/dL) in scenario A with only meal disturbance. The incorporation of the IOB limitation (CC-SMRC) had a similar performance to CC in terms of glucose mean, time in range, and time in hypoglycaemia ($p = 0.195$, $p = 0.806$, and $p = 0.180$, respectively). Nevertheless, the difference between the percentages of time under 54mg/dL was statistically significant. This might be due to the few hypoglycaemia events in the CC performance compared to the zero hypoglycaemia events with the CC-SMRC configuration.

	CC	CC-SMRC	P-value
MG (mg/dL)	129.04 (5.55) 129 [126.19; 131.63]	131.31 (5.53) 131.84 [128.31;133.78]	0.195
TIR(%)	94.13 (3.27) 94.49 [92.11; 96.78]	93.80 (3.47) 94.05 [91.78;96.85]	0.803
>180(%)	5.73 (3.35) 5.43 [2.90;7.89]	6.20 (3.47) 5.95 [3.15; 8.22]	0.268
<70(%)	0.14 (0.30) 0.00 [0.00;0.00]	0.00 (0.06) 0.00 [0.00;0.00]	0.180
<54(%)	0.00 (0.02) 0.00 [0.00;0.00]	0.00 (0.00) 0.00 [0.00; 0.00]	<0.001
INS (U/day)	47.43 (11.52) 44.41 [40.23;53.25]	47.10 (11.48) 44.16 [39.91;53.00]	<0.001
GGON (mg/day)	0.64 (0.54) 0.44 [0.25;0.92]	0.67 (0.56) 0.46 [0.27; 0.97]	<0.001
MAG (mg/dL)	1.20(0.21) 1.19[1.01;1.39]	1.18(0.21) 1.18[0.99;1.38]	0.086
GVP (%)	12.84(3.62) 11.78[9.73;19.96]	12.67(3.66) 11.57[9.49;16.84]	<0.01
LBGI	0.13(0.11) 0.09(0.05;0.16)	0.07(0.07) 0.04[0.03;0.09]	<0.01
IGC	0.32(0.12) 0.31[0.23;0.39]	0.33(0.14) 0.33[0.21;0.41]	0.124

Table 7.7: Statistical analysis for comparison CC vs CC-SMRC, Scenario A.

When a snack was included in the meal daily pattern (Table 7.8 and Figure 7.10), the glucose mean increased from the previous scenario as it was expected. Likewise, the glucose mean was slightly higher in CC-SMRC configuration, but not statistically significant ($p = 0.091$). This difference is mainly because of the different increase of glucose concentration when disturbance is produced, which is possibly due to the slightly higher glucagon delivery. It can be observed in Figure 7.10 at time=39h (i.e., 3pm of the second day) that the median is higher in CC-SMRC. Nevertheless, this detail did not mean that time in hyperglycaemia was higher in CC-SMRC ($p = 0.124$). Hence, both configurations were able to deal with the carbohydrates of the snack without triggering an undesired glycaemic rebound.

The improvement of the CC-SMRC proposal was clearly observed during exercise disturbance (Scenario C). Numerical results are shown in Table 7.9. Time in

	CC	CC-SMRC	P-value
MG (mg/dL)	130.53 (5.53) 130.41 [128.03; 132.95]	132.67 (5.53) 132.32 [130.66; 134.95]	0.091
TIR(%)	94.32 (3.12) 94.92 [92.97;96.49]	93.97 (3.31) 94.61 (92.53;93.30)	0.356
>180(%)	5.57 (3.13) 5.02 [3.39;7.03]	6.02 (3.31) 5.39 [3.70; 7.42]	0.124
<70(%)	0.11 (0.27) 0.00 [0.00;0.11]	0.01(0.04) 0.00 [0.00; 0.00]	0.179
<54(%)	0.00 (0.01) 0.00 [0.00;0.00]	0.00 (0.00) 0.00 [0.00; 0.00]	<0.001
INS (U/day)	48.77 (11.87) 45.31 [41.98;54.94]	48.45 (11.79) 45.02 [41.66;54.60]	<0.001
GGON (mg/day)	0.61 (0.51) 0.47 [0.23;0.94]	0.63 (0.52) 0.49 [0.25;0.99]	<0.001
MAG (mg/dL)	1.21(0.20) 1.21[1.02;1.38]	1.20(0.20) 1.19[1.01;1.38]	0.576
GVP (%)	12.54(3.44) 11.84[9.56;16.00]	12.37(3.44) 11.50[9.39;15.88]	<0.01
LBGI	0.11(0.11) 0.08[0.04;0.14]	0.06(0.07) 0.04[0.03;0.07]	<0.01
IGC	0.33(0.14) 0.31[0.24;0.38]	0.34(0.15) 0.33[0.25;0.39]	0.478

Table 7.8: Statistical analysis for comparison CC vs CC-SMRC, Scenario B.

hypoglycaemia was significantly reduced (1.45% vs 3.40%, $p > 0.001$, considering glucose <70 mg/dL, 0.18% vs 0.73%, $p < 0.001$, considering glucose <54mg/dL). This meant an increase in the time in range (92.98% vs 91.56%, $p = 0.023$) instead of an increment of the time in hyperglycaemia (5.57% vs 5.04%, $p = 0.115$). Moreover, insulin delivery was lower in CC-SMRC (45.91 U/day vs 46.53 U/day, $p = 0.001$) at the expense of higher glucagon delivery to reduce hypoglycaemia (1.03 mg/day vs 0.96 mg/day, $p = 0.001$). The improvements in glycaemic profile due to the CC-SMRC configuration are illustrated in Figure 7.10.

The glycaemic variability assessment of the CC and CC-SMRC configurations shows that the percentage of glycaemic variability (GVP) is improved in scenario A with the CC-SMRC configuration; besides, LBGI is also reduced in all scenarios. Nevertheless, MAG in CC-SMRC is not statistically different from CC since CC is able to reduce successfully the within day variability. On the other hand, IGC is

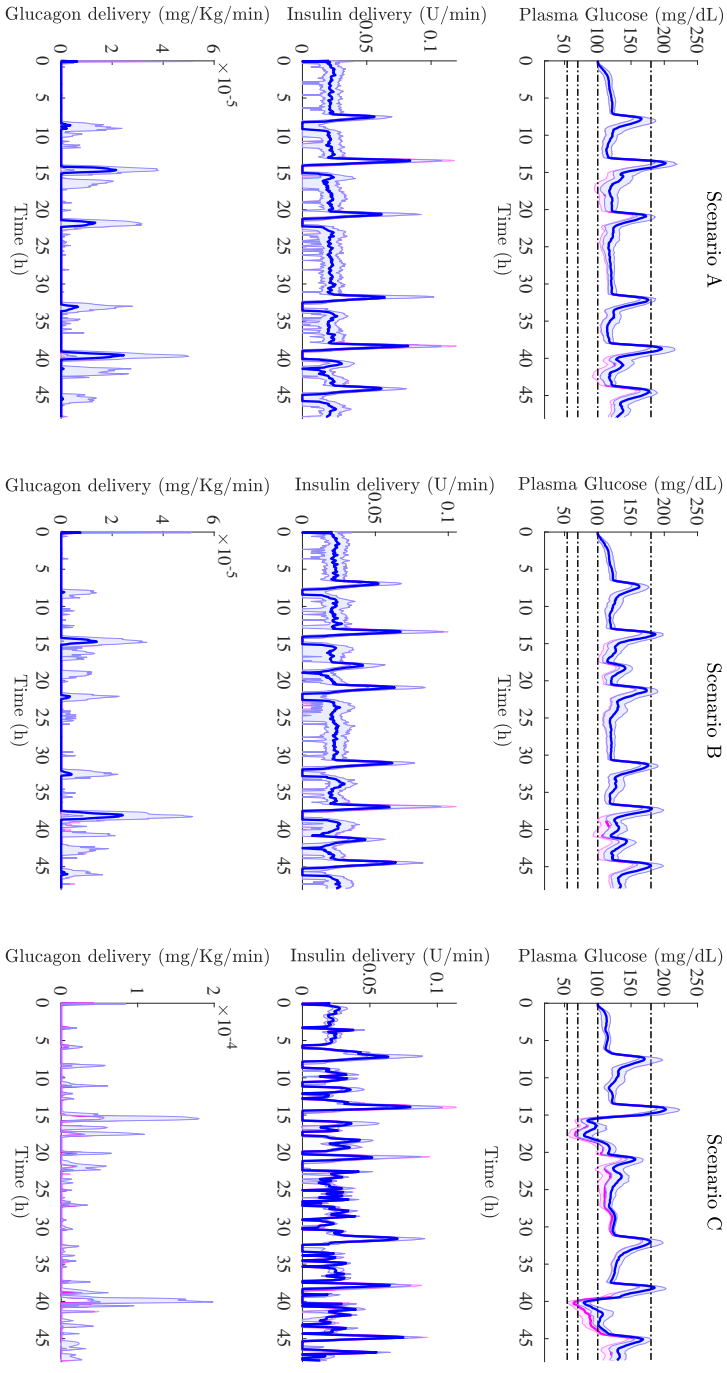

Figure 7.10: Evaluated controllers (CC and CC-SMRC) performance during scenario A, B, and C. Median and percentile 25 and 75 are represented for two simulated days.

	CC	CC-SMRC	P-value
MG (mg/dL)	123.26 (5.72) 121.93 [119.27;126.80]	127.47 (5.87) 126.25 [123.43;130.73]	<0.001
TIR(%)	91.56 (3.42) 91.53 [89.19;94.10]	92.98 (3.24) 93.04 [90.00;95.92]	0.023
>180(%)	5.04 (3.11) 4.24 [2.47;6.88]	5.57 (3.21) 4.94 [2.72;7.53]	0.115
<70(%)	3.40 (2.92) 2.89 [0.95;4.84]	1.45 (2.01) 0.61 [0.09;1.75]	<0.001
<54(%)	0.73 (1.29) 0.15 [0.00;0.72]	0.18 (0.50) 0.00 [0.00; 0.05]	<0.001
INS (U/day)	46.53 (11.22) 44.02 [39.26;52.23]	45.91 (11.16) 43.50 [38.68;51.75]	<0.001
GGON (mg/day)	0.96 (0.79) 0.69 [0.36;1.71]	1.03 (0.83) 0.75 [0.40;1.83]	<0.001
MAG (mg/dL)	1.35(0.21) 1.35[1.17;1.46]	1.33(0.21) 1.34[1.15;1.44]	0.065
GVP (%)	15.64(3.74) 14.75[12.59;17.74]	15.30(3.81) 14.44[12.14;17.50]	0.750
LBGI	0.84(0.57) 0.73[0.43;1.04]	0.44(0.36) 0.32[0.19;0.55]	<0.01
IGC	0.82(0.62) 0.62[0.42;0.94]	0.50(0.32) 0.39[0.28;0.58]	<0.01

Table 7.9: Statistical analysis for comparison CC vs CC-SMRC, Scenario C.

lower in scenario C. It means that the SMRC reduces the time in hypoglycaemia and then, provides better results faced with physical activity.

Looking at the above results, the proposed coordinated glucose control strategy demonstrates the benefits of timely glucagon delivery when the system starts to reduce insulin infusion below basal values, besides that, an optimized usage of both hormones achieves the best possible performance. Moreover, the improvements seen in percentage of time in target and in percentage of time under target with CC-SMRC suggest that the limitation of IOB is capable to avoid the hypoglycaemia. It advocates that an optimal glucagon delivery without an insulin on board limitation is not enough to prevent hypoglycaemia events during more demanding scenarios, such as physical activity.

Hence, the novel parallel control structure with intrinsic coordination among insulin and glucagon delivery and with IOB limitation that have been proposed in this work is able to meet the features of an acceptable Artificial Pancreas control algorithm: important decrease of hypoglycaemia events and reduction of glucose variability.

7.7 Conclusions

A closed-loop glucose control system with automatic insulin and glucagon delivery has the potential to reduce the self-management and the risk of hypo- and hyperglycaemia in type 1 diabetes subjects. A new dual-hormone closed-loop system based on a parallel control structure with intrinsic coordination among insulin and glucagon delivery has been presented in this chapter as a suitable proposal for the artificial pancreas control algorithm.

The benefits of the coordination between both hormones delivery have been proven by the comparison of our coordinated controller with the non-coordinated counterpart based on independent loops for the insulin and glucagon controllers, as currently done in dual-hormone systems. This analysis showed that the coordination distributes differently the hormones delivery such that it is able to reduce the percentage of time in hypoglycaemia and the glycamic variability. It was tested in three scenarios with different disturbances (meal, meal+snack, and meal+scenario). The performance of the coordinated dual-hormone controller was acceptable with the snack and meal disturbances. However, the time in hypoglycaemia during exercise scenario could be further improved. This might be because the fast drop in glucose concentration during exercise cannot be compensated for the glucagon delivery due to the still circulating insulin.

For this reason, a limitation of the insulin-on-board was included in the coordinated control scheme by means of the sliding mode reference conditioning (SMRC) strategy. The results with this additional insulin limitation were similar to the coordinated controller without insulin limitations during scenarios with meal and snack, although it is worth to mention that the glycaemic variability was even more reduced with the SMRC block incorporation. Nevertheless, the important benefit of the IOB limitation lied in exercise periods since it was able to improve the glycaemic control and, then, diminish the percentage of time in hypoglycaemia and the glycaemic variability. Other strong point of the coordinated controller proposed is the total daily glucagon delivered since it is below the acceptable healthy limits.

Simulations were carried out considering the uncertainty between the real model and the linearized one, besides of uncertainty due to the glucose variability, which was included to the simulations as it is explain in Section 7.5.3. The designed controllers handled these conditions, and the glucose levels were successfully controlled. Hence, the designed systems presented robustness against the considered model uncertainty.

The main limitation of this work is the population assumption of some controller parameters, such as IOB_{max}. That is, $IOB_{\max}$ is obtained from the basal IOB value of each patient multiplied by a general factor (1.5). Therefore, in the same way improvements were found in the controllers performance when individual values for insulin and glucagon sensitivity were considered, the multiplying factor of $IOB_{\max}$ could be obtained independently for each subject or even study the existence (or not) of certain relationship between this parameter and the insulin sensitivity. Moreover, other line to explore would be the study of the extra degree of freedom offered by the u_{th} configuration along with the tuning of the $IOB_{\max}$ in order to optimize the performance of the controller.

In addition, it is known that the large glucose intra- and intersubject variability along with physical factors like physical activity or illness among others have an important effect on the glycaemic control. Therefore, the adaptation of the controller parameters would make our system more robust to challenges in a daily life scenario.

On the other hand, it is worth pointing out that despite the limitations of using a linearized plant for the controller design, the performance of the controller was satisfactory, such/as the results showed. However, a future work line could be to explore several techniques to taking into account the nonlinearities and the time-varying dynamics (e.g. LPV controllers or adaptive control).

Finally, the complete validation of our parallel control-based coordinated dual-hormone artificial pancreas with insulin on board limitation is required to assure its good performance demonstrated in silico. To this end, clinical trials will be carried out in the near future in the scope of the mSAFE-AP project.

Chapter 8

Conclusions

In this thesis, several aspects related to the Artificial pancreas were addressed. It is known that patients with type 1 diabetes have a lack of endogenous insulin secretion so they need an exogenous contribution of insulin to regulate the glucose levels and keep them in an euglycaemic range. The automated insulin delivery system, or Artificial pancreas, releases the patient from the current burden of self-control and improves its glycaemic and metabolic control. Nevertheless, the incidence of hypoglycaemia is a problem that still concerns most researchers working in this field because it is not yet solved in the current systems. Therefore, the effort is focused on reducing hypoglycaemia. Likewise, a good control also implies a decrease in glycaemic variability, which is closely related to the long-term complications of diabetes.

This thesis addressed the problem of hypoglycaemia from an analysis in depth of which are the mechanisms involved in it and which physiological changes characterizes it. This allowed to get a hypoglycaemia model as compared to current approaches based on functional black-box models, if even considered. The physiological approach of the model allows to know and better understand the physiology associated with hypoglycaemia phenomenon.

Regarding glycaemic variability, there are multiple metrics to evaluate such phenomenon in the glycaemic profiles. Thus, it is necessary a consensus or a definition of a metrics set to facilitate the assessment of the controllers in terms of improve-

ments in glycaemic variability. In the thesis, a chapter was dedicated to the analysis of them.

Finally, an improvement of the control algorithms that allow to correct an overacting of the controller well in advance is necessary in order to avoid the hypoglycaemia and reduce the glycaemic variability. To achieve this, a dual-hormone configuration of the controller was proposed and assessed in several possible scenarios.

A summary of the thesis contributions addressing the aforementioned problems follows:

- *Study of the physiological response in hypoglycaemia and the development of a hypoglycaemia model which includes the counterregulatory response (chapter 5).*

An exhaustive study of physiology was carried out and the better understanding of counterregulatory mechanisms were achieved. From that study, adrenaline was found as the main counterregulatory hormone during hypoglycaemia events due to glucagon delivery is practically suppressed in T1D patients. The assessment of the adrenaline secretion and action were also conducted in order to extend the Bergman Minimal Model.

From the adrenaline action model, a paradoxical increment of glucose utilization during hypoglycaemia was observed. This led to find some physiological explanation to the phenomenon. Finally, the consideration of FFA mechanisms, which are involved also in the hypoglycaemia avoidance, provided a suitable model approach. Therefore, an extension of Bergman Minimal Model was proposed based on Adrenaline response as the main counterregulation line. The effect of adrenaline was included as a direct effect on glucose concentration and indirectly through the influence on FFA secretion. In addition, the adrenaline secretion model was also incorporate to the model extension presented.

The goodness of fit of the model showed an acceptable performance and an improvement in hypoglycaemia reproduction compared to the Minimal Model. Furthermore, the features of the physiological approach of this model were compared with the functional approach and both worked similarly. Hence, our proposal is able to associate the mathematical terms with physiological mechanisms and interactions.

The main limitation of this work is the reduced number of subjects and the duration of the clamp. Besides, the variability that presents the counterregulatory

response across the subjects is another limiting factor. For this reason, experimental data from clinical studies with longer duration and greater number of participants would provide subjects with a broader range of adrenaline response variation and a better representation of T1D population so that could reinforce our results.

- *Assessment of the multiple variability metrics and control quality indices (chapter 6).*

Several measures of glycaemic variability are described in literature. These can be subdivided into measures to evaluate glycaemic variability (e.g. SD, CV, MAGE, CONGA, MODD, LI, J-Index, M-Value, and MAG), and measures to evaluate glucose control quality that are also sensitive to glycaemic variability (e.g. GRADE, pTIR, ADRR, RI, LBGI, and HBGI). The interrelationship analysis between them suggested that simple metrics such as times in ranges were correlated and could be as informative and useful as the risk indices are, providing that they were good discriminators of glucose variability.

The data presented did not define an absolute gold standard for glycaemic variability measurement but strongly supported the use of MAG as an important glucose variability outcome for people with type 1 diabetes that may be used, alongside HbA1c and a measure of hypoglycaemia, to assess glucose and the impact of interventions in a meaningful way. The most robust time in range was 70 to 180 mg/dL and we advocate standardization of this as the primary time in range metric whereas LBGI and IGC should be considered the optimal glucose quality metrics. LBGI is recommended particularly in performances where the hypoglycaemia assessment is one of the object of study.

- *Development of a parallel Control-based coordinated dual-hormone artificial Pancreas with insulin on board limitation (chapter 7).*

The benefits of the coordination between glucagon and insulin delivery were proven by the comparison of our coordinated controller with the non-coordinated counterpart based on independent loops for the insulin and glucagon controllers, as currently done in dual-hormone systems. The analysis showed that the coordination distributes differently the hormones delivery such that it is able to reduce the percentage of time in hypoglycaemia and the glycamic variability. The performance of the coordinated dual-hormone controller was acceptable with snack and meal disturbances. However, the time in hypoglycaemia during exercise periods could be further improved. Therefore, limitation of the insulin-on-board was included in the coordinated control scheme by means of the sliding mode reference conditioning (SMRC) strategy. The results with this additional insulin limitation

were similar to the coordinated controller without insulin limitations during when meal and snack disturbances were given, the glycaemic variability was even more reduced with the SMRC block incorporation. The important benefit of the IOB limitation was demonstrated during exercise periods since it was able to improve the glycaemic control and, then, diminish the percentage of time in hypoglycaemia and the glycaemic variability. This configuration was able to compensate for the fast drop in glucose concentration during physical activity. In addition, the average total daily glucagon delivered is inside of the acceptable healthy limits.

Therefore, our work recommends sets as a good candidate for further clinical evaluation the parallel control-based coordinated dual-hormone artificial pancreas with insulin on board limitation suggesting a significant improvement in hypoglycaemia mitigation and glycaemic variability, including challenging exercise scenarios.

A word on future work

The future work might follow two different paths:

- From the results of the Bergman Minimal Model extension with the Counterregulatory response:

The main advantage of the proposed extension of the Bergman Minimal Model is that it allows to understand better the physiology of the hypoglycaemia. Nevertheless, the variability of the adrenaline response requires an individualization of the model parameters for each subject or studing a greater number of patients in order to obtain a complete population model. For this reason, a future work could be a validation with experimental data from clinical studies with longer duration and greater number of participants. This would provide subjects with a broader range of adrenaline response variation and a better representation of T1D population.

Notwithstanding, results obtained with the Minimal Model extended with counterregulatory response are successful and relevant.

- From the Dual-hormone coordinated controller proposed for the Artificial Pancreas:

It is known that the large glucose intra- and inter- variability along with physical factors like physical activity or illness among others have an important effect on the glycaemic control. Therefore, a future work that would enhance the features of our dual-hormone controller and would make the system more robust and feasible,

is the adaptation of the controller parameters. Indeed, the continuity of this work is focused on the study of the parameters adaptation by means of machine learning techniques.

On the other hand, the next step in this work will be the complete validation of our parallel control-based coordinated dual-hormone artificial pancreas with insulin on board limitation by means of clinical trials. Indeed, these studies will be carried out in the near future. The goal of the clinical trials will be to compare a single-hormone systems with both a dual-hormone systems presented in this thesis and an the single-hormone systems with carbohydrate recommendation algorithm which have been also developed in our research group.

Publications authored or co-authored

Listed below are all the contributions by the author to the field of the artificial pancreas obtained along the development of this thesis. In particular, publications [1, 6, 8, 13, 16, 17], also highlighted in bold, are related to the direct contributions of this thesis. However, as a result of scientific collaborations with external teams and participation in clinical studies by the group, has resulted in a set of complementary publications which are also listed here, composing the body of contributions to the field of the artificial pancreas.

Journal papers

1. **V. Moscardo, J. Bondia, F. J. Ampudia-Blasco, C. G. Fanelli, P. Lucidi, and P. Rossetti (2018). "Plasma Insulin Levels and Hypoglycemia Affect Subcutaneous Interstitial Glucose Concentration". In: *Diabetes Technology & Therapeutics* 20.4, pp. 263–273**. Indexed in WOS(JCR): Impact factor (2017) 2.921; Quartile Q3 (79/142). Indexed in SCOPUS(SJR): Impact factor (2017) 1.735; Quartile Q1.

2. M. Gimenez, A.J. Tannen, M. Reddy, V. Moscardo, I. Conget, and N. Oliver (2018). "Revisiting the Relationships Between Measures of Glycemic Control and Hypoglycemia in Continuous Glucose Monitoring Datasets". In: *Diabetes Care* 41.2, pp. 326–332. Indexed in WOS(JCR): Impact factor (2017) 13.397; Quartile Q1 (5/142). Indexed in SCOPUS(SJR): Impact factor (2017) 6.69; Quartile Q1.

3. P. Rossetti, C. Quiros, V. Moscardo, A. Comas, M. Giménez, F. J. Ampudia-Blasco, F. León, E. Montaser, I. Conget, J. Bondia, and J. Vehí (2017). "Closed-loop control of postprandial glycemia using an insulin-on-board limitation through continuous action on glucose target". In: *Diabetes Technology & Therapeutics* 19.6, pp. 355–362. Indexed in WOS(JCR): Impact factor (2017) 2.921; Quartile Q3 (79/142). Indexed in SCOPUS(SJR): Impact factor (2017) 1.735; Quartile Q1.

4. M. Giménez, S. Purkayajtha, V. Moscardó, I. Conget, and N. Oliver (2018c). "Intraperitoneal insulin therapy in patients with type 1 diabetes. Does it fit into the current therapeutic arsenal?" In: *Endocrinología, Diabetes y Nutrición* 65.3, pp. 133–188.

Conference papers

5. **V. Moscardó, P. Herrero, J. L. Diez, M. Guimenez, P. Rosseti, and J. Bondia (2019). "In silico evaluation of a Parallel Control-based Coordinated Dual-Hormone Artificial Pancreas with Insulin on Board Limitation". In: *American Control Conference 2019.* Accepted**

6. P. Avari, V. Moscardó, M. Reddy, M. Giménez, and N. Oliver (2018). "The I-HART CGM study: hypoglycaemic episodes reduced with continuous glucose monitoring compared to Flash in adults with type 1 diabetes". In: *The 54th Annual Meeting of the European Association for the Study of Diabetes (EASD).* Berlin, Germany, p. 85.

7. M. Reddy, M. Gimenez, V. Moscardo, and N. Oliver (2018). "The Relationship between A1C and Hypoglycemia in the Diamond Study". In: *The 8th Scientific Sessions of the American Diabetes Association (ADA).* Orlando, USA.

8. **V. Moscardo, P. Rossetti, F.J. Ampudia-Blasco, and J. Bondia (2016b). "Modelling of adrenaline action during hypoglycaemia in Type 1 Diabetes". In: *Proceeding of the 2016 IEEE Conference on Control Applications (CCA).* Buenos Aires, Argentina**.

9. **V. Moscardó, P. Rossetti, F. J. Ampudia-Blasco, and J. Bondia (2015). "Modelling adrenaline secretion during counterregulatory response in Type 1 Diabetes for improved hypoglycaemia prediction". In: *IFAC-PapersOnLine* 48.20, pp. 213–218**.

Conference Abstracts

10. M. Giménez, V. Moscardó, M. Reddy, I. Conget, and N. Oliver (2018a). "Diferencias entre poblaciones de pacientes con diabetes tipo 1 de alto y bajo riesgo de hipoglucemia utilizando sistemas de monitorizacion continua de la glucose". In: *Proceedings of the XXIX Congreso Nacional de la Sociedad Española de Diabetes*. Oviedo, Spain.

11. M. Giménez, A.J. Tannen, M. Reddy, V. Moscardó, I. Conget, and N. Oliver (2018d). "Revising the relationships between measures of glycaemic control and hypoglycaemia in Continuous Glucose Monitoring datasets". In: *The 11th International Conference on Advanced Technologies & treatments for diabetes (ATTD)*. Vienna, Austria.

12. M. Giménez, V. Moscardó, M. Reddy, I. Conget, and N. Oliver (2018b). "Differences between high and low Hypoglycaemia risk populations using Continuous Glucose Monitoring datasets". In: *The 11th International Conference on Advanced Technologies & treatments for diabetes (ATTD)*. Vienna, Austria.

13. V. Moscardó, M. Giménez, P. Avari, M. Reddy, and N. Oliver (2018b). "Influence of ambient temperature on glycaemic behaviour in type 1 Diabetes patients". In: *The 11th International Conference on Advanced Technologies & treatments for diabetes (ATTD)*. Vienna, Austria.

14. **V. Moscardó, J.L. Diez, P. Herrero, M. Giménez, P. Rosseti, and J. Bondia (2018a). "Sliding mode reference conditioning dual hormone coordinated glucose control". In: *The 11th International Conference on Advanced Technologies & treatments for diabetes (ATTD)*. Vienna, Austria**.

15. V. Moscardo, P. Rossetti, F.J. Ampudia-Blasco, and J. Bondia (2016a). "Amperometric glucose sensors' background current is a confounding factor of plasma-interstitium relationship studies during hypoglycaemia". In: *The 16th Annual Diabetes Technology Meeting (DTM)*. Bethesda, USA.

16. P. Rossetti, C. Quirós, V. Moscardó, A. Comas, M. Giménez, J. Ampudia, F. León, E. Montaser, I. Conget, J. Bondia, and J. Vehí (2016). "Better postprandial glucose control with a new developed closed-loop control system as compared with open-loop treatment in patients with type 1 diabetes". In: *The 76th American Diabetes Association (ADA) scientifc sessions*. New Orleans, USA.

Journal Papers under review

17. **V. Moscardó, P. Herrero, J.L. Diez, M. Guimenez, P. Rosseti, P. Georgiou, and J. Bondia (2018d). "Assessment of the Coordinated Control structure in the Dual Hormone Artificial Pancreas". In: *Computers & Chemical Engineering*. Submitted: Second review**.

18. **V. Moscardó, P. Herrero, M. Reddy, N. Hill, P. Georgiou, and N. Oliver (2018e). "Assessment of glucose control metrics by Discriminant Ratio". In: *Diabetes Technology & Therapeutics*. Submitted: First review**.

19. V. Moscardó, M. Gimenez, N. Oliver, and N. Hill (2018c). "Automated assessment of glucose variability in Diabetes". In: *Diabetes Technology & Therapeutics*. Submitted: First review.

Appendices

Appendix A

Glucose Variability metrics

Table A.1: Definition of the Glycaemic Variability metrics.

GLYCAEMIC VARIABILITY METRICS	
SD (Standard deviation) (Whitelaw et al. 2011)	$SD = \sqrt{\sum_{i=1}^{N} \left(G_i - \bar{G}\right)^2 \Big/ (N-1)}$ where G is glucose reading; N is the number of observations; and I is the sample index.
%CV (Coefficient of variation) (Whitelaw et al. 2011)	$\%CV = SD/\bar{G} \cdot 100$
MAGE (Mean amplitude of glucose excursion) (Hill et al. 2007)	$MAGE = \sum_{i=1}^{x} \lambda_i / x \;\; if\, \lambda > v$ where λ is the blood glucose changes from peak to nadir (or nadir to peak); x is the total number of valid observations; and v is 1SD of mean glucose for a 24h period.

CONGAn (Continuous overlapping net glycaemic action over n-hour period) (McDonnell et al. 2005)	$$CONGA_n = \sqrt{\sum_{t=1}^{k} \left(D_t - \bar{D}\right)^2 \Big/ (k-1)},$$ $$D_t = G_t - G_{t-m}$$ where k is the number of observations where there is an observation $n \times 60$ min ago; m is $n \times 60$; G_t is the glucose reading at time t min after start of observations.
MODD (Mean of daily differences) (Molnar et al. 1972)	$$MODD = \sum_{t=t_1}^{t_k} |G_t - G_{t-24h}|/k$$ where k is the number of observations with an observation 24h ago.
M-VALUE (M-value of Schlichtkrull) (Service 2013)	$$M = \sum_{i=1}^{N} \left| 10 \cdot \log_{10}\left(G_i/IGV\right)^3 \right| \Big/ N$$ where G is glucose measured; IGV is the ideal glucose value (default: 100mg/dL); and, N is the total number of readings
J-INDEX (Service 2013)	$$J = 0.001 \cdot \left(\bar{G} + SD\right)^2$$
MAG (Mean absolute glucose) (Service 2013)	$$MAG = \sum_{i=1}^{N-1} (G_i - G_{i+1})/T$$ where G_i is the glucose measured; N is the number of measurements; and, T is the total time (in hours).

AARC (Average absolute rate of change) (Whitelaw et al. 2011)	$$ROC_i = (G(t_i) - G(t_{i+1}))/(t_{i+1} - t_i)\ ,$$ $$i = 1, 2, 3, \ldots, N-1$$ where $G(t_1)$ and $G(t_2)$ are consecutive glucose readings taken at times t_1 and t_2. $$AARC = \sum_{i=1}^{N-1} ROC_i/(N-1)$$
GVP (Glycaemic variability percentage) (Hirsch et al. 2017)	$$GVP = 100 \cdot (L/L_0 - 1)$$ $$L = \sum_{i=1}^{n} \sqrt{{dx_i}^2 + {dy_i}^2}$$ where L_0 is the ideal length for a given temporal duration; dx is de decomposition of the temporal line into horizontal component; dy is de decomposition of the temporal line into vertical component; and n is the total number of glucose recordings.
LI (Lability index) (Ryan et al. 2004)	$$LI = \sum_{i=1}^{N-1} (G_{i+1} - G_i)^2 \Big/ (t_{i+1} - t_i)$$ where G is the glucose measured; N is the total number of glucose readings in a week; and, t is the time.

Table A.2: Definition of the Glucose Control Indices.

GLUCOSE CONTROL INDEXES	
GRADE (Glycaemic risk assessment diabetes Equation) (Hill et al. 2007) $\%GRADE_{hypo}$	$$GRADE = \sum_{i=1}^{N} \min \frac{(50; 425 \cdot \log_{10}(\log_{10}(G_i)))}{N}$$ $$GRADE_{hypo} = \sum_{i=1}^{N_{hypo}} \min \frac{(50; 425 \cdot \log_{10}(\log_{10}(G_{hypo})))}{N_{hypo}}$$ $$\%GRADE_{hypo} = GRADE_{hypo}/GRADE \cdot 100$$ where G is the glucose measured; N is the total number of glucose readings; G_{hypo} is the glucose value lower than hypoglycaemic threshold; N_{hypo} is the number of lower than hypoglycaemic threshold glucose readings.
IGC (Index of glycaemic control) (Rodbard 2009a) (Rodbard 2009b)	$$IGC = Hypo\ Index + Hyper\ Index$$ $$Hypo\ Index = \left(\sum_{i=1}^{k_{hypo}} (LLTR - G_{hypo_i})^b \right) \Big/ (N \cdot d)$$ $$Hyper\ Index = \left(\sum_{i=1}^{k_{hyper}} (G_{hyper_i} - ULTR)^a \right) \Big/ (N \cdot c)$$ where $LLTR$ is the Lower Limit of Target Range (default= 80mg/dL); b is an exponent in the range $[1.0, 2.0]$ (default=2.0); d is a scaling factor to weight hypoglycaemic and hyperglycaemic values (default= 30); $ULTR$ is the upper Limit of Target Range (default=140mg/dL); a is an exponent in the range $[1.0, 2.0]$ (default=1.1); and, c is a scaling factor (default=30).

LBGI (Low blood glucose index) HBGI (High blood glucose index) (Kovatchev et al. 2006)	$$LBGI = \left(\sum_{i=1}^{N} rl\left(x_i\right)\right) \Big/ N$$ $$HBGI = \left(\sum_{i=1}^{N} rh\left(x_i\right)\right) \Big/ N$$ $rl\left(x_i\right) = 22.77 \cdot f\left(x_i\right)^2$ if $f\left(x_i\right) \leq 0$, and 0 otherwise. $rh(x_i) = 22.77 \cdot f\left(x_i\right)^2$ if $f\left(x_i\right) > 0$, and 0 otherwise. $$f\left(x_i\right) = \ln\left(x_i\right)^{1.084} - 5.381$$ where x_i is the glucose recording; and, N is the total number of recordings.
ADRR (Average daily risk range) (Kovatchev et al. 2006)	$$ADRR = \left(\sum_{j=1}^{M} LR^j + HR^j\right) \Big/ M$$ $$LR^j = \max\left(rl\left(x_1\right), \ldots, rl\left(x_n\right)\right)$$ $$HR^j = \max\left(rh\left(x_1\right), \ldots, rh\left(n\right)\right)$$ where j is the day index; M is the total number of days; x_i is the glucose recording; and, n is the total number of recordings per day.

PGS (Personal glycaemic state) (Hirsch et al. 2017)	$$PGS = F\left(GVP\right) + F\left(MG\right) + F\left(PTIR\right) + F(H)$$ $$F\left(GVP\right) = 1 + 9\Big/\left(1 + e^{-0.049\cdot(GVP-65.47)}\right)$$ $$F\left(MG\right) = 1 + 9\Big/\left(1 + e^{0.1139\cdot(MG-72.08)}\right) + 9\Big/\left(1 + e^{-0.1139\cdot(MG-157.57)}\right)$$ $$F\left(PTIR\right) = 1 + 9\Big/\left(1 + e^{0.0833\cdot(PTIR-55.04)}\right)$$ $$F(H) = F_{54}(H) + F_{70}(H)$$ $$F_{54}(H) = 0.5 + 4.5\cdot\left(1 - e^{-0.81093\cdot N_{54}}\right)$$ $$F_{70}(H) = \begin{cases} 0.5714\cdot N_{70} + 0.625 & N_{70} \leq 7.65 \\ 5 & N_{70} > 7.65 \end{cases}$$ where MG is the mean glucose; $PTIR$ ies the percent time in range (70-180mg/dL); N_{54} is the number of hypoglycaemia events per week below the low threshold ($\leq$54mg/dL); and, N_{70} is the number of hypoglycaemia events per week below the high threshold ($\leq$70mg/dL).

Appendix B

Individual parameters identification

B.1 Individual parameters

B.1.1 Adrenaline secretion model

Table B.1: Individual estimation of β_1, β_2, k_{a1}, k_{a2}, and k_e.

#	$\boldsymbol{\beta_1}$ $(10^{-7} dL \cdot \min^{-1})$	$\boldsymbol{\beta_2}$ $(10^{-7} dL \cdot \min^{-1})$	$\mathbf{k_{a1}}$ $(\min^{-1})$	$\mathbf{k_{a2}}$ $(10^{-2}\,\min^{-1})$	$\mathbf{k_e}$ $(\min^{-1})$
1	150.93	1.46	0.52	2.56	0.57
2	197.37	0.01	0.71	8.87	0.49
3	119.41	2.26	5.70	2.33	0.12
4	40.35	0.01	0.09	8.10	0.09
5	376.13	0.02	0.05	1.44	2.35

6	197.44	2.38	0.22	4.25	0.81
7	47.06	0.01	2.33	2.68	0.10
8	139.45	0.57	0.19	2.94	0.62
9	172.55	5.06	1.10	2.05	0.44
10	101.41	5.02	4.66	15.87	0.13
11	394.85	10.11	0.16	12.30	0.53
12	161.43	0.01	1.37	4.56	0.18
13	197.46	5.06	0.03	9.10	0.20
14	394.78	2.20	1.29	18.15	1.84
15	177.10	0.01	4.66	9.30	0.64
16	355.26	0.01	0.56	10.98	1.25
17	397.01	0.01	16.30	6.82	0.38
18	294.68	12.04	16.30	6.45	0.34
19	89.05	0.40	8.07	2.14	0.02
20	235.34	0.01	16.30	3.20	8.11
21	160.76	10.11	0.75	11.67	6.61

B.1.2 Adrenaline action model

Table B.2: Individual estimation of parameters.

#	$\mathbf{p_1}$ (min^{-1})	$\mathbf{p_2}$ (min^{-1})	$\mathbf{p_3}$ ($10^{-5}\,\mathrm{min}^{-1}$)	$\mathbf{p_4}$ ($\mathrm{mg{\cdot}dL^{-1}{\cdot}min^{-1}}$)	$\mathbf{p_a}$ ($10^{7}\,\mathrm{min}^{-1}$)	$\mathbf{p_h}$ (min^{-1})	$\mathbf{G_{b2}}$ (mg/dL)
1	0.013	0.066	9.49	0.641	0.308	0.062	57.374
2	0.004	0.014	2.46	0.288	0.416	0.100	59.248
3	0.004	0.027	2.47	0.418	0.157	0.037	60.597
4	0.004	0.010	1.73	0.309	0.080	0.038	59.259

5	0.009	0.008	2.20	0.472	0.370	0.024	64.386
6	0.008	0.030	5.51	0.309	0.068	0.023	64.160
7	0.001	0.030	7.75	0.257	0.497	0.002	83.842
8	0.000	0.029	7.98	0.298	0.181	0.086	56.567
9	0.013	0.036	11.1	1.286	0.055	0.004	72.230
10	0.021	0.075	16.5	2.499	0.031	0.006	70.528
11	0.027	0.027	5.19	2.611	0.053	0.020	55.023
12	0.004	0.009	2.92	0.312	0.295	0.001	46.534
13	0.018	0.385	26.9	1.216	0.326	0.010	49.360
14	0.004	0.015	1.10	0.198	0.277	0.001	77.460
15	0.010	0.046	6.18	0.821	0.192	0.037	61.937
16	0.016	0.010	1.56	1.079	0.001	0.164	61.937
17	0.004	0.049	6.58	0.327	0.155	0.026	57.054
18	0.014	0.024	3.19	0.567	0.001	0.017	74.747
19	0.000	0.014	2.17	0.401	0.500	0.103	69.435
20	0.020	0.031	3.46	1.468	0.064	0.004	66.786
21	0.018	0.026	3.31	1.455	0.001	0.005	72.225

B.1.3 Minimal model extension based on counterregulatory response

Table B.3: Individual estimation of parameters: Part I.

#	$\mathbf{p_7}$ (min^{-1})	$\mathbf{p_{f2}}$ (min^{-1})	$\mathbf{p_{f3}}$ ($10^{-4}\mathrm{min}^{-1}$)	$\mathbf{F_b}$ (μmol/L)	$\mathbf{G_b}$ (mg/dL)	$\mathbf{k_{1w}}$ ($\mu\mathrm{L}\cdot\mathrm{pg}^{-1}\cdot\mathrm{min}^{-1}$)	$\mathbf{k_{2w}}$ (10^{-3}mL/pg)
1	0.048	1.885	6.39	280.000	90.988	0.011	1.940
2	0.067	1.954	7.86	574.276	76.708	0.073	1.242
3	0.069	0.557	8.39	157.889	119.434	0.046	2.047

4	0.063	1.252	5.22	229.389	88.288	0.151	2.120
5	0.065	1.151	2.08	365.502	54.234	0.079	2.241
6	0.065	1.612	2.17	288.547	86.831	0.173	1.628
7	0.056	1.757	3.00	250.480	89.484	0.030	0.872
8	0.063	1.861	7.48	293.082	78.788	0.046	1.172
9	0.051	0.762	2.97	124.279	99.070	0.023	2.581
10	0.064	1.688	7.27	158.933	96.414	0.022	1.014
11	0.048	1.632	2.89	171.573	97.129	0.165	2.401
12	0.052	0.501	8.16	263.671	89.231	0.108	1.809
13	0.048	0.401	3.71	232.555	87.458	0.102	2.752
14	0.048	1.272	2.53	265.080	84.955	0.023	0.861
15	0.067	2.331	2.95	35.576	97.854	0.131	1.612
16	0.054	1.909	5.75	311.743	65.941	0.116	0.919
17	0.055	1.472	4.65	179.593	93.262	0.063	2.682
18	0.070	0.642	3.72	324.567	40.007	0.095	0.709
19	0.048	1.853	8.40	165.854	68.137	0.073	2.296
20	0.051	0.714	5.51	188.091	79.420	0.010	2.384
21	0.048	1.290	5.24	205.867	80.332	0.042	2.490

Table B.4: Individual parameters estimation: Part II

#	$\mathbf{G_{th2}}$ (mg/dL)	$\mathbf{p_1}$ (min^{-1})	$\mathbf{p_2}$ (min^{-1})	$\mathbf{p_3}$ ($10^{-5}\,\text{min}^{-1}$)	$\mathbf{Vol_G}$ (dL)	$\mathbf{p_a}$ ($10^{7}\,\text{min}^{-1}$)
1	57.374	0.013	0.066	9.486	121.111	0.009
2	49.248	0.012	0.005	1.257	129.604	0.001
3	60.597	0.004	0.027	2.469	156.107	0.003
4	60.259	0.004	0.010	1.733	115.000	0.021

5	64.386	0.009	0.008	2.197	119.454	0.007
6	64.569	0.147	0.026	5.034	160.404	0.046
7	84.448	0.004	0.031	7.859	105.540	0.015
8	57.703	0.245	0.009	2.466	106.042	0.070
9	82.018	0.013	0.036	11.08	164.371	0.001
10	71.261	0.350	0.034	10.89	153.512	0.048
11	63.789	0.032	0.033	5.979	69.753	0.001
12	46.089	0.004	0.009	2.925	137.254	0.003
13	59.515	0.018	0.385	26.86	149.151	0.011
14	78.386	0.004	0.020	1.666	122.500	0.013
15	63.560	0.350	0.005	6.945	118.742	0.065
16	68.892	0.016	0.010	1.560	115.862	0.014
17	57.054	0.004	0.049	6.581	78.676	0.002
18	74.057	0.015	0.027	3.354	102.118	0.006
19	68.621	0.013	0.007	1.211	120.003	0.004
20	71.723	0.028	0.034	3.664	105.409	0.001
21	72.397	0.018	0.026	3.310	127.409	0.000

B.2 Residual analysis

The assessment of the model residuals is carried out with the study of residuals autocorrelation by means of the Ljung-Box Q-test for residual autocorrelation. Besides, the residual independence is tested with the Wald-Wolfowitz Runs tests. In the Ljung-Bos Q-test, the number of lags used was min (20, T-1) as (Box et al. 1994) suggested.

The Ljung-Box test defines:

H_0: The data are independently distributed (i.e. the correlations in the population from which the sample is taken are 0, so that any observed correlations in the data result from randomness of the sampling process).

H_1: The data are not independently distributed; they exhibit serial correlation.

On the other hand, the Wald-Wolfowitz Runs tests determines:

H_0: The data are randomly ordered (i.e. the data are independent).

H_1: The data are not randomly ordered; they show a non-random relationship.

In below-showed tables, the Null hypothesis, H_0, is referred by $H = 0$ whereas Alternative Hypothesis, H_1 is by $H = 1$.

B.2.1 Adrenaline secretion model

Table B.5: Residual analysis of the adrenaline secretion model identification.

Residual analysis				
#	**Ljung-Box Q-test**		**Wald Wolfowitz Run test**	
	H	*p-value*	*H*	*p-value*
1	0	0.117	0	0.755
2	0	0.589	0	0.409
3	0	0.718	0	0.752
4	0	0.174	0	0.140
5	0	0.678	0	0.599
6	0	0.634	0	0.217
7	0	0.694	0	0.392
8	0	0.604	0	0.598
9	0	0.052	0	0.525

10	0	0.052	0	0.755
11	0	0.668	0	1.000
12	0	0.568	0	0.399
13	0	0.518	0	0.597
14	0	0.255	0	0.291
15	0	0.961	0	0.115
16	0	0.604	0	0.160
17	0	0.965	0	0.922
18	0	0.178	0	0.055
19	0	0.842	0	0.596
20	0	0.447	0	0.199
21	0	0.630	0	0.890

B.2.2 Adrenaline action model

Table B.6: Residual analysis of the adrenaline action model identification.

Residual analysis				
#	**Ljung-Box Q-test**		**Wald Wolfowitz Run test**	
	H	*p-value*	*H*	*p-value*
1	0	0.838	0	0.606
2	0	0.057	0	0.339
3	0	0.478	0	0.114
4	0	0.576	0	0.345
5	0	0.890	0	0.761
6	0	0.089	0	0.072
7	0	0.453	0	0.755

8	0	0.733	0	0.836
9	0	0.944	0	0.916
10	0	0.942	0	0.349
11	0	0.795	0	0.249
12	0	0.855	0	0.673
13	0	0.685	0	0.290
14	0	0.992	0	0.590
15	0	0.059	0	0.385
16	0	0.162	0	0.942
17	0	0.851	0	0.665
18	0	0.627	0	0.176
19	0	0.226	0	0.292
20	0	0.306	0	0.833
21	0	0.816	0	0.057

B.2.3 Minimal model extension based on counterregulatory response

Table B.7: Residual analysis of the minimal model extension with counterregulation.

Residual analysis				
#	**Ljung-Box Q-test**		**Wald Wolfowitz Run test**	
	H	*p-value*	*H*	*p-value*
1	0	0.455	0	0.896
2	0	0.276	0	0.686
3	0	0.240	0	0.292
4	0	0.694	0	0.606
5	0	0.921	0	0.842

6	0	0.417	0	0.409
7	0	0.989	0	0.125
8	0	0.603	0	0.174
9	0	0.233	0	0.206
10	0	0.058	0	0.058
11	0	0.742	0	0.140
12	0	0.420	0	1.000
13	0	0.067	0	0.746
14	0	0.190	0	0.673
15	0	0.807	0	0.348
16	0	0.059	0	1.000
17	0	0.081	0	0.615
18	0	0.477	0	0.351
19	0	0.560	0	0.916
20	0	0.125	0	0.061
21	0	0.668	0	0.916

Appendix C

Evaluation of CC and NCC configuration

C.1 Assessment of CC and NCC configuration

Both configurations were evaluated in each scenario (A, B, and C) considering the four threshold switch conditions ($u_{th} \in \{0,\ 0.25u^*,\ 0.5u^*,\ 0.75u^*\}$). The metrics are calculated for the performances of each simulation, and results are shown in the following tables.

Table C.1: Outcomes during scenario A for the four different switch condition in CC.

	$\mathbf{U_{th} = 0}$	$\mathbf{U_{th} = 0.25}$	$\mathbf{U_{th} = 0.5}$	$\mathbf{U_{th} = 0.75}$ **(CC)**
MG (mg/dL)	116.21(4.29) 116.60 [112.97;118.89]	118.77(4.26) 119.44[115.72;121.32]	123.00(4.52) 123.18[120.14;125.95]	129.04(5.55) 129[126.19;131.63]
TIR(%)	94.10 (3,11) 94.73[92.50;96.24]	94.95(2.84) 95.65[93.22;97.14]	95.11(2.86) 95.63[93.24;97.62]	94.13(3.27) 94.49[92.11;96.78]
>180(%)	3.67(2.76) 3.21 [1.33;5.85]	3.90(2.81) 3.50[1.59;6.09]	4.50(2.95) 4.24[1.92;6.68]	5.73(3.35) 5.43[2.90;7.89]
<70(%)	2.23(1.60) 1.95[0.89;3.40]	1.15(1.00) 0.83[0.31;1.87]	0.40(0.54) 0.20[0.00;0.53]	0.14(0.30) 0.00[0.00;0.00]

<54(%)	0.32(0.42) 0.17[0.00;0.51]	0.08(0.14) 0.00[0.00;0.14]	0.02(0.05) 0.00[0.00;0.00]	0.00(0.02) 0.00[0.00;0.00]
INS (U/day)	48.08(11.76) 45.03[40.50;54.38]	48.35(11.78) 45.28[40.78;54.56]	48.30(11.71) 45.33[40.83;54.37]	47.43(11.52) 44.41[40.23;53.25]
GGON (mg/day)	0.32(0.30) 0.15[0.09;0.61]	0.45(0.39) 0.24[0.16;0.88]	0.58(0.49) 0.36[0.22;0.91]	0.64(0.54) 0.44[0.25;0.92]

Table C.2: Outcomes during scenario B for the four different switch condition in CC.

	$\mathbf{U_{th} = 0}$	$\mathbf{U_{th} = 0.25}$	$\mathbf{U_{th} = 0.5}$	$\mathbf{U_{th} = 0.75}$ **(CC)**
MG (mg/dL)	117.53(4.70) 117.39[114.42;120.23]	120.21(4.49) 120.09[117.53;122.42]	124.51(4.63) 124.54[122.36;126.93]	130.53(5.53) 130.41[128.03;132.95]
TIR(%)	94.22(3.20) 94.79[92.06;96.65]	95.12(2.79) 95.67[93.35;97.14]	95.30(2.72) 95.81[93.95;97.43]	94.32(3.12) 94.92[92.97;96.49]
>180(%)	3.47(2.39) 3.03[1.65;4.66]	3.73(2.47) 3.24[1.76;4.99]	4.32(2.67) 3.82[2.27;5.67]	5.57(3.13) 5.02[3.39;7.03]
<70(%)	2.30(2.15) 1.46[0.53;3.82]	1.15(1.26) 0.61[0.10;1.82]	0.38(0.55) 0.05[0.00;0.67]	0.11(0.27) 0.00[0.00;0.11]
<54(%)	0.47(0.68) 0.14[0.00;0.77]	0.15(0.28) 0.00[0.00;0.20]	0.02(0.07) 0.00[0.00;0.00]	0.00(0.01) 0.00[0.00;0.00]
INS (U/day)	49.44(12.13) 45.84[42.22;56.20]	49.74(12.15) 46.12[42.55;56.40]	49.68(12.06) 46.10[42.58;56.17]	48.77(11.87) 45.31[41.98;54.94]
GGON (mg/day)	0.29(0.27) 0.14[0.08;0.53]	0.42(0.36) 0.25[0.14;0.76]	0.55(0.46) 0.39[0.21;0.93]	0.61(0.51) 0.47[0.23;0.94]

Table C.3: Outcomes during scenario C for the four different switch condition in CC.

	$\mathbf{U_{th} = 0}$	$\mathbf{U_{th} = 0.25}$	$\mathbf{U_{th} = 0.5}$	$\mathbf{U_{th} = 0.75}$ **(CC)**
MG (mg/dL)	111.18(3.98) 111.61[107.24;114.75]	113.43(4.10) 114.01[109.38;116.97]	117.26(4.50) 117.00[113.23;120.49]	123.26(5.72) 121.93[119.27;126.80]
TIR(%)	89.14(4.24) 89.06[87.21;91.15]	90.31(3.85) 90.18[88.41;92.22]	91.29(3.53) 91.29[89.26;93.76]	91.56(3.42) 91.53[89.19;94.10]
>180(%)	3.17(2.44) 2.60[1.09;4.94]	3.36(2.50) 2.83[1.26;4.99]	3.85(2.69) 3.11[1.60;5.52]	5.04(3.11) 4.24[2.47;6.88]
<70(%)	7.69(3.97) 8.02[4.54;10.23]	6.32(3.73) 6.44[3.00;8.80]	4.87(3.38) 4.64[1.97;6.82]	3.40(2.92) 2.89[0.95;4.84]
<54(%)	2.62(2.23) 2.62[0.61;3.91]	1.90(1.97) 1.59[0.21;2.74]	1.22(1.68) 0.61[0.00;1.43]	0.73(1.29) 0.15[0.00;0.72]

INS	47.13(11.43)	47.36(11.45)	47.32(11.38)	46.53(11.22)
(U/day)	44.59[39.41;53.26]	44.93[39.66;53.42]	44.98[39.76;53.23]	44.02[39.26;52.23]
GGON	0.61(0.52)	0.74(0.62)	0.87(0.72)	0.96(0.79)
(mg/day)	0.37[0.21;1.20]	0.46[0.27;1.46]	0.60[0.33;1.64]	0.69[0.36;1.71]

Table C.4: Outcomes during scenario A for the four different switch condition in NCC.

	$\mathbf{U_{th} = 0}$ **(NCC-B)**	$\mathbf{U_{th} = 0.25}$	$\mathbf{U_{th} = 0.5}$	$\mathbf{U_{th} = 0.75}$ **(NCC-A)**
MG	121.60(5.52)	126.66(7.53)	133.49(11.66)	141.47(17.58)
(mg/dL)	120.71[117.33;124.59]	124.86[121.80;128,87]	130.62[128.32;133.62]	137.32[134.72;139.59]
TIR(%)	94.58(3.62)	94.12(5.01)	91.90(9.06)	88.18(15.84)
	95.57[92.37; 97.61]	95.55[92.53;97.88]	94.41[91.54;97.28]	92.83[89.96;96.22]
>180(%)	4.53(3.53)	5.67(5.03)	8.06(9.08)	11.81(15.84)
	3.47[1.56;6.78]	4.43[1.98;7.42]	5.59[2.65;8.44]	7.17[3.78;9.98]
<70(%)	0.89(0.95)	0.21(0.29)	0.04(0.09)	0.01(0.04)
	0.57[0.25;1.26]	0.10[0.00;0.35]	0.00[0.00;0.01]	0.00[0.00;0.00]
<54(%)	0.06(0.13)	0.00(0.03)	0.00(0.00)	0.00(0.00)
	0.00[0.00;0.05]	0.00[0.00;0.00]	0.00[0.00;0.00]	0.00[0.00;0.00]
INS	49.10(12.12)	49.98(12.27)	51.15(12.40)	52.49(12.50)
(U/day)	45.80[41.50;55.00]	46.99[42.31;55.76]	49.11[43.28;56.79]	51.17[44.38;58.14]
GGON	0.72(0.75)	1.06(1.12)	1.52(1.70)	2.08(2.48)
(mg/day)	0.31[0.18;1.11]	0.52[0.30;1.48]	0.86[0.46;1.84]	1.21[0.65;2.16]

Table C.5: Outcomes during scenario B for the four different switch condition in NCC.

	$\mathbf{U_{th} = 0}$ **(NCC-B)**	$\mathbf{U_{th} = 0.25}$	$\mathbf{U_{th} = 0.5}$	$\mathbf{U_{th} = 0.75}$ **(NCC-A)**
MG	122.60(5.44)	127.77(7.03)	134.63(10.89)	142.52(16.32)
(mg/dL)	121.42[118.27;126.81]	125.75[123.09;130.95]	131.67[128.99;135.56]	137.99[136.03;141.60]
TIR(%)	94.54(3.67)	94.21(4.72)	92.06(8.58)	88.26(14.66)
	95.54[92.61;97.32]	95.78[92.92;97.30]	94.69[92.10;96.55]	92.77[89.93;95.45]
>180(%)	4.40(3.32)	5.49(4.67)	7.88(8.57)	11.73(14.67)
	3.44[1.96;5.84]	4.04[2.37;6.86]	5.31[3.31;7.55]	7.23[4.55;10.07]
<70(%)	1.06(1.32)	0.30(0.46)	0.06(0.15)	0.02(0.06)
	0.60[0.15;1.38]	0.07[0.00;0.46]	0.00[0.00;0.01]	0.00[0.00;0.00]
<54(%)	0.21(0.43)	0.03(0.08)	0.00(0.01)	0.00(0.00)
	0.00[0.00;0.24]	0.00[0.00;0.00]	0.00[0.00;0.00]	0.00[0.00;0.00]
INS	50.42(12.47)	51.33(12.61)	52.52(12.72)	53.85(12.81)
(U/day)	46.67[43.13;56.68]	48.01[43.85;57.41]	49.50[44.94;58.42]	51.96[46.07;59.76]

GGON	0.66(0.67)	1.00(1.03)	1.47(1.61)	2.01(2.35)
(mg/day)	0.30[0.17;1.12]	0.54[0.31;1.44]	0.88[0.48;1.82]	1.20[0.67;2.18]

Table C.6: Outcomes during scenario C for the four different switch condition in NCC.

	$\mathbf{U_{th} = 0}$ **(NCC-B)**	$\mathbf{U_{th} = 0.25}$	$\mathbf{U_{th} = 0.5}$	$\mathbf{U_{th} = 0.75}$ **(NCC-A)**
MG	120.04(6.84)	124.54(9.22)	130.14(13.01)	136.75(18.28)
(mg/dL)	119.39[115.62;120.30]	122.53[119.58;124.16]	127.03[124.13;128.56]	132.06[129.88;133.96]
TIR(%)	93.15(4.32)	93.22(5.93)	91.96(9.40)	89.26(15.21)
	94.42[90.61;96.34]	95.26[92.72;96.80]	94.92[93.13;96.75]	94.12[92.08;96.01]
>180(%)	4.54(4.44)	5.55(6.22)	7.37(9.61)	10.32(15.36)
	2.91[1.65;5.28]	3.16[1.93;5.49]	4.09[2.42;6.40]	5.43[3.15;7.56]
<70(%)	2.31(1.65)	1.23(1.06)	0.67(0.80)	0.42(0.65)
	2.12[0.84;3.52]	0.87[0.32;2.10]	0.35[0.09;1.00]	0.15[0.00;0.42]
<54(%)	0.36(1.43)	0.11(0.19)	0.05(0.11)	0.02(0.07)
	0.24[0.00;0.58]	0.00[0.00;0.16]	0.00[0.00;0.05]	0.00[0.00;0.00]
INS	48.67(11.70)	49.42(11.83)	50.36(11.97)	51.48(12.13)
(U/day)	46.38[41.27;54.15]	47.39[41.97;54.87]	48.93[42.73;55.67]	50.61[43.44;56.77]
GGON	1.38(1.39)	1.71(1.77)	2.13(2.34)	2.64(3.11)
(mg/day)	0.83[0.43;2.37]	0.97[0.53;2.82]	1.22[0.64;3.13]	1.47[0.78;3.52]

C.2 Statistical analysis of CC vs NCC comparisons

The differences between the eight configurations resulting from the combination of the type of controller (CC and NCC) and the four threshold switch conditions ($u_{th} \in \{0,\ 0.25u^*,\ 0.5u^*,\ 0.75u^*\}$), were assessed non-parametrically using the Kruskal Wallis test with Fisher's LSD post-hoc analysis. This analysis was repeated for each scenario (A, B, and C). Results are shown below:

C.2.1 Scenario A

– Mean glucose concentration (mg/dL)

CC	**0.25**	0.04						
	0.50	<0.01	<0.01					
	0.75	<0.01	<0.01	<0.01				
NCC	**0**	<0.01	0.023	0.262	<0.01			
	0.25	<0.01	<0.01	<0.01	0.056	<0.01		
	0.50	<0.01	<0.01	<0.01	<0.01	<0.01	<0.01	
	0.75	<0.01	<0.01	<0.01	<0.01	<0.01	<0.01	<0.01
	U_{th}	**0**	**0.25**	**0.50**	**0.75**	**0**	**0.25**	**0.50**
		CC				**NCC**		

– Standard deviation (SD)

CC	**0.25**	0.241						
	0.50	0.022	0.262					
	0.75	<0.01	0.056	0.429				
NCC	**0**	0.776	0.375	0.045	<0.01			
	0.25	0.356	0.803	0.171	0.031	0.524		
	0.50	0.222	0.959	0.285	0.063	0.349	0.764	
	0.75	0.181	0.868	0.340	0.081	0.293	0.678	0.908
	U_{th}	**0**	**0.25**	**0.50**	**0.75**	**0**	**0.25**	**0.50**
		CC				**NCC**		

– Percentage of time in range

CC	**0.25**	0.397						
	0.50	0.316	0.877					
	0.75	0.976	0.414	0.331				
NCC	**0**	0.630	0.715	0.603	0.652			
	0.25	0.984	0.408	0.326	0.992	0.645		
	0.50	0.03	<0.01	<0.01	0.028	<0.01	0.028	
	0.75	<0.01	<0.01	<0.01	<0.01	<0.01	<0.01	<0.01
	U_{th}	**0**	**0.25**	**0.50**	**0.75**	**0**	**0.25**	**0.50**
		CC				**NCC**		

– Percentage of time above target

CC	**0.25**	0.822						
	0.50	0.413	0.553					
	0.75	0.041	0.069	0.221				
NCC	**0**	0.395	0.532	0.974	0.233			
	0.25	0.048	0.079	0.245	0.952	0.258		
	0.50	<0.01	<0.01	<0.01	0.021	<0.01	0.018	
	0.75	<0.01	<0.01	<0.01	<0.01	<0.01	<0.01	<0.01
	$\mathbf{U_{th}}$	**0**	**0.25**	**0.50**	**0.75**	**0**	**0.25**	**0.50**
		CC				**NCC**		

– Percentage of time under target

CC	**0.25**	<0.01						
	0.50	<0.01	<0.01					
	0.75	<0.01	<0.01	0.023				
NCC	**0**	<0.01	<0.01	<0.01	<0.01			
	0.25	<0.01	<0.01	0.1	0.524	<0.01		
	0.50	<0.01	<0.01	<0.01	0.352	<0.01	0.117	
	0.75	<0.01	<0.01	<0.01	0.232	<0.01	0.067	0.792
	$\mathbf{U_{th}}$	**0**	**0.25**	**0.50**	**0.75**	**0**	**0.25**	**0.50**
		CC				**NCC**		

– Percentage of time under 54mg/dL

CC	**0.25**	<0.01						
	0.50	<0.01	<0.01					
	0.75	<0.01	<0.01	0.573				
NCC	**0**	<0.01	0.283	0.066	0.016			
	0.25	<0.01	<0.01	0.602	0.966	0.018		
	0.50	<0.01	<0.01	0.510	0.924	0.013	0.890	
	0.75	<0.01	<0.01	0.510	0.924	0.013	0.890	1.00
	U_{th}	**0**	**0.25**	**0.50**	**0.75**	**0**	**0.25**	**0.50**
		CC				**NCC**		

– Insulin delivery (U/day)

CC	**0.25**	0.872						
	0.50	0.899	0.973					
	0.75	0.704	0.588	0.611				
NCC	**0**	0.549	0.662	0.637	0.328			
	0.25	0.263	0.338	0.321	0.134	0.602		
	0.50	0.071	0.100	0.093	<0.01	0.227	0.491	
	0.75	0.01	0.015	0.014	<0.01	<0.01	0.140	0.429
	U_{th}	**0**	**0.25**	**0.50**	**0.75**	**0**	**0.25**	**0.50**
		CC				**NCC**		

– Glucagon delivery (mg/day)

CC	**0.25**	0.443						
	0.50	0.129	0.453					
	0.75	0.060	0.264	0.714				
NCC	**0**	<0.01	0.112	0.402	0.638			
	0.25	<0.01	<0.01	<0.01	0.014	0.047		
	0.50	<0.01	<0.01	<0.01	<0.01	<0.01	<0.01	
	0.75	<0.01	<0.01	<0.01	<0.01	<0.01	<0.01	<0.01
	$\mathbf{U_{th}}$	**0**	**0.25**	**0.50**	**0.75**	**0**	**0.25**	**0.50**
		CC				**NCC**		

C.2.2 Scenario B

– Mean glucose concentration (mg/dL)

CC	**0.25**	0.023						
	0.50	<0.01	<0.01					
	0.75	<0.01	<0.01	<0.01				
NCC	**0**	<0.01	0.044	0.106	<0.01			
	0.25	<0.01	<0.01	<0.01	0.019	<0.01		
	0.50	<0.01	<0.01	<0.01	<0.01	<0.01	<0.01	
	0.75	<0.01	<0.01	<0.01	<0.01	<0.01	<0.01	<0.01
	$\mathbf{U_{th}}$	**0**	**0.25**	**0.50**	**0.75**	**0**	**0.25**	**0.50**
		CC				**NCC**		

– Standard deviation (SD)

CC	**0.25**	0.213						
	0.50	<0.01	0.231					
	0.75	<0.01	<0.01	0.377				
NCC	**0**	0.823	0.142	<0.01	<0.01			
	0.25	0.781	0.333	<0.01	<0.01	0.616		
	0.50	0.684	0.402	<0.01	<0.01	0.528	0.897	
	0.75	0.513	0.555	0.074	<0.01	0.380	0.706	0.805
	U_{th}	**0**	**0.25**	**0.50**	**0.75**	**0**	**0.25**	**0.50**
		CC				**NCC**		

– Percentage of time in range

CC	**0.25**	0.345						
	0.50	0.255	0.846					
	0.75	0.922	0.397	0.298				
NCC	**0**	0.739	0.542	0.421	0.814			
	0.25	0.989	0.339	0.250	0.912	0.729		
	0.50	<0.01	<0.01	<0.01	<0.01	<0.01	<0.01	
	0.75	<0.01	<0.01	<0.01	<0.01	<0.01	<0.01	<0.01
	U_{th}	**0**	**0.25**	**0.50**	**0.75**	**0**	**0.25**	**0.50**
		CC				**NCC**		

– Percentage of time above target

CC	**0.25**	0.782						
	0.50	0.368	0.533					
	0.75	0.025	H1	0.179				
NCC	**0**	0.321	0.475	0.928	0.210			
	0.25	0.032	0.061	0.211	0.927	0.246		
	0.50	<0.01	<0.01	<0.01	0.014	<0.01	0.011	
	0.75	<0.01	<0.01	<0.01	<0.01	<0.01	<0.01	<0.01
	U_{th}	**0**	**0.25**	**0.50**	**0.75**	**0**	**0.25**	**0.50**
		CC				**NCC**		

– Percentage of time under target

CC	**0.25**	<0.01						
	0.50	<0.01	<0.01					
	0.75	<0.01	<0.01	0.065				
NCC	**0**	<0.01	0.538	<0.01	<0.01			
	0.25	<0.01	<0.01	0.588	0.191	<0.01		
	0.50	<0.01	<0.01	0.030	0.745	<0.01	0.103	
	0.75	<0.01	<0.01	0.013	0.518	<0.01	0.051	0.748
	U_{th}	**0**	**0.25**	**0.50**	**0.75**	**0**	**0.25**	**0.50**
		CC				**NCC**		

– Percentage of time under 54mg/dL

CC	**0.25**	<0.01						
	0.50	<0.01	<0.01					
	0.75	<0.01	<0.01	0.614				
NCC	**0**	<0.01	0.136	<0.01	<0.01			
	0.25	<0.01	<0.01	0.958	0.578	<0.01		
	0.50	<0.01	<0.01	0.622	0.991	<0.01	0.586	
	0.75	<0.01	<0.01	0.586	0.968	<0.01	0.50	0.958
	U_{th}	**0**	**0.25**	**0.50**	**0.75**	**0**	**0.25**	**0.50**
		CC				**NCC**		

– Insulin delivery (U/day)

CC	**0.25**	0.865						
	0.50	0.891	0.973					
	0.75	0.701	0.579	0.602				
NCC	**0**	0.577	0.698	0.673	0.346			
	0.25	0.281	0.364	0.346	0.144	0.603		
	0.50	0.079	0.113	0.105	<0.01	0.231	0.497	
	0.75	<0.01	<0.01	<0.01	<0.01	0.050	0.149	0.444
	U_{th}	**0**	**0.25**	**0.50**	**0.75**	**0**	**0.25**	**0.50**
		CC				**NCC**		

– Glucagon delivery (mg/day)

CC	**0.25**	0.411						
	0.50	0.106	0.428					
	0.75	<0.01	0.251	0.723				
NCC	**0**	<0.01	0.137	0.487	0.734			
	0.25	<0.01	<0.01	<0.01	<0.01	<0.01		
	0.50	<0.01	<0.01	<0.01	<0.01	<0.01	<0.01	
	0.75	<0.01	<0.01	<0.01	<0.01	<0.01	<0.01	<0.01
	U_{th}	**0**	**0.25**	**0.50**	**0.75**	**0**	**0.25**	**0.50**
		CC				**NCC**		

C.2.3 Scenario C

– Mean glucose concentration (mg/dL)

CC	**0.25**	0.095						
	0.50	<0.01	<0.01					
	0.75	<0.01	<0.01	<0.01				
NCC	**0**	<0.01	<0.01	<0.01	0.017			
	0.25	<0.01	<0.01	<0.01	0.341	<0.01		
	0.50	<0.01	<0.01	<0.01	<0.01	<0.01	<0.01	
	0.75	<0.01	<0.01	<0.01	<0.01	<0.01	<0.01	<0.01
	U_{th}	**0**	**0.25**	**0.50**	**0.75**	**0**	**0.25**	**0.50**
		CC				**NCC**		

– Standard deviation (SD)

CC	**0.25**	0.400						
	0.50	0.116	0.465					
	0.75	0.081	0.366	0.863				
NCC	**0**	0.038	0.215	0.611	0.737			
	0.25	<0.01	0.072	0.286	0.372	0.577		
	0.50	<0.01	0.043	0.194	0.260	0.42	0.816	
	0.75	<0.01	0.027	0.139	0.192	0.332	0.680	0.858
	U_{th}	**0**	**0.25**	**0.50**	**0.75**	**0**	**0.25**	**0.50**
		CC				**NCC**		

– Percentage of time in range

CC	**0.25**	0.259						
	0.50	0.039	0.348					
	0.75	0.020	0.229	0.793				
NCC	**0**	<0.01	<0.01	0.073	0.126			
	0.25	<0.01	<0.01	0.062	0.109	H1		
	0.50	<0.01	0.113	0.518	0.702	0.251	0.222	
	0.75	0.908	0.31	0.051	0.027	<0.01	<0.01	<0.01
	U_{th}	**0**	**0.25**	**0.50**	**0.75**	**0**	**0.25**	**0.50**
		CC				**NCC**		

– Percentage of time above target

CC	**0.25**	0.848						
	0.50	0.506	0.637					
	0.75	0.067	0.100	0.241				
NCC	**0**	0.179	0.249	0.496	0.623			
	0.25	0.020	0.032	0.095	0.619	0.323		
	0.50	<0.01	<0.01	<0.01	0.023	<0.01	0.075	
	0.75	<0.01	<0.01	<0.01	<0.01	<0.01	<0.01	<0.01
	$\mathbf{U_{th}}$	**0**	**0.25**	**0.50**	**0.75**	**0**	**0.25**	**0.50**
		CC				**NCC**		

– Percentage of time under target

CC	**0.25**	<0.01						
	0.50	<0.01	<0.01					
	0.75	<0.01	<0.01	<0.01				
NCC	**0**	<0.01	<0.01	<0.01	<0.01			
	0.25	<0.01	<0.01	<0.01	<0.01	<0.01		
	0.50	<0.01	<0.01	<0.01	<0.01	<0.01	0.136	
	0.75	<0.01	<0.01	<0.01	<0.01	<0.01	0.029	0.489
	$\mathbf{U_{th}}$	**0**	**0.25**	**0.50**	**0.75**	**0**	**0.25**	**0.50**
		CC				**NCC**		

– Percentage of time under 54mg/dL

CC	**0.25**	<0.01						
	0.50	<0.01	<0.01					
	0.75	<0.01	<0.01	<0.01				
NCC	**0**	<0.01	<0.01	<0.01	0.047			
	0.25	<0.01	<0.01	<0.01	<0.01	0.179		
	0.50	<0.01	<0.01	<0.01	<0.01	0.091	0.727	
	0.75	<0.01	<0.01	<0.01	<0.01	0.063	0.603	0.864
	U_{th}	**0**	**0.25**	**0.50**	**0.75**	**0**	**0.25**	**0.50**
		CC				**NCC**		

– Insulin delivery (U/day)

CC	**0.25**	0.887						
	0.50	0.909	0.977					
	0.75	0.718	0.615	0.635				
NCC	**0**	0.348	0.426	0.410	0.194			
	0.25	0.165	0.213	0.202	0.080	0.652		
	0.50	0.050	0.069	0.065	0.020	0.306	0.567	
	0.75	<0.01	0.013	0.012	<0.01	0.088	0.210	0.495
	U_{th}	**0**	**0.25**	**0.50**	**0.75**	**0**	**0.25**	**0.50**
		CC				**NCC**		

– Glucagon delivery (mg/day)

CC	**0.25**	0.569						
	0.50	0.253	0.566					
	0.75	0.132	0.350	0.718				
NCC	**0**	<0.01	<0.01	0.032	0.075			
	0.25	<0.01	<0.01	<0.01	<0.01	0.163		
	0.50	<0.01	<0.01	<0.01	<0.01	<0.01	0.070	
	0.75	<0.01	<0.01	<0.01	<0.01	<0.01	<0.01	<0.01
	U_{th}	**0**	**0.25**	**0.50**	**0.75**	**0**	**0.25**	**0.50**
		CC				**NCC**		

Bibliography

Abu-Rmileh, A., W. Garcia-Gabin, and D. Zambrano (2010). "A robust sliding mode controller with internal model for closed-loop artificial pancreas". In: *Medical & Biological Engineering & Computing* 48.12, pp. 1191–1201 (cit. on p. 29).

Ali, N. A., J. M. O'Brien Jr., K. Dungan, G. Phillips, C. B. Marsh, S. Lemeshow, A. F. Connors, and J. C. Preiser (2008). "Glucose variability and mortality in patients with sepsis". In: *Critical Care Medicine* 36.8, pp. 2316–2321 (cit. on p. 39).

Allison, B.J. and A.J. Isaksson (1998). "Design and performance of mid-ranging controllers". In: *Journal of Process Control* 8.5-6, pp. 469–474 (cit. on p. 134).

Alvarez-Ramirez, J., A. Velazco, and G. Fernandez-Anaya (2004). "A note on the stability of habituating process control". In: *Journal of Process Control* 14.8, pp. 939–945 (cit. on pp. 135, 137, 139, 141).

Amiel, S.A., P. Aschner, B. Childs, P.E. Cryer, B.E. de Galan, S.R. Heller, B.M. Frier, L. Gonder-Frederick, T. Jones, K. Khunti, L.A. Leiter, R.J. McCrimmon, Y. Luo, E.R. Seaquist, R. Vigersky, S. Zoungas, and International Hypoglycaemia Study Group (2017). "Glucose concentrations of less than 3.0 mmol/L (54 mg/dL) should be reported in clinical trials: a joint position statement of the American Diabetes Association and the European Associa-

tion for the Study of Diabetes". In: *Diabetes Care* 40.1, pp. 155–157 (cit. on p. 62).

Amiel, S.A., R.S. Sherwin, D.C. Simonson, and W.V. Tamborlane (1988). "Effect of intensive insulin therapy on glycemic thresholds for counterregulatory hormone release". In: *Diabetes* 37.7, pp. 901–907 (cit. on pp. 63, 80).

Andreassen, S., J. J. Benn, R. Hovorka, K. G. Olesen, and E. R. Carson (1994). "A probabilistic approach to glucose prediction and insulin dose adjustment: description of metabolic model and pilot evaluation study". In: *Computer Methods and Programs in Biomedicine* 41.3-4, pp. 153–165 (cit. on p. 48).

Atlas, E., R. Nimri, S. Miller, E. A. Grunberg, and M. Phillip (2010). "MD-logic artificial pancreas system: A pilot study in adults with type 1 diabetes". In: *Diabetes Care* 33.5, pp. 1072–2076 (cit. on p. 29).

Audoly, S., G. Bellu, L. D'Angio, M.P. Saccomani, and C. Cobelli (2001). "Global identifiability of nonlinear models of biological systems". In: *IEEE Transactions on biomedical engineering* 48.1, pp. 55–65 (cit. on p. 70).

Auger, A. and N. Hansen (2005). "A restart CMA evolution strategy with increasing population size". In: *The 2005 IEEE Congress on Evolutionary Computation*. Vol. 2. Edinburgh, Scotland, UK, pp. 1769–1776 (cit. on p. 72).

Avari, P., V. Moscardó, M. Reddy, M. Giménez, and N. Oliver (2018). "The I-HART CGM study: hypoglycaemic episodes reduced with continuous glucose monitoring compared to Flash in adults with type 1 diabetes". In: *The 54th Annual Meeting of the European Association for the Study of Diabetes (EASD)*. Berlin, Germany, p. 85 (cit. on p. 172).

Bakhtiani, P. A., L. M. Zhao, J. El Youssef, J. R. Castle, and W. K. Ward (2013). "A review of artificial pancreas technologies with an emphasis on bi-hormonal therapy". In: *Diabetes, Obesity and Metabolism* 15.12, pp. 1065–1070 (cit. on p. 37).

Bakhtiani, P.A., J. El Youssef, A.K. Duell, D.L. Branigan, P.G. Jacobs, M.R. Lasarev, J.R. Castle, and W.K. Ward (2015). "Factors affecting the success of glucagon delivered during an automated closed-loop system in type 1 diabetes". In: *Journal of Diabetes and Its Complications* 29.1, pp. 93–98 (cit. on p. 128).

Beall, C., M.L. Ashford, and R.J. McCrimmon (2012). "The physiology and pathophysiology of the neural control of the counterregulatory response". In: *American Journal of Physiology: Regulatory, Integrative and Comparative Physiology* 302.2, R215–R223 (cit. on pp. 23, 74, 78).

Bellman, R. and K.J. Aström (1970). "On structural identifiability". In: *Mathematical Biosciences* 7.3-4, pp. 329–339 (cit. on p. 69).

Bergman, R. N., Y. Z. Ider, C. R. Bowden, and C. Cobelli (1979). "Quantitative estimation of insulin sensitivity". In: *American Journal of Physiology: Endocrinology And Metabolism* 236.6, E667–E677 (cit. on pp. 46, 51).

Bergman, R. N., L. S. Phillips, and C. Cobelli (1981). "Physiologic evaluation of factors controlling glucose tolerance in man: measurement of insulin sensitivity and beta-cell glucose sensitivity from the response to intravenous glucose". In: *The Journal of Clinical Investigation* 68.6, pp. 1456–1467 (cit. on pp. 45, 55, 82, 83, 106, 107, 131).

Bolli, G.B. (1990). "From physiology of glucose counterregulation to prevention of hypoglycaemia in type 1 diabetes mellitus". In: *Diabetes, Nutrition & Metabolism* 4, pp. 333–349 (cit. on p. 3).

Bolli, G.B. and C.G. Fanelli (1999). "Physiology of glucose counterregulation to hypoglycemia". In: *Endocrinology and Metabolism Clinics of North America* 28.3, pp. 467–493 (cit. on p. 84).

Box, G.E.P., G.M. Jenkins, and G.C. Reinsel (1994). *Time series analysis: forcasting and control*. 3rd ed. New Jersey, USA: Prentice Hall (cit. on p. 187).

— (2015). *Time series analysis: forcasting and control*. 5th ed. New Jersey, USA: John Wiley & Sons (cit. on p. 73).

Bremer, T. and D. A. Gough (1999). "Is blood glucose predictable from previous values? A solicitation for data". In: *Diabetes* 48.3, pp. 445–451 (cit. on p. 4).

Breton, M., A. Farret, D. Bruttomesso, S. Anderson, L. Magni, S. Patek, C. Dalla Man, J. Place, S. Demartini, S. Del Favero, C. Toffanin, C. Hughes-Karvetski, E. Dassau, H. Zisser, F. J. Doyle III, G. De Nicolao, A. Avogaro, C. Cobelli, E. Renard, B. Kovatchev, and International Artificial Pancreas Study Group (2012). "Fully integrated artificial pancreas in type 1 diabetes: mod-

ular closed-loop glucose control maintains near normoglycemia". In: *Diabetes* 61.9, pp. 2230–2237 (cit. on p. 5).

Buckingham, B., H. P. Chase, E. Dassau, E. Cobry, P. Clinton, V. Gage, K. Caswell, J. Wilkinson, F. Cameron, H. Lee, B. W. Bequette, and F. J. Doyle III (2010). "Prevention of nocturnal hypoglycemia using predictive alarm algorithms and insulin pump suspension". In: *Diabetes Care* 33.5, pp. 1013–1017 (cit. on p. 4).

Buckingham, B., E. Cobry, P. Clinton, V. Gage, K. Caswell, E. Kunselman, F. Cameron, and H. P. Chase (2009). "Preventing hypoglycemia using predictive alarm algorithms and insulin pump suspension". In: *Diabetes Technology & Therapeutics* 11.2, pp. 93–97 (cit. on pp. 4, 30).

Burstein, R., C. Polychronakos, C. J. Toews, J.D. MacDougall, H. J. Guyda, and B. I. Posner (1985). "Acute reversal of the enhanced insulin action in trained athletes: association with insulin receptor changes". In: *Diabetes* 34.8, pp. 756–760 (cit. on p. 39).

Cameron, F., G. Niemeyer, K. Gundy-Burlet, and B. Buckingham (2008). "Statistical hypoglycemia prediction". In: *Journal of Diabetes Science and Technology* 2.4, pp. 612–621 (cit. on p. 4).

Capel, I., G. Rigla M.and García-Sáez, A. Rodríguez-Herrero, B. Pons, D. Subías, F. García-García, M. Gallach, M. Aguilar, E. Pérez-Gandía C.and Gómez, A. Caixas, and M.E. Hernando (2014). "Artificial pancreas using a personalized rule-based controller achieves overnight normoglycemia in patients with type 1 diabetes". In: *Diabetes technology & therapeutics* 16.3, pp. 172–179 (cit. on p. 29).

Carson, E. and C. Cobelli (2014). *Modelling methodology for physiology and medicine*. 2nd ed. London, UK: Elsevier (cit. on p. 70).

Castle, J. R., J. El Youssef, L.M. Wilson, R. Reddy, N. Resalat, D. Branigan, K. Ramsey, J. Leitschuh, B. Rajhbeharrysingh U. and Senf, S.M. Sugerman, V. Gabo, and P.G. Jacobs (2018). "Randomized Outpatient Trial of Single- and Dual-Hormone Closed-Loop Systems That Adapt to Exercise Using Wearable Sensors". In: *Diabetes Care* 41.7, pp. 1471–1477 (cit. on pp. 5, 37).

Castle, J. R., J. M. Engle, J. El Youssef, R. G. Massoud, K. C. J. Yuen, R. Kagan, and W. K. Ward (2010). "Novel use of glucagon in a closed-loop system for prevention of hypoglycemia in type 1 diabetes". In: *Diabetes Care* 33.6, pp. 1282–1287 (cit. on p. 33).

Cavallo, M. G., S. Romeo, G. Coppolino, and P. Pozzilli (2001). "Continuous glucose monitoring during the European Soccer cup semifinal, Italy against Holland". In: *Diabetologia* 44.2, pp. 268–268 (cit. on p. 39).

Cerasi, E., G. Fick, and M. Rudemo (1974). "A mathematical model for the glucose induced insulin release in man". In: *European Journal of Clinical Investigation* 4.4, pp. 267–278 (cit. on p. 48).

Cevantes, I. and J. Alvarez-Ramirez (2004). "A simple chaos control strategy for DC-DC power converters". In: *30th Annual Conference of IEEE Industrial Electronics Society (IECON 2004)*. Busan, South Korea, pp. 193–198 (cit. on p. 135).

Children Network (DirecNet) Study Group, Diabetes Research in (2004). "Lack of accuracy of continuous glucose sensors in healthy, nondiabetic children: results of the Diabetes Research in Children Network (DirecNet) accuracy study". In: *The Journal of Pediatrics* 144.6, pp. 770–775 (cit. on p. 4).

— (2006). "The effects of aerobic exercise on glucose and counterregulatory hormone concentrations in children with type 1 diabetes". In: *Diabetes Care* 29.1, pp. 20–25 (cit. on p. 38).

Choleau, C., P. Dokladal, J. C. Klein, W. K. Ward, G. S. Wilson, and G. Reach (2002). "Prevention of hypoglycemia using risk assessment with a continuous glucose monitoring system". In: *Diabetes* 51.11, pp. 3263–3273 (cit. on p. 4).

Cinar, A. and K. Turksoy (2018). *Advances in Artificial Pancreas Systems: Adaptive and Multivariable Predictive Control*. Springer (cit. on p. 29).

Clarke, W. L., S. Anderson, M. Breton, S. Patek, L. Kashmer, and B. Kovatchev (2009). "Closed-loop artificial pancreas using subcutaneous glucose sensing and insulin delivery and a model predictive control algorithm: the Virginia experience". In: *Journal of Diabetes Science and Technology* 3.5, pp. 1031–1038 (cit. on p. 31).

Clutter, W.E., D.M. Bier, S.D. Shah, and P.E. Cryer (1980). "Epinephrine plasma metabolic clearance rates and physiologic thresholds for metabolic and hemodynamic actions in man". In: *The Journal of Clinical Investigation* 66.1, pp. 94–101 (cit. on pp. 92, 105).

Cobelli, C. and E. Carson (2008). *Introduction to modeling in physiology and medicine*. Biomedical Engineering. London, UK: Academic Press (cit. on p. 96).

Cobelli, C., A. Caumo, and M. Omenetto (1999). "Minimal model S_G overestimation and S_I underestimation: improved accuracy by a Bayesian two-compartment model". In: *American Journal of Physiology: Endocrinology And Metabolism* 277.3, E481–E488 (cit. on p. 54).

Cobelli, C., C. Dalla Man, M. G. Pedersen, A. Bertoldo, and G. Toffolo (2014). "Advancing our understanding of the glucose system via modeling: a perspective". In: *IEEE Transactions on Biomedical Engineering* 61.5, pp. 1577–1592 (cit. on p. 48).

Cobelli, C., C. Dalla Man, G. Sparacino, L. Magni, G. De Nicolao, and B. P. Kovatchev (2009). "Diabetes: models, signals, and control". In: *IEEE Reviews in Biomedical Engineering* 2, pp. 54–96 (cit. on pp. 31, 46).

Cobelli, C., G. Pacini, G. Toffolo, and L. Sacca (1986). "Estimation of insulin sensitivity and glucose clearance from minimal model: new insights from labeled IVGTT". In: *American Journal of Physiology: Endocrinology And Metabolism* 250.5, E591–E598 (cit. on p. 54).

Colmegna, P., F. Garelli, H. De Battista, and R. Sánchez-Peña (2018a). "Automatic regulatory control in type 1 diabetes without carbohydrate counting". In: *Control Engineering Practice* 74, pp. 22–32 (cit. on p. 33).

Colmegna, P., R. S. Sanchez Peña, R. Gondhalekar, E. Dassau, and F. J. Doyle III (2014). "Reducing risks in type 1 diabetes using H_∞ control". In: *IEEE Transactions on Biomedical Engineering* 61.12, pp. 2939–2947 (cit. on p. 29).

Colmegna, P., R.S. Sánchez Peña, and R. Gondhalekar (2018b). "Linear parameter-varying model to design control laws for an artificial pancreas". In: *Biomed. Signal Proc. and Control* 40, pp. 204–213 (cit. on p. 47).

Colmegna, P.H. and R.S. Sánchez-Peña (2014). "Linear parameter-varying control to minimize risks in type 1 diabetes". In: *IFAC Proceedings Volumes* 47.3, pp. 9253–9257 (cit. on p. 29).

Colmegna, P.H., R.S. Sánchez-Peña, R. Gondhalekar, E. Dassau, and F.J. Doyle III (2016a). "Reducing glucose variability due to meals and postprandial exercise in T1DM using switched LPV control: In silico studies". In: *Journal of diabetes science and technology* 10.3, pp. 744–753 (cit. on p. 29).

Colmegna, P.H., R.S. Sánchez-Peña, R. Gondhalekar, E. Dassau, and F.J. Doyle (2016b). "Switched LPV glucose control in type 1 diabetes". In: *IEEE Transactions on Biomedical Engineering* 63.6, pp. 1192–1200 (cit. on p. 29).

Control, Diabetes and Complications Trial Research Group (1993). "The effect of intensive treatment of diabetes on the development and progression of long-term complications in insulin-dependent diabetes mellitus". In: *New England Journal of Medicine* 329.14, pp. 977–986 (cit. on p. 1).

Cooperberg, B. A. and P. E. Cryer (2009). "β-Cell-mediated signaling predominates over direct α-cell signaling in the regulation of glucagon secretion in humans". In: *Diabetes Care* 32.12, pp. 2275–2280 (cit. on p. 37).

Cooperberg, B.A. and P.E. Cryer (2010). "Insulin reciprocally regulates glucagon secretion in humans". In: *Diabetes* 59.11, pp. 2936–2940 (cit. on p. 129).

Cryer, P. E. (1994). "Hypoglycemia: the limiting factor in the management of IDDM". In: *Diabetes* 43.11, pp. 1378–1389 (cit. on p. 23).

— (2001). "Hypoglycemia-associated autonomic failure in diabetes". In: *American Journal of Physiology: Endocrinology And Metabolism* 281.6, E1115–E1121 (cit. on pp. 22, 24, 25, 60, 63).

Dalla Man, C., F. Micheletto, D. Lv, M. Breton, B. Kovatchev, and C. Cobelli (2014). "The UVA/PADOVA type 1 diabetes simulator: new features". In: *Journal of Diabetes Science and Technology* 8.1, pp. 26–34 (cit. on pp. 35, 46, 50, 55, 60, 84, 106, 107, 148).

Dalla Man, C., D. M. Raimondo, R. A. Rizza, and C. Cobelli (2007a). "GIM, simulation software of meal glucose-insulin model". In: *Journal of Diabetes Science and Technology* 1.3, pp. 323–330 (cit. on p. 50).

Dalla Man, C., R. A. Rizza, and C. Cobelli (2007b). "Meal simulation model of the glucose-insulin system". In: *IEEE Transactions on Biomedical Engineering* 54.10, pp. 1740–1749 (cit. on pp. 4, 46, 50, 131).

Daskalaki, E., K. Nørgaard, T. Züger, A. Prountzou, P. Diem, and S. Mougiakakou (2013). "An early warning system for hypoglycemic/hyperglycemic events based on fusion of adaptive prediction models". In: *Journal of Diabetes Science and Technology* 7.3, pp. 689–698 (cit. on p. 4).

Dassau, E., F. Cameron, H. Lee, B. W. Bequette, H. Zisser, L. Jovanovic, H. P. Chase, D. M. Wilson, B. A. Buckingham, and F. J. Doyle (2010). "Real-time hypoglycemia prediction suite using continuous glucose monitoring: a safety net for the artificial pancreas". In: *Diabetes Care* 33.6, pp. 1249–1254 (cit. on p. 4).

de Galan, B.E., S.J. Rietjens, C.J. Tack, S.P. van der Werf, C.G.J. Sweep, J. Lenders W.M., and P. Smits (2003). "Antecedent adrenaline attenuates the responsiveness to but not the release of counterregulatory hormones during subsequent hypoglycemia". In: *The Journal of Clinical Endocrinology & Metabolism* 88.11, pp. 5462–5467 (cit. on pp. 74, 78, 80).

DeFronzo, R.A., R. Hendler, and N. Christensen (1980). "Stimulation of counterregulatory hormonal responses in diabetic man by a fall in glucose concentration". In: *Diabetes* 29.2, pp. 125–131 (cit. on pp. 92, 93, 95).

DeFronzo, R.A., D. Simonson, and E. Ferrannini (1982). "Hepatic and peripheral insulin resistance: a common feature of type 2 (non-insulin-dependent) and type 1 (insulin-dependent) diabetes mellitus". In: *Diabetologia* 23.4, pp. 313–319 (cit. on p. 3).

Dejgaard, A., J. Hilsted, J.H. Henriksen, and N.J. Christensen (1989). "Plasma adrenaline kinetics in Type 1 (insulin-dependent) diabetic patients with and without autonomie neuropathy". In: *Diabetologia* 32.11, pp. 810–813 (cit. on pp. 76, 78).

Diabetes Research in Children Network (DirecNet) Study Group, E. Tsalikian, C. Kollman, W. B. Tamborlane, R. W. Beck, R. Fiallo-Scharer, L. Fox, K. F. Janz, K. J. Ruedy, D. Wilson, D. Xing, and S. A. Weinzimer (2006). "Prevention of hypoglycemia during exercise in children with type 1 diabetes by

suspending basal insulin". In: *Diabetes Care* 29.10, pp. 2200–2204 (cit. on p. 39).

Dimitriadis, G. D. and J. E. Gerich (1983). "Importance of timing of preprandial subcutaneous insulin administration in the management of diabetes mellitus". In: *Diabetes Care* 6.4, pp. 374–377 (cit. on p. 3).

Dovc, K., M. Macedoni, N. Bratina, D. Lepej, R. Nimri, E. Atlas, I. Muller, O. Kordonouri, T. Biester, T. Danne, M. Phillip, and T. Battelino (2017). "Closed-loop glucose control in young people with type 1 diabetes during and after unannounced physical activity: a randomised controlled crossover trial". In: *Diabetologia* 60.11, pp. 2157–2167 (cit. on pp. 5, 29).

El Hachimi, M., A. Ballouk, I. Khelafa, and A. Baghdad (2017). "Development of a model predictive controller for an artificial pancreas". In: *2017 International Conference on Electrical and Information Technologies (ICEIT)*. Rabat, Morocco, pp. 1–6 (cit. on p. 31).

El Youssef, J., J. R. Castle, D. L. Branigan, R. G. Massoud, M. E. Breen, P. G. Jacobs, B. W. Bequette, and W. K. Ward (2011). "A controlled study of the effectiveness of an adaptive closed-loop algorithm to minimize corticosteroid-induced stress hyperglycemia in type 1 diabetes". In: *Journal of Diabetes Sciences and Technologies* 5.6, pp. 1312–1326 (cit. on pp. 29, 39, 40).

El Youssef, J., J.R. Castle, P.A. Bakhtiani, A. Haidar, D.L. Branigan, M. Breen, and W.K. Ward (2014). "Quantification of the glycemic response to microdoses of subcutaneous glucagon at varying insulin levels". In: *Diabetes Care* 37.11, pp. 3054–3060 (cit. on pp. 36, 128).

Elleri, D., J.M. Allen, J. Harris, K. Kumareswaran, M. Nodale, L. Leelarathna, C.L. Acerini, A. Haidar, M.E. Wilinska, N. Jackson, A.M. Umpleby, Evans M.L., D.B. Dunger, and R. Hovorka (2013). "Absorption patterns of meals containing complex carbohydrates in type 1 diabetes". In: *Diabetologia* 56.5, pp. 1108–1117 (cit. on p. 40).

Ellingsen, C., E. Dassau, H. Zisser, B. Grosman, M.W. Percival, L. Jovanovic, and F.J. Doyle III (2009). "Safety constraints in an artificial pancreatic β cell: an implementation of model predictive control with insulin on board". In: *Journal of Diabetes Science and Technology* 3.3, pp. 536–544 (cit. on pp. 5, 31, 33, 34, 128).

Enoksson, S., S. K. Caprio, F. Rife, G.I. Shulman, W.V. Tamborlane, and R.S. Sherwin (2003). "Defective activation of skeletal muscle and adipose tissue lipolysis in type 1 diabetes mellitus during hypoglycemia". In: *The Journal of Clinical Endocrinology & Metabolism* 88.4, pp. 1503–1511 (cit. on p. 84).

Fabietti, P. G., V. Canonico, M. O. Federici, M. M. Benedetti, and E. Sarti (2006). "Control oriented model of insulin and glucose dynamics in type 1 diabetics". In: *Medical and Biological Engineering and Computing* 44.1-2, pp. 69–78 (cit. on pp. 47, 49).

Fanelli, C., S. Pampanelli, L. Epifano, A.M. Rambotti, M. Ciofetta, F. Modarelli, A. Di Vincenzo, B. Annibale, M. Lepore, C. Lalli, P. Del Sindaco, P. Brunetti, and G.B. Bolli (1994). "Relative roles of insulin and hypoglycaemia on induction of neuroendocrine responses to, symptoms of, and deterioration of cognitive function in hypoglycaemia in male and female humans". In: *Diabetologia* 37.8, pp. 797–807 (cit. on p. 22).

Fanelli, C.G., P. De Feo, F. Porcellati, G. Perriello, E. Torlone, F. Santeusanio, P. Brunetti, and G.B. Bolli (1992). "Adrenergic mechanisms contribute to the late phase of hypoglycemic glucose counterregulation in humans by stimulating lipolysis." In: *The Journal of Clinical Investigation* 89.6, pp. 2005–2013 (cit. on p. 105).

Federation of European Nurses in Diabetes (2008). *Diabetes. The policy puzzle: Is Europe making progress?* Available: `https://ec.europa.eu/health/sites/health/files/major_chronic_diseases/docs/policy_puzzle_2008.pdf` (cit. on p. 1).

Finan, D. A., F. J. Doyle III, C. C. Palerm, W. C. Bevier, H. C. Zisser, L. Jovanovic, and D. E. Seborg (2009). "Experimental evaluation of a recursive model identification technique for type 1 diabetes". In: *Journal of Diabetes Science and Technology* 3.5, pp. 1192–1202 (cit. on p. 3).

Forsman, K. and T. Glad (1990). "Constructive algebraic geometry in nonlinear control". In: *Decision and Control, 1990, Proceedings of the 29th IEEE Conference*, pp. 2825–2827 (cit. on p. 71).

Galassetti, P., D. Tate, R. A. Neill, A. Richardson, S.Y. Leu, and S.N. Davis (2006). "Effect of differing antecedent hypoglycemia on counterregulatory re-

sponses to exercise in type 1 diabetes". In: *American Journal of Physiology: Endocrinology and Metabolism* 290.6, E1109–E1117 (cit. on pp. 63, 80).

Gerich, J., J. Davis, M. Lorenzi, R. Rizza, N. Bohannon, J. Karam, S. Lewis, R. Kaplan, T. Schultz, and P. Cryer (1979). "Hormonal mechanisms of recovery from insulin-induced hypoglycemia in man". In: *American Journal of Physiology: Endocrinology and Metabolism* 236.4, E380–E385 (cit. on p. 22).

Gibney, M. (2013). *The race for the artificial pancreas.* URL: `https://www.fiercepharma.com/r-d/race-for-artificial-pancreas` (cit. on p. 2).

Giménez, M., V. Moscardó, M. Reddy, I. Conget, and N. Oliver (2018a). "Diferencias entre poblaciones de pacientes con diabetes tipo 1 de alto y bajo riesgo de hipoglucemia utilizando sistemas de monitorizacion continua de la glucose". In: *Proceedings of the XXIX Congreso Nacional de la Sociedad Española de Diabetes.* Oviedo, Spain (cit. on p. 173).

— (2018b). "Differences between high and low Hypoglycaemia risk populations using Continuous Glucose Monitoring datasets". In: *The 11th International Conference on Advanced Technologies & treatments for diabetes (ATTD).* Vienna, Austria (cit. on p. 173).

Giménez, M., S. Purkayajtha, V. Moscardó, I. Conget, and N. Oliver (2018c). "Intraperitoneal insulin therapy in patients with type 1 diabetes. Does it fit into the current therapeutic arsenal?" In: *Endocrinología, Diabetes y Nutrición* 65.3, pp. 133–188 (cit. on p. 172).

Gimenez, M., A.J. Tannen, M. Reddy, V. Moscardo, I. Conget, and N. Oliver (2018). "Revisiting the Relationships Between Measures of Glycemic Control and Hypoglycemia in Continuous Glucose Monitoring Datasets". In: *Diabetes Care* 41.2, pp. 326–332 (cit. on pp. 6, 112, 171).

Giménez, M., A.J. Tannen, M. Reddy, V. Moscardó, I. Conget, and N. Oliver (2018d). "Revising the relationships between measures of glycaemic control and hypoglycaemia in Continuous Glucose Monitoring datasets". In: *The 11th International Conference on Advanced Technologies & treatments for diabetes (ATTD).* Vienna, Austria (cit. on p. 173).

Gondhalekar, R., E. Dassau, and F. J. Doyle III (2015a). "Tackling problem nonlinearities and delays via asymmetric, state-dependent objective costs in MPC

of an artificial pancreas". In: *IFAC-Papers OnLine* 48.23, pp. 154–159 (cit. on p. 29).

Gondhalekar, R., E. Dassau, and F. J. Doyle (2015b). "Velocity-weighting to prevent controller-induced hypoglycemia in MPC of an artificial pancreas to treat T1DM". In: *Proceedings of the 2015 American Control Conference (ACC).* Chicago, IL, USA, pp. 1635–1640 (cit. on p. 31).

Gondhalekar, R., E. Dassau, H.C. Zisser, and F.J. Doyle III (2013). "Periodic-zone model predictive control for diurnal closed-loop operation of an artificial pancreas". In: *Journal of Diabetes Science and Technology* 7.6, pp. 1446–1460 (cit. on p. 31).

Grodsky, G. M. (1972). "A threshold distribution hypothesis for packet storage of insulin and its mathematical modeling". In: *The Journal of Clinical Investigation* 51.8, pp. 2047–2059 (cit. on p. 48).

Grosman, B., E. Dassau, H.C. Zisser, L. Jovanovic, and F.J. Doyle III (2010). "Zone model predictive control: a strategy to minimize hyper-and hypoglycemic events". In: *Journal of Diabetes Science and Technology* 4.4, pp. 961–975 (cit. on p. 31).

Guilmin-Crépon, S., J. C. Carel, J. Schroedt, E. Scornet, C. Alberti, N. Tubiana-Rufi, and Start-In! Study Group (2018). "How Should We Assess Glycemic Variability in Type 1 Diabetes? Contribution of Principal Component Analysis for Interstitial Glucose Indices in 142 Children". In: *Diabetes Technology & Therapeutics* 20.6, pp. 440–447 (cit. on p. 125).

Guyton, J. R., R. O. Foster, J. S. Soeldner, M. H. Tan, C. B. Kahn, L. Koncz, and R. E. Gleason (1978). "A model of glucose-insulin homeostasis in man that incorporates the heterogeneous fast pool theory of pancreatic insulin release". In: *Diabetes* 27.10, pp. 1027–1042 (cit. on p. 49).

Haidar, A. (2012). "External artificial pancreas for type 1 diabetes: Modeling and control". Available: `http://digitool.library.mcgill.ca/thesisfile117039.pdf`. PhD. Dissertation. Montreal, Canada: McGill University (cit. on p. 40).

— (2016). "The artificial pancreas: How closed-loop control is revolutionizing diabetes". In: *IEEE Control Systems* 36.5, pp. 28–47 (cit. on p. 40).

Haidar, A., L. Legault, M. Dallaire, A. Alkhateeb, A. Coriati, V. Messier, P. Cheng, M. Millette, B. Boulet, and R. Rabasa-Lhoret (2013). "Glucose-responsive insulin and glucagon delivery (dual-hormone artificial pancreas) in adults with type 1 diabetes: A randomized crossover controlled trial". In: *Canadian Medical Association Journal* 185.4, pp. 297–305 (cit. on pp. 33, 37, 128).

Haidar, A., L. Legault, V. Messier, T.M. Mitre, C. Leroux, and R. Rabasa-Lhoret (2015). "Comparison of dual-hormone artificial pancreas, single-hormone artificial pancreas, and conventional insulin pump therapy for glycaemic control in patients with type 1 diabetes: an open-label randomised controlled crossover trial". In: *The Lancet Diabetes & Endocrinology* 3.1, pp. 17–26 (cit. on p. 37).

Haidar, A., V. Messier, L. Legault, M. Ladouceur, and R. Rabasa-Lhoret (2017). "Outpatient 60-hour day-and-night glucose control with dual-hormone artificial pancreas, single-hormone artificial pancreas, or sensor-augmented pump therapy in adults with type 1 diabetes: An open-label, randomised, crossover, controlled trial". In: *Diabetes, Obesity and Metabolism* 19.5, pp. 713–720 (cit. on p. 37).

Hansen, N. (2006). "The CMA evolution strategy: a comparing review". In: *Towards a new evolutionary computation*. Springer, pp. 75–102 (cit. on p. 72).

— (2016). *The CMA evolution strategy: A tutorial*. arXiv: 1604.00772 (cit. on p. 72).

Hansen, N., S. D. Müller, and P. Koumoutsakos (2003). "Reducing the time complexity of the derandomized evolution strategy with covariance matrix adaptation (CMA-ES)". In: *Evolutionary Computation* 11.1, pp. 1–18 (cit. on p. 72).

Harvey, R. A., E. Dassau, W. C. Bevier, D. E. Seborg, L. Jovanovic, F. J. Doyle III, and H. C. Zisser (2014). "Clinical evaluation of an automated artificial pancreas using zone-model predictive control and health monitoring system". In: *Diabetes Technology & Therapeutics* 16.6, pp. 348–357 (cit. on p. 40).

Harvey, R. A., E. Dassau, H. C. Zisser, W. Bevier, D. E. Seborg, L. Jovanovic, and F. J. Doyle III (2012). "Clinically relevant hypoglycemia prediction metrics

for event mitigation". In: *Diabetes Technology & Therapeutics* 14.8, pp. 719–727 (cit. on p. 4).

Health Research (JCHR), Jaeb Center for (2018). *Diabetes Research Studies.* URL: `http://diabetes.jaeb.org/Dataset.aspx` (cit. on pp. 39, 117).

Heinemann, L. (2017). "Future of Diabetes Technology". In: *Journal of Diabetes Science and Technology* 11.5, pp. 863–869 (cit. on pp. 18, 21).

Heller, S.R. and I.A. Macdonald (1996). "The measurement of cognitive function during acute hypoglycaemia: experimental limitations and their effect on the study of hypoglycaemia unawareness". In: *Diabetic Medicine* 13.7, pp. 607–615 (cit. on p. 23).

Henson, M.A., B.A. Ogunnaike, and J.S. Schwaber (1995). "Habituating control strategies for process control". In: *American Institute of Chemical Engineers Journal* 41.3, pp. 604–618 (cit. on pp. 134, 135).

Hermans, M. P., J. C. Levy, R. J. Morris, and R. C. Turner (1999). "Comparison of insulin sensitivity tests across a range of glucose tolerance from normal to diabetes". In: *Diabetologia* 42.6, pp. 678–687 (cit. on p. 115).

Hermans, M. P., F. M. Sacks, S. A. Ahn, and M. F. Rousseau (2011). "Non-HDL-cholesterol as valid surrogate to apolipoprotein B 100 measurement in diabetes: Discriminant Ratio and unbiased equivalence". In: *Cardiovascular Diabetology* 10.20, pp. 1–7 (cit. on p. 115).

Herrero, P., J. Bondia, N. Oliver, and P. Georgiou (2017). "A coordinated control strategy for insulin and glucagon delivery in type 1 diabetes". In: *Computer Methods in Biomechanics and Biomedical Engineering* 20.13, pp. 1474–1482 (cit. on p. 37).

Herrero, P., P. Georgiou, N. Oliver, D. G. Johnston, and C. Toumazou (2012). "A bio-inspired glucose controller based on pancreatic β-cell physiology". In: *Journal of Diabetes Science and Technology* 6.3, pp. 606–616 (cit. on pp. 33, 37, 128, 146).

Herrero, P., P. Georgiou, N. Oliver, M. Reddy, D. Johnston, and C. Toumazou (2013). "A composite model of glucagon-glucose dynamics for in silico test-

ing of bihormonal glucose controllers". In: *Journal of Diabetes Science and Technology* 7.4, pp. 941–951 (cit. on pp. 131, 133).

Hill, N. R., P. C. Hindmarsh, R. J. Stevens, I. M. Stratton, J. C. Levy, and D. R. Matthews (2007). "A method for assessing quality of control from glucose profiles". In: *Diabetic medicine* 24.7, pp. 753–758 (cit. on pp. 42, 114, 177, 180).

Hill, N. R., N. S. Oliver, P. Choudhary, J. C. Levy, P. Hindmarsh, and D. R. Matthews (2011). "Normal reference range for mean tissue glucose and glycemic variability derived from continuous glucose monitoring for subjects without diabetes in different ethnic groups". In: *Diabetes technology & therapeutics* 13.9, pp. 921–928 (cit. on p. 39).

Hinshaw, L., C. Dalla Man, D. K. Nandy, A. Saad, A. E. Bharucha, J. A. Levine, R. A. Rizza, R. Basu, R. E. Carter, C. Cobelli, Y. C. Kudva, and A. Basu (2013). "Diurnal pattern of insulin action in type 1 diabetes: implications for a closed loop system". In: *Diabetes* 62.7, pp. 2223–2229 (cit. on p. 51).

Hirsch, I. B., A. K. Balo, K. Sayer, A. Garcia, B. A. Buckingham, and T. A. Peyser (2017). "A simple composite metric for the assessment of glycemic status from continuous glucose monitoring data: implications for clinical practice and the artificial pancreas". In: *Diabetes technology & therapeutics* 19.S3, S38–S48 (cit. on pp. 43, 179, 182).

Hövelmann, U., B.V. Bysted, U. Mouritzen, F. Macchi, D. Lamers, B. Kronshage, D.V. Møller, and T. Heise (2018). "Pharmacokinetic and pharmacodynamic characteristics of dasiglucagon, a novel soluble and stable glucagon analog". In: *Diabetes Care* 41.3, pp. 531–537 (cit. on p. 38).

Hovorka, R. (2006). "Continuous glucose monitoring and closed-loop systems". In: *Diabetic Medicine* 23.1, pp. 1–12 (cit. on p. 28).

Hovorka, R., J.M. Allen, D. Elleri, L.J. Chassin, J. Harris, D. Xing, C. Kollman, T. Hovorka, A.M. Larse, M. Nodale, A. De Palma, M. E. Wilinska, C.L. Acerini, and D.B. Dunger (2010). "Manual closed-loop insulin delivery in children and adolescents with type 1 diabetes: A phase 2 randomised crossover trial". In: *The Lancet* 375.9716, pp. 743–751 (cit. on pp. 4, 40).

Hovorka, R., V. Canonico, L.J. Chassin, U. Haueter, M. Massi-Benedetti, M.O. Federici, T.R. Pieber, H.C. Schaller, L. Schaupp, T. Vering, and M.E. Wilinska (2004). "Nonlinear model predictive control of glucose concentration in subjects with type 1 diabetes". In: *Physiological Measurement* 25.4, pp. 905–920 (cit. on pp. 3, 4, 35, 46, 49, 131, 156).

Hovorka, R., L. Chassin, S. D. Luzio, R. Playle, and D. R. Owens (1998). "Pancreatic β-cell responsiveness during meal tolerance test: model assessment in normal subjects and subjects with newly diagnosed noninsulin-dependent diabetes mellitus". In: *The Journal of Clinical Endocrinology & Metabolism* 83.3, pp. 744–750 (cit. on p. 46).

Hovorka, R., F. Shojaee-Moradie, P. V. Carroll, L. J. Chassin, I. J. Gowrie, N. C. Jackson, R. S. Tudor, A. M. Umpleby, and R. H. Jones (2002). "Partitioning glucose distribution/transport, disposal, and endogenous production during IVGTT". In: *American Journal of Physiology: Endocrinology and Metabolism* 282.5, E992–E1007 (cit. on pp. 49, 54).

Iscoe, K.E. and M.C. Riddell (2011). "Continuous moderate-intensity exercise with or without intermittent high-intensity work: effects on acute and late glycaemia in athletes with Type 1 diabetes mellitus". In: *Diabetic Medicine* 28.7, pp. 824–832 (cit. on p. 38).

Jaeb Center for Health Research (2018). *JDRF/NIDDK Artificial Pancreas Project Consortium*. URL: `%5Curl%7Bhttp://jdrfconsortium.jaeb.org/ViewPage.aspx?PageName=Home%7D` (cit. on p. 2).

Jain, R. and E. Lammert (2009). "Cell-cell interactions in the endocrine pancreas". In: *Diabetes, Obesity and Metabolism* 11, pp. 159–167 (cit. on pp. 37, 129).

Kanderian, S. S., S. A. Weinzimer, and G. M. Steil (2012). "The identifiable virtual patient model: comparison of simulation and clinical closed-loop study results". In: *Journal of Diabetes Science and Technology* 6.2, pp. 371–379 (cit. on pp. 46, 131).

Kanderian, S., M. F. Saad, K. Rebrin, and G. M. Steil (2006). "Modeling glucose profiles obtained using closed loop insulin delivery-Implications for controller optimization". In: *Diabetes* 55.Suppl 1, A98–A98 (cit. on p. 49).

Kelley, D. E. (2003). "Sugars and starch in the nutritional management of diabetes mellitus". In: *The American Journal of Clinical Nutrition* 78.4, 858S–864S (cit. on p. 3).

El-Khatib, F. H., S.J. Russell, D.M. Nathan, R.G. Sutherin, and E.R. Damiano (2010). "A bihormonal closed-loop artificial pancreas for type 1 diabetes". In: *Science Translational Medicine* 2.27, 27ra27 (cit. on pp. 4, 29, 33, 36, 40, 128).

Kilpatrick, E. S., A. S. Rigby, K. Goode, and S. L. Atkin (2007). "Relating mean blood glucose and glucose variability to the risk of multiple episodes of hypoglycaemia in type 1 diabetes". In: *Diabetologia* 50.12, pp. 2553–2561 (cit. on pp. 39, 112).

Kircher, R., J. Lee, D. Matheson, and R. Mauseth (2015). "Efficacy and Computational Efficiency of the Dose Safety Hypoglycemia Prevention Module (HPM)". In: *Diabetes technology & Therapeutics*. Vol. 17, A96–A96 (cit. on pp. 32, 34).

Kohnert, K. D., P. Heinke, L. Vogt, and E. Salzsieder (2015). "Utility of different glycemic control metrics for optimizing management of diabetes". In: *World Journal of Diabetes* 6.1, pp. 17–29 (cit. on p. 113).

Kovács, L., B. Kulcsár, J. Bokor, and Z. Benyó (2008). "Model-based nonlinear optimal blood glucose control of type I diabetes patients". In: *30th Annual International Conference of the IEEE Engineering in Medicine and Biology Society*. Vancouver, Canada, pp. 1607–1610 (cit. on p. 29).

Kovatchev, B. and C. Cobelli (2016). "Glucose variability: timing, risk analysis, and relationship to hypoglycemia in diabetes". In: *Diabetes Care* 39.4, pp. 502–510 (cit. on p. 39).

Kovatchev, B., C. Cobelli, E. Renard, S. Anderson, M. Breton, S. Patek, W. Clarke, D. Bruttomesso, A. Maran, S. Costa, A. Avogaro, C. Dalla Man, A. Facchinetti, L. Magni, G. De Nicolao, J. Place, and A. Farret (2010). "Multinational study of subcutaneous model-predictive closed-loop control in type 1 diabetes mellitus: summary of the results". In: *Journal of Diabetes Science and Technology* 4.6, pp. 1374–1381 (cit. on p. 4).

Kovatchev, B., L. S. Farhy, D. J. Cox, M. Straume, V. I. Yankov, L. A. Gonder-Frederick, and W. L. Clarke (1998). "Modeling Insulin-Glucose Dynamics during Insulin Induced Hypoglycemia. Evaluation of Glucose Counterregulation". In: *Journal of Theoretical Medicine* 1.4, pp. 313–323 (cit. on pp. 55, 60).

Kovatchev, B., E. Otto, D. Cox, L. Gonder-Frederick, and W. Clarke (2006). "Evaluation of a new measure of blood glucose variability in diabetes". In: *Diabetes care* 29.11, pp. 2433–2438 (cit. on pp. 42, 43, 60, 181).

Kowalski, A.J. (2009). "Can we really close the loop and how soon? Accelerating the availability of an artificial pancreas: a roadmap to better diabetes outcomes". In: *Diabetes Technology & Therapeutics* 11.S1, S113–S119 (cit. on p. 2).

Krinsley, J. S. (2008). "Glycemic variability: a strong indepentent predictor of mortality in critically ill patients". In: *Critical care medicine* 36.11, pp. 3008–3013 (cit. on p. 39).

Kudva, Y. C., R. E. Carter, C. Cobelli, R. Basu, and A. Basu (2014). "Closed-loop artificial pancreas systems: physiological input to enhance next-generation devices". In: *Diabetes care* 37.5, pp. 1184–1190 (cit. on p. 41).

Kumareswaran, K., D. Elleri, J. M. Allen, J. Harris, D. Xing, C. Kollman, M. Nodale, H. R. Murphy, S. A. Amiel, S. R. Heller, M. E. Wilinska, C. L. Acerini, M. L. Evans, D. B. Dunger, and R. Hovorka (2011). "Meta-analysis of overnight closed-loop randomized studies in children and adults with type 1 diabetes: the Cambridge cohort". In: *Journal of Diabetes Science and Technology* 5.6, pp. 1352–1362 (cit. on p. 4).

Lackinger, C., F. Reiterer, D. Moser, P. Schrangl, and L. del Re (2017). "Chance-constrained model predictive control for blood glucose management in diabetes". In: *2017 IEEE 56th Annual Conference on Decision and Control (CDC)*. Melbourne, VIC, Australia, pp. 4703–4708 (cit. on p. 31).

Lee, J. B., R. Gondhalekar, E. Dassau, and F. J. Doyle III (2016). "Shaping the MPC Cost Function for Superior Automated Glucose Control". In: *IFAC Papers On Line* 49.7, pp. 779–784 (cit. on p. 31).

Leese, G. P., J. Wang, J. Broomhall, P. Kelly, A. Marsden, W. Morrison, B. M. Frier, and A. D. Morris (2003). "Frequency of severe hypoglycemia requiring emergency treatment in type 1 and type 2 diabetes: a population-based study of health service resource use". In: *Diabetes care* 26.4, pp. 1176–1180 (cit. on p. 22).

Lehmann, E.D., T. Deutsch, A.V. Roudsari, E.R. Carson, and P.H. Sonksen (1993). "Validation of a metabolic prototype to assist in the treatment of insulin-dependent diabetes mellitus". In: *Medical Informatics* 18.2, pp. 83–101 (cit. on p. 48).

Levy, J., R. Morris, M. Hammersley, and R. Turner (1999). "Discrimination, adjusted correlation, and equivalence of imprecise tests: application to glucose tolerance". In: *American Journal of Physiology: Endocrinology and Metabolism* 276.2, E365–E375 (cit. on p. 115).

Li, Y., C.C. Chow, A.B. Courville, A.E. Sumner, and V. Periwal (2016). "Modeling glucose and free fatty acid kinetics in glucose and meal tolerance test". In: *Theoretical Biology and Medical Modelling* 13.1, p. 8 (cit. on p. 100).

Lurie, B. and P. Enright (2011). *Classical feedback control: with MATLAB*. 2nd ed. Boca Raton, FL, USA: CRC Press-Taylor & Francis Group (cit. on p. 134).

Maahs, D. M., B. A. Buckingham, J. R. Castle, A. Cinar, E. R. Damiano, E. Dassau, J. H. DeVries, F. J. Doyle III, S. C. Griffen, A. Haidar, L. Heinemann, R. Hovorka, T. W. Jones, C. Kollman, B. Kovatchev, B. L. Levy, R. Nimri, D. N. O'Neal, M. Philip, E. Renard, S. J. Russell, S. A. Weinzimer, H. Zisser, and J. W. Lum (2016). "Outcome measures for artificial pancreas clinical trials: a consensus report". In: *Diabetes Care* 39.7, pp. 1175–1179 (cit. on pp. 114, 149).

Macdonald, I. A. and P. King (2007). "Normal Glucose Metabolism and Responses to Hypoglycaemia". In: *Hypoglycaemia in clinical diabetes*. Ed. by B. M. Frier and M. Fisher. 2nd ed. Chichester, England: John Wiley & Sons. Chap. 1, pp. 1–22 (cit. on p. 17).

Magni, L., M. Forgione, C. Toffanin, C. Dalla Man, B. Kovatchev, G. De Nicolao, and C. Cobelli (2009). *Run-to-run tuning of model predictive control for type 1 diabetes subjects: in silico trial* (cit. on p. 4).

Magni, L., D. M. Raimondo, C. Dalla Man, G. De Nicolao, B. Kovatchev, and C. Cobelli (2007). "Model predictive control of type 1 diabetes: an in silico trial". In: *Journal of Diabetes Science and Technology* 1.6, pp. 804–812 (cit. on p. 4).

— (2008). "Model predictive control of glucose concentration in subjects with type 1 diabetes: an in silico trial". In: *IFAC Proceedings Volumes* 41.2, pp. 4246–4251 (cit. on p. 31).

Maran, A., P. Pavan, B. Bonsembiante, E. Brugin, A. Ermolao, A. Avogaro, and M. Zaccaria (2010). "Continuous glucose monitoring reveals delayed nocturnal hypoglycemia after intermittent high-intensity exercise in nontrained patients with type 1 diabetes". In: *Diabetes Technology & Therapeutics* 12.10, pp. 763–768 (cit. on p. 38).

Mari, A. (1992). "Estimation of the rate of appearance in the non-steady state with a two-compartment model". In: *American Journal of Physiology: Endocrinology and Metabolism* 263.2, E400–E415 (cit. on p. 46).

Marty, N., M. Dallaporta, and B. Thorens (2007). "Brain glucose sensing, counter-regulation, and energy homeostasis". In: *Physiology* 22.4, pp. 241–251 (cit. on p. 63).

Mauseth, R., I. B. Hirsch, J. Bollyky, R. Kircher, D. Matheson, S. Sanda, and C. Greenbaum (2013). "Use of a "fuzzy logic" controller in a closed-loop artificial pancreas". In: *Diabetes Technology & Therapeutics* 15.8, pp. 628–633 (cit. on pp. 29, 32).

Mauseth, R., S.M. Lord, I.B. Hirsch, R.C. Kircher, D.P. Matheson, and C.J. Greenbaum (2015). "Stress testing of an artificial pancreas system with pizza and exercise leads to improvements in the system's fuzzy logic controller". In: *Journal of Diabetes Science and Technology* 9.6, pp. 1253–1259 (cit. on p. 32).

Mazor, E., A. Averbuch, Y. Bar-Shalom, and J. Dayan (1998). "Interacting multiple model methods in target tracking: A survey". In: *Diabetes Technology & Therapeutics* 34.1, pp. 103–123 (cit. on p. 40).

McDonnell, C. M., S. M. Donath, S. I. Vidmar, G. A. Werther, and F. J. Cameron (2005). "A novel approach to continuous glucose analysis utilizing glycemic variation". In: *Diabetes Technology & Therapeutics* 7.2, pp. 253–263 (cit. on pp. 42, 178).

McLain, R.B., M.J. Kurtz, M.A. Henson, and F.J. Doyle (1996). "Habituating control for nonsquare nonlinear processes". In: *Industrial & Engineering Chemistry Research* 35.11, pp. 4067–4077 (cit. on pp. 134, 135).

Melmed, S., K. S. Polonsky, P. R. Larsen, and H. M. Kronenberg (2016). *Williams textbook of endocrinology*. 13th ed. Philadelpia, PA, USA: Elsevier (cit. on pp. 19–21).

Mitrakou, A., C. Ryan, T. Veneman, M. Mokan, T. Jenssen, I. Kiss, J. Durrant, P. Cryer, and J. Gerich (1991). "Hierarchy of glycemic thresholds for counterregulatory hormone secretion, symptoms, and cerebral dysfunction". In: *American Journal of Physiology: Endocrinology And Metabolism* 260.1, E67–E74 (cit. on pp. 22, 23).

Moheet, A., A. Kumar, L.E. Eberly, J. Kim, R. Roberts, and E.R. Seaquist (2014). "Hypoglycemia-associated autonomic failure in healthy humans: comparison of two vs three periods of hypoglycemia on hypoglycemia-induced counterregulatory and symptom response 5 days later". In: *The Journal of Clinical Endocrinology & Metabolism* 99.2, pp. 664–670 (cit. on p. 80).

Molnar, G. D., W. F. Taylor, and M. M. Ho (1972). "Day-to-day variation of continuously monitored glycaemia: A further measure of diabetic instability". In: *Diabetes Technology & Therapeutics* 8.5, pp. 342–348 (cit. on pp. 42, 178).

Monnier, L., C. Colette, and D. R. Owens (2008). "Glycemic variability: the third component of the dysglycemia in diabetes. Is it important? How to measure it?" In: *Journal of Diabetes Science and Technology* 2.6, pp. 1094–1100 (cit. on p. 112).

Monnier, L., E. Mas, C. Ginet, F. Michel, L. Villon, J. P. Cristol, and C. Colette (2006). "Activation of oxidative stress by acute glucose fluctuations compared with sustained chronic hyperglycemia in patients with type 2 diabetes". In: *Journal of the American Medical Association* 295.14, pp. 1681–1687 (cit. on p. 39).

Monroy-Loperena, R., R. Solar, and J. Alvarez-Ramirez (2004). "Balanced control scheme for reactor/separator processes with material recycle". In: *Industrial & Engineering Chemistry Research* 43.8, pp. 1853–1862 (cit. on p. 135).

Moscardo, V., J. Bondia, F. J. Ampudia-Blasco, C. G. Fanelli, P. Lucidi, and P. Rossetti (2018). "Plasma Insulin Levels and Hypoglycemia Affect Subcutaneous Interstitial Glucose Concentration". In: *Diabetes Technology & Therapeutics* 20.4, pp. 263–273 (cit. on pp. 39, 63, 171).

Moscardó, V., J.L. Diez, P. Herrero, M. Giménez, P. Rosseti, and J. Bondia (2018a). "Sliding mode reference conditioning dual hormone coordinated glucose control". In: *The 11th International Conference on Advanced Technologies & treatments for diabetes (ATTD)*. Vienna, Austria (cit. on p. 173).

Moscardó, V., M. Giménez, P. Avari, M. Reddy, and N. Oliver (2018b). "Influence of ambient temperature on glycaemic behaviour in type 1 Diabetes patients". In: *The 11th International Conference on Advanced Technologies & treatments for diabetes (ATTD)*. Vienna, Austria (cit. on p. 173).

Moscardó, V., M. Gimenez, N. Oliver, and N. Hill (2018c). "Automated assessment of glucose variability in Diabetes". In: *Diabetes Technology & Therapeutics*. Submitted: First review (cit. on p. 174).

Moscardó, V., P. Herrero, J. L. Diez, M. Guimenez, P. Rosseti, and J. Bondia (2019). "In silico evaluation of a Parallel Control-based Coordinated Dual-Hormone Artificial Pancreas with Insulin on Board Limitation". In: *American Control Conference 2019*. Accepted (cit. on p. 172).

Moscardó, V., P. Herrero, J.L. Diez, M. Guimenez, P. Rosseti, P. Georgiou, and J. Bondia (2018d). "Assessment of the Coordinated Control structure in the Dual Hormone Artificial Pancreas". In: *Computers & Chemical Engineering*. Submitted: Second review (cit. on p. 174).

Moscardó, V., P. Herrero, M. Reddy, N. Hill, P. Georgiou, and N. Oliver (2018e). "Assessment of glucose control metrics by Discriminant Ratio". In: *Diabetes Technology & Therapeutics*. Submitted: First review (cit. on p. 174).

Moscardó, V., P. Rossetti, F. J. Ampudia-Blasco, and J. Bondia (2015). "Modelling adrenaline secretion during counterregulatory response in Type 1 Diabetes for improved hypoglycaemia prediction". In: *IFAC-PapersOnLine* 48.20, pp. 213–218 (cit. on p. 172).

Moscardo, V., P. Rossetti, F.J. Ampudia-Blasco, and J. Bondia (2016a). "Amperometric glucose sensors' background current is a confounding factor of

plasma-interstitium relationship studies during hypoglycaemia". In: *The 16th Annual Diabetes Technology Meeting (DTM)*. Bethesda, USA (cit. on p. 173).

— (2016b). "Modelling of adrenaline action during hypoglycaemia in Type 1 Diabetes". In: *Proceeding of the 2016 IEEE Conference on Control Applications (CCA)*. Buenos Aires, Argentina (cit. on p. 172).

Mukaka, M. M. (2012). "A guide to appropriate use of correlation coefficient in medical research". In: *Malawi Medical Journal* 24.3, pp. 69–71 (cit. on p. 121).

Neylon, O. M., P. A. Baghurst, and F. J. Cameron (2014). "The minimum duration of sensor data from which glycemic variability can be consistently assessed". In: *Journal of Diabetes Science and Technology* 8.2, pp. 273–276 (cit. on pp. 117, 119).

Nimri, R., E. Atlas, M. Ajzensztejn, S. Miller, T. Oron, and M. Phillip (2012). "Feasibility study of automated overnight closed-loop glucose control under MD-logic artificial pancreas in patients with type 1 diabetes: the DREAM Project". In: *Diabetes Technology & Therapeutics* 14.8, pp. 728–735 (cit. on p. 32).

Omar, M. A., A. Kok, D. Khutsoane, S. Joshi, M. Ramaboea, M. L. I. Mashitisho, V. Chetty, L. J. Koopman, L. Johnson, and on behalf of the IO HAT investigator group (2018). "Incidence of hypoglycaemia among insulin-treated patients with type 1 or type 2 diabetes mellitus: South African cohort of International Operations Hypoglycaemia Assessment Tool (IO HAT) study". In: *Journal of Endocrinology, Metabolism and Diabetes of South Africa* 23.1, pp. 1–8 (cit. on p. 22).

Palerm, C. C. and B. W. Bequette (2004). "Issues on hypoglycemia prediction and detection". In: *Proceedings of the IEEE 30th Annual Northeast Bioengineering Conference*. Springfield, MA, USA, pp. 81–82 (cit. on p. 4).

— (2007). "Hypoglycemia detection and prediction using continuous glucose monitoring: A study on hypoglycemic clamp data". In: *Journal of Diabetes Science and Technology* 1.5, pp. 624–629 (cit. on p. 4).

Pańkowska, E., M. Błazik, and L. Groele (2012). "Does the fat-protein meal increase postprandial glucose level in type 1 diabetes patients on insulin pump:

the conclusion of a randomized study". In: *Diabetes Technology & Therapeutics* 14.1, pp. 16–22 (cit. on p. 39).

Parker, R. S. and F. J. Doyle III (2001). "Control-relevant modeling in drug delivery". In: *Advanced Drug Delivery Reviews* 48.2-3, pp. 211–228 (cit. on p. 47).

Parker, R. S., F. J. Doyle III, and N. A. Peppas (1999). "A model-based algorithm for blood glucose control in type I diabetic patients". In: *IEEE Transactions on Biomedical Engineering* 46.2, pp. 148–157 (cit. on p. 49).

Parker, R. S., F. J. Doyle III, J. H. Ward, and N. A. Peppas (2000). "Robust H_∞ glucose control in diabetes using a physiological model". In: *American Institute of Chemical Engineers Journal* 46.12, pp. 2537–2549 (cit. on p. 49).

Patek, S.D., M.D. Breton, Y. Chen, C. Solomon, and B. Kovatchev (2007). "Linear quadratic gaussian-based closed-loop control of type 1 diabetes". In: *Journal of Diabetes Science and Technology* 1.6, pp. 834–841 (cit. on p. 31).

Patek, S.D., L. Magni, E. Dassau, C. Karvetski, C. Toffanin, G. De Nicolao, S. Del Favero, M. Breton, C. Dall Man, E. Renard, H. Zisse, F.J. Doyle III, C. Cobelli, B.P. Kovatchev, and International Artificial Pancreas (iAP) Study Group (2012). "Modular closed-loop control of diabetes". In: *IEEE Transactions on Biomedical Engineering* 59.11, pp. 2986–2999 (cit. on p. 3).

Periwal, V., C.C. Chow, R.N. Bergman, M. Ricks, G.L. Vega, and A.E. Sumner (2008). "Evaluation of quantitative models of the effect of insulin on lipolysis and glucose disposal". In: *American Journal of Physiology: Regulatory, Integrative and Comparative Physiology* 295.4, R1089–R1096 (cit. on p. 100).

Quagliaro, L., L. Piconi, R. Assaloni, R. Da Ros, A. Maier, G. Zuodar, and A. Ceriello (2005). "Intermittent high glucose enhances ICAM-1, VCAM-1 and E-selectin expression in human umbilical vein endothelial cells in culture: The distinct role of protein kinase C and mitochondrial superoxide production". In: *Atherosclerosis* 183.2, pp. 259–267 (cit. on p. 39).

Rabasa-Lhoret, R., J. Bourque, F. Ducros, and J.L. Chiasson (2001). "Guidelines for premeal insulin dose reduction for postprandial exercise of different intensities and durations in type 1 diabetic subjects treated intensively with a basal-bolus insulin regimen (ultralente-lispro)". In: *Diabetes Care* 24.4, pp. 625–630 (cit. on p. 39).

Radziuk, J., T. J. McDonald, D. Rubenstein, and J. Dupre (1978). "Initial splanchnic extraction of ingested glucose in normal man". In: *Metabolism: Clinical Experimental* 27.6, pp. 657–669 (cit. on p. 46).

Reddy, M., M. Gimenez, V. Moscardo, and N. Oliver (2018). "The Relationship between A1C and Hypoglycemia in the Diamond Study". In: *The 8th Scientific Sessions of the American Diabetes Association (ADA)*. Orlando, USA (cit. on p. 172).

Renard, E., A. Farret, J. Kropff, D. Bruttomesso, M. Messori, J. Place, R. Visentin, R. Calore, C. Toffanin, F. Di Palma, L. Giordano, P. Magni, F. Boscari, S. Galasso, A. Avogaro, P. Keith-Hynes, B. Kovatchev, S. Del Favero, C. Cobelli, L. Magni, and J. H. DeVries (2016). "Day-and-night closed-loop glucose control in patients with type 1 diabetes under free-living conditions: results of a single-arm 1-month experience compared with a previously reported feasibility study of evening and night at home". In: *Diabetes Care* 39.7, pp. 1151–1160 (cit. on p. 31).

Renard, E., J. Place, M. Cantwell, H. Chevassus, and C.C. Palerm (2010). "Closed-loop insulin delivery using a subcutaneous glucose sensor and intraperitoneal insulin delivery: feasibility study testing a new model for the artificial pancreas". In: *Diabetes care* 33.1, pp. 121–127 (cit. on p. 28).

Revert, A., F. Garelli, J. Picó, H. De Battista, P. Rossetti, J. Vehí, and J. Bondia (2013). "Safety auxiliary feedback element for the artificial pancreas in type 1 diabetes". In: *IEEE Transactions on Biomedical Engineering* 60.8, pp. 2113–2122 (cit. on pp. 5, 30, 33, 34, 128, 155).

Rico-Azagra, J., M. Gil-Martínez, and J. Elso (2014). "Quantitative Feedback Control of Multiple Input Single Output Systems". In: *Mathematical Problems in Engineering* 2014, pp. 1–17 (cit. on pp. 133, 134).

Riddell, M.C., O. Bar-Or, B.V. Ayub, R.E. Calvert, and G.J.F. Heigenhauser (1999). "Glucose ingestion matched with total carbohydrate utilization attenuates hypoglycemia during exercise in adolescents with IDDM". In: *International Journal of Sport Nutrition* 9.1, pp. 24–34 (cit. on p. 39).

Riddell, M.C., D.P. Zaharieva, L. Yavelberg, A. Cinar, and V.K. Jamnik (2015). "Exercise and the development of the artificial pancreas: one of the more

difficult series of hurdles". In: *Journal of Diabetes Science and Technology* 9.6, pp. 1217–1226 (cit. on p. 38).

Rizza, R.A., P.E. Cryer, and J.E. Gerich (1979). "Role of glucagon, catecholamines, and growth hormone in human glucose counterregulation: effects of somatostatin and combined α-and β-adrenergic blockade on plasma glucose recovery and glucose flux rates after insulin-induced hypoglycemia". In: *The Journal of Clinical Investigation* 64.1, pp. 62–71 (cit. on p. 22).

Rodbard, D. (2009a). "Interpretation of continuous glucose monitoring data: glycemic variability and quality of glycemic control". In: *Diabetes Technology & Therapeutics* 11.S1, S55–S67 (cit. on pp. 39, 43, 114, 180).

— (2009b). "New and improved methods to characterize glycemic variability using continuous glucose monitoring". In: *Diabetes Technology & Therapeutics* 11.9, pp. 551–565 (cit. on pp. 43, 180).

— (2018). "Metrics to Evaluate Quality of Glycemic Control: Comparison of Time in Target, Hypoglycemic, and Hyperglycemic Ranges with "Risk Indices"". In: *Diabetes Technology & Therapeutics* 20.5, pp. 325–334 (cit. on p. 123).

Rodriguez-Diaz, R., M.H. Abdulreda, A.L. Formoso, I. Gans, C. Ricordi, P.O. Berggren, and A. Caicedo (2011a). "Innervation patterns of autonomic axons in the human endocrine pancreas". In: *Cell Metabolism* 14.1, pp. 45–54 (cit. on p. 37).

Rodriguez-Diaz, R., R. Dando, M.C. Jacques-Silva, A. Fachado, J. Molina, M.H. Abdulreda, C. Ricordi, S.D. Roper, P.O. Berggren, and A. Caicedo (2011b). "Alpha cells secrete acetylcholine as a non-neuronal paracrine signal priming beta cell function in humans". In: *Nature Medicine* 17.7, pp. 888–892 (cit. on p. 129).

Rossetti, P., F. Porcellati, C. G. Fanelli, G. Perriello, E. Torlone, and G. B. Bolli (2008). "Superiority of insulin analogues versus human insulin in the treatment of diabetes mellitus". In: *Archives of Physiology and Biochemistry* 114.1, pp. 3–10 (cit. on pp. 16, 21).

Rossetti, P., C. Quiros, V. Moscardo, A. Comas, M. Giménez, F. J. Ampudia-Blasco, F. León, E. Montaser, I. Conget, J. Bondia, and J. Vehí (2017).

"Closed-loop control of postprandial glycemia using an insulin-on-board limitation through continuous action on glucose target". In: *Diabetes Technology & Therapeutics* 19.6, pp. 355–362 (cit. on pp. 5, 30, 36, 113, 155, 172).

Rossetti, P., C. Quirós, V. Moscardó, A. Comas, M. Giménez, J. Ampudia, F. León, E. Montaser, I. Conget, J. Bondia, and J. Vehí (2016). "Better postprandial glucose control with a new developed closed-loop control system as compared with open-loop treatment in patients with type 1 diabetes". In: *The 76th American Diabetes Association (ADA) scientifc sessions*. New Orleans, USA (cit. on p. 173).

Roy, A. and R. S. Parker (2006a). "Dynamic modeling of exercise effects on plasma glucose and insulin levels". In: *International Symposium on Advanced Control of Chemical Processes*. Gramado, Brazil, pp. 509–514 (cit. on p. 54).

— (2006b). "Dynamic modeling of free fatty acid, glucose, and insulin: An extended "minimal model"". In: *Diabetes Technology & Therapeutics* 8.6, pp. 617–626 (cit. on pp. 52, 53, 87, 93, 94, 100).

Ruiz, J.L., J.L. Sherr, E. Cengiz, L. Carria, A. Roy, G. Voskanyan, W.V. Tamborlane, and S.A. Weinzimer (2012). "Effect of insulin feedback on closed-loop glucose control: a crossover study". In: *Journal of Diabetes Science and Technology* 6.5, pp. 1123–1130 (cit. on p. 30).

Russell, S. J., F. H. El-Khatib, D. M. Nathan, K. L. Magyar, J. Jiang, and E. R. Damiano (2012). "Blood glucose control in type 1 diabetes with a bihormonal bionic endocrine pancreas". In: *Diabetes Care* 35.11, pp. 2148–2155 (cit. on p. 5).

Rutscher, A., E. Salzsieder, and U. Fischer (1994). "KADIS: model-aided education in type I diabetes". In: *Computer Methods and Programs in Biomedicine* 41.3-4, pp. 205–215 (cit. on p. 48).

Ryan, E. A., T. Shandro, K. Green, B. W. Paty, P. A. Senior, D. Bigam, A. M. J. Shapiro, and M. C. Vantyghem (2004). "Assessment of the severity of hypoglycemia and glycemic lability in type 1 diabetic subjects undergoing islet transplantation". In: *Diabetes* 53.4, pp. 955–962 (cit. on pp. 42, 179).

Saccomani, M.P., S. Audoly, G. Bellu, L. D'Angio, and C. Cobelli (1997). "Global identifiability of nonlinear model parameters". In: *IFAC Proceedings Volumes* 30.11, pp. 233–238 (cit. on pp. 70, 87).

Sánchez Peña, R. S. and A. S. Ghersin (2010). "LPV control of glucose for Diabetes type I". In: *2010 Annual International Conference of the IEEE Engineering in Medicine and Biology*. Buenos Aires, Argentina, pp. 680–683 (cit. on p. 29).

Sánchez-Peña, R., P. Colmegna, F. Garelli, H. De Battista, D. García-Violini, M. Moscoso-Vásquez, N. Rosales, E. Fushimi, E. Campos-Náñez, M. Breton, et al. (2018). "Artificial Pancreas: Clinical Study in Latin America Without Premeal Insulin Boluses". In: *Journal of diabetes science and technology* 12.5, pp. 914–925 (cit. on pp. 5, 33).

Sánchez-Peña, R., P. Colmegna, L. Grosembacher, M. Breton, H. De Battista, F. Garelli, W.H. Belloso, E. Campos-Nánez, V. Simonovich, V. Beruto, P. Scibona, and D. Chernavvsky (2017). "Artificial pancreas: first clinical trials in Argentina". In: *IFAC-PapersOnLine* 50.1, pp. 7731–7736 (cit. on pp. 5, 33).

Scheiner, G. and B.A. Boyer (2005). "Characteristics of basal insulin requirements by age and gender in Type-1 diabetes patients using insulin pump therapy". In: *Diabetes research and clinical practice* 69.1, pp. 14–21 (cit. on p. 32).

Schiavon, M., L. Hinshaw, A. Mallad, C.D. Man, G. Sparacino, M. Johnson, and A. Basu (2013). "Postprandial glucose fluxes and insulin sensitivity during exercise: a study in healthy individuals". In: *American Journal of Physiology: Endocrinology and Metabolism* 305.4, E557–E566 (cit. on p. 148).

Schiekofer, S., M. Andrassy, J. Chen, G. Rudofsky, J. Schneider, T. Wendt, N. Stefan, P. Humpert, A. Fritsche, M. Stumvoll, E. Schleicher, H.U. Häring, P.P. Nawroth, and A. Bierhaus (2003). "Acute hyperglycemia causes intracellular formation of CML and activation of ras, p42/44 MAPK, and nuclear factor κB in PBMCs". In: *Diabetes* 52.3, pp. 621–633 (cit. on p. 39).

Schroeck, S.J., W.C. Messner, and R.J. McNab (2001). "On compensator design for linear time-invariant dual-input single-output systems". In: *IEEE/ASME Transactions On Mechatronics* 6.1, pp. 50–57 (cit. on p. 134).

Schwartz, N.S., W.E. Clutter, S.D. Shah, and P.E. Cryer (1987). "Glycemic thresholds for activation of glucose counterregulatory systems are higher

than the threshold for symptoms". In: *The Journal of Clinical Investigation* 79.3, pp. 777–781 (cit. on pp. 22, 55, 61, 78, 93).

Sedaghat, A. R., A. Sherman, and M. J. Quon (2002). "A mathematical model of metabolic insulin signaling pathways". In: *American Journal of Physiology: Endocrinology and Metabolism* 283.5, E1084–E1101 (cit. on p. 48).

Service, F. J. (2013). "Glucose variability". In: *Diabetes* 62.5, pp. 1398–1404 (cit. on pp. 42, 114, 178).

Shaw, J. E., R. A. Sicree, and P. Z. Zimmet (2010). "Global estimates of the prevalence of diabetes for 2010 and 2030". In: *Diabetes Research and Clinical Practice* 87.1, pp. 4–14 (cit. on p. 1).

Shinskey, FG (1978). "Control systems can save energy". In: *Chemical Engineering Progress* 74.5, pp. 43–46 (cit. on p. 134).

Signal, M., A. Le Compte, D.L. Harris, P.J. Weston, J.E. Harding, and J.G. Chase (2012). "Using Stochastic modelling to identify unusual continuous glucose monitor measurements and behaviour, in newborn infants". In: *Biomedical Engineering Online* 11.45, pp. 1–12 (cit. on p. 4).

Sorensen, J. T. (1985). "A physiologic model of glucose metabolism in man and its use to design and assess improved insulin therapies for diabetes". PhD thesis. Cambirdge, MA, USA: Dept. of Chemical Engineering, Massachusetts Institute of Technology (cit. on pp. 47, 48).

Ståhl, F. and R. Johansson (2009). "Diabetes mellitus modeling and short-term prediction based on blood glucose measurements". In: *Mathematical Biosciences* 217.2, pp. 101–117 (cit. on p. 3).

Steele, R., C. Bjerknes, I. Rathgeb, and N. Altszuler (1968). "Glucose uptake and production during the oral glucose tolerance test". In: *Diabetes* 17.7, pp. 415–421 (cit. on p. 46).

Steil, G.M., C.C. Palerm, N. Kurtz, G. Voskanyan, A. Roy, S. Paz, and F.R. Kandeel (2011). "The effect of insulin feedback on closed loop glucose control". In: *The Journal of Clinical Endocrinology & Metabolism* 96.5, pp. 1402–1408 (cit. on pp. 3, 30, 34, 40).

Steil, G.M., K. Rebrin, C. Darwin, F. Hariri, and M.F. Saad (2006). "Feasibility of automating insulin delivery for the treatment of type 1 diabetes". In: *Diabetes* 55.12, pp. 3344–3350 (cit. on p. 30).

Steil, G.M., K. Rebrin, R. Janowski, C. Darwin, and M.F. Saad (2003). "Modeling β-cell insulin secretion-implications for closed-loop glucose homeostasis". In: *Diabetes Technology & Therapeutics* 5.6, pp. 953–964 (cit. on p. 29).

Sun, J., F. Cameron, and B. W. Bequette (2012). "A habituating blood glucose control strategy for the critically ill". In: *Journal of Process Control* 22.8, pp. 1411–1421 (cit. on p. 135).

Swan, K.L., J.D. Dziura, G.M. Steil, G.R. Voskanyan, K.A. Sikes, A.T. Steffen, M.L. Martin, W.V. Tamborlane, and S.A. Weinzimer (2009). "Effect of age of infusion site and type of rapid-acting analog on pharmacodynamic parameters of insulin boluses in youth with type 1 diabetes receiving insulin pump therapy". In: *Diabetes Care* 32.2, pp. 240–244 (cit. on p. 39).

Taleb, N., A. Emami, C. Suppere, V. Messier, L. Legault, M. Ladouceur, J.L. Chiasson, A. Haidar, and R. Rabasa-Lhoret (2016). "Efficacy of single-hormone and dual-hormone artificial pancreas during continuous and interval exercise in adult patients with type 1 diabetes: randomised controlled crossover trial". In: *Diabetologia* 59.12, pp. 2561–2571 (cit. on pp. 5, 37).

Taplin, C.E., E. Cobry, L. Messer, K. McFann, H.P. Chase, and R. Fiallo-Scharer (2010). "Preventing post-exercise nocturnal hypoglycemia in children with type 1 diabetes". In: *The Journal of Pediatrics* 157.5, pp. 784–788 (cit. on pp. 39, 40).

Tesfaye, N. and E. R. Seaquist (2010). "Neuroendocrine responses to hypoglycemia". In: *Annals of the New York Academy of Sciences* 1212.1, pp. 12–28 (cit. on pp. 61–63, 78, 93).

Thomaseth, K., A. Brehm, A. Pavan, G. Pacini, and M. Roden (2014). "Modeling glucose and free fatty acid kinetics during insulin-modified intravenous glucose tolerance test in healthy humans: role of counterregulatory response". In: *American Journal of Physiology: Regulatory, Integrative and Comparative Physiology* 307.3, pp. 321–331 (cit. on p. 60).

Toffanin, C., M. Messori, F. Di Palma, G. De Nicolao, C. Cobelli, and L. Magni (2013). "Artificial pancreas: Model predictive control design from clinical experience". In: *Journal of Diabetes Science and Technology* 7.6, pp. 1470–1483 (cit. on p. 40).

Trajanoski, Z. and P. Wach (1998). "Neural predictive controller for insulin delivery using the subcutaneous route". In: *IEEE Transactions on Biomedical Engineering* 45.9, pp. 1122–1134 (cit. on p. 29).

Trout, K.K., M.R. Rickels, M.H. Schutta, M. Petrova, E.W. Freeman, N.C. Tkacs, and K.L. Teff (2007). "Menstrual cycle effects on insulin sensitivity in women with type 1 diabetes: a pilot study". In: *Diabetes Technology & Therapeutics* 9.2, pp. 176–182 (cit. on p. 40).

van Heusden, K., E. Dassau, H.C. Zisser, D.E. Seborg, and F.J. Doyle III (2012). "Control-relevant models for glucose control using a priori patient characteristics". In: *IEEE Transactions on Biomedical Engineering* 59.7, pp. 1839–1849 (cit. on p. 47).

Velasco-Pérez, A., J. Álvarez-Ramírez, and R. Solar-González (2011). "Control múltiple entrada una salida (MISO) de un CSTR". In: *Revista Mexicana de Ingeniería Química* 10.2, pp. 321–331 (cit. on p. 135).

Velasco-Perez, A., J.J. Alvarez-Ramirez, S.E. Vigueras-Carmona, A. Osorio-Miron, L.A. Sanchez-Bazan, V. Cruz-Garrido, and A. Rodriguez-Rivera (2009). "Algorithm for parallel control for an aerobic reactor". In: *The Third International Meeting on Environmental Biotechnology and Engineering*. Palma de Mallorca, Spain (cit. on p. 135).

Verkest, K.R., L.M. Fleeman, J.S. Rand, and J.M. Morton (2010). "Basal measures of insulin sensitivity and insulin secretion and simplified glucose tolerance tests in dogs". In: *Domestic Animal Endocrinology* 39.3, pp. 194–204 (cit. on p. 115).

Vicini, P., A. Caumo, and C. Cobelli (1997). "The hot IVGTT two-compartment minimal model: indexes of glucose effectiveness and insulin sensitivity". In: *American Journal of Physiology: Endocrinology And Metabolism* 273.5, E1024–E1032 (cit. on p. 46).

Visentin, R., E. Campos-Náñez, M. Schiavon, D. Lv, M. Vettoretti, M. Breton, B. P. Kovatchev, C. Dalla Man, and C. Cobelli (2018). "The UVA/Padova Type 1 Diabetes Simulator Goes From Single Meal to Single Day". In: *Journal of Diabetes Science and Technology* 12.2, pp. 273–281 (cit. on p. 50).

Walter, E. and L. Pronzato (1997). *Identification of parametric models from experimental data*. London: Springer Verlag (cit. on p. 69).

Wang, C., L. Lv, Y. Yang, D. Chen, G. Liu, L. Chen, Y. Song, L. He, X. Li, H. Tian, W. Jia, and X. Ran (2012). "Glucose fluctuations in subjects with normal glucose tolerance, impaired glucose regulation and newly diagnosed type 2 diabetes mellitus". In: *Clinical Endocrinology* 76.6, pp. 810–815 (cit. on p. 39).

Wang, L.X. (1997). *A Course in Fuzzy Systems and Control*. Upper Saddle River, NJ, USA: Prentice-Hall, Inc. (cit. on p. 32).

Ward, W.K., J. Engle, H.M. Duman, C.P. Bergstrom, S.F. Kim, and I.F. Federiuk (2008). "The benefit of subcutaneous glucagon during closed-loop glycemic control in rats with type 1 diabetes". In: *IEEE Sensors Journal* 8.1, pp. 89–96 (cit. on pp. 37, 128).

Watts, A.G. and C.M. Donovan (2010). "Sweet talk in the brain: glucosensing, neural networks, and hypoglycemic counterregulation". In: *Frontiers in Neuroendocrinology* 31.1, pp. 32–43 (cit. on p. 63).

Weinzimer, S. A., G. M. Steil, K. L. Swan, J. Dziura, N. Kurtz, and W. V. Tamborlane (2008). "Fully automated closed-loop insulin delivery versus semiautomated hybrid control in pediatric patients with type 1 diabetes using an artificial pancreas". In: *Diabetes Care* 31.5, pp. 934–939 (cit. on pp. 5, 29, 30).

Weisman, A., J.W. Bai, M. Cardinez, C.K. Kramer, and B.A. Perkins (2017). "Effect of artificial pancreas systems on glycaemic control in patients with type 1 diabetes: a systematic review and meta-analysis of outpatient randomised controlled trials". In: *The Lancet Diabetes & Endocrinology* 5.7, pp. 501–512 (cit. on p. 37).

Whitelaw, B. C., P. Choudhary, and D. Hopkins (2011). "Evaluating rate of change as an index of glycemic variability, using continuous glucose monitoring data".

In: *Diabetes Technology & Therapeutics* 13.6, pp. 631–636 (cit. on pp. 39, 41, 42, 177, 179).

Wilinska, M. E., L. J. Chassin, C. L. Acerini, J. M. Allen, D. B. Dunger, and R. Hovorka (2010). "Simulation environment to evaluate closed-loop insulin delivery systems in type 1 diabetes". In: *Journal of Diabetes Science and Technology* 4.1, pp. 132–144 (cit. on p. 46).

Wilinska, M. E. and R. Hovorka (2008). "Simulation models for in silico testing of closed-loop glucose controllers in type 1 diabetes". In: *Drug Discovery Today: Disease Models* 5.4, pp. 289–298 (cit. on pp. 49, 50).

Yardley, J.E., G. P. Kenny, B. A. Perkins, M. C. Riddell, N. Balaa, J. Malcolm, P. Boulay, F. Khandwala, and R. J. Sigal (2012). "Resistance versus aerobic exercise: acute effects on glycemia in type 1 diabetes". In: *Diabetes Care* 36.3, pp. 537–542 (cit. on p. 39).

Yu, C.C. and W.L. Luyben (1986). "Analysis of valve-position control for dual-input processes". In: *Industrial & Engineering Chemistry Fundamentals* 25.3, pp. 344–350 (cit. on p. 134).